DIET, DISEASE STATE, AND THE SPACE ENVIRONMENT MODIFY THE INTESTINAL MICROBIOTA AND MUCOSAL ENVIRONMENT VIA MICROBIOTA-DIRECTED ALTERATIONS IN COLONOCYTE SIGNALLING

A Dissertation

by

LAUREN ELIZABETH RITCHIE

Submitted to the Office of Graduate and Professional Studies of
Texas A&M University
in partial fulfillment of the requirements for the degree of

DOCTOR OF PHILOSOPHY

Chair of Committee,	Nancy D. Turner
Committee Members,	Robert S. Chapkin
	Joanne R. Lupton
	Penny K. Riggs
	Joseph M. Sturino
Intercollegiate Faculty Chair,	Craig J. Coates

December 2013

Major Subject: Genetics

ABSTRACT

Microbial dysbiosis and toll-like receptor (TLR) signaling play a role in colonic injury and inflammation. Ulcerative colitis and radiation are known to alter microbiota, and diets containing polyphenols impact bacterial populations. We hypothesized that diet can mitigate dextran sodium sulfate (DSS) colitis (sorghum bran diets containing polyphenols) and space environment-induced alterations (normal iron content) in colonic microbiota and TLR signaling. To test this we utilized two experimental paradigms; DSS-induced colitis (3% DSS, 48-hr, 3 exposures, 2 wk separation), and three models to emulate the space environment: 1) fractionated low linear energy transfer (LET) γ radiation (RAD) (3 Gy) and high Fe diet (IRON) (650 mg/kg), 2) high LET Si particle exposure (50 cGy) and 1/6 G hind limb unloading (HLU), and 3) 13 d spaceflight.

Bran diets upregulated proliferation, and repair protein (TFF3 and TGFβ) and short chain fatty acid (SCFA) transporter (Slc16a1 and Slc5a8) expression post-DSS. Diet significantly affected 24-hr fecal butyrate production, with Cellulose and Black bran having numerically higher concentrations. Two predominant phyla were identified, Firmicutes and Bacteroidetes, and this ratio was higher in Cellulose DSS. Post DSS#3 the proportion of Bacteroidales, Clostridiales, and Lactobacillales was reduced compared to post DSS#2 for all diets. Black bran non-DSS rats had the highest richness and diversity. Colonic injury negatively correlated with the proportion of Firmicutes, Actinobacteria, and Lactobacillales, and positively correlated with Unknown and

Unclassified groups. Bran diets reduced the severity of epithelial injury, maintained fecal butyrate, and prevented microbial dysbiosis and depletion during DSS-induced colitis.

IRON+RAD decreased SCFA concentrations. Low and high LET radiation, HLU, IRON and spaceflight increased Bacteroidetes and decreased Firmicutes. HLU and spaceflight increased Clostridiales and decreased Lactobacillales. RAD and IRON+RAD animals had increased Lactobacillales and significantly lower Clostridiales compared to CON and IRON. TLR9 and IL-6 were downregulated by RAD. TLR4, TFF3 and TGFβ differentially changed with IRON and spaceflight. Microgravity independently affected the microbiota, regardless of radiation energy or dose.

Each environmental insult differentially altered the microbiota and mucosal gene expression, with distinct diet, microgravity, and radiation effects observed. Bran diets mitigated deleterious effects of colitis, maintained barrier integrity, and prevented microbiota dysbiosis.

DEDICATION

For my mother

ACKNOWLEDGEMENTS

I would like to thank my entire committee for their guidance throughout the course of my research, particularly my advisor, Dr. Nancy Turner, for allowing me to work with her on these projects and opening the door to amazing experiences with the NSBRI fellowship program. We thank the staff of the NASA Johnson Space Center Nutritional Biochemistry Laboratory and Jane Krauhs for their assistance in performing biochemical analyses and immune system assays, as well as editorial assistance in Chapter IV. Additionally, I would like to thank Dr. Laurie Davidson for her guidance and methodology expertise that played an integral part in my research experience. Finally, I would like to specially thank Stella Taddeo for her never-ending dedication and encouragement. I appreciate all you do!

To all my friends and family, thank you for your support throughout my entire academic career. A special thanks to Bethany, Erika, Leigh Ann, and Taylor whom have helped me in more ways than they know. Finally to my mother, I appreciate your ever present prayers and reassurance.

This work was supported by fellowships to Ms. Ritchie from the National Space Biomedical Research Institute (EO01001) through NASA NCC 9658642, the Whole Systems Genomics Initiative, and the Office of Graduate and Professional Studies at Texas A&M University. Research was funded by the grant support from United Sorghum Checkoff Board Roo31A609, HVM006-12, and NASA HRP MTL 730.

NOMENCLATURE

ALT alanine transaminase

AST aspartate transaminase

CD crohn's disease

CON control group

COX cyclooxygenase

CRC colorectal cancer

CRP C-reactive protein

ddH2O distilled deionized water

DRI Dietary Reference Intake

DSS dextran sodium sulfate

EDTA ethylenediaminetetraacetic acid

ELISA enzyme-linked immunosorbent assay

EtOH ethanol

FDR false discovery rate

FGF fibroblast growth factor

FITC fluorescein isothiocyanate

GI gastrointestinal

GPX glutathione peroxidase

HEPES 4-(2-hydroxyethyl)-1-piperazineethanesulfonic acid

HTA-Br hexadecyltrimethylammonium bromide

IBD inflammatory bowel disease

IL interleukin

IRON high iron/sham group

IRON + RAD high iron/radiation

ISS International Space Station

LPS lipopolysaccharide

LS least squares

MCT-1 monocarboxylate transporter-1

MPO myeloperoxidase

MyD88 myeloid differentiation factor-88

NF-κB nuclear transcription factor kappa B

PBS phosphate buffered solution

PC5 phycoerythrin cyanin 5

PCR polymerase chain reaction

PE phycoerythrin

PFA paraformaldehyde

RAD control/radiation group

ROS reactive oxygen species

RT-PCR real-time polymerase chain reaction

SEM standard error of the mean

SLC5A8 sodium-coupled monocarboxylate transporter-1

SCFA short chain fatty acids

SOD superoxide dismutase

TAC total antioxidant capacity

TBI total body iron

TCR T-cell receptor

TGF transforming growth factor

TFF-3 trefoil factor-3

TLR toll-like receptor

TNF tumor necrosis factor

TNFR tumor necrosis factor receptor

Tollip toll interacting protein

UC ulcerative colitis

TABLE OF CONTENTS

Page

Page

LIST OF FIGURES

Page

Page

LIST OF TABLES

Page

CHAPTER I

INTRODUCTION AND LITERATURE REVIEW

Introduction

Chronic inflammation in the bowel is known to increase the risk of colorectal cancer, which is the 2nd most lethal cancer worldwide (1-3). During repeated bouts of intestinal inflammation, the activation of signaling pathways promotes the release of inflammatory cytokines and stimulates cellular proliferation, thereby increasing the risk of developing colonic neoplasias (1, 4). The etiology of gastrointestinal (GI) diseases such as inflammatory bowel disease (IBD), which includes both ulcerative colitis and Crohn's disease, are not well understood but both are associated with acute or chronic bouts of inflammation in the GI tract. Although genome-wide searches have implicated some gene loci in disease susceptibility, increasing diagnosis of these GI diseases has pointed researchers toward environmental effects such as intestinal microbiota dysbiosis and disruptions in signaling through toll-like receptors (TLR) as mitigating factors (5).

The intestinal microbiota is composed of trillions of bacteria, and it is estimated to be comprised of over 100 different phylotypes (6). It is universally accepted that the intestinal microbiota plays an important role in the health status of the host by influencing nutrient absorption, providing a defense mechanism against invading pathogens, and interacting with the host immune system through TLR signaling. However, increasing evidence suggests that initiation and pathogenesis of IBD is caused by a disruption in the host immune response to the commensal microbiota,

including oversensitization of TLR to bacterial ligands and alterations to TLR expression (7-8). Additionally, epithelial cell inflammation and oxidative stress can affect barrier function, which if compromised can allow the host to be exposed to bacteria and bacterial antigens from the lumen and initiate innate and adaptive immune responses (5). Understanding the role of the microbiota in GI diseases might help elucidate mechanisms that influence the onset and perturbation of inflammatory bouts.

Characterizing how the luminal environment and oxidative stress affect the intestinal microbiota is important to understanding its role in IBD. It is well documented that dietary constituents can affect intestinal bacterial populations (9-12), particularly dietary fiber (i.e., nondigestible food sources such as resistant starch and plant cell wall material), which reaches the colon and serves as substrates for the microbiota (13). Additionally, some secondary plant metabolites such as polyphenols can reach the colon and undergo bacterial transformations or have a bactericidal effect. Numerous studies have been performed that highlight how these dietary bioactive compounds have an effect on the predominant bacterial groups that reside in the GI tract (9, 14-16). As the host diet fluctuates, changes in the quality and quantity of bacterial substrates can alter the gut environment by affecting transit time and lumen pH (17-18). Additionally, the primary and secondary bacterial metabolites produced can shift bacterial populations and promote changes to epithelial cell metabolic regulation (19-20). Environmental factors that cause oxidative stress, such as radiation exposure and a high oxidant load diet (e.g., elevated dietary iron (Fe)), can have deleterious effects on colonic epithelial cells such as formation of reactive oxygen species (ROS) and DNA damage (21-22), but little is

known regarding the effect on the microbiota. Therefore, studies characterizing how dietary components, particularly polyphenols, and environmental insults that cause oxidative stress (i.e., radiation exposure and high Fe diet) affect the intestinal microbiota are warranted; as alterations to the GI environment and bacterial populations present in the intestine could affect the onset and progression of intestinal inflammation.

Sorghum grain is a common staple in dry, arid areas such as Africa and South America. Epidemiological data show that the incidence of colorectal cancer in both men and women is lower in countries that consume sorghum daily (23-24). Sorghum grain can be decorticated to isolate the bran fraction, which contains concentrated levels of bioactive compounds such as anthocyanins and tannins (25-26). These polyphenols have been characterized as potent antioxidants, and it has been demonstrated that sorghum bran has an *in vitro* antioxidant capacity (ORAC) higher than that of fruits such as blueberries, and pomegranate (27). Additionally, bran is a source of dietary fiber, which has been reported to have a positive impact on overall health by improving serum lipid concentrations, regulating blood glucose concentrations, lowering blood pressure and reducing the risk of developing GI disorders and colon cancer (13, 28). Previous animal studies demonstrated that, in comparison to a diet containing cellulose as a fiber source, sorghum bran can significantly reduce the occurrence of aberrant crypt foci (ACF), a precursor to colon adenomas (24).

Based on this evidence it is likely that properties of sorghum bran, including the bioactive compounds (anthocyanins and tannins), could be beneficial in suppressing the effects of chronic inflammation in the intestine by affecting the intestinal microbiota, its

metabolites, and downstream signaling through TLR. Furthermore, characterizing alterations to the microbiota caused by environmental insults (i.e., radiation exposure and diets containing elevated iron) will elucidate its role in propagating oxidative stress, and help identify mechanisms to reduce the risk of intestinal inflammation and cancer.

Literature Review

Implications of intestinal inflammation and IBD

Epidemiological studies suggest that those suffering from chronic intestinal inflammation, due to GI diseases such as ulcerative colitis, have between a 2-18% increased risk (dependent upon age), of developing colon cancer (1-3), which is the third most common diagnosed cancer in males and second highest in females (23). Similar to sporadic colon cancer, colitis-associated colorectal cancer can be associated with genetic mutations and alterations to molecular patterns in intestinal epithelial cells (4). For example, there is increasing evidence that methylation and allelic deletion of genes such as p53 are associated with colitis-associated cancer (4). Additionally, the presence of reactive oxygen species (ROS), often elevated in GI diseases such as IBD, can mutate or methylate regulatory genes, oncogenes, and those involved in DNA repair (29-30). ROS also have been implicated in inducing gene expression of key regulators of the inflammatory process such as nuclear factor kappa B (NF-κB), COX-2, and TNF-α (31-34). It has been reported that neoplastic regions of the mucosa are associated with chronic inflammation, and increased levels of NF-κB and its downstream mediators have been reported in intestinal biopsies from patients with ulcerative colitis (32). Therefore, suppression of these inflammatory cytokines by reducing ROS species in the bowel

might provide a reasonable countermeasure to mitigate the effects of GI diseases and the increased risk of colitis-associated cancer.

Commensal intestinal microbiota

In healthy individuals the commensal bacteria residing in the intestine, or microbiota, plays a major role in the health of the host by affecting the ability to digest dietary fiber, altering bowel motility and pH, and interacting with the host immune system (35-36). Additionally, these bacterial groups can provide protection against invading pathogens by effectively competing for host adhesion sites, secretion of bacteriocidal compounds, and improving the efficacy of epithelial cell tight junctions (36-37). Dietary fiber remains undigested and intact until it reaches the large intestine where the microbiota ferments it to produce metabolites that can influence mucosal metabolism (28, 38). These metabolites include SCFA, lactate, ethanol, ammonia and nitrates, which can be utilized by other bacteria or serve as a fuel source for the host epithelia. It is estimated that 8-10% of energy from the diet absorbed by the host is derived from byproducts of bacterial fermentation (39). The SCFA butyrate is a primary fuel source for colonocytes and has been shown to stimulate proliferation and affect migration in these cells, and is reported to have anti-inflammatory properties (40-42).

As mentioned previously, although the etiologies of many chronic enteropathies are unknown, there is increasing evidence that points away from genetic influences to other factors such as disruption in the homeostasis between the commensal bacterial species residing in the bowel and the host. Although in healthy individuals these bacteria provide benefits to the host, they can in fact become detrimental and often exacerbate GI

diseases (43-46). Additionally it has been reported that alterations in the production of SCFA may be involved in the development of colitis and colon cancer (47-48).

The effect of SCFA on intestinal homeostasis

SCFA play a major role in normal bowel function, and lumen concentrations predominantly consist of butyrate, acetate, and propionate (20, 38, 42). Numerous studies have analyzed the pleiotrophic effects of SCFA on colonocytes, in particular butyrate, which includes anti-inflammatory activity, the induction of gene expression, cellular differentiation, apoptosis, cell cycle arrest, and interference with transcription factors critical for pro-inflammatory cytokine production (20, 41-42, 47, 49-51). However, the effect of SCFA on the progression of IBD is not well understood. It has been reported that patients with ulcerative colitis have impaired fatty acid β-oxidation, which could suggest that alterations to butyrate uptake or metabolism in enterocytes is a possible pathogenetic mechanism (52-53).

Differential effects have been reported regarding butyrate's influence on cytokine production and the initiation of inflammation in the bowel. *In vitro* and *in vivo* studies have reported that butyrate plays a major role in the onset of an inflammatory state in the intestine by affecting cytokine production and epithelial cellular migration (54-59), however, SCFA supplementation has been reported to improve symptoms of patients with GI disorders (50, 60). Several *in vitro* studies have reported that butyrate suppresses (CaCo2) and enhances (HT-29 and LIM 1215) levels of IL-8 in colon cancer cells lines (57-59). One potential mechanism for influencing cytokine levels is the modification of transcription factors such as NF-κB, which activates the transcription of a multitude of

pro-inflammatory genes. It has been reported that butyrate can interfere with NF-κB transactivation by increasing IκB production or inhibition of IκB degradation, which leads to NF-κB remaining arrested in the cytoplasm (54-56, 61-62). Two *in vitro* studies reported that when intestinal cells were exposed to butyrate, NF-κB dimer activity and downstream cytokine production was suppressed (56, 61). Wu *et al* reported that IκB expression was increased in the surface epithelium, further suggesting that butyrate aids in suppressing the onset of inflammation through the NF-κB pathway. Similar results were reported in two studies by Kanauchi *et al* , which used both a transgenic mouse and dextran sodium sulfate (DSS) colitis rat model to demonstrate that increased levels of luminal butyrate (produced by feeding a germinated barley based diet) suppressed NF-κB activity (54-55). Another *in vivo* study utilizing a different colitis mouse model (i.e., trinitrobenzene sulfonic acid (TNBS)) also reported butyrate's ability to suppress NF-κB activity (62).

Studies focusing on the effect of SCFA on colon cancer progression reported that butyrate inhibited growth and promoted terminal differentiation in a variety of colon cancer cell lines and an animal model (47-49, 56, 63). One study reported that, of all the SCFA tested (i.e., acetate, butyrate, propionate), only butyrate demonstrated an ability to induce differentiation in LIM1215 colon carcinoma cells (48). Using a growth study assay, it was shown that the doubling time of these model cancer cells decreased markedly with the addition of a 1 mmol/l butyrate solution to the cell culture (48). Another study using a rat model reported that when fed diets containing fermentable

fibers, which increased the concentration of butyrate in the colon, animals had a decreased incidence of tumors (64).

More recent studies have proposed molecular mechanisms for how SCFA might exert cellular effects such as differentiation and apoptosis. It has been established that butyrate can enhance apoptosis in colonocytes, and has been reported to have the most potent cellular effects *in vitro* compared to other SCFA such as acetate and propionate (48, 65-66). Two studies reported the human colon carcinoma cell line, HT-29, demonstrates enhanced levels of differentiation and apoptosis when exposed to butyrate (47, 65). Hinnebusch *et al* further showed that when p21 is deleted in colon cancer cell lines SCFA have no effect on proliferation, suggesting that growth arrest *in vitro* requires the p21 gene. Also, it was reported that the effect of butyrate on colon cancer cell differentiation is protein kinase C and JNK dependant (65). Similar results were reported in YAMC and YAMC-Ras transformed cell lines, where butyrate (5 mM) and *n*-3 polyunsaturated fatty acids (PUFA) supplementation had a synergistic effect by significantly increasing apoptosis (66).

Butyrate is thought to produce these cellular effects, in part, by inhibiting histone deacetylase (HDAC), which affects gene transcription by enhancing histone acetylation (i.e., DNA relaxation and increased transcription factor access) (47, 51, 67-68). Although it was reported that propionate and valerate could inhibit HDAC *in vitro*, butyrate stimulated the greatest increase in overall H4 acetylation (47). These results have been confirmed *in vivo*, where a positive correlation between luminal butyrate levels and histone acetylation (H4) was reported (67). In a study published just last year,

researchers identified that butyrate can additionally stimulate histone acetylase (HAT) activity (69). Although both mechanisms increase histone acetylation, different gene loci were up or down regulated depending on how butyrate was utilized in the cell. Additionally they demonstrated that butyrate has differential effects on cell lines and this effect is dependent upon the cells metabolic state. Donohoe et al. (69) simulated the Warburg effect (i.e., glycolysis followed by cytosolic lactic acid fermentation versus oxidation of pyruvate in the mitochondria) *in vitro*, which is commonly found in cancer cells. They observed that butyrate concentrations were not depleted in these cells as observed in normal colonocytes, and thereby affected transcription of different gene loci (69). This is thought to be due to inefficient metabolism of butyrate due to the Warburg effect, allowing for accumulation of butyrate in the nucleus and inhibition of HDACs. These studies are a first step in better understanding the butyrate paradox, and how this metabolite can epigenetically regulate the expression of different target genes associated with proliferation and apoptosis.

Microbial signaling in the intestine

In addition to acting as a physical barrier, the intestinal epithelium is very important in the regulation of intestinal homeostasis. Microbe-epithelial cell interactions are important in maturation of intestinal epithelium and the development of the innate and acquired mucosal immune system (35, 70). Bacteria present in the bowel, either commensal or pathogenic, can communicate with the host immune system through pathogen-associated molecular patterns (PAMPs) or an increasingly used term, microbe-associated molecular patterns (MAMPs) (71). The most common and characterized

receptors are TLR, with over 13 being reported in mice and humans. TLR recognize various microbial ligands including lipoproteins, lipopolysaccharide (LPS), flagellin, and CpG DNA (72-73). Once activated, TLR can trigger a downstream signaling cascade through the MyD88 pathway, which includes NF-κB activation, known to upregulate the expression of various chemokines (73-74). In healthy individuals, the host epithelium tolerates the presence of luminal bacteria and does not mount an inflammatory response. Furthermore, this relationship is required for normal function and involved in various beneficial effects such as epithelial cell proliferation, IgA production, mucin gene expression, goblet cell dynamics and differentiation, and the maintenance of tight junctions (44, 74-75).

As mentioned previously, the etiology of GI diseases such as Crohn's and IBD is not well established. However, chronic stimulation or uncontrolled signaling between commensal bacteria and the host has been implicated as a cause for the initiation and pathogenesis of IBD (5). Alterations to these interactions can lead to acute or chronic bouts of inflammation in the bowel, which mentioned previously, can lead to increased susceptibility to colorectal cancers. Other references indicate that mutations/differential expression of TLR, nod-like receptors (NLR), and downstream mediators of the NF-κB pathway can break microbial tolerance and have been implicated in GI diseases such as IBD and Crohn's (7, 76-77). It was reported that patients with IBS had significantly up and down regulated expression of TLRs compared to healthy controls, indicating that affecting the interaction between these receptors and the commensal bacteria present in the bowel could potentiate GI diseases (7).

It has been reported that interactions between TLR and the commensal bacteria also maintain epithelial cell barrier function and have been implicated in the inhibition of colonic inflammation (37, 72, 75). Studies using gnotobiotic or knockout (KO) animals (e.g., TLR pathway) or experimental models that induce an inflammatory state in the bowel using DSS or TNBS can help elucidate the effect of the intestinal microbiota on health and disease states (78-81). It has been demonstrated that animals raised in a germ-free environment, containing no GI bacterial populations, are more susceptible to DSS induced colitis suggesting the interaction between TLR and microbes are essential to maintaining intestinal homeostasis (80, 82). Additionally, it has been hypothesized that if the intestinal microbiota does not contain species with TLR ligands, there could be an increase in epithelium permeability and therefore increased ability for infiltration by pathogens (37). To better understand how TLR signaling can affect barrier stability, one *in vitro* study looked at the effect of a synthetic lipopeptide on two different epithelial cell lines (37). It was reported that these lipopeptides, which are similar to that of commensal bacteria, interact with TLR2 and enhance epithelial cell barrier function by activating protein kinase C. Other important interactions of commensal bacteria and TLR were demonstrated in a recent *in vivo* study where transgenic mice were used to better understand the relationship between commensal bacteria and epithelial inflammation (75). In this study, intestinal inflammation was induced by a chemical agent and the effect of TLR signaling (induced by commensal bacteria) in the MyD88 pathway was shown to confer protection against colonic bleeding and intestinal epithelium damage. In addition, mice without commensal bacteria present had a lower

survival rate than animals with selected commensal bacteria (by antibacterial administration) in the GI tract, which suggests that the commensal bacteria can produce these protective effects (37).

Many studies have been performed to better understand the role of TLR in inflammatory and immune disorders in the gut (83-86). One study reported that defective IL-10 signaling from TLR causes a constitutive activation of certain inflammatory cytokines, and can lead to the development of chronic enterocolitis (86). Another recent study also implicated TLR and interleukin activities in the etiology of enterocolitis (83). In this study, a variety of transgenic knockout mice were used to understand how the absence of IL-10 signaling induces colitis. Kobayashi et al. reported that introduction of TLR4 deficiency in mutant mice diminished intestinal inflammation in these animals, which demonstrates that TLR recognition of pathogenic ligands in the intestine can trigger the development of chronic enterocolitis (83). Two studies performed by the same research group demonstrated that TLR9-mediated microbial recognition inhibits colonic inflammation in a mouse model (84-85). These two studies induced colitis in wild-type and transgenic animals and demonstrated that certain probiotic bacterial strains had anti-inflammatory effects when interacting with TLR. In particular they demonstrated that TLR-triggered IFN-α/β production, thereby mediating innate immunity, can provide a protective effect against colitis (84). It has also been suggested that the absence of TLR in epithelial cells might contribute to a hypo- responsive tone toward commensal bacteria and lead to inflammation in the GI tract (87).

These studies indicate that TLR may play a role in the etiology of different GI disorders. It has been suggested that TLR are probably involved in other aspects of immune responses, even in the absence of infection (73). Many aspects of the interactions between TLR and bacterial ligands are unknown, and additional studies are warranted to better understand how their relationship affects the physiology of the host. Additionally, a complete phylogenetic characterization of the bacterial groups present in healthy and diseased individuals is important and will allow researchers to better understand how shifts in the commensal microbiota or activation of pro-inflammatory pathways through TLR can affect the onset or progression of IBD.

Characterization of the intestinal microbiota and its role in IBD

Early studies characterizing the intestinal microflora used traditional microbiological culture techniques, in which samples are plated on selective culture media and are grown in an aerobic or anaerobic environment and further identified by various morphological and biochemical tests (88). However, it is established that microbiological culture techniques fail to accurately characterize bacterial communities in complex environmental samples (e.g., the gastrointestinal tract) (89-90). This is due to the fact that only an estimated 10% - 50% of bacteria present in the mammalian gut are cultivable due to unknown growth requirements, poor selectivity of culture media, and microorganism metabolic plasticity (90). Furthermore, culture-based techniques for studying complex biological samples such as intestinal content are laborious and time-consuming.

In recent years, the intestinal microflora in many mammalian species has been studied using molecular-based methods that amplify the 16S ribosomal RNA gene (16S rDNA) (91-93). Bacterial 16S rRNA genes generally contain nine hypervariable regions that demonstrate considerable sequence diversity among different bacterial species and can be used for species identification (94). Since these hypervariable regions are flanked by conserved regions, universal bacterial primers can be designed that enable PCR amplification of target sequences, which results in amplification of all bacteria present in a given sample. Therefore, molecular-based methods allow identification of both cultivable and non-cultivable bacteria. In many studies, molecular techniques have resulted in the observation of an increased bacterial diversity in the intestine compared to strictly culture-based methods (89-90, 92). Additionally, next generation sequencing techniques have allowed for the rapid and in-depth analysis of complex bacterial communities such as the intestinal microbiota. Within the past decade, numerous studies have employed a 454-pyrosequencing technique and reported that this method produces taxonomic classifications down to phylotypes below the genus level (93, 95).

Numerous studies have focused on identifying shifts in intestinal bacterial populations that might initiate or propagate intestinal inflammation in GI diseases (summarized in Table 1). Patients with ulcerative colitis and Crohns disease demonstrate a decreased microbial diversity, in particular, depletion of certain bacterial species that are thought to be beneficial to GI tract health (e.g., lactic acid producing bacteria) (96-99). Other organisms thought to be involved are species that are cytotoxic and/or possibly adherent or invasive to the gut epithelium, including *Escherichia coli* (*E.coli*),

Table 1. Documented microbiota alterations in IBD patients and *in vivo* models of ulcerative colitis.

Changes in microbiota	Phylum	Class	Order	Family	Genus	Species	Method	Model	Author
	↓ Firmicutes						FISH, CL	CD patients	Manichanh et al, 2006
↓ Bacterial species richness							T-RFLP	IBD patients	Sepehri et al, 2007
	Firmicutes	**↑Clostridia**							
Diff in CD & UC biopsies							CL, qPCR	IBD patients	Frank et al, 2007
	↑Proteobacteria						CL, qPCR	IBD patients	Frank et al, 2007
	↓ Bacteroidetes						CL, qPCR	IBD patients	Frank et al, 2007
	Firmicutes	Clostridia	Clostridiales	**↓ Lachnospiraceae**			CL, qPCR	IBD patients	Frank et al, 2007
	Firmicutes	Bacilli	Bacillales	Bacillaceae	**↑ Bacillus**		CL, qPCR	IBD patients	Frank et al, 2007
	↓ Bacteroidetes						MA, qPCR	IBS patients	Rajilic-Stojanovic, 2011
	↑ Firmicutes						MA, qPCR	IBS patients	Rajilic-Stojanovic, 2011
	Firmicutes	Clostridia	Clostridiales	Clostridiaceae	**↑ Clostridium**		MA, qPCR	IBS patients	Rajilic-Stojanovic, 2011
	Actinobacteria	Actinobacteria	Bificobacteriales	Bifidobacteriaceae	**↓ Bifidobacterium**		MA, qPCR	IBS patients	Rajilic-Stojanovic, 2011
↓ Bacterial diversity							FISH, FC	IBD patients	Sokol et al, 2006
↓ Bacterial diversity							CL, T-RFLP, qPCR	DSS induced colitis	Nagalingam et al, 2011
	↓ Bacteroidetes						CL, T-RFLP, qPCR	DSS induced colitis	Nagalingam et al, 2011
	↑ Firmicutes						CL, T-RFLP, qPCR	DSS induced colitis	Nagalingam et al, 2011
	Firmicutes	Clostridia	Clostridiales	**↑ Lachnospiraceae**			CL, T-RFLP, qPCR	DSS induced colitis	Nagalingam et al, 2011
↓ Bacterial diversity							qPCR, DGGE	DSS in WT, TLR2 -/-,	Heimesaat et al, 2007
	Firmicutes	Clostridia	**↑ Clostridiales**				qPCR, DGGE	TLR4 -/- &	Heimesaat et al, 2007
	Proteobacteria	γ-Proteobacteria	Enterobacteriales	**↑Enterobacteriaceae**			qPCR, DGGE	TLR 2/4 -/-	Heimesaat et al, 2007
	Firmicutes	Bacilli	Lactobacillales	Lactobacillaceae	**↓Lactobacillus**		qPCR, DGGE		Heimesaat et al, 2007
↓ Bacterial diversity							T-RFLP	IBD patients	Andoh et al, 2011
	Firmicutes	Clostridia	Clostridiales	Clostridiaceae	**↓Clostridium**		T-RFLP	IBD patients	Andoh et al, 2011
	Firmicutes	Clostridia	Clostridiales	Clostridiaceae	**↑Clostridium**		qPCR	UC patients	Verma et al, 2010
	Bacteroidetes	Bacteroidetes	Bacteroidales	Bacteroidaceae	**↓Bacteroides**		qPCR	UC patients	Verma et al, 2010
	Firmicutes	Bacilli	Lactobacillales	Lactobacillaceae	**↓Lactobacillus**		qPCR	UC patients	Verma et al, 2010
	Actinobacteria	Actinobacteria	Bificobacteriales	Bifidobacteriaceae	**↓Bifidobacterium**		qPCR	UC patients	Verma et al, 2010
↓ Bacterial diversity							DGGE	UC patients	Noor et al, 2010
	Bacteroidetes	Bacteroidetes	Bacteroidales	Bacteroidaceae	**↓Bacteroides**	***vulgatus***	DGGE	UC patients	Noor et al, 2010
	Bacteroidetes	Bacteroidetes	Bacteroidales	Bacteroidaceae	**↓Bacteroides**	***uniformis***	DGGE	UC patients	Noor et al, 2010
	Bacteroidetes	Bacteroidetes	Bacteroidales	Bacteroidaceae	**↓Bacteroides**	***ovatus***	DGGE	UC patients	Noor et al, 2010
Mucus and feces differences							FISH	UC patients	Takaishi et al, 2008
	Firmicutes	Bacilli	Lactobacillales	Lactobacillaceae	**↑ Lactobacillus**		Culture	UC patients	Takaishi et al, 2008
	Actinobacteria	Actinobacteria	Bificobacteriales	Bifidobacteriaceae	**↓Bifidobacterium**		Culture	UC patients	Takaishi et al, 2008
	Bacteroidetes	Bacteroidetes	Bacteroidales	Bacteroidaceae	**↓Bacteroides**	***vulgatus***	qPCR	UC patients	Takaishi et al, 2008
	Bacteroidetes	Bacteroidetes	Bacteroidales	Bacteroidaceae	**↓Bacteroides**	***ovatus***	qPCR	UC patients	Takaishi et al, 2008
	Bacteroidetes	Bacteroidetes	Bacteroidales	Bacteroidaceae	**↓Bacteroides**	***thetaiotaomicron***	qPCR	UC patients	Takaishi et al, 2008
	Bacteroidetes	Bacteroidetes	Bacteroidales	Bacteroidaceae	**↓Bacteroides**	***fragilis***	qPCR	UC patients	Takaishi et al, 2008
	Firmicutes	Clostridia	Clostridiales	Clostridiaceae	**↑ Clostridium**	***leptum***	qPCR	UC patients	Takaishi et al, 2008
	↑ Firmicutes						CL	UC patients	Gophna et al, 2006
	↓ Bacteroidetes						CL	UC patients	Gophna et al, 2006
	Firmicutes	**↑Clostridia**					CL	UC patients	Gophna et al, 2006
↓ Bacterial diversity							Culture		Fabia et al, 1993
↓ Anaerobic Gram (-) bacteria							Culture	UC patients, AA	Fabia et al, 1993
	Firmicutes	Bacilli	Lactobacillales	Lactobacillaceae	**↓Lactobacillus**		Culture		Fabia et al, 1993
↓ Bacterial diversity							SSCP & qPCR	UC patients	Ott et al, 2004
	↓ Bacteroidetes						SSCP & qPCR	UC patients	Ott et al, 2004
	Proteobacteria	γ-Proteobacteria	Enterobacteriales	**↓Enterobacteriaceae**			SSCP & qPCR	UC patients	Ott et al, 2004
	Firmicutes	Bacilli	Lactobacillales	Lactobacillaceae	**↓Lactobacillus**		SSCP & qPCR	UC patients	Ott et al, 2004
	↑ Increased compared to controls								
	↓ Decreased compared to controls								
	CL, clone library; FISH, flourescent in situ hybridization; FC, Flow cytrometry; T-RFLP, terminal restriction length fragment polymorphism; qPCR, quantitative PCR;								
	DGGE, denaturing gradient gel electrophoresis; SSCP, single strand conformation polymorphism; CD, Crohns disease; UC, ulcerative colitis;								
	IBD, inflammatory bowel disease; TLR, toll-like receptor AA, amino acid induced colitis; WT, wild type								

and *Shigella*, *Streptococcus*, *Salmonella*, and *Clostridium* species (46, 100). Additionally, a dysbiosis of the predominant bacterial phyla, Bacteriodes and Firmicutes, has been implicated in the etiology of IBD (101).

Using a variety of phylogenetic characterization techniques, multiple studies showed that the microbiota in patients with a GI disorder (ulcerative colitis and Crohn's disease) differed from the flora of healthy individuals (97-98, 102). One study used principal component analysis (PCA) to assess the differences in 155 bacterial species from patients with ulcerative colitis, Crohns disease, and healthy controls. They reported a clear separation between these groups when comparing the microbiota of fecal samples (102). However, varying results from patient to patient and across studies suggest that no one particular phyla is responsible for the onset of inflammation in the intestine. For example, some studies reported a marked decrease in 'good' or beneficial bacteria (i.e., bacteria that provide health benefits to the host), such as Lactobacilli and Bifidobacteria, compared to healthy controls. These species have also been reported to reduce intestinal inflammation in an animal colitis model, further suggesting their role in suppressing inflammation in patients with GI diseases (103). Yet another study reported an increase in *Clostridium* species has been reported in biopsies and luminal contents from patients with ulcerative colitis. In contrast, Frank *et al* reported a depletion of the 'normal flora', namely bacteria belonging to the Bacteriodes and Firmicutes (contains *Clostridium* spp.) phyla in patients with ulcerative colitis and Crohn's diesase (96). Additionally, conflicting results have been reported regarding the bacteria associated with inflamed mucosa. When comparing intestinal biopsies from patients with GI disorders, one study

cited differences in the bacterial species isolated from inflamed areas of tissue versus non-inflamed areas (97), while another study reported no significant differences between inflamed or non-inflamed mucosa (98). Differences in these studies could be due to disease progression of each patient, sampling technique, or method of phylogenetic classification. Therefore, a better understanding of what bacterial populations are present in a diseased state is important and should be characterized.

Alterations to intestinal microbiota by diet and bioactive compounds

The composition of the intestinal microbiota can be altered by changes in the host's diet, GI disease, antibiotics, and the presence of pathogens. A change in diet composition is very influential in altering the bacterial groups that reside in the GI tract (11-12). Dietary compounds such as tannins, polyphenols, and other antioxidants have been studied within the last few decades because of their numerous beneficial effects for the host (i.e., antimicrobial capabilities, elimination of free radicals, and anti-inflammatory effects) (15, 104-105). In addition, numerous studies have shown that these dietary compounds can have an effect on the survival of certain bacterial taxa, which allow certain bacterial groups to thrive while suppressing or eliminating others in the gut (9, 14-16, 104-105).

Tannins are the second most abundant group of plant polyphenols and are different from other polyphenols due to their ability to precipitate proteins from solution (106). In addition, tannins are bacteriostatic compounds that are able to inhibit the growth of certain microorganisms and resist microbial attack (16, 107-109). Tannins are found in a variety of fruits, vegetables and other plants and can be found in two different

forms, hydrolysable and condensed (9). Many studies have been performed to ascertain the effect of these tannins on the microbiota in different mammals, including humans (9, 16).

Some previous studies used stock bacterial strains, previously identified as constituents of the intestinal microbiota, and tested the *in vitro* effect of tannins using culture based methods (9, 14, 107). One study reported that some hydrolysable tannins (gallic acid and methyl gallate) derived from the Galla Rhios plant have inhibitory properties against some *Clostridium* species in culture (14). They reported that large doses of methyl gallate (10 mg) had an inhibitory effect on potentially harmful bacterial strains such as *C. perfringens, C. paraputrificum, E. limosum, B. fragilis, S. aureus*, and *E. coli*, but only had slight effect on some 'beneficial' lactic acid bacteria (LAB) strains (Bifidobacteria and Lactobacilli) (14). An additional *in vitro* study showed the effects of dietary tannins (gallic acid, tannic acid and its ester forms, propyl gallate and methyl gallate) on common human GI microbes that were previously isolated from the human intestine (9). Similar to Ahn et al. (14), they reported that gram positive bacterial species such as *B. fragilis*, *C. clostridiiforme*, *E. coli*, and *S. typhimurium* were inhibited by these tannins (excluding gallic acid) while LAB species were not (i.e., *B. infantis*, *L. acidophilus*) (9). Osawa *et al* reported that *Lactobacillus* species isolated from human fecal samples expressed the enzymatic capability to break down tannin ester bonds, suggesting that their presence in the flora could alter dietary tannins ability to effectively bind proteins (105).

Another study testing the effect of different tannins on the GI microbiota *in vivo* also reported similar gram positive bacteria inhibition (16). This study used denaturing gel electrophoresis (DGGE) to elucidate how tannins derived from the *Acacia angustissima* shrub affected the bacterial diversity of the GI tract in laboratory rats. Extracted condensed tannins were added to a basal rodent diet (0.7% and 2.0%, low and Hi Tannin diet respectively) for 3.5 weeks, with non-supplemented basal diet fed for 3 weeks prior and 3.5 weeks after tannin supplementation. They reported that there was a significant difference in the diversity of fecal samples in rodents fed a diet supplemented with tannins based off DGGE fingerprints (16). Predominant bands from the control and tannin supplemented animal DGGE gels were excised and sequenced to obtain phylogenetic information on these bacterial groups. Phylogenetic classification showed a significant decrease in the *C. leptum* sub-group in rats fed a tannin supplemented diet, while other enteric bacteria such as species classified in the *B. fragilis* and *Bacteroides-Prevotella-Porphyromonas* groups increased significantly (16).

Although the mechanisms that allow some bacterial species to be tannin-resistant are not completely known, some have suggested that tannins cause an iron deficiency thereby inhibiting the growth of bacterial species that require iron as a cofactor for metabolism (107, 110). However, some hydrolysable tannins, such as propyl and methyl gallate, do not bind iron; therefore, other mechanisms must be considered to fully understand the antimicrobial capacities of tannins (9).

Other dietary compounds such as tea polyphenols and other antioxidants have been reported to alter the composition of the intestinal microbiota (15, 104). One study

observed that Xanthohumol, an antimicrobial flavonoid found in hops, had a significant effect on the diversity of bacterial groups in rat feces using DGGE fingerprint analysis (104). Similar results were observed in a study that characterized how tea polyphenols affected GI microbial diversity in humans (15). Using culture based methods, it was observed that tea polyphenols had an effect on the bacterial diversity of human fecal samples. Those that were administered tea polyphenols had decreased proportion of *Clostridium* spp. and an increased proportion of *Bifidobacterium* spp. compared to those that did not consume these polyphenols (15).

In addition to dietary bioactive compounds, other dietary constituents (e.g., elevated dietary iron) can have a profound impact on oxidative stress in the lumen. Dietary iron can be found in heme (predominant Fe form in red meat) and non-heme forms (found in plants), with the latter having numerous chemical permutations (e.g., ferric citrate) that affect bioavailability and absorption. Studies have demonstrated that elevated levels of heme in the diet can have deleterious effects to the luminal environment and intestinal epithelium, including production of cytotoxic compounds and free radicals, barrier damage, hyperproliferation, downregulating repair mechanisms, as well as altering the microbiota and luminal concentration of SCFA (111-113). Although no studies directly assess the effect of non-heme high dietary iron on intestinal bacterial metabolism, it is known that butyrate producing bacteria strongly depend on Fe as a cofactor for butyrate production (110). One study did report that diets supplemented with ferric citrate (1.3 umol/g) can suppress SCFA concentrations in fecal water (111), however, they didn't phylogenetically classify the microbiota or perform metagenomics

to assess changes to metabolism. Other independent studies have reported that dietary iron depletion variably promote and inhibit the microbiota, including taxa that are known butyrate producers (114-115). It has been reported that cecum SCFA concentrations and the proportion of butyrate-producing bacteria can be increased when iron depleted animals are fed diets fortified with iron (115), however, there is little literature that describes the effect of non-heme high dietary iron on the microbiota or bacterial metabolism.

Epidemiological data and research based evidence suggests that a diet containing bran sources can alter the luminal environment and may be protective against the onset of colon cancer (23-24, 27-28, 116). Sorghum bran in particular, has been characterized as containing high levels of dietary bioactive compounds that could be beneficial to those with GI disorders by removing ROS from the lumen and providing beneficial changes to the microbiota and their metabolites (25-27). Black and brown sorghums are known to contain high concentrations of 3-deoxyanthocyanins and condensed tannins, respectively, and have been reported to have a significantly higher antioxidant capacity compared to wheat bran, whole grains, and fruits such as blueberries and pomegranate (27, 117). One study reported that animals fed a diet containing 6% fiber from sorghum bran had differential effects on luminal SCFA concentrations and were more protected against the promotion of colon cancer (24). Aberrant crypt foci, a preneoplastic lesion used as a biomarker for carcinogenesis in animals, were significantly lower in animals fed a black or brown sorghum compared to cellulose control animals. Additionally, it was demonstrated that these bran diets can affect the proliferation and apoptosis of

colonocytes, further suggesting that the differential actions of the sorghum bran may be beneficial in suppressing colon cancer (24).

Studies indicating that bran based diets and high dietary iron can alter luminal SCFA concentrations suggest alterations to the intestinal microbiota. In addition, it has been reported that bioactive compounds, particularly tannins, have the ability to enhance or suppress the growth of different constituents of the microbiota. Furthermore, tannins and other polyphenols with antioxidant characteristics can affect intestinal homeostasis and could be utilized in a diet to mitigate the effects of chronic inflammation or the progression of colon cancer. Additional studies are warranted to better understand the interactions and mechanisms that bioactive compounds found in sorghum bran have with the microbiota, and their combined effects on the health of the host.

Effect of radiation exposure on intestinal homeostasis

When radioactive particles come into contact with the human body, it can affect cells by either direct energy absorption or by the production of free radicals. Radiation has many deleterious effects on the biological systems including the formation of reactive oxygen species (ROS), and DNA damage, which includes base pair loss, single or double strand breakage, and chromosomal aberrations (118-119). The GI tract is one of the most radiosensitive organs and exposure affects numerous cellular mechanisms including membrane stability, differentiation, and apoptosis (118, 120). Additionally, preliminary studies suggest radiation exposure can alter the microbiota (114). Countermeasures such as antioxidant supplementation and probiotics might be effective at counteracting some of the negative effects of radiation on the gastrointestinal tract, as

it has been reported they have the ability to reduce intestinal inflammation and mitigate symptoms of IBD (108, 121-124).

When radiation comes into contact with cells, the "biological key substances", or protein, DNA, and RNA, are affected either directly or indirectly and the degree of damage directly correlates to the number of transformed molecules (21). In radiobiology, understanding linear energy transfer (LET), or the amount of energy that is transferred to a substance as the radiation passes through, is important in understanding the effect of radiation on biological systems (118). Low LET radiation such as gamma and x-rays is more likely to have indirect effects on cells by the formation of free radicals such as H•, •OH, H_2O_2, and e^-_{aq}, while high LET radiation will directly damage cell membranes, organelles and DNA (118, 125). High LET DNA damage is more complex and difficult to repair compared to low LET injuries induced by free radicals.

ROS interactions with DNA can cause a myriad of structural lesions such as the base loss, base modification, single or double strand break and the formation of dimers and DNA-protein cross-links (21, 118, 125). Direct effects of radiation produce similar chromosomal injuries and can influence cell survival. Throughout the cell cycle, check points monitor the viability of the DNA and can either repair or shuttle cells into an apoptotic, or programmed cell death, pathway. Two main repair mechanisms include base pair excision (BPE) and non-homologous end joining (NHEJ) (119). Once a cell becomes irradiated (directly or indirectly), the outcome can be mutations, division delay, apoptosis, reproductive failure or cellular arrest, and transformation to a possibly carcinogenic cell (21, 119).

The mucosal surface of the small and large intestine has shown increased propensity for radiation induced mucosal injury, and complications are magnified in the small and large intestines due to the high proliferative capacity of the mucosal cells (22). As mentioned previously, irradiation can cause mitosis to halt in epithelial cells. If proliferation is halted at the base of the intestinal crypt, the continued migration and sloughing of cells from the villi causes the intestinal wall to become denuded and can allow for entry of bacteria and toxins from the lumen (126). Additionally, it has been shown that radiation exposure can activate apoptosis in the small and large intestine through a variety of pathways. It has been reported that the incidence of apoptosis in the small intestine directly correlates to increasing doses of radiation and this induction plateaus around 1 Gy (127). However, the type and position of the cells undergoing apoptosis differ in the small and large bowel crypts (128). The reason the small and large intestine differ so greatly in regards to radiation induced apoptosis is still unknown, however, it has been suggested that diet, presence of food, transit time, and the bacterial populations populating the lumen could play a role.

Radiation induced injury to the intestinal tract has numerous deleterious effects, including direct mucosal toxicity, delayed gastric emptying and secretion, release of prostaglandins, morphological effects such as villous shortening, and alterations to the diversity of the intestinal microbiota (21-22, 120, 129-130). Radiation exposure has also been implicated in stimulating the secretion of intestinal fluid and transcellular electrolytes, which results in diarrhea. This elevated secretion could be due to the epithelial cell loss described above, however, it has been reported that epithelial

dysregulation can occur prior to the epithelial cell loss. For example, two animal studies reported that responsiveness to secretagogues, or a substance causing another substance to be secreted, is reduced in animals with acute radiation enteritis (120, 126). Although the mechanisms causing this hyporesponsiveness to secretagogues are unclear, it has been proposed that irradiation has an effect on intestinal mast cell populations, which control the responsiveness to secretagogues via enteric nerve stimulation (131). Additionally, it has been reported that the inducible form of nitric oxide (NO) synthase (iNOS) expression, is increased post-radiation (132). Due to the increased permeability and decreased responsiveness to secretagogues, it has been suggested that a luminal factor, such as the commensal bacteria, might be involved in the etiology of radiation induced intestinal dysregulation (120).

Effect of radiation on intestinal microbiota

As mentioned previously, the intestinal bacterial populations, or microbiota, play a significant role in gastrointestinal health of both humans and animals and disruption of the homeostatic balance between the host and commensal bacteria has been implicated in the etiology of gastrointestinal disorders in humans and many animals (18, 35-36, 43, 45). Although little is known in regards to the effects of the microbiota in an irradiated state, early studies in the 1950's and 1960's reported that germ-free animals had more protection against radiation at differing doses compared to animals with a conventional microbiota. McLaughlin *et al.* reported that with differing doses of radiation (4.82-8.33 Gy), germ-free mice always had a greater survival rate compared to conventional and *E.coli* mono-contaminated (germ-free mice inoculated with bacteria) animals. It was

suggested that the presence of bacteria in the bowel has an effect on proliferation of intestinal mucosal cells, and these underlying mechanisms might play a role in the protective effect shown (131). These reports have been confirmed in a more recent study as well, which reported that germ-free animals exposed to 10-22 Gy showed no signs of radiation enteritis induced injury to their small intestine compared to conventional (containing a normal microbiota) or conventionalized (germ-free mice inoculated with bacteria) mice which showed the classical injury response (133). Additionally, much higher doses of radiation were administered to these animals (~16 Gy) and the same effect was observed where germ-free animals had a significantly higher survival rate compared to animals with a functional microbiota. Both of these studies showed that there is an interaction with radiation and the microbiota and further studies are warranted to investigate these mechanisms.

Described previously, commensal bacteria have been shown to influence the response to intestinal injury through the transcription factor, NF-κB, which is activated downstream of many TLR pathways (74). It has been reported that disruption of this pathway by knocking out IκB kinase, allowing IκB to permanently sequester NF-κB in the cytoplasm, causes increased epithelial cell apoptosis in mice exposed to radiation (134). This increase in apoptosis corresponded with increased expression and activation of p53, similar to reports from Hendry *et al* (127). Another study used a knockout mouse model for the p50 subunit of NF-κB, and reported that animals without NF-κB signaling were more susceptible to radiation lethality than wild type animals (135). Additionally, production of prostaglandins via TLR activation has been shown to protect intestinal

crypts against radiation exposure (136). These studies show a direct link of the intestinal microbiota, NF-κB activation, production of prostaglandins, and the regulation of radiation induced apoptosis.

To our knowledge, little information is published that characterizes changes in the bacterial groups or TLR expression in the intestine after radiation exposure. It has been reported that long term effects of radiation enteropathy are associated with an overgrowth of gram-negative bacilli and bowel dysmotility, however, no molecular analysis was performed to identify a particular bacterial taxa involved with the etiology of radiation induced intestinal dysfunction (137). One small pilot study used denaturing gradient gel electrophoresis (DGGE) to identify changes in the bacterial diversity of fecal samples from patients suffering from acute post-radiotherapy diarrhea, and those with no gastrointestinal distress after radiation treatment (total exposure of 4,300-5,400 cGy) (114). They observed that the microbial profiles of the individuals in each group (i.e., control, no diarrhea and diarrhea group), clustered in similar sets, suggesting that specific bacterial taxa could be associated with risk or protection after radiation exposure. Subjects with clinical signs (i.e., diarrhea) showed a marked modification of their microbial profile compared to those that did not have gastrointestinal complications. Additionally, it was reported that the proportion of *Bacilli* species and bacteria characterized in the Actinobacteria phylum were markedly higher in individuals with diarrhea compared to those without diarrhea following radiation treatment (114). Based on the findings, it suggests that the bacterial groups that compose the intestinal microbiota could be a determinant if an individual is susceptible to post-irradiation

diarrhea. Additionally, these results suggest that radiation might play a role in the proportion of different bacterial groups present in the intestine. Unfortunately little phylogenetic classification was performed in this pilot study which could provide more insight into which specific bacterial taxa might be involved in the etiology of intestinal dysfunction caused by radiation, or which bacterial groups might be altered by exposure to radiation.

The majority of the experiments described above are predominately large, acute radiation doses comparable to exposures seen in warfare or accidental exposures. Unfortunately, little is known regarding how GI homeostasis can be affected by low and/or fractionated radiation doses from medical diagnostic tests, occupational radiation exposure, and those encountered by airline and spaceflight crews. NASA is concerned with the health risks to astronauts, particularly those associated with radiation exposure, and alterations to the luminal environment and intestinal epithelium following large radiation doses is an indicator that GI dysfunction may be a risk during and after space flight. To our knowledge there are no studies analyzing the effect of fractionated, low doses of radiation on the microbiota, SCFA production, and TLR signaling. Results from these studies will further elucidate mechanisms responsible for the observed perturbations to normal GI function, and will also allow doctors and researchers to create more specific countermeasures for gastrointestinal dysfunction for these types of radiation exposures.

Hypothesis and Specific Aims

Our overall goal is to better understand how intestinal inflammation and injury is initiated by environmental insults such as chemical exposure, radiation, and a high oxidant load diet. Our overarching hypothesis is that each insult will have an effect on inflammation and injury by changing the colonic bacterial populations and by affecting signaling between the bacterial populations and colonocytes. Our secondary hypothesis is that through an appropriate dietary intervention, we can mitigate the inflammation and injury caused by these environmental insults. The experiments designed to test these hypotheses will utilize two experimental paradigms; one using a chemical inducer of inflammation/injury (DSS) and the other using various forms of radiation, weightlessness and diets commonly consumed in the space environment.

Aim 1: Determine if the perturbations in the intestinal environment leading to intestinal inflammation and injury caused by DSS exposure can be mitigated by diets containing bioactive compound-enriched sorghum brans.

Hypothesis 1: DSS induced colonic inflammation will affect the colon luminal environment by altering bacterial populations, their metabolites, and TLR signaling in colonocytes.

Hypothesis 2: Sorghum brans containing 3-deoxyanythocyanins, condensed tannins, or a combination of both compounds, will mitigate the effects of repeated inflammation in the bowel by restoring commensal bacterial populations, suppressing TLR-induced elevations in pro-inflammatory mediator expression, and upregulating epithelial repair mechanisms.

Aim 2: Determine how environmental insults associated with space flight (i.e., radiation exposure, microgravity, high oxidant load diet) affect intestinal inflammation and injury.

Hypothesis 1: Exposure to radiation, microgravity, and high oxidant load diets will initiate an inflammatory state in the GI tract by altering the microbiota, its metabolites, and TLR signaling in colonocytes.

CHAPTER II

NOVEL SORGHUM BRANS ATTENUATE THE SEVERITY OF DSS-INDUCED COLITIS AND UPREGULATE EPITHELIAL BARRIER PROLIFERATION AND REPAIR PROTEIN EXPRESSION

Introduction

Chronic inflammation has been shown to increase the risk of numerous forms of cancer, and epidemiological studies suggest that those suffering from gastrointestinal (GI) diseases such as ulcerative colitis (UC) have between a 2-18% increased risk (dependent upon age) of developing colon cancer (138). Ulcerative colitis consists of varying degrees of mucosal inflammation that extends proximally from the rectum, and these regions of inflammation are commonly associated with ulcerations and mucin depletion (5). The complete etiology of UC is still not fully understood, but recent research has indicated that a disruption in the host immune response to the commensal bacterial populations in the intestine, or microbiota, could be a major factor in the progression of this disease (5, 8, 78).

It is well documented that the intestinal microbiota plays a role in the health of the host by affecting the luminal environment and interacting with the host epithelial cells. This includes the fermentation of dietary fiber, altering intestinal motility and pH, and can provide protection against invading pathogens and increase efficacy of tight junctions (35-36, 72). Fermentation of dietary fiber produces metabolites including lactate and short chain fatty acids (SCFA) such as butyrate, which is the preferred fuel

source for colonocytes (38, 139). SCFA also have been shown to affect the induction of gene expression, cellular differentiation, and have anti-inflammatory activity (20, 139-140). In addition, the microbiota affects the innate immunity of the host by signaling through pathogen-associated molecular patterns such as toll-like receptors (TLR), which signal through the NFκB pathway (72-73, 87). This signaling pathway can affect the transcription of pro-inflammatory cytokines, and epithelial cell proliferation and apoptosis. Furthermore, dysregulation of the TLR pathway has been associated with the progression of intestinal inflammation and the pathogenesis of UC (72-74, 84-85).

The composition of the microbiota can be altered by numerous environmental factors including antibiotic use and stress. Additionally, it has been demonstrated that changing certain dietary constituents can have a dramatic affect on the proportions of certain bacterial taxa in the intestine (11-12, 116, 141). In recent years secondary plant metabolites, such as polyphenols, have been reported to alter the intestinal microbiota (14, 16, 107, 142-145). Recent *in vivo* studies have reported the ability of polyphenols such as hydrocaffeic acid, tea polyphenols, and tannic acid to have differential effects on bacterial populations by enhancing certain taxa and eliminating others in the intestine (9, 15, 143). Additionally, numerous polyphenols are known antioxidants and may prove to have beneficial effects during inflammatory bouts associated with UC (9, 15, 107, 143, 145).

Sorghum is a grain predominately grown in dry, arid areas and is a common staple in some African and South American countries. Certain black and brown sorghum varieties contain large quantities of 2-deoxyanthocyanins and condensed tannins, which

are known antioxidants (25-26, 117). The antioxidant capacity in decorticated bran is even higher than other bran sources (i.e., wheat, oat) and fruits such as pomegranates and blueberries (27). Additionally, limited research demonstrates that diets containing sorghum bran have the potential to protect against the progression of colon cancer and can affect the intestinal microbiota and its metabolites (24). Other sources of dietary polyphenols have been reported to mitigate some of the deleterious effects of colitis, including modulating alterations to the intestinal microbiota (108-109, 121, 146). Based on this information, we hypothesize that DSS induced colonic inflammation will affect the colon luminal environment by altering bacterial metabolites and TLR signaling in colonocytes. Furthermore, we hypothesize that feeding sorghum brans will mitigate the effects of repeated inflammation in the bowel by suppressing TLR-induced elevations in pro-inflammatory mediator expression and upregulating epithelial repair mechanisms. Therefore, in order to elucidate the effects of sorghum grain on the deleterious effects of UC, we aim to characterize the effects of consumption of sorghum bran diets containing 3-deoxyanthocyanins, condensed tannins, or both polyphenols on the production of secondary microbial metabolites, TLR signaling and epithelial cell proliferation, apoptosis, and repair during repeated dextran sodium sulfate (DSS) exposures.

Materials and Methods

Animals and diets

Eighty male Sprague-Dawley rats (21 d old) were stratified by body weight and assigned to one of four experimental diets (n=20/ diet). The four diets contained 6% dietary fiber from 1) cellulose, or bran isolated from sorghum grains that contain: 2) high

levels of 3-deoxyanthocyanins (Black bran), 3) high levels of condensed tannins and low levels of 3-deoxyanthocyanins (Sumac bran), or 4) both 3-deoxyanthocyanins and condensed tannins (Hi Tannin bran). Antioxidant capacity, total polyphenol content, tannin content, and proportions of soluble and insoluble fiber were quantified for each experimental diet (Table 2). Prior to beginning the experimental diet (at 40 d of age), animals were maintained on a standard pelleted rodent diet.

Table 2. Antioxidant capacity, phenol levels, and fiber content for all experimental diets. Composite analysis was performed on a sample taken when each experimental diet was mixed. Over time analysis was performed on a sample containing fractions of each experimental diet collected throughout the course of the study.

	Sample	ABTS[†]	Total Phenols[‡]	Tannins[‡]	% Total Fiber	% Soluble	% Insol.
Over time	Cellulose	ND	ND	ND			
	Sumac bran	172.30	11.92	14.01			
	Hi Tannin bran	123.50	8.37	13.18			
	Tx430 Black bran	62.09	4.35	0.01			
Composite	Cellulose	ND	ND	ND	6.68	0.41	6.27
	Sumac bran	182.41	11.56	14.02	5.98	0.71	5.27
	Hi Tannin bran	136.31	8.75	13.49	6.4	0.41	5.99
	Tx430 Black bran	64.16	5.43	0.15	6.98	0.66	6.32
	ND= not determined						
	[†]Antioxidant capacity using ABTS method						
	[‡]Absorbance measured at 600 nm for Total Phenols and 500 nm for Tannins						

After 21 d of experimental diets, half of the rats were exposed to three sequential 48 h dextran sodium sulfate (DSS) (MP Biomedicals, Irvine, CA) treatments (3% DSS) in their drinking water, with 14 d between each DSS exposure (Figure 1). Between DSS

exposures, distilled water was supplied to treated animals to mimic remissions experienced by human chronic UC patients (147). The remaining half of the animals received distilled water throughout the course of the study.

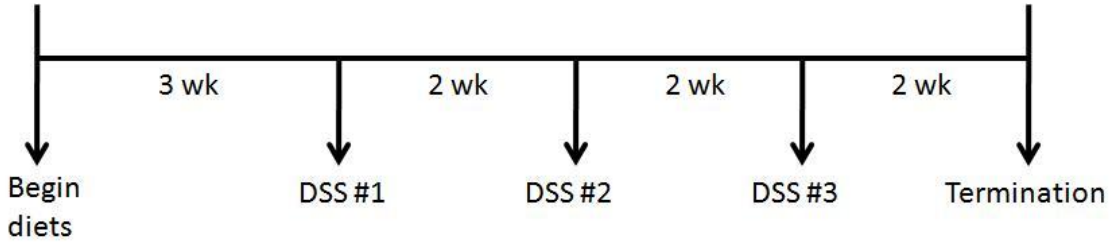

Figure 1. Timeline of DSS treatments for DSS rats in each experimental group. After 21 d of experimental diets, DSS exposures began (3% DSS for 48 h, 14 d separation, 3 treatments total).

Body weight and food intake were routinely monitored. Rats were weighed upon arrival (d 1), prior to beginning experimental diets (d 19), 48 hr before each DSS exposure, and prior to termination (d 82). Additionally, food intake was measured prior to the first DSS treatment (d 35), following the second DSS treatment (d 56), and prior to termination (d 77, following third DSS treatment). On day 82, animals were euthanized by CO_2 asphyxiation. The colon was resected, and two 1 cm sections were removed for histological preparations and the remainder was scraped.

Fecal collections and processing

Fresh fecal samples were collected for fermentation metabolite analysis prior to DSS exposure, and 48 h after each DSS exposure.

Fecal samples were thawed and placed into a weighed pan prior to drying in a 60°C oven for 72 h. Samples were cooled in a vacuum dessicator before being weighed and the procedure was repeated until weight became static.

Short chain fatty acid analysis

Fresh fecal samples were collected immediately following defecation. Samples were transferred to sterile cryotubes, snap-frozen in liquid nitrogen, and stored at -80°C. Frozen samples were processed and SCFA extracted and quantified by a Varian 3900 gas chromatograph (Walnut Creek, CA) as described previously (28). Standards and blanks were run to facilitate calibration and to calculate SCFA (acetic acid, propionic acid, isobutyric acid, butyric acid, isovaleric acid, valeric acid) concentrations. The concentrations were multiplied by the 24 hr feces weight to calculate daily SCFA excretion (See Appendix B for calculations).

Tissue fixation for immunohistological processing

After fecal material was removed from the colon the two, 1 cm segments removed from the distal end of the colon, rinsed with RNase free Phosphate-Buffered Saline (PBS), and fixed in either a 4% PFA or 70% EtOH solution prior to embedding in paraffin.

Mucosal samples

The remaining colon was washed twice in RNase free PBS, scraped on a chilled RNase free surface, and 2/3 of the material was transferred to an RNase free homogenization tube along with 500 µl of Denaturation Solution (Ambion, Austin, TX) and the remaining 1/3 transferred to a homogenization tube with 400 µl of protein

buffer. Scraped mucosa for RNA analysis was homogenized in Denaturation Solution for 6-7 strokes and then transferred to a 2 ml epitube for storage at -80°C (148). Scraped mucosa for protein analysis was homogenized, centrifuged (15,000 g x 30 min at 40°C), and the supernatant was stored at -80°C (149).

Inflammation and injury histological scores

The degree of inflammation and morphological injury caused by DSS exposure was assessed in H&E stained tissue slides. Histologic examination was performed in a blinded manner by a board-certified pathologist, and the degrees of inflammation (score of 0–3) and epithelial injury (score of 0–3) on microscopic cross sections of the colon were graded as described previously (150).

Activated NF-κB measurement

Activated NF-**κ**B was assessed from scraped mucosa samples using the manufacturer's protocol for whole cell lysates with the TransAM™ NF-**κ**B Chemi Lysis buffer (Active Motif, Carlsbad, CA). Activated NF-κB (p50/p65 subunits) extracted from each sample was added to an oligonucleotide coated plate, bound to a primary antibody, and identified with a secondary antibody. Only activated NF-**κ**B subunits can bind to the oligonucleotide coated plate and are accessible to primary antibodies for detection. A nuclear extract of Jurkat cells was used as a positive control for the p65 NF-**κ**B subunit. An aliquot of protein buffer and lysis buffer was run as a negative control.

Immunohistological measurement of proliferation and apoptosis

Cell proliferation was measured using a monoclonal antibody to proliferating cell nuclear antigen (PCNA; Anti-PC-10, Covance, Emeryville, CA) as described by

Vanamala et al. (151). The total number of proliferating cells, position of the highest proliferating cell and total cell number/crypt column (crypt column height) was assessed in 25 crypt columns/rat.

Paraffin sections of the 4% PFA fixed tissues were used to measure apoptosis with the TUNEL assay (151). Total numbers of apoptotic cells were determined in 50 crypt columns/rat, and an apoptotic index (apoptotic cells/crypt column height) was determined for each crypt.

Measurement of gene expression using real-time PCR

Total RNA was isolated from mucosal samples using Phase Lock Gel™ tubes (5 Prime, Gaithersburg, MD) and the ToTALLY RNA™ Kit (Ambion, Austin, TX) followed by DNase treatment (DNA-*free*™ Kit, Ambion, Austin, TX). RNA quality was assessed using an Agilent Bioanalyzer and mRNA concentrations were measured using spectrophotometry prior to storage at -80°C. First strand cDNA was synthesized using random hexamers, oligo dT primer (Promega, Madison, WI), and Superscript™ III Reverse Transcriptase following manufacturer's instructions (Invitrogen, Carlsbad, CA).

Real-time PCR was performed using an ABI 7900 HT thermocycler (Applied Biosystems, Foster City, CA) on select genes (TOLLIP, TFF3, ZO-1, Slc16a1, IL-6, IL-1β, IL-12b, TNFα, SLC5A8, TGFβ, TLR4, TLR2, MyD88, Rela/p65, COX-2). Selected primers were pre-loaded to Taqman® Array Micro Fluidic Cards (Applied Biosystems, Foster City, CA) and used for subsequent qPCR analysis (Assay IDs for all primers compiled in Appendix B). Expression levels were normalized to 18S gene expression.

Statistical analysis

Data were analyzed using two-way analysis of variance (ANOVA) including variables of diet and DSS exposure in SAS 9.1 (SAS Institute, Inc.) considering a p-value of <0.05 as significant. Sample size in each experimental group for all analyses is N=10, except for relative expression of selected gene targets (i.e., TOLLIP, TFF3, Slc16a1, IL-6, IL-12b, SLC5A8, Rela/p65) and 24 SCFA production on d 72. Relative expression of the aforementioned targets were greater than 2.5 SD from the mean for one animal in the Sumac DSS group and therefore excluded from further analysis. Sample size for 24 SCFA production on d 72 was N=9 for all experimental groups since 24 hr dry weight measurements were not taken at this time point. All data are reported as least squares (LS) means ± standard error of the mean (SEM), using a significance of $p<0.05$.

Results

Body weight, intake and fecal moisture content

There were no significant differences in initial body weights (d 1), d 19 (start of experimental diet treatment), d 67, d 77, or at termination (d 82) (Appendix A-1). Hi Tannin control rats had higher body weights than Cellulose control rats on d 37 ($p=0.0321$), d 39 ($p=0.0273$), d 53 ($p = 0.0248$), and d 58 ($p=0.0415$) (Figure 2); however, there were no significant differences for any other experimental groups during these time points. On d 37 (prior to DSS#1), we observed a slightly lower food intake in Cellulose DSS rats compared to Sumac DSS rats ($p<0.05$), however, there were no significant differences in intake for any experimental groups on d 58 (post DSS#2), or d 79 (post DSS #3) (Table 3).

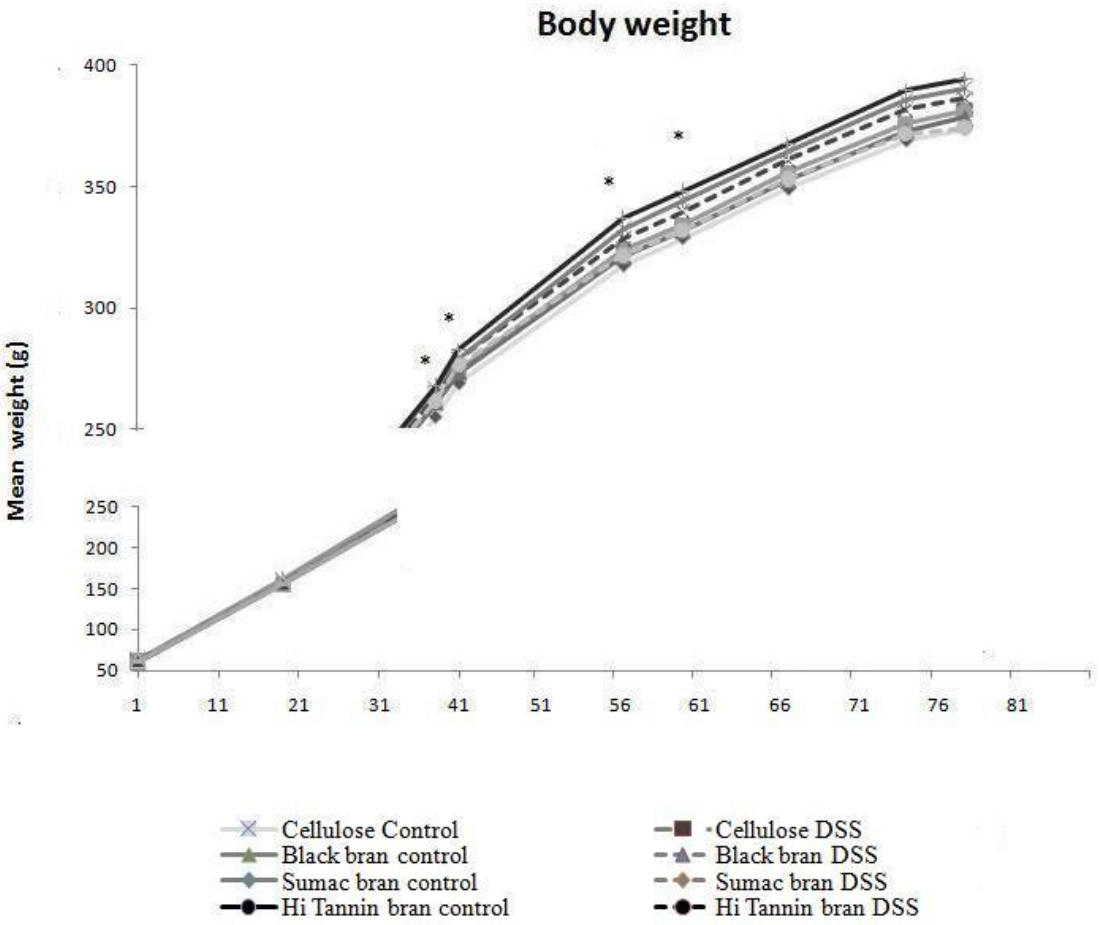

Figure 2. Mean body weight (g) on d 37, 39, 53, and 58. Values are LS means and collection dates with (*) indicate significant differences ($p<0.05$) between Hi Tannin control rats compared to Cellulose control rats. See Appendix A-1 for actual values.

Table 3. Intake (g) measured prior to DSS#1 (d 35), following DSS#2 (d 56), and following DSS#3 (d 77).

		Cellulose		Black bran		Sumac bran		Hi Tannin bran				
		Control	**DSS**	**Control**	**DSS**	**Control**	**DSS**	**Control**	**DSS**	**Diet**	**DSS**	**Diet* DSS**
Total diet consumed g/24 hrs	**Intake 1 Pre DSS #1**	19.0±0.7^{ab}	18.1±0.7^{a}	19.6±0.7^{ab}	19.1±0.7^{ab}	19.6±0.7^{ab}	20.0±0.7^{b}	19.5±0.7^{ab}	18.9±0.7^{ab}			
	Intake 2 Post DSS#2	19.6±0.6^{a}	19.1±0.6^{a}	19.5±0.6^{a}	19.9±0.6^{a}	20.2±0.6^{a}	19.5±0.6^{a}	19.3±0.6^{a}	19.2±0.6^{a}			
	Intake 3 Post DSS#3	21.5±0.7^{a}	21.3±0.7^{a}	20.5±0.7^{a}	20.4±0.7^{a}	21±0.7^{a}	19.9±0.7^{a}	21.2±0.7^{a}	20.0±0.7^{a}			
		Values are LS mean ± SEM.										
		Means without common superscripts differ (p<0.05).										

Fecal moisture content in bran fed rats (i.e., Black, Sumac and Hi Tannin) was significantly higher than Cellulose fed rats on d 38 (prior to DSS treatments) and all other collections (d 44, 58, 81). These values remained relatively constant throughout the study and didn't markedly increase following DSS treatments for any experimental diet group (≤6 %; Table 4). However, on d 44 (post DSS #1) and d 58 (post DSS#2) Sumac DSS rats had a slightly higher fecal moisture content compared to Sumac control rats. We do not observe any other significant differences in fecal moisture content in DSS rats compared to their diet matched control for Cellulose, Black or Hi Tannin bran for this time point or on d 58 (post DSS#2) or d 81 (post DSS#3).

Table 4. Fecal moisture was significantly higher in bran fed rats throughout the study. DSS exposure increased fecal moisture in Sumac DSS rats on d 44 and d 58, but did not increase in any other groups.

		% fecal moisture			
		d 38	d 44	d 58	d 81
Cellulose	**Control**	39.81±0.89^{a}	38.68±0.83^{a}	40.41±0.89^{a}	43.25±1.11^{a}
	DSS	38.87±1.00^{a}	39.98±0.75^{a}	41.53±0.42^{a}	40.89±0.47^{a}
Black bran	**Control**	47.60±0.49^{b}	47.74±0.20^{b}	47.91±0.21^{b}	48.05±0.51^{b}
	DSS	46.47±0.75^{b}	47.74±0.20^{b}	48.28±0.62^{b}	49.57±0.41^{bc}
Sumac bran	**Control**	52.25±0.57^{c}	50.28±0.55^{c}	51.41±1.03^{c}	53.23±0.54^{d}
	DSS	53.05±0.43^{c}	54.98±1.43^{d}	53.79±0.76^{d}	55.61±0.89^{d}
Hi Tannin bran	**Control**	48.40±0.30^{b}	49.43±0.92^{bc}	49.63±0.56^{bc}	50.06±0.39^{c}
	DSS	47.89±0.34^{b}	48.90±0.65^{bc}	50.34±0.77^{c}	49.97±0.51^{c}
Diet		<0.0001	<0.0001	<0.0001	<0.0001
DSS			0.0163	0.0241	
Diet*DSS			0.0062		0.003
		Values are LS mean ± SEM.			
		Means without common superscripts differ (p<0.05).			

Immunohistochemical analysis of distal colon

There was only one significant difference in inflammation scores, with Cellulose DSS rats having a significantly lower score compared to all other diet and treatment groups (Figure 3A) ($p<0.05$). Cellulose controls had lower injury scores than Black and Sumac bran controls ($p<0.05$, Figure 3B). DSS treatment elevated injury scores in all experimental diets, with significantly higher scores observed in Hi Tannin DSS rats compared to Hi Tannin control rats ($p=0.0072$). DSS treated rats fed bran diets had significantly higher injury scores compared to Cellulose DSS rats ($p<0.05$).

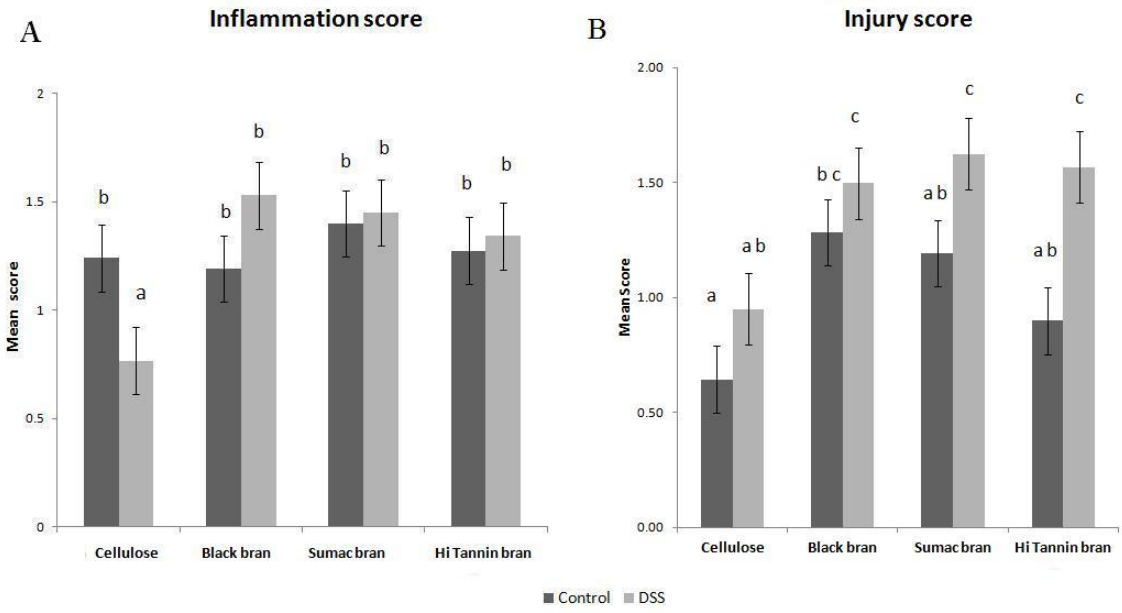

Figure 3. A) Inflammation score was significantly lower in Cellulose DSS rats compared to all other groups ($p<0.05$). B) DSS exposure elevated injury scores in all experimental groups, with Hi Tannin DSS having a significantly higher score compared to their diet matched controls. Values are LS mean ± SEM. Means without common superscripts differ ($p<0.05$).

DSS-treated rats for all diets had shorter crypts compared to control rats ($p<0.05$, Table 5). Black bran control rats had the lowest proliferative index, which was significantly lower than Black, Sumac and Hi Tannin bran DSS rats ($p<0.05$, Table 5). In addition, Black bran control had a significantly lower proliferative zone compared to Cellulose control, and Sumac and Hi Tannin bran DSS rats ($p<0.05$). In bran fed rats, DSS treatment elevated proliferative index and zone; however, we observe the tendency for a lower proliferative index and zone for Cellulose DSS rats compared to their diet-

matched control. Aside from Black bran DSS having a significantly higher proliferative index than Black bran controls (p=0.0049), there were no significant differences between control and DSS rats in the other experimental diet groups for either proliferative zone or proliferative index. There were no significant differences in apoptotic index between control and DSS rats for all experimental diets, however, Sumac control rats had a significantly higher index than Hi Tannin DSS rats (p=0.0208, Table 5).

Fecal short chain fatty acid (SCFA) analysis

We used fecal SCFA excretion as an indicator of SCFA production. Prior to DSS treatments (d 38), we observed a significant diet effect on 24 hr SCFA production (umol/24 hr) for all SCFA analyzed (i.e., acetic, propionic, isobutyric, butyric, isovaleric, valeric) (Table 6). The proportion of excreted butyrate compared to total SCFA produced was lowest in Sumac fed rats (10-11%) compared to Cellulose, Black and Hi Tannin bran diets (18-21%, 23-24%, 15-17%, respectively). We observed a significant diet effect for all other collections (d 44, 66, 72, 81) for propionic, isobutyric, butyric, isovaleric, valeric (except for propionic on d 81, p=0.055) (Appendix A-2, A-3, A-4, and Table 7, respectively).

Following recovery from DSS#2 and DSS#3, we did not observe a significant effect of DSS treatment on 24 hr SCFA production except a significant interaction between diet and DSS exposure on d 44 (post DSS#2) for isobutyric and on d 66 (post DSS#3) for acetic (umol/24 hr) (Appendix A-2 and A-3).

Fecal samples following recovery from all DSS treatments (d 81) represents the luminal environment closest to termination. On d 81 we observed the same significant diet effects on 24 hr SCFA production as observed on d 38 (prior to DSS treatments) for all SCFA except for acetic and propionic acid (umol/24 hr; $p<0.05$) (Table 7). Diet significantly affected 24 hr butyrate production following all DSS treatments (d 81) with Cellulose and Black bran rats having numerically higher concentrations (16.4 and 20.1 µmol/24 hr, respectively) compared to Sumac and Hi Tannin bran (8.8 and 14.1 µmol/24 hr, respectively). In DSS rats (d 81), the proportion of excreted butyrate compared to total short chains produced was lower in Sumac bran rats (9%) compared to Cellulose, Black or Hi Tannin rats (19, 23, 15%, respectively) on a wet weight basis (umol/g), which is similar to values observed prior to DSS exposure (Figure 4).

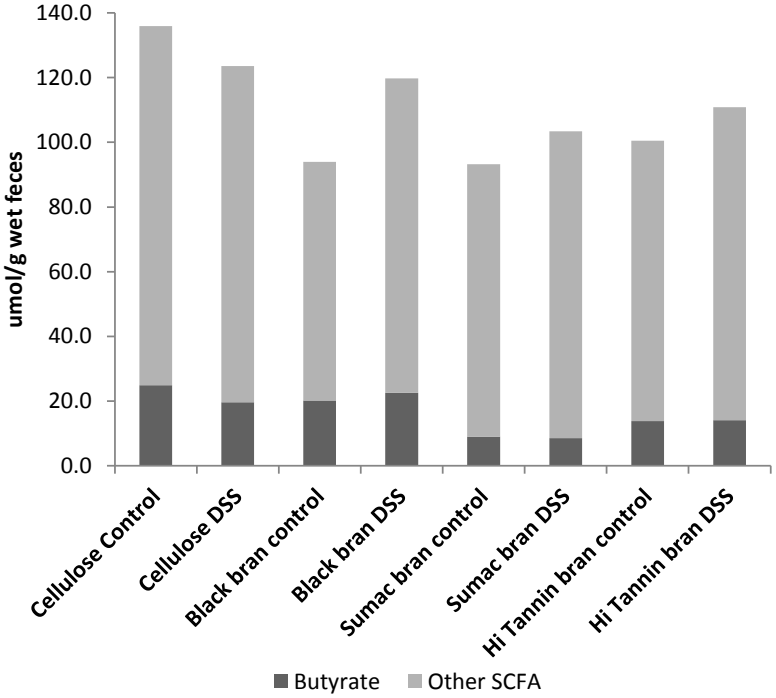

Figure 4. Prior to termination (d 81), the concentration of butyrate compared to total SCFA was lower in Sumac bran fed animals compared to other experimental groups (umol/ g wet wt). Values are LS mean.

Table 5. DSS treatment significantly affected proliferative index, with bran fed DSS rats having a higher and Cellulose DSS rats having a lower proliferative zone compared to their diet matched controls. DSS treatment significantly affected crypt height, with DSS rats in all experimental groups having lower crypt height compared to their diet matched controls ($p<0.05$). Values are LS mean ± SEM. Means without common superscripts differ ($p<0.05$).

	Cellulose		Black bran		Sumac bran		Hi Tannin bran				
	Control	**DSS**	**Control**	**DSS**	**Control**	**DSS**	**Control**	**DSS**	**Diet**	**DSS**	**Diet* DSS**
Proliferative index	9.59±2.88^{ab}	9.35±3.44^{ab}	8.15±3.20^{a}	11.18±3.00^{b}	9.83±3.15^{ab}	10.75±3.79^{b}	9.17±3.02^{ab}	10.89±3.35^{b}		0.0112	
Proliferative zone	36.96±6.54^{b}	34.45±6.50^{ab}	31.49±5.39^{a}	35.18±5.08^{ab}	36.29±7.26^{ab}	37.52±5.57^{b}	34.91±5.95^{ab}	37.72±7.04^{b}			
Apoptotic index	0.18±0.01^{ab}	0.18±0.01^{ab}	0.15±0.01^{ab}	0.18±0.01^{ab}	0.29±0.01^{b}	0.22±0.01^{ab}	0.23±0.01^{ab}	0.09±0.01^{a}			
Crypt height	30.00±0.74^{b}	27.73±0.76^{a}	30.74±0.77^{b}	26.62±0.88^{a}	32.02±0.72^{b}	27.08±1.01^{a}	31.23±0.68^{b}	26.29±0.98^{a}		<.0001	

Table 6. SCFA production on d 38 (umol/24 hr). Diet significantly affected 24 hr SCFA production for acetic, propionic, isobutyric, butyric, isovaleric, and valeric.

		Cellulose		Black bran		Sumac bran		Hi Tannin bran				
		Control	**DSS**	**Control**	**DSS**	**Control**	**DSS**	**Control**	**DSS**	**Diet**	**DSS**	**Diet* DSS**
Total SCFA prod (umol)/ 24 hr	**Acetic**	43.01±6.70^{a}	32.55±6.34^{abc}	29.63±2.76^{bc}	26.95±2.16^{c}	32.52±2.97^{abc}	39.96±5.52^{ab}	28.518±2.05^{c}	25.94±2.59^{c}	0.0299		
	Propionic	8.72±0.92^{c}	7.85±1.11^{c}	11.78±1.22^{b}	11.27±1.20^{bc}	18.53±1.42^{a}	17.60±1.82^{a}	13.641±0.86^{b}	12.409±1.01^{b}	0.0001		
	Isobutyric	1.44±0.16^{b}	1.35±0.13^{b}	1.49±0.13^{b}	1.48±0.15^{b}	2.91±0.30^{a}	2.82±0.28^{a}	3.164±0.18^{a}	3.02±0.27^{a}	0.0001		
	Butyric	13.34±2.54^{ab}	12.79±2.30^{ab}	16.13±1.17^{a}	14.36±1.08^{ab}	8.15±0.77^{c}	8.18±0.63^{c}	12.987±0.85^{ab}	11.84±1.16^{bc}	0.0001		
	Isovaleric	2.89±0.39^{b}	2.74±0.28^{b}	3.70±0.31^{b}	3.65±0.36^{b}	7.73±0.81^{a}	7.49±0.58^{a}	8.463±0.50^{a}	8.176±0.78^{a}	0.0001		
	Valeric	4.40±0.40^{b}	4.17±0.48^{b}	5.60±0.70^{b}	5.55±1.04^{b}	1.75±0.96^{b}	1.50±0.73^{b}	8.389±0.99^{b}	16.518±7.90^{a}	0.0035		
	Total	73.80±9.62^{a}	61.46±9.35^{a}	68.33±5.81^{a}	63.26±5.52^{a}	71.59±4.67^{a}	81.32±7.49^{a}	75.163±3.67^{a}	77.90±8.97^{a}			
		Values are LS mean ± SEM.										
		Means without common superscripts differ (p<0.05).										

Table 7. SCFA production on d 81 (umol/24 hr). Diet significantly affected 24 hr SCFA production for isobutyric, butyric, isovaleric, and valeric.

		Cellulose		Black bran		Sumac bran		Hi Tannin bran				
		Control	**DSS**	**Control**	**DSS**	**Control**	**DSS**	**Control**	**DSS**	**Diet**	**DSS**	**Diet* DSS**
Total SCFA prod (umol)/ 24 hr	**Acetic**	49.19±6.70^{a}	48.45±6.33^{a}	26.04±2.76^{b}	33.71±2.17^{ab}	40.33±2.98^{ab}	50.24±5.52^{a}	51.30±2.05^{b}	37.20±2.59^{ab}			
	Propionic	10.79±0.92^{b}	12.59±1.11^{ab}	9.10±1.22^{b}	22.43±1.20^{a}	22.40±1.42^{a}	23.98±1.82^{a}	22.06±0.86^{a}	17.14±1.01^{ab}			
	Isobutyric	1.52±0.16^{c}	1.53±0.13^{c}	1.14±0.13^{c}	1.54±0.15^{c}	3.75±0.30^{b}	3.77±0.28^{b}	5.85±0.18^{a}	4.53±0.27^{ab}	0.0001		
	Butyric	19.67±2.54^{a}	16.45±2.30^{ab}	15.98±1.17^{ab}	20.07±1.08^{a}	9.20±0.77^{b}	8.80±0.63^{b}	20.24±0.85^{a}	14.08±1.16^{ab}	0.0065		
	Isovaleric	2.83±0.39^{c}	2.94±0.28^{c}	2.99±0.31^{c}	3.78±0.36^{c}	9.48±0.81^{b}	9.28±0.58^{b}	14.91±0.50^{a}	11.35±0.78^{ab}	0.0001		
	Valeric	4.17±0.40^{b}	4.46±0.48^{b}	3.98±0.70^{b}	5.04±1.04^{b}	0.71±0.96^{b}	0.55±0.73^{b}	14.39±0.99^{a}	12.11±7.90^{a}	0.0001		
	Total	88.08±9.62^{ab}	86.41±9.35^{ab}	59.22±5.81^{a}	86.55±5.53^{ab}	85.88±4.67^{ab}	96.61±7.48^{ab}	128.74±3.67^{a}	96.41±8.97^{ab}			
		Values are LS mean ± SEM.										
		Means without common superscripts differ (p<0.05).										

Mucosal gene expression and NFκB activity

We did not observe any diet or diet*treatment effects for any gene targets except COX-2 and IL-12b (diet*treatment effect, p=0.025 and p=0.017, respectively), which are both upregulated by signals derived from NFκB pathway activation. We observed a significant treatment effect for gene targets involved in the TLR pathway, including TLR2 (p=0.0179), TLR4 (p=0.0436), MyD88 (p=0.0098), RelA/p65 (regulatory subunit of NFκB) (p=0.0039), Tollip (p=0.0039), cytokines TNFα (p=0.0018), IL-12b (p=0.0017), IL-6 (p=0.0042), and COX-2 (p=0.0063), as well as injury repair proteins TGFβ (p=0.0069) and TFF3 (p=0.0152) (Table 8). These targets relative expression (except TNFα and IL-12b) was upregulated in bran DSS rats and downregulated in Cellulose DSS rats compared to their diet matched controls. Relative expression of TLR2, TLR4, RelA/p65, Tollip, COX-2, IL-12b, TFF3, and TGFβ was upregulated in Hi Tannin DSS rats, with COX-2, IL-12b and TGFβ having significantly higher expression compared to all other groups ($p<0.05$; Figure 5). Relative expression of proinflammatory cytokine IL-6 was elevated in bran fed DSS rats, with Sumac and Hi Tannin DSS rats having significantly higher relative expression compared to their diet matched controls ($p<0.05$).

Relative expression of SCFA transporters (i.e., Slc16a1 and Slc5a8) was numerically higher in Cellulose controls and Black, Sumac and Hi Tannin bran DSS rats compared to their diet-matched counterparts, and these expression levels paralleled total SCFA concentrations observed on d 81 (prior to termination) (Figure 6). Hi Tannin DSS

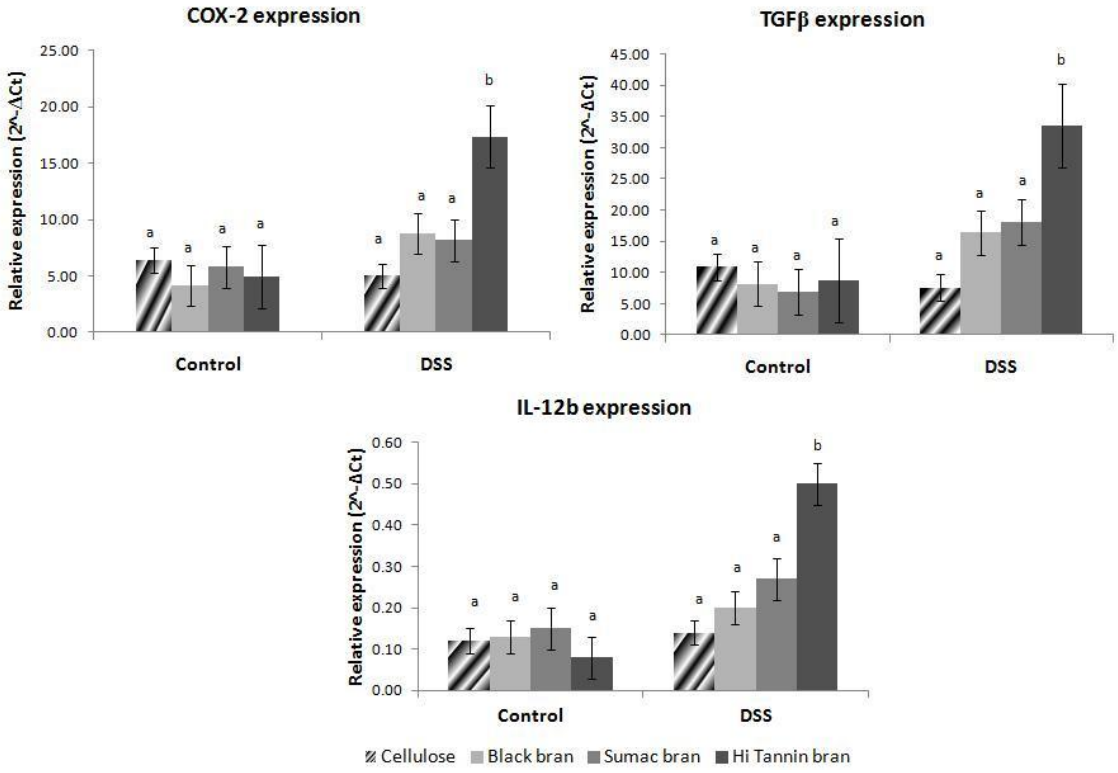

Figure 5. Relative expression (2^-ΔCt) of COX-2, IL-12b and TGFβ was significantly higher in Hi Tannin bran DSS rats compared to all other experimental groups ($p<0.05$). Values are LS mean ± SEM. Means without common superscripts differ ($p<0.05$). See Table 8 for actual values.

rats had significantly higher relative expression of Slc16a1 and Slc5a8 compared to their diet matched controls ($p= 0.0033$ and $p= 0.0157$, respectively).

Mucosal NFκB activity was numerically elevated in DSS treated rats for all experimental diets, with activity becoming significantly higher in Hi Tannin bran DSS rats compared to Cellulose controls ($p=0.0278$; Figure 7). The relationship between the change in injury score and NF-κB activity induced by DSS was determined to assess

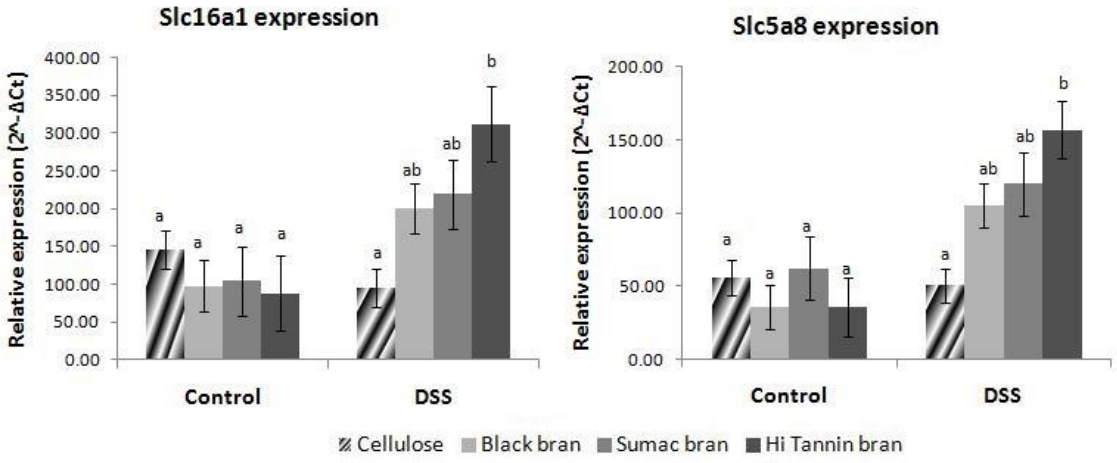

Figure 6. Relative expression (2^-ΔCt) of SCFA transporters, Slc16a1 and Slc5a8, was elevated in bran fed DSS rats, which was significantly higher in Hi Tannin bran DSS rats compared to their diet matched controls ($p<0.05$). Values are LS mean ± SEM. Means without common superscripts differ ($p<0.05$). See Table 8 for actual values.

whether these changes were unique to the specific diets. We observed a linear relationship between the change in injury score and NF-κB activity ($p=0.01$, $R^2=0.98$), with the Black bran diet resulting in the lowest value compared to Cellulose, Sumac and Hi Tannin, respectively (Figure 8).

Table 8. Relative expression of selected gene targets (2^-ΔCt). Values are LS mean ± SEM. Means without common superscripts differ ($p<0.05$).

	Cellulose		Black bran		Sumac bran		Hi Tannin bran				
	Control	DSS	Control	DSS	Control	DSS (n=9-10)	Control	DSS	Diet	DSS	Diet* DSS
TLR2	2.21±0.5^{ab}	2.11±0.57^{ab}	0.83±0.11^{a}	3.29±1.75^{ab}	1.94±0.93^{ab}	4.25±2.01^{ab}	1.06±0.29^{ab}	5.46±2.32^{b}		0.018	
TLR4	23.72±4.59^{ab}	19.98±3.67^{a}	18.22±2.73^{a}	50.1±23.04^{ab}	36.45±10.06^{ab}	41.92±11.75^{ab}	20.1±3.77^{a}	56.34±18.18^{b}		0.044	
MyD88	36.81±8.93^{ab}	24.77±3.93^{ab}	23.64±3.01^{a}	68.64±28.63^{bc}	30.46±5.17^{ab}	47.81±11.56^{abc}	23.65±4.77^{ab}	82.95±24.48^{c}		0.010	
RelA/p65	47.13±11.33^{ab}	38.61±5.62^{ab}	35.06±4.13^{ab}	81.66±25.6^{bc}	45.45±6.65^{ab}	80.52±20.81^{bc}	33.47±6.44^{ab}	112.18±34.75^{c}		0.0039	
Tollip	57.24±12.44^{ab}	50.18±9.85^{ab}	31.38±5.03^{ab}	99.09±32.07^{bc}	51.2±11.0^{ab}	117.27±41.5^{bc}	35.22±7.38^{ab}	158.14±62.81^{c}		0.0039	
TNFα	1.68±0.42^{ab}	1.84±0.43^{ab}	1.54±0.25^{a}	3.32±0.78^{abc}	1.6±0.42^{ab}	4.3±1.62^{c}	1.18±0.28^{a}	3.8±1.03^{bc}		0.002	
COX-2	6.41±1.33^{a}	5.01±0.87^{a}	4.12±0.72^{a}	8.81±2.87^{a}	5.8±1.43^{a}	8.18±2.28^{a}	4.92±0.86^{a}	17.36±4.72^{b}		0.006	0.026
Tff3	647.57±149.62^{ab}	540.8±89.22^{a}	442.63±51.92^{a}	1226.52±515.32^{ab}	629.67±159.77^{ab}	992.00±302.79^{ab}	410.29±89.38^{a}	1492.93±548.66^{b}		0.0152	
TGFβ	10.95±3.03^{a}	7.61±1.2^{a}	8.22±1.16^{a}	16.42±5.93^{a}	6.86±1.17^{a}	18.09±6.23^{a}	8.7±2.24^{a}	33.53±11.12^{b}		0.007	
Il-12b	0.12±0.03^{a}	0.14±0.03^{a}	0.13±0.03^{a}	0.20±0.05^{a}	0.15±0.03^{a}	0.27±0.07^{a}	0.08±0.02^{a}	0.50±0.15^{b}		0.0017	0.017
Il-1b	83.64±67.48^{b}	0.74±0.23^{a}	0.69±0.20^{a}	2.89±2.23^{a}	0.74±0.32^{a}	1.22±0.30^{a}	0.59±0.17^{a}	3.62±1.36^{a}			
Il-6	0.89±0.21^{a}	0.66±0.17^{a}	0.56±0.11^{a}	1.29±0.53^{ab}	0.72±0.21^{a}	2.10±0.83^{b}	0.48±0.13^{a}	2.09±0.61^{b}		0.0042	
Slc16a	146.45±30.3^{a}	96.03±16.71^{a}	98.19±13.53^{a}	201.18±54.23^{ab}	104.71±22.81^{a}	219.38±68.19^{ab}	88.22±19.07^{a}	311.93±111.45^{b}		0.0102	
Slc5a8	56.27±13.37^{a}	50.47±10.53^{a}	35.53±5.43^{a}	105.49±50.06^{ab}	62.34±18.78^{a}	119.80±44.07^{ab}	35.83±7.45^{a}	156.88±68.24^{b}		0.0162	
	Values are LS mean ± SEM.										
	Means without common superscripts differ ($p<0.05$).										

Discussion

Observed symptoms and severity of colonic injury

With the incidence of GI diseases such as ulcerative colitis (UC) on the rise worldwide (138), it is imperative to identify mechanisms to mitigate the onset or progression of chronic inflammation in the intestine. Diets containing bioactive compounds may provide protection against UC due to their ability to alter the intestinal microbiota, as well as provide anti-inflammatory effects and eliminate free radicals (9, 14-15, 104, 143, 145). Additionally, diets rich in fiber have been shown to reduce the risk of developing GI disorders and colon

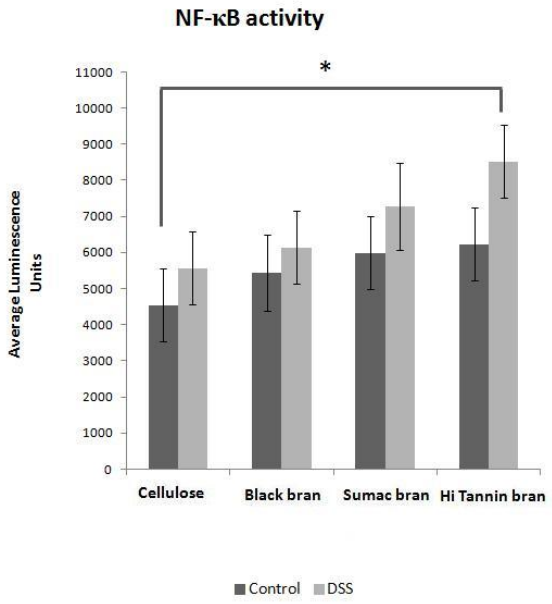

Figure 7. NF-κB activity was elevated in DSS rats in all experimental groups. Average NF-κB activity was significantly higher in Hi Tannin DSS rats compared to Cellulose control rats ($p<0.05$). Values are LS mean ± SEM.

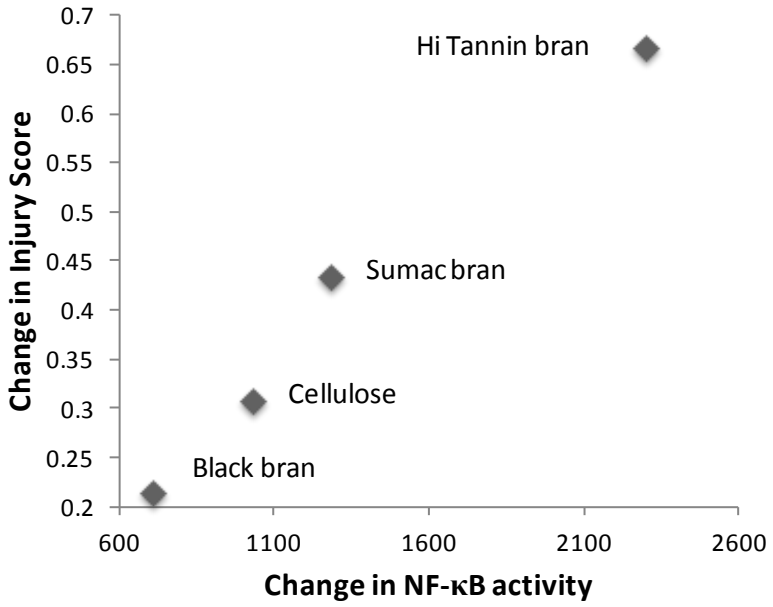

Figure 8. A linear relationship was observed between the change in injury score and change in NF-κB activity ($p=0.01$, $R^2=0.98$) with the Black bran diet resulting in the lowest value.

cancer (13, 28). Sorghum bran is a fiber source that has been shown to contain high levels of bioactive compounds, particularly, 3-deoxyanthocyanins, condensed tannins, or a combination of both compounds (25-26, 117). Previous studies indicate that these compounds can reduce the occurrence of preneoplastic lesions in AOM treated animals (24), however, the ability of sorghum bran based diets to mitigate UC has not been investigated.

DSS administration is a commonly used technique to induce experimental colitis, and it is well documented that exposure can produce symptoms such as watery and

bloody stools, weight loss and injury to the colonic mucosa (152). We investigated the ability of sorghum bran diets to mitigate the effects of repeated DSS exposure (3% DSS concentration for 48 hrs, 3 exposures with 2 wk recovery between bouts). Our observations suggest that disease severity in DSS rats was minimal, as we observed no significant differences in body weight, diet intake, or marked increases in fecal moisture content (≤ 6%) following DSS exposures. Maintenance of fecal moisture content during inflammatory bouts could be due to the composition of the sorghum bran, which contains a high proportion of insoluble fiber (~95%). Soluble and insoluble fibers are both required for optimum health, but carry out different physiological roles in the body. Insoluble fibers are known to be beneficial for regularity by increasing fecal bulk, reducing diarrhea and binding deleterious compounds such as carcinogens (153). Although some soluble fibers are known to ease constipation and have been shown to improve symptoms of UC (154), our lab previously reported that rats fed experimental diets containing 6% pectin, a predominately soluble fiber source, demonstrated significantly higher fecal moisture content and bloody diarrhea following the same DSS treatments used in this study (155). Similar to our results, other studies reported that insoluble fiber can attenuate the deleterious effects of DSS-induced colitis (2-3.5% DSS for 5-6 d) (54-55). These studies reported that experimental diets containing dietary fiber from germinated barley provides numerous beneficial effects in vivo including weight maintenance, elevated fecal butyrate, reduction in the presence of bloody stool and incidence of diarrhea, and attenuating elevations in circulating IL6 and mucosal NFκB (54-55). Thus, these results indicate consuming a diet containing insoluble dietary fiber

may have the ability to ameliorate negative clinical effects such as weight loss and bloody diarrhea associated with UC.

Immunohistochemical examination of the distal colon revealed that crypt height was significantly reduced in DSS treated rats for all experimental diets. However, mucosal injury and inflammatory cell infiltration remained confined to the epithelial membrane and rarely extended into the submucosa. Injury scores were elevated in DSS treated rats for all experimental diets, but, these were generally described as discrete lesions with only occasional mucosal erosion. One explanation for differing injury scores in bran fed animals compared to Cellulose could be due to the structure of the bran particles. Black bran in particular is reported to have a different bran composition and larger particle size compared to Sumac and Hi Tannin brans, which could explain an elevated injury score in Black bran control rats that did not receive DSS compared to control rats from other experimental diets (156). Observations in animals that received 3 cycles of DSS contrasts other studies that utilized similar DSS treatments (3-5%), which reported elevated fecal moisture content, mucosal erosion, complete loss of crypts, as well as erosion that extended into the intestinal wall (155, 157-158). Two of these studies fed a standard chow, while the other utilized an experimental diet containing pectin as the sole dietary fiber source. As mentioned previously, fiber composition has numerous implications for gut health and could be one reason for the disparity in these results.

Chronic intestinal inflammation can lead to epithelial barrier dysfunction, and preservation of colonocyte proliferation is crucial for maintaining barrier integrity.

PCNA analysis indicates that proliferation levels (i.e., proliferative index and proliferative zone) were increased at termination (2 weeks post DSS#3) for all bran fed DSS rats compared to their diet matched control, with Black bran DSS rats having significantly higher proliferative index than Black bran controls ($p=0.0049$). This observation could be due to the presence of 3-deoxyanthocyanins in this bran. Other studies reported diets containing anthocyanin rich blueberries reduce epithelial injury, bacterial translocation, and inflammation in multidrug resistance gene deficient mice and during DSS induced colitis (5% DSS for 10 d). Although proliferation was not measured in these studies, the authors hypothesize the ability to maintain epithelial barrier integrity could be, in part, by modulating epithelial proliferation (121, 159).

In addition to maintaining epithelial cell proliferation, proteins responsible for epithelial migration and tight junction formation allow for restitution of the epithelial barrier and wound healing following colonic injury (160-163). We observe upregulated expression of apical (trefoil factor 3, TFF3) and basolateral (transforming growth factor β ,TGFβ) repair proteins in colonic mucosa of bran DSS rats compared to their diet matched controls. Moreover, relative expression of TGFβ was significantly higher in Hi Tannin DSS rats compared to their diet-matched controls. Trefoil factor proteins are expressed on the apical side of colonic epithelial cells, and have been shown to be produced by intestinal goblet cells and be associated with excreted mucins. Although the complete mechanism of TFF3 in colonic epithelial repair has not been elucidated, TFF3 has been shown to be involved in cellular migration and suppressing apoptosis (162-164). It has been reported that TFF3 expression is suppressed in TNBS models of

experimental colitis (161, 165), and the absence of TFF3 expression in DSS induced colitis (2.5% for 5d) significantly delays healing of mucosal injury up to 12 d post DSS exposure (166). Our results contrast these reports, as we observe elevated relative expression of this protein in colonic mucosa of bran DSS rats following repeated DSS treatments (14 d post DSS#3). Furthermore, we observe a significant elevation in TGFβ in Hi Tannin DSS rats compared to all other experimental groups. TGFβ is expressed on the basolateral side of the colonic epithelial membrane and is thought to play a major role in epithelial cellular differentiation, migration, and has been implicated in the restitution of monolayer would healing *in vitro* (160, 167). Furthermore, it has been reported that TGFβ induces the expression of COX2 *in vitro* (167), which is similar to our findings in Hi Tannin DSS rats that demonstrated significantly higher relative expression of TGFβ and COX2 in colonic mucosa.

In general we observe that repeated DSS exposure does not cause drastic mucosal damage as described in similar experimental colitis models (155, 157-158). Although injury scores were higher in bran fed DSS rats, our results indicate that bran based diets could have the ability to repair the mucosal damage associated with UC by modulating epithelial cell proliferation and the expression of repair proteins. Interestingly, we do not observe enhanced proliferation or increased relative expression of repair proteins in Cellulose DSS rats, which could be an indicator that properties of sorghum bran diets (i.e., presence of bioactive compounds) could be a factor in upregulating epithelial repair mechanisms. Additionally, examination of distal colon using TUNEL revealed no significant differences in apoptotic index between healthy and

diseased animals and we observe no distinct link between apoptosis and mucosal TNFα expression.

Historically, diets containing condensed tannins (similar to those found in Sumac and Hi Tannin bran) have been used to treat patients with UC (168). More recent studies have shown that plant polyphenols such as anthocyanins and condensed tannins can mitigate colonic injury and improve UC symptoms, however, the mechanism behind these benefits have not been elucidated (9, 16, 143, 169-170). The beneficial properties of bioactive compounds could be, in part, due to modulating the luminal environment and microbiota, which is well documented to have a profound effect on the progression and severity of UC. Therefore, we sought to elucidate how sorghum bran diets can alter the luminal environment and microbiota by analyzing fecal short chain fatty acids (SCFA) and mucosal gene expression of toll-like receptors (TLR) and downstream mediators of this signaling pathway.

Bacterial metabolites and mucosal gene expression

The intestinal microbiota has a profound impact on the host immune system, and dysbiosis of these bacterial populations has been implicated in UC (35, 75, 96-97). Patients with UC have demonstrated alterations to the predominant bacterial populations (i.e., Bacteroidetes and Firmicutes) as well as decreased species diversity, which can have a major impact on the luminal environment by altering the concentrations of microbial metabolites such as SCFA (6, 19, 43, 45, 99, 171-173). Of particular importance is butyrate, which is not only the preferred fuel for colonocytes, but has other plieotrophic effects including anti-inflammatory activity and the ability to induce gene

expression and cellular differentiation in epithelial cells (38, 47, 69, 174-175). Additionally, it has been demonstrated that butyrate supplementation can improve symptoms of UC (54, 62, 174).

We observe very few significant treatment or diet*treatment differences in fecal SCFA concentrations and no distinct patterns between control and DSS rats for any experimental diets following DSS#1, DSS#2 or DSS#3 (d 44, d 66, and d 72 respectively). We observe a diet*treatment effect on d 44 (post DSS#2) for isobutyric and on d 66 (post DSS#3) for acetic (umol/24 hr). Throughout the study we observe a significant effect of diet on numerous SCFA. Following recovery from all DSS treatments and just prior to termination (d 81), we observe similar fecal SCFA concentrations as observed prior to DSS treatments (d 38). We do not observe a significant reduction in fecal butyrate or other SCFA (umol/24 hr) in bran fed rats during an active disease state, which suggests DSS induced inflammation did not affect microbial fermentation patterns in these animals. In contrast, Cellulose DSS rats had significantly lower 24 hr butyrate production following DSS#2 & DSS#3 compared to their diet matched controls ($p=0.032$ and $p=0.015$, respectively). In DSS rats, the proportion of excreted butyrate compared to total short chains produced was lower in Sumac and Hi Tannin bran rats (9% and 14% respectively) compared to Cellulose and Black bran rats (19% and 23%, respectively) prior to termination (d 81). One possible explanation for lower fecal concentrations of butyrate is enhanced uptake and utilization by coloncytes. Although we did not directly measure butyrate absorption, we observe an upregulation of SCFA transporter (i.e., Slc16a1 and Slc5a8) expression in bran fed DSS

rats. Interestingly, Tannin DSS rats had significantly higher relative expression of both Slc16a1 and Slc5a8 ($p<0.05$) compared to their diet matched controls, which could explain the reduced fecal butyrate observed in these animals.

It has previously been reported that patients with UC have suppressed SCFA production and impaired butyrate oxidation (176-177). Although we did not measure butyrate oxidation in this experiment, we do not observe a significant decrease in fecal butyrate following DSS exposure when fed a bran based diet. Additionally, studies have shown a decrease in SCFA transporter expression in diseased tissues and patients with IBD (52-53, 178-179), but in our study DSS induced colitis did not suppress relative expression of Slc16a1 or Slc5a8 when fed bran based diets, particularly Hi Tannin. We observe suppressed 24 hr butyrate production and expression of these transporters in Cellulose DSS rats, suggesting that properties of bran diets could be protective against suppression of both SCFA production and SCFA transporter expression commonly associated with intestinal inflammation and UC (177-180).

In addition to affecting the luminal environment and influencing epithelial cell metabolism, the microbiota also plays a major role in the status of the epithelial barrier by interacting with pattern recognition receptors (PRR) such as TLR. TLR signaling, mediated through the NFκB pathway, provides homeostatic interactions between the microbiota and host. However, in a disease state this pathway has been shown to upregulate the immune response as well as cause hyperproliferation which increases the risk of tumorigenesis (34, 181-182). Studies have shown that experimental models of UC and patients with chronic intestinal inflammation have differential TLR expression

(183), and in our study we observe a significant effect of DSS treatment on TLR2 and TLR4 ($p=0.0179$ and $p=0.0436$, respectively). Furthermore, we observe a significant effect of DSS treatment on other targets associated with the TLR signaling cascade (i.e., MyD88, RelA/p65 (regulatory subunit of NFκB), TNFα, IL-12b, IL-6, and COX-2). Relative expression of these gene targets was numerically elevated in colonic mucosa of bran DSS rats but not Cellulose DSS rats. Compared to their diet matched controls, Hi Tannin DSS rats had significantly higher relative expression of TLR4 ($p=0.0365$), which has been previously reported to be upregulated in patients with UC (7). TLR4 has been reported to regulate COX-2 expression in DSS induced colitis (184), which is similar to our results in Hi Tannin DSS rats which had upregulated TLR4 and significantly higher relative expression of COX-2 ($p<0.05$) compared to all other experimental groups. Activated NFκB was elevated in colonic mucosa of DSS treated rats; however, we observe no significant differences between healthy and diseased animals for any experimental diet. Upregulation of TLR signaling pathways and NFκB activity is more severe in DSS rats fed bran based diets that contain condensed tannins (i.e., Sumac and Hi Tannin bran) compared to bran containing 3-deoxyanthocyanins (Black bran). Black bran DSS rats had relative expression and activated NFκB that was closer to their diet-matched controls. To elucidate the relationship of NFκB activation and epithelial injury, the relationship between changes in injury and NFκB within each diet was assessed. We observe a linear relationship ($p=0.01$, $R^2=0.98$) in activated NFκB and epithelial injury, with the Black bran diet resulting in the lowest value. As mentioned previously, Black bran DSS rats had significantly higher proliferative zone than their diet matched control

and this upregulation could explain why we observe very little difference in injury score between these groups.

Additionally, upon immunohistochemical examination of distal colon, DSS treated rats fed a bran based diet demonstrated no significant differences in inflammatory infiltration compared to their diet matched controls. The inflammation score observed for all experimental groups in this study demonstrate the presence of increased number of inflammatory cells in the lamina propria, but little infiltration into the submucosa. These results suggest that feeding a bran diet may modulate an immune response and infiltration of inflammatory cells into the colonic mucosa during an inflammatory challenge. Surprisingly, Cellulose control rats have a significantly higher inflammation score than Cellulose DSS rats. One explanation for this disparate result could be mucosal gene expression of pro-inflammatory cytokine IL-1b, which was significantly higher in Cellulose control compared to all other experimental groups.

Conclusions

Although we observe significantly higher expression of certain gene targets associated with TLR signaling in DSS rats, we do not observe a drastic upregulation in the relative expression of proinflammatory cytokines and changes in NFκB activity between healthy and diseased animals is relatively low. These relatively small differences could be due to the number of days between the last DSS treatment and tissue collection in our study (14 days). Other studies using DSS induced experimental colitis observed that expression of IL-1b peaked following DSS treatment and decreased progressively and returned to baseline just four days after treatment (183). These results

suggest that we may observe a more severe upregulation of the TLR/NFκB signaling pathway during a more active disease state immediately after DSS exposure. Our SCFA observations indicate that there may be differences in the bacterial populations or their metabolism between experimental groups, and previous studies have identified anthocyanins and hydrolysable tannins from other dietary constituents (e.g., tea leaves, grapes, Galla Rhois plant) that have differential effects on intestinal bacterial populations (14-16, 185-186). Additionally, since TLR expression has been shown to be dependent upon microbiota composition (74, 187), phylogenetic classification of the intestinal bacterial populations in this study is warranted to further elucidate changes caused by inflammation and bran based diets on microbial metabolites and TLR signaling.

To our knowledge this is the first study to analyze the effects of sorghum bran based diets on UC. We observe distinct differences among bran diets that contain differing bioactive compounds (i.e., 3-deoxyanthocyanins, condensed tannins, or a combination of both compounds) and a Cellulose control diet, suggesting that the presence of these dietary constituents may influence the luminal and colonic mucosal environments. Our results indicate that by feeding bran based diets, it is possible to reduce the severity of epithelial injury and alleviate symptoms such as diarrhea that have been observed in similar DSS induced colitis models and patients suffering from UC. We demonstrate these diets may be able to mitigate colonic injury and epithelial dysfunction associated with repeated colonic inflammation by upregulating epithelial repair protein (i.e., TFF3 and TGFβ) and SCFA transporter (i.e., Slc16a1 and Slc5a8)

expression. Furthermore, we do not observe a drastic inflammatory cell infiltration in the distal colon nor fold changes in relative expression of mucosal proinflammatory cytokine gene expression (i.e., TNFα, COX2, Il-12b, Il-1b, IL6), which is commonly associated with an overactive TLR/ NFκB signaling cascade in experimental colitis models and patients diagnosed with UC. Further classification of the microbiome and metabolomics will help elucidate mechanisms by which bioactive compounds in sorghum bran may alter the luminal environment and mitigate UC.

CHAPTER III

NOVEL SORGHUM BRANS ALTER COLON MICROBIOTA AND DIFFERENTIALLY RESTORE SPECIES DIVERSITY AND SPECIES RICHNESS IN RESPONSE TO DSS-INDUCED COLITIS

Introduction

The incidence of inflammatory bowel disease (IBD), which encompasses Crohn's disease and ulcerative colitis (UC), affects nearly 1.4 million people in the United States alone (188), and the incidence is increasing worldwide (138). Complications include abdominal cramping, constipation, abnormal bowel movements, and it is associated with an increased risk in colorectal cancers (1, 4, 189). Although the complete etiology of these diseases are unknown, factors point to dysbiosis of the inherent bacterial populations residing in the gastrointestinal (GI) tract, or microbiota, as being a significant factor in the progression and severity of these diseases (5, 78, 96).

Numerous studies over the past decade have sought to elucidate alterations to the microbiota or identify which bacterial populations might be associated with the onset or perturbation of GI diseases (5, 78, 188, 190). Although some studies have implicated an increase in pathogenic bacteria or a depletion of beneficial bacteria such as lactic acid bacteria (LAB) (191-193), it is becoming more apparent that not one particular bacterial group can be implicated in the cause of IBD. However, studies have reported alterations in the ratio of the predominant bacterial phyla, Firmicutes and Bacteroidetes, in patients

affected with IBD compared to controls (190, 194-195). Another common observation in patients with IBD is a reduction in bacterial diversity and species richness (99, 171).

It is well documented that diet can also have profound effects on the intestinal microbiota. Alterations to the diet can affect the luminal environment by affecting transit time, luminal pH, and the production of microbial metabolites (e.g., butyrate) (12, 18, 196). Additionally, dietary constituents containing secondary plant metabolites such as polyphenols have been reported to differentially affect luminal bacterial populations, suppressing certain taxa while allowing others to thrive, by affecting bacterial metabolism or evoking a bactericidal effect (9, 15, 142). In recent years diets containing bioactive compounds, such as polyphenols and tannins, have been identified as probable interventions for IBD due to their antimicrobial and antioxidant capacity. In vitro studies have shown that tannins, the second most abundant plant polyphenol, and other bioactive compounds can dramatically affect the survival of bacterial groups typically present in the GI tract (14, 185, 197). Moreover, numerous *in vivo* studies have also characterized how these compounds can enhance certain beneficial or probiotic bacteria (i.e., *Bifidobacterium* & *Lactobacillus* spp.), while suppressing or eliminating other pathogenic bacteria such as *C. perfringens* and *C. difficile* in the intestine (15-16, 145). Additionally, one study demonstrated that hydrocaffeic acid, a polyphenol metabolite derived from colonic microbiota, produced anti-inflammatory affects including suppression of pro-inflammatory cytokine production (i.e., TNFα, IL-8, IL-1β) and a reduction in oxidative DNA damage in rat colonic mucosa (143).

Bran from specific varieties of sorghum has been characterized as containing high levels of dietary polyphenols, including 3-deoxyanthocyanins and condensed tannins, and certain strains are reported to have a significantly higher antioxidant capacity compared to wheat bran and "super fruits" such as blueberries and pomegranates (25-27, 117). Research based evidence demonstrates that certain black and brown varieties of sorghum can affect the colonic mucosal environment by altering concentrations of fecal microbial metabolites (e.g., short chain fatty acids (SCFA)), which indicates a change to the intestinal microbiota (24, 198). Based off these results, we hypothesize that DSS induced colonic inflammation will affect the colon luminal environment by altering the microbiota, and by feeding sorghum bran diets we can mitigate this dysbiosis. Therefore the aim of this study was to characterize the effect of sorghum bran based diets containing 3-deoxyanthocyanins, condensed tannins, or both polyphenols on the intestinal microbiota. Furthermore, we aim to ascertain if sorghum bran diets can mitigate alterations to the microbiota during repeated inflammatory bouts produced by dextran sodium sulfate (DSS) challenge.

Materials and Methods

Animals and diets

Eighty male Sprague-Dawley rats (21 d old) were stratified by body weight and assigned to one of four experimental diets (n=20/ diet). The four diets contained 6% dietary fiber from cellulose, or bran isolated from sorghum grains that contain high levels of 3-deoxyanthocyanins, high levels of condensed tannins and low levels of 3-deoxyanthocyanins, or both 3-deoxyanthocyanins and condensed tannins. Prior to

beginning the experimental diet, animals (40 d old) were maintained on a standard pelleted diet for 19 d in order to adjust to the new environment.

After 21 d of experimental diets, half of the rats were exposed to three sequential 48 h dextran sodium sulfate (DSS) (MP Biomedicals, Irvine, CA) treatments (3% DSS) in their drinking water, with 14 d between each DSS exposure. Between DSS exposures, distilled water was supplied to treated animals. The remaining half of the animals received distilled water throughout the course of the study.

Body weight and food intake were routinely monitored (Chapter II). Rats were weighed upon arrival, prior to beginning experimental diets, before and after each DSS exposure, and prior to termination. Additionally, food intake was measured prior to the first DSS treatment, following the second DSS treatment, and prior to termination (following third DSS treatment). On day 63, animals were euthanized by CO_2 asphyxiation.

Inflammation and injury histological scores

A 1 cm segment was removed from the distal end of the colon and fixed in 70% EtOH solution prior to embedding in paraffin. The degree of inflammation and morphological injury caused by DSS exposure was assessed by H&E staining. Histologic examination was performed in a blinded manner by a board-certified pathologist, and the degrees of inflammation (score of 0–3) and epithelial injury (score of 0–3) on microscopic cross sections of the colon were graded as described previously (150) (Appendix B).

Sample collection and microbial DNA isolation

Following recovery from the second (d 47 N=9 or 10 for Cellulose & Black or Sumac & Hi Tannin DSS rats, respectively) and third (d 62 N=5/diet for control rats and N=10/diet for DSS rats) DSS exposures, and fresh fecal samples were collected immediately following defecation. Samples were transferred to sterile cryotubes, placed on ice, then stored at -80°C. DNA was isolated from homogenized fecal samples using a FastDNA SPIN kit according to the manufacturer's instructions (MP Biomedicals, Solon, OH) (Appendix B). Purified DNA was stored at -80°C. A negative control containing H_2O instead of sample was purified in parallel to each extraction batch to screen for contamination of extraction reagents.

16S rRNA bacterial tag-encoded FLX amplicon pyrosequencing (bTEFAP)

Initial amplification of the V1-V2 region of the bacterial 16S rDNA was performed on total DNA isolated from fecal samples. Master mixes for these reactions used the Qiagen Hotstar Hi-Fidelity Polymerase Kit (Qiagen, Valencia CA) with a forward primer composed of the Roche Titanium Fusion Primer A (5'-CCATCTCATCCCTGCGTGTCTCCGACTCAG -3'), a 10 bp Multiplex Identifier (MID) sequence (Roche, Indianapolis, IN) unique to each of the samples, and the universal bacteria primer 8F (5'-AGAGTTTGATCCTGGCTCAG-3') (199). Incorporation of MID sequences to the PCR amplicons essentially "barcodes" samples and allow for multiplexed assays. Samples are pooled prior to the pyrosequencing reaction. The reverse primer was composed of the Roche Titanium Primer B (5'-CCTATCCCCTGTGTGCCTTGGCAGTCTCAG -3'), the identical 10 bp MID

sequence as the forward primer and the reverse bacteria primer 338R (5'-GCTGCCTCCCGTAGGAGT-3') (200) which span the V1-V2 hypervariable region of the bacterial 16S rDNA. The thermal profile for the amplification of each sample had an initial denaturing step at 94°C for 5 minutes, followed by a cycling of denaturing of 94°C for 45 seconds, annealing at 50°C for 30 seconds and a 90 second extension at 72°C (35 cycles), a 10 minute extension at 72°C and a final hold at 4°C. Each sample was individually gel purified using the E-Gel Electrophoresis System (Life Technologies, Invitrogen). To ensure equal representation of each sample in the sequencing run, each barcoded sample was standardized by calculating equimolar amounts prior to pooling. Pooled samples of the 16S rDNA multiplexed amplicons were sequenced on a Roche 454 Genome Sequencer FLX Titanium instrument (Microbiome Core Facility, Chapel Hill NC) using the GS FLX Titanium XLR70 sequencing reagents and protocols.

bTEFAP data analysis

Analysis of deep sequencing data was carried out using the QIIME pipeline (201). Briefly, the combined raw sequencing data plus metadata describing the samples were de-multiplexed and filtered for quality control. Next, data were denoised using Denoiser software as described previously (202). Chimeric sequences were depleted from the trimmed data set using Chimera Slayer (203). Sequences were grouped into OTUs (Operational Taxonomic Units) at a 97% level to approximate species-level phylotypes using Uclust (204). OTU sequences were aligned and OTU tables containing the counts of each OTU in each sample were used to calculate mean species diversity of

each sample (alpha diversity) and the differentiation among samples (beta diversity). Alpha and beta diversity measures were used to calculate a Chao species richness estimate and a Shannon Weaver diversity index for each OTU. To evaluate the similarities between bacterial communities a combination of Unifrac significance, principal coordinate analysis (PCoA) using Fast Unifrac (205) and network analysis (206-207) were performed to compare samples based on sample time and treatment. ANOVA, the G test of independence, Pearson correlation, or a paired t-test were used within Qiime to identify OTUs that are differentially represented across experimental treatments or measured variables.

Statistical analysis

Data were analyzed using two-way analysis of variance (ANOVA) including variables of diet and DSS exposure in SAS 9.1 (SAS Institute, Inc.) considering a p-value of <0.05 as significant. Relationships between microbial populations and colonic injury score were assessed by calculating Pearson's product moment correlation coefficient.

Results

Body weight and experimental diet intake

There were no significant differences in initial body weights (d 1 of experimental diet treatment), d 14, d 70, d 81, or at termination (d 84) (Chapter II). Hi Tannin control rats had significantly higher body weights than Cellulose control on d 39 ($p=0.0321$), d 42 ($p=0.0273$), d 56 ($p = 0.0248$), and d 60 ($p=0.0415$); however, there were no significant differences for any other experimental groups during these time points. On d

39 (prior to DSS#1), we observed a significantly lower food intake in Cellulose DSS animals compared to Sumac DSS rats ($p<0.05$), however, there were no significant differences in intake for any experimental groups on d 60 (post DSS#2), or d 81 (post DSS #3) (Chapter II).

Multivariate analysis of bacterial populations

Unifrac and principal components analysis (PCA) of all sequences for each sample, represented as a discrete data point without overlap, revealed distinct clustering of samples based on experimental diet (Figure 9). Variation of data points along PC2 (10.3%) indicates clear clusters and therefore distinct differences in bacterial communities between rats fed the Cellulose, Black, Sumac, and Hi Tannin bran diets, with Black bran diet samples having the smallest variation from Cellulose followed by Hi Tannin and Sumac bran, respectively. Hi Tannin bran, which contains both condensed tannins and 3-deoxyanthocyanins, had bacterial communities that clustered near both Black bran (contains 3-deoxyanthocyanins) and Sumac bran (contains condensed tannins). Additionally, rats fed bran diets that contain condensed tannins (i.e., Sumac and Hi Tannin bran) had bacterial communities that clustered together. Spatial relation of data points along PC3 (6.28%) revealed that rats consuming the Sumac bran diet had samples with the least amount of variation, or clustered tightly together, compared to other experimental diets. Furthermore, samples collected on d 47 (post DSS#2) predominately clustered in the right half of the plot, whereas samples collected on d 62 (post DSS#3) clustered on the left half. Differences in the spatial relation of

samples suggest distinct differences in bacterial communities based on diet and the number of DSS exposures.

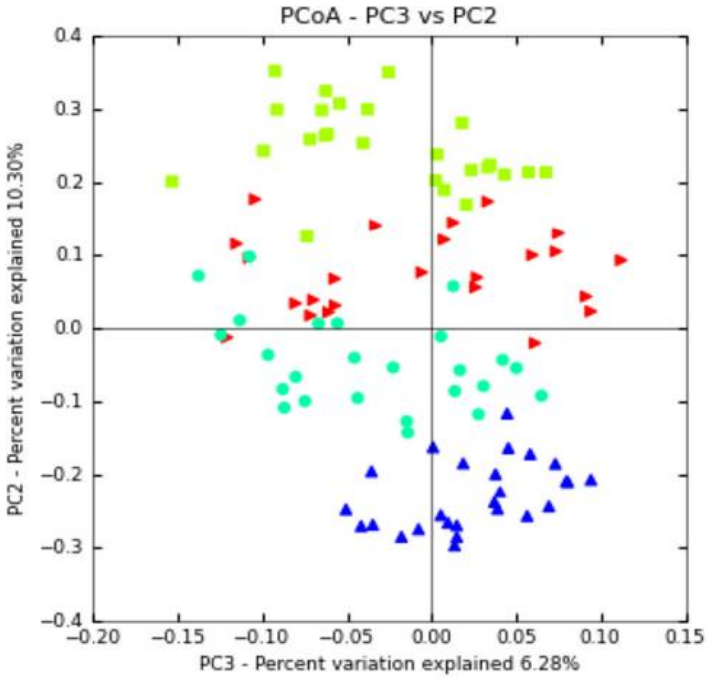

Figure 9. PCA plot of samples from d 47 and d 62. Green squares (Cellulose), red triangles (Black bran), light blue circles (Hi Tannin bran), and blue triangles (Sumac bran), illustrate differences in bacterial populations due to experimental diet treatment. Samples collected on d 47 and d 62 clustered in the right and left halves of the plot, respectively.

Microbial taxonomic structure analysis

Phylogenetic classification of OTUs revealed two predominant phyla, Bacteroidetes and Firmicutes, for all experimental diets on d 47 (post DSS#2) and d 62 (post DSS#3) (Figure 10). OTUs were also classified in the Actinobacteria and Proteobacteria phyla, but proportions did not exceed 5% for any experimental group at either time point. We observed a significant diet effect for all classified phyla at both time points (Appendix A-5). For all experimental diets at both time points there were OTUs that did not match any known sequences in the RDP database, and the proportion of OTUs classified as "Unknown" or "Unclassified" was elevated in all experimental diets on d 62 compared to d 47 (≥2 fold increase).

We observed a significant effect of DSS on both the Firmicutes and Bacteroidetes phylum ($p=0.0006$ and $p<0.0001$, respectively) on d 62, and patients with IBD have been shown to have elevated Firmicutes to Bacteroidetes ratios. Thus, ratios of these phyla were calculated to characterize any dysbiosis to the predominant bacterial groups on d 47 and d 62 (Table 9). The highest ratio was observed in Cellulose control rats (112.02), and was markedly higher than that of Black (26-fold), Sumac (114-fold), and Hi Tannin bran control rats (35-fold). The ratio of Firmicutes to Bacteroidetes was higher in Cellulose DSS rats on d 47 and d 62 compared to Black, Sumac, and Hi Tannin bran DSS rats (Table 9).

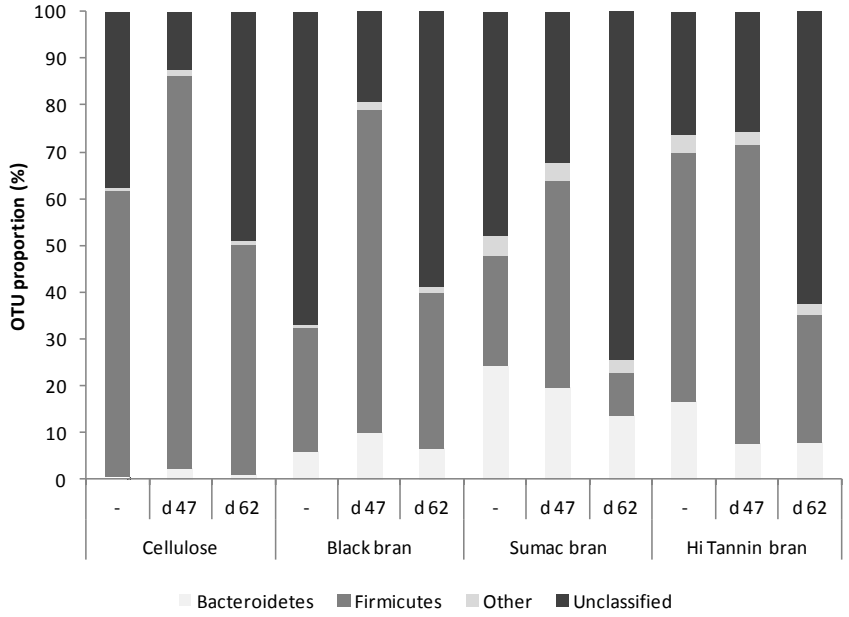

Figure 10. Phylogenetic classification of OTUs at the phylum level for control rats d 62 (-) and DSS treated rats (d 47 and d 62) for all diets. Data are LS±SEM. Actual values in Appendix A-5.

Table 9. Firmicutes/Bacteoridetes ratio on d 47 and d 62. The highest ratio was observed in Cellulose control rats and was markedly higher than that of Black, Sumac, and Hi Tannin bran control rats.

		Cellulose		Black bran		Sumac bran		Hi Tannin bran	
			DSS (n=9)		DSS (n=9)		DSS (n=10)		DSS (n=10)
Day 47	Firmicutes		0.84		0.69		0.44		0.64
	Bacteroidetes		0.02		0.10		0.19		0.08
	Firmicutes/ Bacteroidetes		**35.32**		**7.08**		**2.29**		**8.50**
		Control (n=5)	**DSS (n=10)**	**Control (n=5)**	**DSS (n=9)**	**Control (n=5)**	**DSS (n=10)**	**Control (n=5)**	**DSS (n=9)**
Day 62	Firmicutes	0.61	0.49	0.26	0.33	0.24	0.09	0.53	0.27
	Bacteroidetes	0.01	0.01	0.06	0.07	0.24	0.14	0.17	0.08
	Firmicutes/ Bacteroidetes	**112.02**	**51.70**	**4.33**	**5.12**	**0.98**	**0.69**	**3.21**	**3.39**

Further phylogenetic analysis of OTUs revealed three predominant bacterial orders (Bacteroidales, Clostridiales, and Lactobacillales) in all collected samples (Table 10, Figure 11). We observe significant diet effects on d 47 for bacteria in the Bacteroidales ($p<0.0001$), Clostridiales ($p=0.0205$) and Lactobacillales orders ($p=0.0417$). Sumac DSS rats had significantly higher proportion of OTUs classified in the Bacteroidales order, and Hi Tannin DSS rats had significantly higher proportions of Lactobacillales compared to all other experimental diets ($p<0.05$).

On d 62, proportions of OTUs classified in the predominant bacterial orders (i.e., Bacteroidales, Clostridiales, and Lactobacillales) were reduced in DSS treated rats compared to d 47 (post DSS#2) for all experimental diets (Figure 11), with the highest reduction observed in the Clostridiales order (56%-79%, Figure 12). Additionally, we observe significant diet, treatment and diet*treatment effects for the Bacteroidales ($p<0.0001$, $p<0.0001$, and $p=0.0005$, respectively) and Clostridiales ($p=0.0387$, $p=0.0005$, and $p<0.0001$, respectively) orders at this time point (Table 10). In Sumac control rats, we observe a significantly higher proportion of OTUs classified in the Bacteriodales order, and a significantly higher proportion of Clostridiales in Hi Tannin control rats compared to other experimental diets ($p<0.05$). We observe a significant effect of diet and treatment for OTUs classified in the Lactobacillales order ($p<0.001$ and 0.0377, respectively). Cellulose controls had a significantly higher proportion of OTUs classified in this order ($p<0.05$) compared to all other experimental groups. Additionally, DSS treated rats fed Cellulose, Sumac and Hi Tannin bran diets had lower proportions of the Lactobacillales order compared to their diet matched controls.

When comparing Sumac and Hi Tannin DSS treated rats to their diet matched controls, we observe a significant reduction in numerous bacterial orders (Table 10). Sumac DSS rats had significantly lower proportions of the orders Bacteroidales, Clostridiales, and Burkholderiales, and Hi Tannin DSS lower proportions of orders Bacteroidales, Clostridiales, and Eryspelotrichales compared to their diet matched controls ($p<0.05$). In contrast, Black bran DSS rats had numerical elevations in the proportion of bacteria classified in the Bacteroidales, Lactobacillales, Clostridiales, and Burkholderiales orders, and Cellulose DSS rats had numerical elevations in Bacteroidales, Clostridiales, and Erysipelotrichales orders compared to their diet-matched controls.

Diversity and species richness comparisons

To analyze the effect of diet and DSS induced inflammation on bacterial species richness and diversity, sequences from each sample were used to perform alpha and beta diversity analysis and calculate a Chao species richness estimate and Shannon Weaver diversity index. We observe a significant diet effect on species richness and diversity ($p<0.0001$ for both) on d 62, with Black bran controls having a significantly higher species richness ($p<0.05$) compared to Sumac and Hi Tannin bran controls, and a significantly higher diversity index ($p<0.05$) compared to all other controls (Table 11).

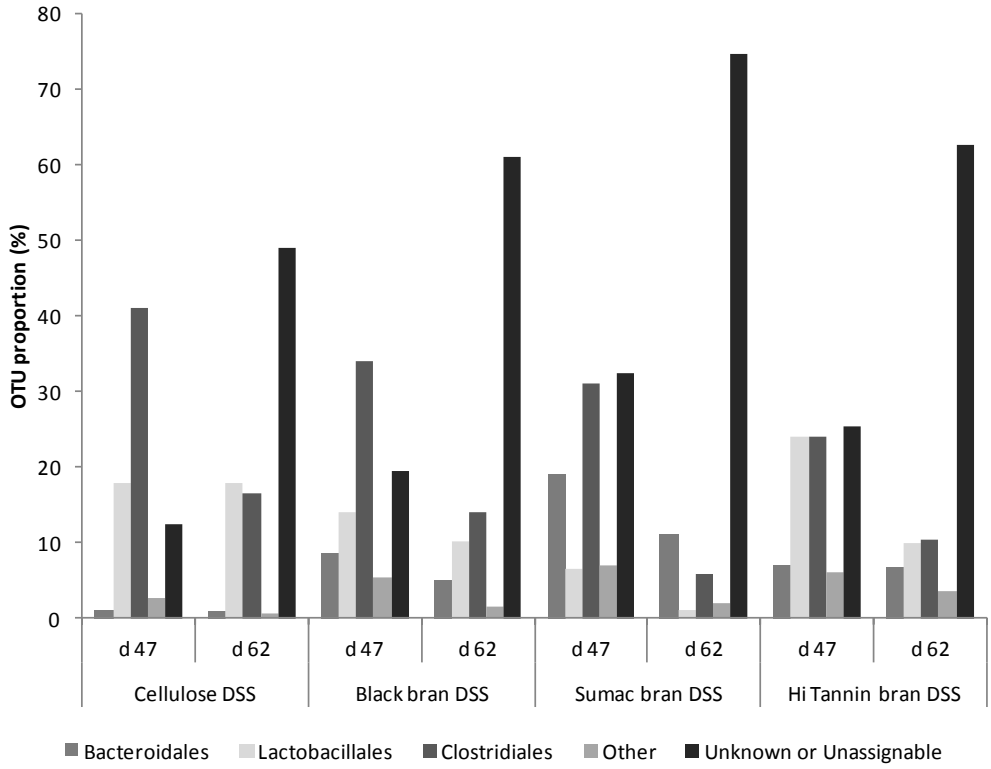

Figure 11. Proportion of OTUs at the order level in DSS treated animals over time. On d 62 (post DSS#3), proportions of OTUs classified in Bacteroidales, Clostridiales, and Lactobacillales were reduced in DSS treated rats compared to d 47 (post DSS#2) for all experimental diets. Actual values found in Table 10.

Table 10. Phylogenetic classification of samples at the order level on d 47 and d 62. On d 62, proportions of OTUs classified in as Bacteroidales, Clostridiales, and Lactobacillales were reduced in DSS treated rats compared to d 47 (post DSS#2) for all experimental diets, with the highest reduction observed in the Clostridiales order. Means without common superscripts differ ($p<0.05$).

		Cellulose		Black bran		Sumac bran		Hi Tannin bran				
			DSS (n=9)		DSS (n=9)		DSS (n=10)		DSS (n=10)	Diet		
Day 47 (Post DSS#2): Order level classification (% OTUs)	Bacteroidales		1.31±0.60^{a}		8.59±2.71^{b}		19.29±2.75^{c}		7.30±2.37^{ab}	<0.0001		
	Lactobacillales		18.19±6.73^{ab}		14.08±3.44^{ab}		6.54±2.17^{a}		24.18±4.14^{b}	0.0417		
	Clostridiales		41.90±5.68^{b}		34.26±3.30^{ab}		30.96±3.32^{ab}		23.72±3.04^{a}	0.0205		
	Erysipelotrichales		1.93±0.52^{a}		3.95±0.79^{ab}		4.95±1.33^{b}		4.23±1.23^{ab}			
	Burkholderiales		0.69±0.18^{a}		1.48±0.32^{ab}		1.99±0.50^{b}		2.24±0.54^{b}			
	Unknown		7.97±1.43^{a}		10.88±1.69^{ab}		16.49±2.38^{b}		13.31±2.90^{ab}			
	Unassignable		4.50±0.51^{a}		8.51±0.91^{ab}		15.95±1.73^{c}		12.44±2.88^{bc}	0.0007		
		Control (n=5)	DSS (n=10)	Control (n=5)	DSS (n=9)	Control (n=5)	DSS (n=10)	Control (n=5)	DSS (n=9)	Diet	DSS	Diet* DSS
Day 62 (Post DSS#3): Order level classification (% OTUs)	Bacteroidales	0.44±0.23^{a}	0.76±0.17^{a}	4.83±0.84^{ab}	4.81±1.66^{ab}	23.59±4.72^{d}	11.19±0.80^{c}	15.85±3.36^{c}	6.69±0.58^{b}	<0.0001	<0.0001	0.0005
	Bacillales	0±0.00^{b}	0±0.00^{b}	0±0.00^{b}	0±0.00^{b}	0±0.00^{b}	0±0.00^{b}	3.22±3.22^{a}	0±0.00^{b}			
	Lactobacillales	30.73±3.90^{d}	17.96±5.00^{c}	6.87±3.55^{ab}	10.27±3.25^{bc}	3.20±1.68^{ab}	1.11±0.43^{a}	19.61±2.21^{cd}	9.94±1.94^{bc}	<0.0001	0.0377	0.1019
	Clostridiales	12.37±4.25^{bc}	16.61±1.60^{c}	14.24±1.09^{bc}	13.21±1.98^{bc}	16.41±2.95^{c}	5.80±0.45^{a}	23.46±2.2^{d}	10.29±0.78^{ab}	0.0387	0.0005	<0.0001
	Erysipelotrichales	0.22±0.16^{a}	0.51±0.18^{a}	0.93±0.44^{abc}	0.64±0.26^{ab}	2.14±0.60^{c}	1.17±0.26^{abc}	4.2±1.23^{d}	1.71±0.46^{bc}			
	Burkholderiales	0.14±0.09^{a}	0.11±0.04^{a}	0.37±0.10^{a}	0.81±0.28^{ab}	2.99±0.54^{d}	0.87±0.27^{ab}	1.72±0.43^{bc}	1.82±0.60^{c}			
	Unknown	20.61±3.28^{a}	27.51±2.39^{b}	39.43±2.55^{d}	33.28±1.84^{cd}	28.10±4.10^{bc}	45.15±0.63^{de}	15.80±2.35^{a}	36.37±1.40^{d}	<.0001	<.0001	<.0001
	Unassignable	16.92±0.93^{b}	21.44±1.19^{c}	27.48±1.03^{de}	25.68±1.22^{d}	19.80±3.41^{bc}	29.50±1.26^{e}	10.38±1.41^{a}	26.28±0.87^{de}	<.0001	<.0001	<.0001
		†Data represents predominant phylogenetic groups (>1%) and are LS mean±SEM										

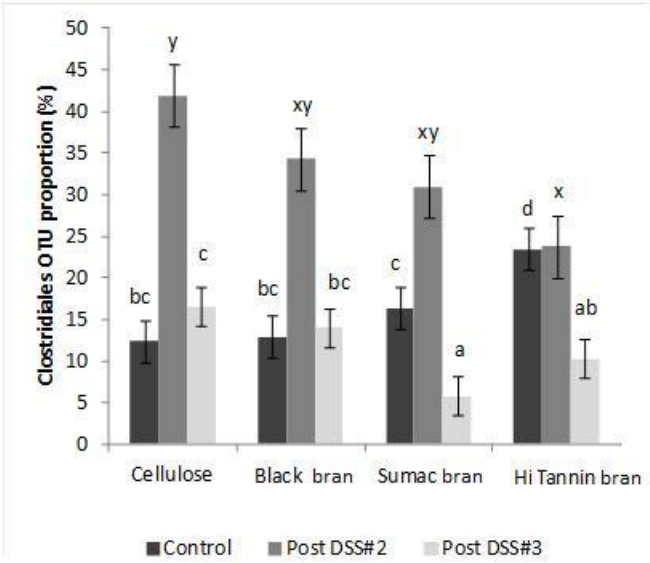

Figure 12. Proportion of OTUs classified in the Clostridiales order. On d 62 (post DSS#3) the Clostridiales order was reduced in DSS treated rats compared to d 47 (post DSS#2) for all experimental diets. Data are LS±SEM. Means without common superscripts differ ($p<0.05$). Actual values found in Table 10.

Sumac controls had numerically lower species richness and diversity indices compared to all other experimental diets. Following DSS#2 (d 47), we observe no significant differences in bacterial diversity between Cellulose, Black, Sumac or Hi Tannin bran DSS rats. Sumac DSS rats had a significantly lower species richness compared to Cellulose, Black and Hi Tannin bran DSS rats ($p<0.05$) at this time point. DSS treated rats on d 47 had numerically lower species richness and diversity indices. However, on d 62 there was an increase in diversity (13.6-25%) and species richness (39-62%) compared to d 47 for Cellulose and Black, Sumac and Hi Tannin bran DSS rats (Table 11).

On d 62, we observe a significant diet*DSS effect on species richness and diversity ($p<0.0001$ and $p=0.0003$, respectively), in which Cellulose and Black bran DSS rats had a significantly lower Chao compared to their diet-matched controls ($p<0.05$). Sumac bran DSS rats had significantly higher richness ($p=0.0199$) and numerically higher diversity index compared to Sumac controls, and Hi Tannin DSS rats had significantly higher richness and diversity indices ($p<0.001$ and $p=0.013$, respectively) compared to Hi Tannin controls at this time point (Table 11).

DSS induced injury of distal colon

DSS treatment elevated injury scores in rats consuming all experimental diets, with significantly higher increases in scores observed in Hi Tannin DSS rats compared to Hi Tannin control rats ($p=0.0072$, Chapter II). DSS treated rats fed bran diets had significantly higher injury scores compared to Cellulose DSS rats ($p<0.05$). Cellulose controls had the lowest injury scores, which were significantly lower than Black and Sumac bran controls ($p<0.05$).

Correlation between phylogenetic data and colonic injury score

The proportion of OTUs classified in each taxa were correlated to colonic injury score and significant correlations were observed for three phylogenetic groups (Table 12). At the phylum level, both Firmicutes and Actinobacteria negatively correlated to colonic injury ($p=0.003$ and $p=0.019$). Within the Firmicutes phylum, all classified taxa at the order level (i.e., Clostridiales, Erysipelotrichales, Lactobacillales) negatively correlated to colonic injury and was significant for Lactobacillales ($p=0.045$). The

Table 11. Chao and Shannon Weaver indices for all treatment groups on d 47 and d 62. Sumac DSS rats had significantly lower species richness compared to Cellulose, Black and Hi Tannin bran DSS rats on d 47. On d 62 Cellulose and Black bran DSS rats had a significantly lower and Sumac and Hi Tannin had significantly higher Chao compared to their diet-matched controls. Black bran DSS had a significantly lower and Hi Tannin DSS rats had a significantly higher diversity index compared to their diet matched controls on d 62. Means without common superscripts differ ($p<0.05$).

		Cellulose		Black bran		Sumac bran		Hi Tannin bran				
			DSS (n=9)		DSS (n=9)		DSS (n=10)		DSS (n=10)	Diet		
Day 47	Chao		117.33±4.78^{b}		124.74±6.23^{b}		92.76±2.12^{a}		112.98±5.91^{b}	0.0005		
	Shannon Weaver index		4.00±0.18^{a}		4.35±0.16^{a}		4.17±0.08^{a}		4.17±0.12^{a}			
		Control (n=5)	DSS (n=10)	Control (n=5)	DSS (n=9)	Control (n=5)	DSS (n=10)	Control (n=5)	DSS (n=9)	Diet	DSS	Diet* DSS
Day 62	Chao	207.32±14.08^{d}	169.29±5.45^{c}	222.91±12.47^{d}	173.79±14.27^{c}	118.27±6.85^{a}	155.08±6.87^{bc}	133.45±13.05^{ab}	210.40±9.17^{d}	<0.0001		<0.0001
	Shannon Weaver index	4.79±0.33^{cd}	4.86±0.15^{c}	5.82±0.04^{a}	5.13±0.15^{bc}	4.39±0.14^{d}	4.78±0.08^{cd}	4.73±0.16^{cd}	5.5±0.10^{ab}	<0.0001		0.0003
		Data are LS mean±SEM										

abundance of OTUs classified as “Unknown” or “Unclassified” (OTUs that did not match any known sequences in the RDP database) both positively correlated to colonic injury (both p=0.003, Table 12).

Discussion

The intestinal microbiota is composed of trillions of bacteria and over 400 individual species have been identified thus far. These bacterial populations provide numerous benefits to the host including immune system development, epithelial barrier maintenance, and providing fuel for colonocytes (6, 35-36, 71, 110). It is now understood that perturbations to the microbiota is involved in the onset and recurrence of intestinal inflammation and an important factor in the etiology of inflammatory bowel diseases (IBD) such as ulcerative colitis (UC) (45, 96-97, 171, 173). Another environmental input that has been shown to affect the microbiota is diet composition, and recent focus has been put on bioactive compounds and their possible role in mitigating the deleterious effects of intestinal inflammation (16-17, 19, 39, 143, 208-209).

Table 12. Correlation of intestinal microbiota and colonic injury score with significant coefficients indicated ($p<0.05$).

Taxon		Correlation coefficient
Actinobacteria		-0.308†
Bacteroidetes		0.076
	Bacteroidales	0.049
Firmicutes		-0.387†
	Clostridiales	-0.123
	Erysipelotrichales	-0.096
	Lactobacillales	-0.264†
Proteobacteria		-0.012
	Burkholderiales	0.08
Unknown		0.382†
Unclassified		0.387†

†Indicates phylogenetic groups which proportion correlated significantly to injury score

Previous work in our lab demonstrated that sorghum bran diets containing bioactive compounds can alter fecal short chain fatty acid (SCFA) concentrations, a microbial metabolite, suggesting the ability to alter the composition of the microbiota or microbial fermentation (198). PCA analysis from this study suggests that there are distinct bacterial communities in animals fed experimental diets containing Cellulose, Black, Sumac or Hi Tannin bran diets. Additionally, samples collected at different time points (post DSS#2 and DSS#3) also grouped in different quadrants of the plot, suggesting DSS treatment and colonic inflammation also creates distinct microbial

populations. Little research has been done to understand how the bioactive compounds found in sorghum (i.e., 2-deoxyanthocyanins and condensed tannins) can alter the luminal environment, particularly the intestinal bacterial populations. Therefore the goal of this work was to characterize alterations to the microbiota during DSS induced colitis and determine if these diets have the ability to mitigate the dysbiosis associated with UC.

Intestinal microbiota composition in UC

Although ample research has been done to understand the role of the microbiota in UC, it is becoming more apparent that not one constituent of the intestinal flora is to blame. However, global shifts and overall dysbiosis in the ratio of predominant bacterial populations (i.e., Firmicutes and Bacteroidetes phylum) have been observed in patients with IBD. An increased Firmicutes to Bacteroidetes ratio has been documented in both feces and biopsies of IBD patients and experimental models of obesity and UC (194-195, 210-211). In our study we do not observe an elevated Firmicutes/Bacteroidetes ratio in DSS treated animals fed a bran based diet at either time point, suggesting that DSS exposure didn't drastically alter these phyla. Furthermore, when comparing healthy and diseased animals fed a bran diet we do not see a marked difference in this ratio. The Firmicutes/Bacteroidetes ratio observed in Cellulose fed animals (both control and DSS) was at least ten fold higher than that of bran fed animals, which could be in part due to the presence of cellulose fermenting bacterial species within this phylum (e.g., *Ruminococcus* spp.) (212). Additionally, this result could suggest that properties of bran, such as the presence of bioactive compounds, may be involved in maintaining a healthy distribution of bacteria during colonic inflammation.

A recent review documented the numerous changes observed in experimental models and patients with IBD, and no agreement has been reached on the association of specific microbial groups and UC (213). Studies have documented elevated levels and enhanced epithelial adherence of pathogenic bacteria species (e.g., *E. coli*) in patients with IBD and DSS induced colitis (100). Our study contrasts this report, as we observe less than 5% of OTUs classified in the Proteobacteria phylum at both time points. A low proportion of this phylum following DSS exposure is positive, since it includes numerous pathogenic genera such as *Escherichia*, *Salmonella*, *Vibrio*, and *Helicobacter*.

Previous studies in experimental models and patients with UC have also documented a depletion in bacterial species that provide benefit to the host such as Bifidobacterium and Lactobacillus (96, 100, 195), which produce antimicrobial substances and compete with pathogens for epithelial and mucin binding sites (214). Furthermore, it has been demonstrated that supplementation of these probiotic species has helped attenuate symptoms and maintain remission of UC (123-124, 215). In this study, we observe virtually undetectable levels of OTUs classified in the Actinobacteria phylum (≤0.80%), suggesting Bifidobacteria is not a major constituent of the microbiota in any of our experimental groups. However, we do observe significant diet and treatment effects on the proportion of OTUs classified in the Lactobacillales order. During an active disease state (following DSS#2), we observe significantly higher proportion of this order in Hi Tannin DSS animals compared to Cellulose, Black and Sumac bran DSS animals. However, following DSS#3, we observe a suppression of the Lactobacillales order in DSS treated animals fed Cellulose, Sumac and Hi Tannin bran

diets, which is similar to other reports in patients and experimental models of UC that documented a suppression of LAB (100). In contrast, Black bran DSS animals had numerically elevated proportion of Lactobacillales compared to their diet matched controls at both time points, suggesting that the presence of 3-deoxyanthocyanins may have a positive influence on maintaining this bacterial population.

Alterations in other bacterial populations that are prevalent constituents of the commensal intestinal flora have been reported in experimental models and patients with UC, and both an elevation and suppression have been observed in species such as *Bacteroides* and *Clostridium* in feces and colonic tissue (172, 216-219). Similarly, when comparing healthy and diseased animals in our study we observe both increased and decreased proportions of numerous bacterial populations at the order level that differ across experimental diets. For example, following DSS treatments (both d 47 and d 62) diseased animals fed Sumac and Hi Tannin bran had a lower proportion of bacterial populations such as Bacteroidales and Clostridiales, while DSS animals fed Black bran had an elevated proportion of these and other bacterial groups (i.e., Bacteroidales, Lactobacillales, Clostridiales, and Burkholderiales) compared to their diet matched controls. Previous studies reported elevations in Clostridiales and Lachnospiraceae (a bacterial family within Clostridiales) during DSS induced colitis, which is similar to our observations in Black bran DSS animals (100, 211). To better understand how the predominant bacterial populations were fluctuating during different stages of inflammation, we compared DSS treated animals on d 47 (post DSS#2) to d 62 (post DSS#3) and observe distinct differences across experimental diets. Decreased

proportions of the Bacteroidales, Clostridiales, and Lactobacillales orders were observed in DSS animals for all experimental diets following DSS#3, with the highest reduction observed in the Clostridiales order (56%-79%). The Clostridiales order is of particular importance, as it harbors bacterial species that have the ability to produce important bacterial metabolites such as butyrate (220-221). Alterations to this particular population could be detrimental to colonic health, as butyrate is not only the predominant fuel for colonocytes, but suppressed availability and uptake of this metabolite have been implicated in the etiology of IBD (177, 179-180, 222).

As demonstrated in this study and the literature, both elevated and suppressed proportions of various bacterial populations have been observed in patients and experimental models of UC (100, 211, 213, 216-219). Observed differences could be due, in part, to the progression of inflammation or severity of epithelial barrier injury in these subjects and the animals in this study. It has been previously reported that areas of inflammation harbor different bacterial populations than non-inflamed tissues from the same individual, suggesting that the variations we observe could be dependent on disease state (96-98). Additionally, previous studies have shown correlations between bacterial populations and disease severity which can further elucidate the relationship between the microbiota and UC. We report a negative correlation between colonic injury and numerous phylogenetic groups, including significant correlation to Firmicutes, Actinobacteria, and Lactobacillales. Similar to our results, one study reported that the abundance of certain taxa in the Firmicutes phylum (i.e., Clostridium clusters IV and IX) were negatively correlated to disease symptom score (e.g., abdominal pain, distention) in

patients with irritable bowel syndrome (194). In contrast to our results, another study illustrated a positive correlation between the abundance of cecal *E. coli* and histologic colon score in HLA-B27 transgenic rats (223). Our results could differ from previous studies due to the experimental model utilized, tissue analyzed (i.e., feces versus colonic tissue), and phylogenetic characterization technique differences (e.g., FISH, T-RFLP, DGGE, microbiological culture). Further analysis can be done to further characterize the composition of bacterial populations, particularly probiotic bacterial taxa such as Bifidobacteria and LAB. Utilizing species specific PCR probes and identifying closest neighbors to unclassified and unidentified OTUs will further elucidate the significance of these bacterial groups and their relation to colonic injury in our experimental groups.

Although we observed a decrease in the predominant bacterial orders on d 62, there was not a reduction in bacterial diversity and species richness at this time point, which is a common observation in patients with UC and DSS induced colitis (99-100, 172, 193, 211). Following the second DSS treatment, we observed a decrease in both species richness and diversity; however, the values of these indices are elevated following recovery from DSS#3. Furthermore, following all DSS exposures diseased animals fed brans containing condensed tannins (i.e., Sumac and Hi Tannin bran) had bacterial richness and diversity that was higher than their diet matched controls. Black bran DSS rats were unable to fully restore richness and diversity, but Black bran controls had numerically higher indices compared to other experimental diets and perhaps more recovery time would allow for complete restoration. A diminished flora could be detrimental due to decreased colonization resistance, imbalances in microbial-host

signaling through pattern recognition receptors such as toll like receptors (TLR), as well as allowing for pathogenic bacteria to thrive (224). This data suggests that even though the bacterial populations may be affected during an active disease state, feeding bran based diets, particularly those containing condensed tannins, may be useful to restore diminished bacterial species richness and diversity associated with UC.

Effect of diet and polyphenol composition on the microbiota

In addition to intestinal inflammation, differences in fecal microbial populations in our study could be due to the bioactive compound composition of these sorghum brans. Previous research and analysis of each experimental diet in this study (Chapter II) indicates that bran from these sorghum varieties contain concentrated levels of 3-deoxyanthocyanins, condensed tannins, or a combination of these compounds (Black bran, Sumac Bran and Hi Tannin bran, respectively) (25-26, 117). Due to their high antioxidant capacity and bacteriocidal effects, plant polyphenols similar to those utilized in this study have been studied to mitigate the effects of IBD and also been found to affect the microbiota (9, 14, 16, 121-122, 145, 208, 225). Two previous studies used stock bacterial strains, previously identified as constituents of the intestinal microbiota, and reported that hydrolysable tannins (i.e., gallic acid, methyl gallate, propyl gallate) have inhibitory properties against some *Clostridium* species and potentially harmful bacterial strains such as *C. perfringens, C. paraputrificum, E. limosum, B. fragilis, S. aureus,* and *E. coli* in culture (9, 14). This inhibitory effect could be one reason for the lack of bacterial species characterized in the Proteobacteria phylum in our study (≤4.29%), which as mentioned previously harbors numerous pathogenic bacteria species

such as *S. aureus* and *E. coli*. Furthermore, these studies reported hydrolysable tannins only had slight effect on LAB strains (e.g., *B. infantis*, *L. acidophilus*) (9, 14), which parallels Hi Tannin DSS animals having a significantly higher proportion of Lactobacillales compared to Cellulose, Black, and Sumac DSS animals on d 47. Another study testing the effect of condensed tannins on the GI microbiota *in vivo* also reported similar gram positive bacteria inhibition (16). This study used denaturing gel electrophoresis (DGGE) and reported that tannins derived from the *Acacia angustissima* shrub significantly increased murine fecal bacterial diversity (16). Phylogenetic classification of DGGE bands showed a significant decrease in the *C. leptum* sub-group in rats fed a tannin supplemented diet, while other enteric bacteria such as species classified in the *B. fragilis* and *Bacteroides-Prevotella-Porphyromonas* groups increased significantly (16). Our observations are similar to these reports, as animals fed a bran diet containing tannins (i.e., Sumac and Hi Tannin) had higher proportions of bacteria classified in the Bacteroidales order compared to Cellulose and Black bran fed animals. Interestingly Sumac bran not only contains the highest concentration of tannins, but animals fed this experimental diet had significantly higher proportions of Bacteroidales in controls and on d 47 (Sumac DSS animals) compared to other experimental groups. Other dietary compounds such as tea polyphenols and other flavanoids have been reported to alter the composition of the intestinal microbiota (15, 104). One study observed that Xanthohumol, an antimicrobial flavonoid found in hops, had a significant effect on the diversity of bacterial groups in rat feces using DGGE fingerprint analysis (104). Similar results were observed in a study that characterized how tea polyphenols

affected GI microbial diversity in humans (15). Those that were administered tea polyphenols had decreased proportion of *Clostridium* spp. and an increased proportion of *Bifidobacterium* spp. compared to those that did not consume these polyphenols (15).

Previous studies and our results indicate that plant polyphenols not only have the ability to alter bacterial populations and intestinal diversity, but their effects vary substantially and may be dependent upon the polyphenolic structure and the ability of microbes to metabolize these compounds. Very little is known regarding microbial metabolism of the 3-deoxyanthocyanins and condensed tannins found in sorghum bran. In general, polyphenols are poorly absorbed and therefore available to be catabolized by the colonic microbiota. Microbial metabolism of polyphenols is extremely complex and numerous microbial catalytic and hydrolytic enzymes have been identified [76], therefore a complete description is beyond the scope of this paper. However, unlike other flavonoids, many anthocyanins do not undergo extensive metabolism and their structure is stabilized in acidic conditions (226). Furthermore, condensed tannins such as those described in this study are large non-hydrolysable proanthocyanindins, with three or more polymerizations, that are not easily fractionated by water and tannases (227). One study demonstrated that condensed tannins isolated from sorghum bran were only isolated in excrement and not absorbed in chickens (228). Furthermore, both animal and human studies have shown that anthocyanins from berries (i.e., bilberry & raspberry) are poorly absorbed in the small intestine and typically <0.1% of the quantities ingested are detected in urine within 24 h of consumption (229-230). This implies that although the gut and its microbiota may be closely involved in the metabolism of some polyphenols,

previous studies report that compounds similar to those found in this study may not be absorbed or metabolized and therefore concentrated in the intestinal lumen. Metagenome and metabolomics analyses may help elucidate the relationship of the microbiota and the bioactive compounds found in sorghum, however, due to the large number of genes and metabolites identified in these analyses it could be quite difficult to elucidate the biomolecular mechanisms involved in the observed beneficial effects.

Conclusions

To our knowledge, there are no studies that describe the effect of sorghum bran on the microbiota. We demonstrate that sorghum bran diets may be able to mitigate some of the deleterious effects associated with UC, such as preventing an overall dysbiosis of predominant bacterial populations and decreased microbial diversity. Furthermore, we observe distinct differences among experimental diets suggesting that the presence of bioactive compounds such as 3-deoxyanthocianins and condensed tannins may be a factor in these diets ability to alter the luminal environment and microbial populations. Additional analysis such as species-specific bacterial primers could elucidate additional population changes not captured in this study. Future studies elucidating mechanisms by which these bioactive compounds affect the intestinal microbiota during a healthy and diseased state are warranted.

CHAPTER IV

INCREASED DIETARY IRON AND RADIATION IN RATS PROMOTE OXIDATIVE STRESS, INDUCE LOCALIZED AND SYSTEMIC IMMUNE SYSTEM RESPONSES, AND ALTER COLON MUCOSAL ENVIRONMENT

Introduction

Iron is a micronutrient involved in many cellular processes, including oxygen binding and electron transport, and it serves as a cofactor for hundreds of enzymes. As with many nutrients, a sensitive balance exists between the deleterious effects of iron deficiency and iron excess (231). Physiological adaptations to microgravity and an iron-rich food supply contribute to altered iron homeostasis during space flight (232-233). A decrease in red blood cell mass during flight, an increase in serum ferritin, and a decrease in transferrin receptors after long-duration flight provide evidence for increased iron storage as a result of space travel (233-236). Additionally, the astronauts' diet may also contribute to increased iron stores because the iron content of many items on the International Space Station (ISS) menu is very high due to fortification (232).The standard ISS menu contains 20 ± 6 mg iron/d (232, 237), with some crews' intake occasionally being as high as 47 mg iron/d (232). The current U.S. Dietary Reference Intake (DRI) is 8 mg/d for males and 10 mg/d for females, and the tolerable upper limit of intake is 45 mg/d (238). For ISS astronauts, the defined space flight requirement is 8-10 mg/d for both men and women (232, 237). It is worth noting that the typical American consumes 30 - 120% more than the DRI depending on gender (239), making

chronic subclinical iron overload a potential issue for the general public. Elevated iron stores have been associated with a number of diseases, including cardiovascular disease and cancer (240-242), and reduced stores (related to blood donation) have been associated with lower disease risk (243-244). Thus, maintenance of iron homeostasis within normal ranges is extremely important for human health on Earth, and in space.

In addition to the physiological effects of microgravity on the human body, radiation exposure is a major concern for space travel. The free radicals, including reactive oxygen species (ROS), which are generated in cells immediately after radiation exposure are responsible for deleterious effects on cell function and survival (245). In animal models, exposure to ionizing radiation (ranging from 0.1 Gy to 8 Gy) increases oxidative damage in many tissues (246-248). Risks associated with radiation exposure in space include central nervous system effects, carcinogenesis, and other degenerative tissue defects such as cataracts, heart disease, and digestive diseases (249-251).

Elevated iron stores and radiation are expected to promote oxidative stress and damage, as both generate ROS (252-253). Elevated oxidative stress associated with increased body iron stores may increase radiation sensitivity by decreasing cellular oxygen radical scavenging capabilities of enzymes like superoxide dismutase (SOD), glutathione peroxidase (GPX), and catalase (254-256). Evidence also exists that some types of radiation exposure and oxidative stress can release ferrous iron (Fe^{2+}) from ferritin (257-258), further adding to free iron load.

The effects of oxidative stress on immunity can be both localized and systemic. The local immune response in the gut is an important defense against pathogens. The

intestinal immune system must recognize commensal bacteria while preserving its capacity to respond to pathogenic species (259). The gut monitors bacterial populations by recognizing pathogen-associated molecular patterns (such as bacterial ligands including lipopolysaccharide, ligand presenting assembly, and flagellin), thereby inducing innate and adaptive immune responses (260-261) that are mediated through toll-like receptors TLR (262-263) and downstream activation of NF-κB. Changes in the molecular patterns produced by the commensal colon microflora or the ratio of pathogenic to beneficial bacteria (dysbiosis) caused by elevated dietary iron and radiation may perturb these activation pathways, inducing transcription of proinflammatory cytokines (e.g., TNFα, IL-1b, IL-6, and COX-2) that initiate inflammatory reactions with systemic implications (264-265). Interestingly, previous research has shown that agonists of the TLR5 pathway have radioprotective effects against lethality (266). Colonic dysbiosis has long-term implications because an increased inflammatory tone is thought to play a role in the etiology of gastrointestinal disorders such as inflammatory bowel disease, which promotes colon carcinogenesis (267-269). Changes in the microbiota and their functional state can be monitored by measuring their metabolites, such as short-chain fatty acids (SCFA) (270). In addition to indicating changes in the microbiota, the concentrations of SCFA, such as butyrate, influence colon health and ability to maintain epithelia barrier functions, because butyrate is the preferred substrate for colon epithelial cell metabolism (271-272).

Persistent alterations to the immune system may also have adverse systemic effects on immune function. Reactive species are produced as a normal consequence of

immune activation or inflammation. In the immune system, these reactive molecules are actually beneficial, supporting pathogen elimination through respiratory bursts that are balanced by antioxidant production by immunocytes. Chronic inflammation, however, may overwhelm antioxidant defenses and lead to cellular damage as described above. Persistent exposure to space radiation may induce a chronic low level of inflammation in astronauts. Plasma cytokine data during long-duration space flight suggests this, with levels of IL-8, CXC5, and IL-1ra significantly elevated for the duration of a 6-month orbital flight**.** Oxidative stress also negatively affects T-cell function (273), and diminished T-cell function was recently documented to occur during space flight (274)**.** Investigators have also found reactivation of latent herpes viruses during short-duration flight (275-276), and oxidative injury is a component of several neurotropic viral infections (277)**.** The extent to which oxidative damage plays a beneficial role, versus a pathologic role, in viral infection is an emerging area of investigation. Dysregulation of other hematologic and immunologic variables has also been found to occur immediately after space flight (278-279), and altered cell-mediated immunity has occurred during long-duration flight (280). Any persistent immune dysregulation during exploration deep-space missions might result in specific clinical risks for crewmembers (281).

In this study, we characterized the combined effects of radiation exposure and high dietary iron on multiple physiological systems. Specifically, we investigated the effects of these treatments on: 1) iron status and oxidative stress markers, 2) systemic immune responses, 3) production of colon bacterial metabolites, and 4) colon mucosal gene expression and inflammatory markers. These systems will be used to develop an

integrated physiological response to the effects of radiation and high dietary iron as they relate to space flight.

Materials and Methods

Animals used in this study were housed, irradiated, and terminated at the animal test facility at Johnson Space Center. Following tissue collection, described below, feces and colonic mucosa was transported to the Turner lab at Texas A&M University for analysis. Remaining analyses, including biochemical analyses and immune system assays of liver, blood, and serum, were completed at Johnson Space Center.

Animals

This project was approved by the NASA Johnson Space Center Institutional Animal Care and Use Committee. Four groups (*n*=8/group) of 4-month-old Sprague Dawley male rats (Charles River Laboratories, Wilmington, MA, USA) were fed a control iron diet (45 mg iron/kg diet) and exposed to sham (0 Gy) radiation (control/sham, designated CON), fed a high-iron diet (650 mg iron/kg diet) and exposed to sham radiation (high iron/sham, designated IRON), fed the control iron diet and exposed to fractionated (0.375 Gy of Cs-137 every other day for 16 d for a total of 3 Gy) radiation (control/radiation, designated RAD), or fed a high-iron diet and exposed to fractionated radiation (high iron/radiation, designated IRON+RAD).

After arrival at the animal test facility at Johnson Space Center, rats were acclimated to the environment and control diet (AIN-93G; Research Diets, New Brunswick, NJ, USA) for 20 d (Day -20 to Day 0). They were housed individually with a 12-h light/dark cycle, in a temperature- and humidity-controlled room (21 ± 1°C). After

20 d (defined as study day 0), half the animals were given the high-iron diet (AIN-93G with 650 mg iron /kg; Research Diets, New Brunswick, NJ, USA). Food intake was determined three times per week to ensure that food consumption and animal weights were similar between groups, and that pair-feeding was not required. On study day 14 the first radiation dose was administered to the radiation groups. Animals in both the sham and radiation groups were placed in a restraint tube (Battelle, Geneva, Switzerland) for about 10 min per session to be either irradiated or sham treated. The last irradiation was performed on study day 28.

Treatments

The dietary iron content of 650 mg iron/kg has been used by others as a moderately high iron intake known to induce oxidative damage (282). The low, fractionated dose of gamma radiation was intended to provide enough total dose (3 Gy) to induce an oxidative stress signal, and also to approximate the level of radiation exposure expected over a long-duration space mission outside low Earth orbit (283). Based on recent radiation measurements taken during the rover Curiosity's trip to Mars, the calculated radiation exposures of the shortest round trip to Mars are estimated to be 0.66 ± 0.12 sievert (or about 0.66 Gy of gamma irradiation) (284).

Tissue collection

At the time of termination (24 h after the last radiation exposure) all animals had been fasted for 12 hours, and were anesthetized with isofluorane before blood was collected by cardiac puncture. Samples of liver, colon mucosa, and feces were collected. The liver was removed, weighed, rinsed with phosphate-buffered saline (PBS), sectioned

into small pieces, placed in cryovials, and flash frozen in liquid nitrogen. All tissues and samples were stored at -80ºC until further processing. Samples of the blood were placed in lithium-heparin, ethylenediaminetetraacetic acid (EDTA), or serum separator tubes. Whole blood (EDTA) was used for erythrocyte count and leukocyte analyses. Samples were centrifuged at 3500 RPM (1780 x *g*) for 15 min, then aliquoted for individual tests.

The colon was resected, feces were removed and snap frozen at -80°C, and the colon was washed twice in RNase-free PBS and scraped on a chilled RNase-free surface. Half of the scraped mucosa was homogenized by pipetting with 500 μL of denaturation solution (Ambion, Austin, TX) and transferred to a 2-ml Eppendorf tube for RNA isolation. The remainder was snap frozen in liquid nitrogen, and both samples were stored at -80°C. Scraped mucosa for RNA analysis was homogenized in denaturation buffer (285).

Biochemical analyses

Biochemical analyses and immune system assays were performed at Johnson Space Center.

Liver protein and mineral analysis

For protein assays, a ~0.2-g section of liver was homogenized in buffer (20 mM HEPES, 1 mM ethylene glycol tetraacetic acid, 90 mM mannitol, and 70 mM sucrose). Samples were centrifuged at 3500 RPM (1780 x *g*) for 15 min, and the supernatant was aliquoted for SOD, catalase, GPX, and total protein analysis. Samples were stored at -80°C until assays were performed. For mineral analysis, a ~0.2 g section of liver was dried at 70°C for 24 h (Fisher Scientific Isotemp oven) and the dry samples were

weighed and then placed in acid-washed Teflon microwave digestion vials with 2 ml of ultrapure nitric acid (Aldrich, St. Louis, MO, USA). Samples were digested using a CEM MARS XP1500Plus microwave digestion system using the method designed for bovine liver (ramp to 200°C over 15 min and hold at 200°C for 15 min). Samples were clear with low surface tension after cooling. Samples were transferred to centrifuge tubes, using 3 ml of 18 MΩ water to rinse the Teflon digestion vessels, and weighed. Samples were diluted 1:50 with 10% nitric acid and 10% ethanol for mineral analysis on an inductively coupled plasma mass spectrometer (SCIEX ELAN DRC II, Perkin Elmer Inc., Waltham, MA, USA). Copper, iron, selenium, and zinc were measured using gallium as the internal standard. Process blanks revealed that there was no significant contamination of Cu, Fe, Se, or Zn during processing.

Oxidative stress and iron status analyses

Whole-blood SOD and catalase were measured colorimetrically using commercially available kits (Cayman Chemical Company, Scottsdale, AZ, USA). Whole-blood GPX was measured on an Ace Alera autoanalyzer using the Randox GPX method and reagents (Randox, Crumlin, United Kingdom). Serum ferritin was measured using a commercially available rat ferritin ELISA assay (Alpco Immunoassay, Salem, NH, USA). Plasma iron was measured using a Beckman Coulter AU analyzer. Plasma heme was measured using the Quantichrom Heme Assay Kit, from BioAssay Systems (Hayward, CA, USA). Serum C-reactive protein was measured using the Rat C-reactive Protein ELISA kit from EIAab (Wuhan, China). Serum n-telopeptide was measured using a Rat NTX ELISA Kit from Cusabio (Wuhan, China). Oxidized low-density

lipoprotein was measured using a Rat OxLDL ELISA Kit from Cusabio (Wuhan, China). Serum total antioxidant capacity was measured using Randox reagents on a Beckman Coulter AU analyzer, with a blank measurement being taken of each sample before reagents were added. This allows subtraction of any contribution from urate, ascorbate, and albumin. Liver total protein was measured using the Pierce® BCA protein assay kit from Thermo Scientific (Rockford, IL, USA). Hematocrit was measured on a Coulter LH750 hematology analyzer (Coulter, Brea, CA, USA).

Immune system assays

Leukocyte subset analysis

Total leukocyte count was determined after erythrocyte lysis using a Hemocue leukocyte analyzer with a DNA intercalating dye. The major subsets (granulocytes, lymphocytes, monocytes) were determined by analysis on a Beckman Coulter LH750 hematology analyzer. The percentages of T cells and CD4+ and CD8+ T-cell subsets were determined by flow cytometry. The antibody matrix and fluorescent labels were as follows: CD8, fluorescein isothiocyanate (FITC); CD3, phycoerythrin (PE); CD4, phycoerythrin cyanin 5 (PC5) (Beckman Coulter, Miami, FL, USA). Antibody staining and erythrocyte lysis were performed as previously described (274), and analysis was performed on a Beckman-Coulter EPICS XL flow cytometer. Lymphocytes were resolved and gated from granulocytes and monocytes by scatter properties (FSC/SSC). T cells (CD3+) were resolved and gated from unstained cell populations by plotting CD3 versus side scatter from the lymphocyte gate. CD4+ and CD8+ T cells were plotted and enumerated from the T-cell gate.

T-cell blastogenesis

T cells were activated by culturing 100 µl of heparinized blood in 1.0 ml RPMI medium and 0.5 µg/ml each of anti-CD3 and anti-CD28 for 24 hours to trigger the T-cell receptor (TCR) and provide co-stimulation (anti-CD28) (286). Cultured whole blood was then stained as described above, using an anti-CD25-FITC, CD3-PE, CD4-PC5 antibody matrix. Lymphocytes were resolved and gated from granulocytes/monocytes by scatter properties (FSC/SSC). T-cell subsets were resolved and gated from unstained cell populations by plotting CD3 versus CD4 from the lymphocyte gate. Finally, CD25 expression for both the CD4+ and CD8+ (defined as CD4 negative) T-cell subsets were plotted from the appropriate gates.

Mitogen-stimulated cell cultures

Whole-blood cultures (heparinized blood) were set up as described above, with mitogenic stimulation generated by 0.5 µg/ml anti-CD3 and 0.5 µg/ml anti-CD28 antibodies (T cells), 10 ng/ml PMA+ 2.0 µg/ml ionomycin (a stronger stimulus affecting all cell populations), or 10 µg/ml lipopolysaccharide (monocytes). Cultures were incubated for 48 h to allow for cytokine production and accumulation. After 48 h, supernatants were removed and frozen until they were analyzed.

Cytokine analysis

Concentrations of soluble cytokines, from either plasma or mitogen-stimulated culture supernatants, were determined by using bead-array technology and a Luminex-100 analyzer. The analysis array was obtained from R&D Systems, Inc., and consisted of

separate bead-based cytokine analysis reagents for IL-1b, IL-6, TNFα, IL-2, IFNγ, IL-4, and IL-10.

Fecal and colon analyses

All fecal and colon analyses were performed and data analyzed by the Turner lab group at Texas A&M University.

Short-chain fatty acid analyses

Frozen fecal samples were ground, mixed with an internal standard (2-ethylbutyric acid), and extracted in 70% ethanol. After centrifugation, the supernatant was removed and mixed with a second internal standard, heptanoic acid, before it was injected into an HP-FFAP column (Agilent Technologies, Santa Clara, CA, USA) in a Varian 3900 gas chromatograph (Walnut Creek, CA, USA). Concentrations of short-chain fatty acids were calculated based on comparison of sample peak areas with those produced by a commercially available mix of standards (287).

Gene expression using quantitative real-time PCR

Total RNA was isolated from mucosal samples using Phase Lock Gel™ tubes (5 Prime, Gaithersburg, MD) and the ToTALLY RNA™ Kit (Ambion, Austin, TX, USA) followed by DNase treatment (DNA-*free*™ Kit, Ambion, Austin, TX, USA) (285). RNA quality was assessed using an Agilent Bioanalyzer before storage of the treated samples at -80°C. First-strand cDNA was synthesized using random hexamers, oligo dT primer (Promega, Madison, WI, USA), and Superscript™ III Reverse Transcriptase, following the manufacturer's instructions (Invitrogen, Carlsbad, CA, USA). RT-PCR was performed on select genes (TOLLIP, TFF3, Slc16a1, IL-6, IL-1β, TNFα, TNFα1a,

TNFα1b, RipK1, SLC5A8, TGFβ, TLR9, TLR5, TLR4, TLR2, MyD88, NF-κB, COX-2 [PTGS2]) using Taqman® Array Micro Fluidic Cards (Applied Biosystems, Foster City, CA, USA) and an ABI 7900 HT thermocycler (Applied Biosystems, Foster City, CA, USA). Expression levels were normalized to GAPDH gene expression.

Myeloperoxidase assay

Myeloperoxidase (MPO) concentration was measured in scraped mucosa according to the manufacturer's instructions (Cell Technology, Inc., Mountainview, CA, USA). Mucosa samples were weighed and homogenized in 250 µl of 1X assay buffer containing 10 mM N-ethylmaleimide then aspirated through a 23-gauge needle twice, and centrifuged at 12,000 x g at 4°C for 20 min. The resulting proteinaceous pellet was homogenized in 500 µl 1X assay buffer containing 0.5% HTA-Br (w/v), sonicated (Sonic Dismembrator, Fisher Scientific, Pittsburgh, PA, USA), and subjected to two cycles of freezing and thawing before being centrifuged at 8,000 x *g* at 4°C for 20 min. The supernatant was incubated with 20 mM 3-amino-1,2,4-triazole (Sigma Chemical, St. Louis, MO, USA) for 60 min, followed by incubation in the dark at room temperature with 50 µl reaction cocktail for 60 min. Fluorescence was measured at 530-570 nm excitation and 590-600 nm emission wavelengths in a fluorescent plate reader with the 1X assay buffer serving as a negative control.

Statistical analyses

Statistical analyses were performed using Stata IC software (v 12.1, StataCorp, College Station, TX, USA) and setting 2-tailed α to reject the null hypothesis at 0.05. Some dependent variables required log transformation to satisfy the required statistical

assumptions. The variables requiring transformation are indicated in the tables. Overly influential observations (i.e., statistical outliers) were excluded from analysis if the standardized residual exceeded ± 1.96 units away from the mean (also identified in the tables).

Data were analyzed by 2-way ANOVA with diet and radiation as the main factors. Pairwise comparisons of all possible pairs were made for all analytes. Pearson correlations were performed on select analytes. For RT-PCR, 2-way ANOVA was run on change in expression ($2^{-\Delta CT}$) relative to reference gene (GAPDH) as the dependent variable. On completion of all analyses, the uncorrected *P*-values were submitted to a single multiple-testing correction (810 hypothesis tests) using the Krieger false discovery rate (FDR) method (288). The FDR was set at 10%, thereby accepting that up to 10% of the rejected null hypothesis may be a result of type 1 error. As this was a small study examining a wide range of analytes, the use of a more conservative FDR value or method (Bonferroni) is not warranted. Unadjusted *P*-values are presented in the tables and text with an asterisk indicating that the results remained significant after adjusting for multiple comparisons. The residuals from Anti: CD3-IFNγ, PMA: IL-1β, and Plasma: IFNγ, IL-10, IL-1β, and IL-4 could not be normalized and therefore statistical analyses were not performed on these assays. Nonetheless, the data are presented in Table 15. All data are presented as mean ± SD.

Results

The following data were collected and analyzed at Johnson Space Center to determine the independent and combined effects of exposure to gamma radiation and

elevated body iron stores on markers of oxidative damage and antioxidant status. Additionally, these data were collected to determine the relationships between oxidative damage markers and markers of immune and liver enzyme function.

Neither high dietary iron nor the radiation exposure changed food intake or body mass gain (data not shown). There were no differences in liver weights at the time of termination [11.07 ± 1.35 g (CON), 10.72 ± 2.02 g (IRON), 11.69 ± 1.33 g (RAD), 12.50 ± 2.51 g (IRON+RAD).

Iron metabolism was significantly altered as a result of both high dietary iron and radiation, as evidenced by both blood (Table 13) and liver analyses (Table 14). Plasma iron concentration increased by 37% in IRON+RAD relative to CON ($P = 0.007$). Liver iron concentrations increased as a result of diet alone ($P = 0.004$), with a 17% increase in the IRON group relative to CON and a 36% increase in the IRON+RAD group relative to RAD. Liver iron and plasma iron were positively correlated for all groups ($r=0.36$, $P = 0.044$, data not shown). In addition to the changes in iron status, several markers of plasma and liver oxidative stress were affected by the dietary iron and radiation exposures. High dietary iron increased plasma catalase ($P = 0.0008$) and liver GPX

Table 13. Blood markers of iron status and oxidative stress. Mean ± SD.

	Outliers	CON	IRON	RAD	IRON+RAD		Main Effect	
Test		.				Diet	Rad	Inter
		Serum						
ALT, U/l	1	25 ± 4 a	24 ± 4 a	21 ± 5 ab	19 ± 2 b*		<0.01*	
AST, U/l	1	102 ± 29 a	113 ± 50 a	87 ± 37 a	82 ± 22 a			
Transferrin, mg/ml	0	1.3 ± 0.2 a	1.4 ± 0.1 a	1.4 ± 0.2 a	1.4 ± 0.1 a			
Ferritin, ng/ml	1	130 ± 70 a	166 ± 45 ab	213 ± 86 b	241 ± 87 b*		<0.01*	
Hepcidin, ng/ml	0	33 ± 6 a	34 ± 11 a	30 ± 13 a	26 ± 9 a			
Oxidized LDL, ng/ml	0	51 ± 16 a	52 ± 21 a	49 ± 20 a	48 ± 18 a			
C-reactive protein, mg/l	0	372 ± 50 a	322 ± 50 b	325 ± 45 b	324 ± 35 b			
N-telopeptide, nM	1	142 ± 37 a	142 ± 25 a	161 ± 44 a	166 ± 46 a			
		Whole Blood						
Hemoglobin, g/l	0	143 ± 6 ab	145 ± 5 b	138 ± 6 a	143 ± 4 ab			
Hematocrit, %	0	42 ± 2 a	42 ± 1 a*	40 ± 2 b	41 ± 2 ab		<0.05	
Oxidized Glutathione, µM	1	7 ± 3 a	9 ± 4 a	10 ± 5 a	9 ± 5 a			
Glutathione Ratio	1	73 ± 35 a	61 ± 15 a	67 ± 21 a	53 ± 42 a			
Peroxidase, U/g hgb	0	507 ± 22 a	484 ± 26 a	498 ± 27 a	481 ± 22 a	<0.05		
Peroxidase, U/ml	0	72 ± 2 a	70 ± 3 ab	69 ± 2 b	69 ± 2 b*		<0.05	
RBC Folate, ng/ml	0	936 ± 66	942 ± 59	978 ± 54	899 ± 81			
		Plasma						
Iron, µmol/l	1	25 ± 6 a	32 ± 7 ab	34 ± 12 b	47 ± 10 c*	<0.01*	<0.001*	
Copper, µmol/l	0	15 ± 2 a	16 ± 1 a	15 ± 2 a	16 ± 2 a			
Selenium, µmol/l	0	7 ± 1 a	7 ± 1 a	6 ± 1 a	6 ± 1 a			
Zinc, µmol/l	0	21 ± 3 a	22 ± 4 a	25 ± 4 a	24 ± 4 a			
U/ml	0	22 ± 10 a	22 ± 4 a	19 ± 6 a	22 ± 6 a			
Catalase, nmol/min/ml §	1	41 ± 14 a	54 ± 15 ab	41 ± 9 a	70 ± 23 b*	<0.001*		
capacity, mmol/l	0	1.2 ± 0.1 a	1.2 ± 0.1 ab	1.1 ± 0.0 b	1.1 ± 0.1 ab		<0.05	
Heme, µmol/l	2	18 ± 3 a	21 ± 6 a	21 ± 6 a	20 ± 5 a			
	a, b, c - different letters indicate the unadjusted pairwase comparison found a significant							
	difference between groups, P <0.05. comparisons.							
	* Remained significant after adjusting for multiple compariosns, § log transformed							

Table 14. Liver markers of iron status and oxidative stress. Mean ± SD.

	Outliers	CON	IRON	RAD	IRON+RAD		Main Effect	
Test		.				Diet	Rad	Inter
Catalase, µmol/mg protein	0	1.2 ± 0.3 a	1.2 ± 0.3 a	1.2 ± 0.3 a	1.3 ± 0.4 a			
Copper, µg/g dry wt.	1	19 ± 2 a	19 ± 4 a	20 ± 3 a	19 ± 1 a			
Glutathion Peroxidase, U/g protein	0	32 ± 4 a	38 ± 7 ab	34 ± 7 a	41 ± 7 b*	<0.01*		
Iron, µg/g dry wt.	0	621 ± 123 ab	728 ± 140 a	559 ± 106 b	758 ± 169 a*	<0.01*		
Selenium, µg/g dry wt.	0	4 ± 1 a	4 ± 1 a	4 ± 1 a	4 ± 1 a			
Superoxide Dismutase, U/mg protein	2	64 ± 12 a	75 ± 16 a	74 ± 14 a	75 ± 17 a			
Total Antioxidant Capacity, mmol/g protein	0	0.6 ± 0.1 a	0.7 ± 0.1 b	0.8 ± 0.1 b*	0.8 ± 0.1 b*			<0.05
Total Protein, mg/ml	0	12 ± 4 a	13 ± 3 a	11 ± 2 a	13 ± 3 a			
Zinc, µg/g dry wt.	0	114 ± 12 a	105 ± 15 a	112 ± 13 a	112 ± 16 a			
	a, b, c - different letters indicate the unadjusted pairwase comparison found a							
	significant difference between groups, P <0.05. comparisons.							
	* Remained significant after adjusting for multiple compariosns							

(P = 0.005). Liver GPX was positively correlated with liver iron for all groups (r=0.47, P = 0.006) (Figure 13). Radiation exposure increased serum ferritin (P = 0.007) and decreased alanine transaminase (ALT) (P = 0.002), erythrocyte GPX (P = 0.02), hematocrit (P = 0.03), and plasma total antioxidant capacity (TAC) (P = 0.03). There was a tendency for both aspartate transaminase (AST) and hemoglobin to be lower in the radiation-treated groups, but these did not reach statistical significance. Dietary iron and radiation had an interactive effect on liver TAC (P = 0.03), in that liver TAC increased in the IRON group relative to the CON group (P = 0.03), but dietary iron did not further increase liver TAC in the IRON+RAD group beyond that which occurred with radiation alone (RAD).

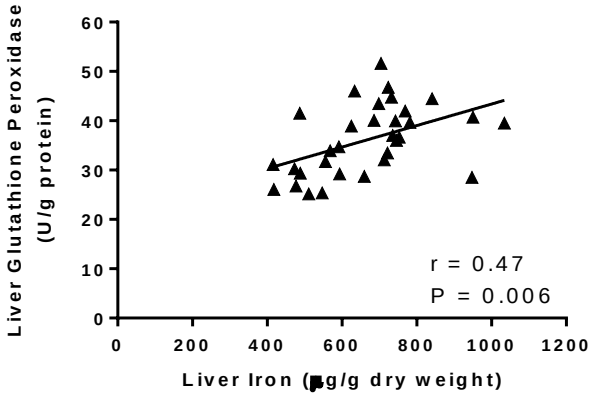

Figure 13. An increase in liver iron was correlated with an increase in liver glutathione peroxidase, indicating that oxidative load on the liver increased as a result of increased iron stores.

Both radiation exposure and a high-iron diet resulted in alterations to both cellular distribution and functional aspects of the immune system (Table 15). Diet and radiation had an interactive effect on leukocytes ($P = 0.02$). The percentage of leukocytes increased in the IRON group relative to the CON group ($P = 0.003$); however, diet had no significant effect in the radiation group (IRON+RAD relative to RAD).

Radiation induced alterations to the immune cell subset percentages, including an increase in the granulocyte percentage ($P = 0.001$), a decrease in total lymphocyte percentage ($P = 0.0009$), and a reduction in percentage of CD4+ T cells ($P < 0.0001$) and an increase in percentage of CD8+ T cells ($P < 0.0001$), which corresponded to an overall decrease in the CD4+:CD8+ T-cell ratio ($P < 0.0001$). There was a significant correlation between serum ferritin and CD4+ T cells ($r = -0.44$, $P = 0.01$, Figure 14), CD8+ T cells ($r = 0.45$, $P = 0.01$), and the CD4+:CD8+ ratio ($r = -0.45$, $P = 0.01$). Diet had no main effect on these T-cell subset percentages. Generally the plasma concentrations of the inflammatory and adaptive immunity cytokines that were measured were not altered. However, radiation did decrease the plasma concentration of TNFα ($P = 0.03$), which was decreased in the IRON+RAD group relative to CON and IRON.

As a measure of functional capability, cytokine production was determined after T-cell stimulation via triggering of the TCR and co-stimulation (anti-CD3/CD28). Radiation induced a significant stimulatory effect on T-cell cytokine production. Cytokines IL-6 and TNFα both increased as a result of radiation after co-stimulation

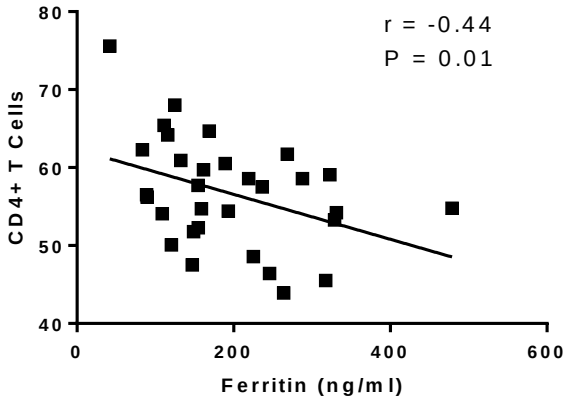

Figure 14. An increase in serum ferritin concentrations was correlated with a decrease in CD4+ T cells, indicating that an inflammatory response was affecting T-cell distribution.

with anti-CD3/CD28 ($P = 0.002$; $P = 0.009$). Production of IL-10 and IL-4 after co-stimulation showed an interactive effect ($P < 0.0001$; $P = 0.02$): a significant increase occurred in IL-10 and IL-4 production in the RAD group relative to the CON group ($P < 0.0001$; $P = 0.006$), but production of these cytokines in the IRON+RAD group was not significantly different from production in the CON or IRON group ($P < 0.0001$; $P = 0.02$). The high-iron diet seemed to ameliorate the effect of radiation. However, after anti-CD3/CD28 stimulation, T-cell production of IL-2 actually decreased as a result of diet ($P < 0.001$) and was reduced to the greatest extent in the IRON+RAD group.

Cytokine profiles were also determined after pan-leukocyte activation using a more powerful pharmacologic stimulus consisting of PMA (PKC activator) and ionomycin (calcium ionophore). A suppressive effect was observed after radiation. Radiation decreased IFNγ, IL-4, IL-6 and TNFα ($P = 0.0005$, $P = 0.0005$, $P = 0.01$;

Table 15. Immune markers. Mean ± SD.

	Outliers	CON	IRON	RAD	IRON+RAD		Effect	
Test		.				Diet	Rad	Inter
Leukocytes, count §	0	4 ± 1 a	7 ± 3 b*	3 ± 1 a	3 ± 1 a			<0.05
Granulocytes, %	0	14 ± 12 a	13 ± 16 a	30 ± 5 b*	28 ± 12 b		<0.01*	
Lymphocytes, %	1	76 ± 18 a	90 ± 8 b*	68 ± 6 a	67 ± 11 a		<0.001*	
Monocytes, %	1	0.2 ± 0.1 a	0.4 ± 0.9 a	0.5 ± 0.8 a	0.6 ± 0.8 a			
CD4+ T cells	0	62 ± 6 a	60 ± 4 a	53 ± 4 b*	51 ± 5 b*		<0.001*	
CD8+ Tcells	0	35 ± 8 a	37 ± 4 a	45 ± 4 b*	47 ± 6 b*		<0.001*	
CD4+/CD8+, ratio	0	2 ± 1 a	2 ± 0 ab	1 ± 0 b*	1 ± 0 b*		<0.001*	
	Staphlyococcus Entertoxin							
T cell function CD4+	0	7.0 ± 1.6 a	7.6 ± 2.5 a*	4.3 ± 2.4 b	6.4 ± 2.7 ab		<0.05	
T cell function CD8+	0	1.9 ± 0.6 a	1.7 ± 0.5 a	1.2 ± 0.9 a	1.8 ± 1.3 a			
	Plasma Concentrations							
IFNγ, pg/ml plasma	0	0 ± 0	0 ± 0	0 ± 0	0 ± 0	†		
IL-10, pg/ml plasma	0	0.2 ± 0.5	0.3 ± 0.7	3.2 ± 6.2	0.1 ± 0.3	†		
IL-1b, pg/ml plasma	0	15 ± 37	0 ± 0	2 ± 4	7 ± 15	†		
IL-2, pg/ml plasma §	0	3 ± 2 a	8 ± 11 a	6 ± 5 a	9 ± 10 a			
IL-4, pg/ml plasma	0	0.2 ± 0.4	0.0 ± 0.0	0.0 ± 0.0	0.1 ± 0.1	†		
IL-6, pg/ml plasma §	0	8 ± 13 a	21 ± 42 a	22 ± 27 a	6 ± 11 a			
Tnfα, pg/ml plasma §	0	4 ± 4 a	10 ± 11 a	7 ± 10 ab	1 ± 1 b		<0.05	
	Anti CD3/CD28							
IFNγ, pg/ml supernatant	0	3.9 ± 8.0	1.3 ± 3.7	53.7 ± 56.8	4.7 ± 12.0	†		
IL-10, pg/ml supernatant §	0	4 ± 4 a	3 ± 1 a	88 ± 95 b*	3 ± 4 a			<0.001*
IL-1b, pg/ml supernatant §	0	2 ± 4 a	1 ± 2 a	22 ± 25 a	14 ± 25 a			
IL-2, pg/ml supernatant §	0	28 ± 13 a*	16 ± 5 a	58 ± 53 a*	9 ± 13 b	<0.001*		
IL-4, pg/ml supernatant §	0	0.2 ± 0.2 a*	1.7 ± 3.8 a	5.3 ± 5.5 b	1.1 ± 2.0 a*			<0.05
IL-6, pg/ml supernatant §	0	62 ± 44 a*	45 ± 36 a*	1,525 ± 1,849 b	927 ± 1,233 ab		<0.01*	
Tnfα, pg/ml supernatant §	0	3.6 ± 4.2 a	2.4 ± 1.2 a	45.0 ± 43.8 b*	7.3 ± 8.8 a		<0.01*	
	PMA/Ionomycin							
IFNγ, pg/ml supernatant	1	81 ± 26 a*	65 ± 40 a*c	18 ± 7 b	38 ± 36 bc		<0.001*	
IL-10, pg/ml supernatant §	0	27 ± 39 a*	10 ± 26 b	5 ± 4 ab	12 ± 16 a			<0.01*
IL-1b, pg/ml supernatant	0	13 ± 19	10 ± 20	0 ± 0	0 ± 1	†		
IL-2, pg/ml supernatant	0	857 ± 330 a	471 ± 229 b*	259 ± 75 b*	428 ± 394 b*			<0.05*
IL-4, pg/ml supernatant §	0	3 ± 3 a	1 ± 1 ab	0 ± 0 b*c	0 ± 0 c*		<0.001*	
IL-6, pg/ml supernatant §	0	255 ± 287 a	162 ± 346 ab	34 ± 23 b*	53 ± 39 b		<0.05*	
Tnfα , pg/ml supernatant §	0	37.0 ± 54.4 a	12.3 ± 16.4 ab	4.7 ± 4.0 b*	5.2 ± 4.2 b*		<0.001*	
		LPS						
IFNγ, pg/ml supernatant§	0	12 ± 21 a	0 ± 0 c*	10 ± 13 b	3 ± 3 ab	<0.01*	<0.001*	
IL-10, pg/ml supernatant §	0	40 ± 16 a	23 ± 6 b	22 ± 7 b*	18 ± 13 b*	<0.05*	<0.01*	
IL-1b, pg/ml supernatant	0	56 ± 10 a	60 ± 13 a	52 ± 9 a	47 ± 16 a			
IL-2, pg/ml supernatant §	0	17.3 ± 12.2 a	10.6 ± 6.3 a	17.9 ± 11.8 a	9.4 ± 6.5 a			
IL-4, pg/ml supernatant §	0	0.2 ± 0.2 a*	0.4 ± 0.9 a	0.7 ± 0.4 b	1.4 ± 1.8 b*		<0.001*	
IL-6, pg/ml supernatant	0	408 ± 187 a	322 ± 138 a	270 ± 98 a	338 ± 297 a			
Tnfα, pg/ml supernatant	0	52 ± 15 a	58 ± 11 a	66 ± 12 a	57 ± 22 a			
	a, b, c - different letters indicate the unadjusted pairwise comparison found a significant							
	difference between groups, P <0.05.							
	* Remained significant after adjusting for multiple comparsons. § log transformed.							
	†Insufficient signal to run ANOVA.							

P = 0.001). There was an interactive effect of diet and radiation for IL-10 and IL-2 production (P = 0.01; P = 0.01). There was a significant decrease in IL-10 and IL-2 in the IRON group relative to the CON group (P = 0.007; P = 0.01) but no decrease in the IRON+RAD group relative to RAD. IL-2 decreased in both RAD and IRON+RAD relative to CON (P < 0.0001; P = 0.007). After monocyte stimulation with bacterial endotoxin (lipopolysaccharide, LPS), production of IFNγ and IL-10 was decreased with both high dietary iron and radiation exposure (P = 0.0002, P = 0.005; P = 0.006, P = 0.02), whereas IL-4 production increased with radiation exposure (P = 0.0006). An increase in plasma iron was correlated with a decrease in IL-10 production after LPS stimulation (r = -0.54, P = 0.002, Figure 15).

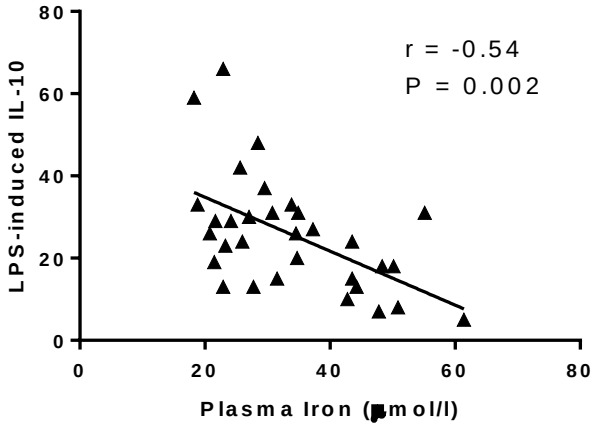

Figure 15. An increase in plasma iron was correlated with a decrease in IL-10 production after LPS stimulation, indicating that adaptive Th1 and Th2 responses to pathogens may be diminished after either radiation exposure or increased dietary iron.

The following data were collected and analyzed by the Turner lab group at Texas A&M University to determine independent and combined effects of exposure to gamma radiation and elevated body iron stores on functional indicators of the modification of colon bacteria by examining changes in short-chain fatty acid concentrations in feces. Furthermore, this data was collected to identify any alterations to expression of butyrate transporters, TLR and their downstream inflammatory mediators, and localized inflammatory state (i.e., myeloperoxidase (MPO) activity) in colon mucosa.

Feces analysis showed significant changes in SCFA in response to dietary iron and radiation (Table 16). Both diet and radiation had significant main effects on SCFA; both treatments caused a decrease in total SCFA ($P = 0.04$), which was greatest in the IRON+RAD group relative to CON. Additionally, dietary iron decreased fecal butyric acid ($P = 0.051$), and dietary iron and radiation combined decreased isovaleric acid concentration ($P = 0.05$, $P = 0.04$).

Dietary iron and radiation had significant effects on expression of selected gene targets in the scraped colon mucosa (Table 17). There was a reduction in expression of TLR9 ($P < 0.001$), TNFα ($P = 0.001$) and IL-6 ($P < 0.001$) with radiation exposure. Dietary iron decreased expression of TLR4 ($P = 0.03$) and TFF3 ($P = 0.04$). Expression of TNFα1b increased with dietary iron ($P = 0.01$) but decreased with radiation exposure ($P < 0.001$). Slc5a8 expression was affected by iron and radiation interactively ($P = 0.004$). With a reduction in expression of Slc5a8 in the IRON group relative to the CON group, but no decrease as a result of diet in the IRON+RAD relative to the RAD

Table 16. Short chain fatty acids. Mean ± SD.

	Outliers, no.;	CON	IRON	RAD	IRON+RAD		Effect	
Test	transform	.				Diet	Rad	Inter
Acetic acid, µmol/g wet wt.	0	68 ± 18 a*	61 ± 15 ab	60 ± 18 ab	48 ± 11 b			
Propionic acid, µmol/g wet wt.	0	23 ± 6 a*	20 ± 7 ab	20 ± 5 ab	15 ± 6 b			
Isobutyric acid, µmol/g wet wt.	0	5 ± 1 a*	4 ± 1 ab	4 ± 1 ab	4 ± 1 b			
Butyric acid, µmol/g wet wt.	0	19 ± 4 a*	16 ± 3 ab	16 ± 5 ab	14 ± 4 b			
Isovaleric acid, µmol/g wet wt.	0	10 ± 1 a*	9 ± 2 ab	9 ± 3 ab	7 ± 2 b	<0.05	<0.05	
Valeric acid, µmol/g wet wt.	0	8 ± 1 a*	7 ± 1 ab	7 ± 3 ab	5 ± 2 b			
Total fatty acids, µmol/g wet wt.	0	134 ± 29 a*	116 ± 24 ab	116 ± 31 ab	93 ± 23 b	<0.05	<0.05	
	a, b, c - different letters indicate the unadjusted pairwise comparison found							
	a significant difference between groups, P <0.05.							
	* Remained significant after adjusting for multiple comparisons.							

group. MPO activity, an inflammatory marker in the colon mucosa, increased with radiation exposure (P = 0.04), with the IRON+RAD group being significantly higher than the CON group (P = 0.04, Table 17).

Discussion

The combined effects of increased dietary iron and radiation have implications for astronauts on long-duration space flights. Recent reports have documented a relationship between iron stores, oxidative damage, and bone health in astronauts (289), along with animal studies of radiation and bone health (290-292). We report here an animal model for the combined effects of iron and radiation, with implications for

Table 17. Change in gene expression in colon relative to GAPDH [($2^{\Delta-Ct}$)*1000] and MPO concentration. Mean ± SD.

	Outliers	CON	IRON	RAD	IRON+RAD		Effect	
Test		.				Diet	Rad	Inter
TLR2	0	1.39 ± 0.68 a	1.37 ± 0.71 a	1.27 ± 0.41 a	1.26 ± 0.42 a			
TLR4	0	10.93 ± 2.69 a*	6.98 ± 1.14 b	11.18 ± 3.45 a*	10.63 ± 3.39 a	<0.05		
TLR5	0	4.23 ± 1.75 a	5.38 ± 2.94 a	4.70 ± 1.55 a	4.09 ± 2.21 a			
TLR9 §	0	0.44 ± 0.25 a	0.65 ± 0.30 a	0.13 ± 0.06 b*	0.18 ± 0.15 b*		<0.001*	
MyD88	0	14.16 ± 2.54 a	11.99 ± 1.13 a	13.26 ± 2.33 a	12.27 ± 2.33 a			
IκB	0	17.89 ± 4.10 a	16.89 ± 2.26 a	17.10 ± 4.01 a	15.26 ± 2.23 a			
NFκB	0	22.24 ± 3.78 a	18.23 ± 1.45 b	20.16 ± 4.12 ab	19.70 ± 3.96 ab			
TNFα §	0	0.42 ± 0.41 ac	0.83 ± 0.80 a	0.10 ± 0.15 b*	0.12 ± 0.10 bc		<0.01*	
TNFα1α §	0	20.15 ± 7.06 a	18.06 ± 4.01 a	17.78 ± 4.68 a	17.83 ± 2.55 a			
TNFα1b §	0	1.35 ± 0.53 a	1.85 ± 0.50 b*	1.03 ± 0.21 a	1.17 ± 0.18 a	<0.05*	<0.001*	
Tollip	0	8.86 ± 1.78 a	8.13 ± 0.83 a	8.18 ± 1.74 a	8.53 ± 1.19 a			
Ripk1	0	8.46 ± 1.45 a	8.93 ± 1.09 a	8.86 ± 1.42 a	7.99 ± 0.85 a			
Tff3 §	0	684.85 ± 97.83 a	564.48 ± 151.12 a	748.23 ± 259.02 a	596.01 ± 129.14 a	<0.05		
TGFβ	0	2.36 ± 0.92 a	2.93 ± 0.84 a	2.73 ± 0.83 a	2.29 ± 1.10 a			
IL-1b §	0	0.32 ± 0.17 a	0.53 ± 0.39 a	0.32 ± 0.11 a	0.28 ± 0.11 a			
IL-6	0	0.10 ± 0.04 ab	0.14 ± 0.05 a*	0.06 ± 0.02 b	0.06 ± 0.05 b		<0.001*	
Ptgs2 (COX-2)	0	1.62 ± 0.53 a	1.39 ± 0.39 ab	1.41 ± 0.41 ab	1.17 ± 0.35 b			
Slc16a1	1	88.49 ± 14.16 a	85.91 ± 10.50 a	86.85 ± 12.60 a	81.77 ± 6.62 a			
Slc5a8	0	30.43 ± 7.40 a	17.09 ± 3.30 b*	27.53 ± 5.39 a	27.84 ± 7.35 a			<0.01*
		.						
Myeloperoxidase, U/mg	0	3,979 ± 1,752 a	4,239 ± 855 ab	4,789 ± 809 ab	5,333 ± 1,324 b		<0.05	

a, b, c - different letters indicate the unadjusted pairwase comparison found a significant difference between groups, P <0.05.

* Remained significant after adjusting for multiple compariosns. § log transformed.

hepatic and immune system function, and gastrointestinal health. Studies such as these will be critical in understanding integrated physiological responses to space flight and ultimately in developing countermeasures to any pathologic adaptations, particularly in light of the emerging field of osteoimmunology, which links perturbations in immune health with bone loss (293).

Iron status

The relatively short-term high dietary intake of iron increased iron stores as well as liver iron content. Increased iron stores and liver iron content reflect an increase in total body iron, as has been shown in humans (294). This relationship is important because some of the markers of oxidative stress observed in this study are not limited to effects on liver tissue alone. In this study, liver iron increased 17% in the IRON group, the same percentage increase observed for body iron (estimated from ferritin and transferrin receptors) in the first 15-30 days of long-duration space flight (289).

The increase in serum iron observed in the high-iron diet groups further indicates an increase in the iron load. Plasma iron was also increased in the radiation group, causing an additive effect in the IRON+RAD group, but liver iron (and thus total body iron) was not affected by radiation exposure. One remaining question pertains to the source of the increased serum iron shown to result from radiation. One possibility may be an inhibition of erythrocyte formation. It is known that hematopoietic stem cells are radiosensitive and are easily disrupted by radiation exposure (295). In this study, this phenomenon seems to have occurred in radiation-exposed animals as evidenced by lower hematocrit levels and decreased erythrocyte GPX. If radiation prevents new

erythrocytes from forming, then the age of circulating erythrocytes will increase and as a result, the cellular GPX will seem to decrease, which was observed in this study.

Oxidative stress markers

Increasing dietary iron increased iron status, and the increase was related to markers of oxidative stress. Liver iron was correlated with serum catalase ($r=0.49$, $P=0.005$), and both increased with high dietary iron. This relationship could be caused by an increase in oxidative stress from the increase in TBI or by liver damage, which is also known to increase serum catalase (296). Nonetheless, increasing dietary iron increased serum catalase, indicating that an increase in oxidative stress occurred as a result of high dietary iron. Liver iron was positively correlated with liver GPX ($r=0.47$, $P=0.006$; Figure 13), indicating that a greater oxidative load on the liver was associated with increased iron stores. Also supportive of potential liver damage or aging of the cell population was the decrease in liver enzymes (ALT, with a trend for AST) with radiation exposure. This ALT response to radiation has been observed in previous studies in which radiation doses ranged from 5 Gy to 25 Gy; the ALT response is dose-dependent for doses lower than 15 Gy (297).

Radiation induced an acute-phase inflammatory response, as indicated by an increase in serum ferritin. In addition to being an iron storage protein, ferritin is also an acute-phase protein that is upregulated during an inflammatory response (298). C-reactive protein (CRP), another acute-phase protein, did not increase in response to radiation. Ferritin significantly increased with radiation but not with dietary iron, indicating that the ferritin response was most likely due to inflammation resulting from

radiation exposure and not to increased iron load. The timing of any change in CRP expression may have been missed in this study with only one time point, or CRP may behave differently when the radiation dose is fractionated over 16 days (299-301).

Systemic immune response

The immunological monitoring for this study consisted of determining basic leukocyte distribution and plasma cytokine levels, to monitor both *in vivo* immune activation and various mitogen-stimulated cytokine production profiles and detect dysregulation of cellular functional capacity. The data indicated that the IRON group alone had an elevated leukocyte count but a normal subset distribution relative to the CON group. Both radiation groups, independent of diet, had an increase in granulocyte percentage, which may protect against radiation injury (302-303). Both radiation groups had a decrease in the total percentage of lymphocytes and a decrease in the T-cell CD4:CD8 ratio. The decrease in CD4+ T cells was expected because of the radiation dose given: 3 Gy. A ~10% decrease corresponded to ~3% per Gy (304). The decrease in CD4+ T cells also correlated with an increase in serum ferritin concentrations ($r= -0.44$ $p=0.01$, Figure 14), indicating that a radiation-induced inflammatory response was affecting T-cell distribution.

Alterations in plasma cytokine levels may indicate constitutive immune activation. After radiation treatment, the plasma concentration of TNFα was significantly reduced, and this response paralleled the observations from the colon mucosal cells (to be discussed later). Other studies have indicated that plasma TNFα increases after radiation exposure (305). This discrepancy could be due to the fractionated radiation

doses of 0.375 Gy, which is a lower single dose than is typically administered. Although it was not statistically significant because of the large error bar, TNFα increased in the IRON group to a magnitude similar to that observed by Tsay et al. (306) in their iron overload study. No further alterations occurred in the plasma levels of cytokines associated with inflammation or adaptive immune processes.

The absence of constitutive immune activation may have diminished cellular functional capacity, resulting in an increased health risk. Previous studies showed that radiation alone has a negative effect on early blastogenesis of T cells but a positive effect on T-cell function in a murine model (307-308). For this study, whole-blood cultures were stimulated with cell-specific mitogen to produce in vitro cellular activation, and supernatant cytokine levels were measured as an indicator of functional capacity. Whole-blood culture is perceived to more closely represent in vivo conditions, as all potential cell-cell interactions are preserved and plasma soluble factors are present.

T cells were stimulated by triggering the TCR and costimulatory molecule; these actions model in vivo activation via an antigen-presenting cell. Elevated dietary iron reduced T-cell IL-2 production, whereas radiation increased T-cell production of TNFα and IL-6. The RAD group showed an increase in IL-4 and IL-10, but the IRON+RAD group negated this increase. This diet effect was not observed in the sham group. Thus, a high-iron diet seems to inhibit both constitutive immune functional responses and the elevated functional responses observed after radiation treatment.

Radiation exposure resulted in demonstrable alterations in leukocyte cytokine production after mitogenic stimulation with PMA-I. This mitogen, consisting of a

phorbol ester/PKC activator and calcium ionophore, bypasses much of the signal transduction used by surface molecule mitogens, and is more powerful. Radiation resulted in decreased production of TNFα, IL-6, IFNγ, and IL-4, a grouping that spans both inflammatory, Th1, and Th2 cytokine categories. The decrease in TNFα and IL-6 in these cells, again, parallels the observations from the colon, suggesting that radiation has systemic as well as localized impacts on immune function. Production of some cytokines (IL-2 and IL-10) was also diminished in the IRON group compared to CON, although this diet effect was not observed when comparing the RAD and IRON+RAD group.

LPS generally serves as an activator of monocytes and B cells. After culture of whole blood in the presence of LPS, IL-10 and IFNγ production decreased with as a result of radiation exposure and high dietary iron. Production of IL-4 actually increased as a result of radiation exposure. Plasma iron concentration was negatively correlated with IL-10 after LPS simulation ($r=-0.54$, $p=0.002$; Figure 15). These data generally indicate that adaptive Th1 and Th2 responses (IFNγ and IL-10, respectively) to pathogens may be diminished after either radiation exposure or increased dietary iron. With respect to radiation exposure, however, the elevation in IL-4 production may be considered discordant with this conclusion. Diminished cytokine production profiles are consistent with recent reports of space flight-associated immune dysregulation in astronauts.

"Colon responses" and "Colonic mucosa gene expression and inflammatory markers" sections were contributions by the Turner lab group at Texas A&M University.

Colon responses

The total concentration of all SCFA analyzed (acetic, propionic, isobutyric, butyric, isovaleric, and valeric acid) decreased in other groups relative to the CON group, with a maximum decrease occurring in the IRON+RAD group. Changes in the concentration of fecal SCFA could be caused by alterations in the bacterial populations and/or changes in bacterial metabolism after an increase in dietary iron or exposure to radiation. To our knowledge, no studies have shown an effect of high dietary iron or radiation on intestinal bacterial metabolism, although it is known that butyrate-producing bacteria strongly depend on iron as a cofactor for butyrate production (309). Independent studies have reported that radiation therapy (4.3-5.4 Gy) and dietary iron depletion variably promote and inhibit the microbiota, including taxa that are known butyrate producers (310-311). It has been reported that cecum SCFA concentrations and the proportion of butyrate-producing bacteria can be increased when iron-depleted animals are fed diets fortified with iron (311); however, no reports describe the effect of high dietary iron on the microbiota or bacterial metabolism. Another potential explanation for the observed reduction in fecal SCFA is an alteration in the absorption of SCFA into colonocytes, which was not directly assessed in this experiment. However, we observed alterations in gene expression of SCFA transporters (described below), which may contribute to the observed fecal SCFA concentrations.

Colonic mucosa gene expression and inflammatory markers

Exposure to genotoxic stress, including ionizing radiation and oxidative ROS, can initiate physiological responses in the intestine such as cell cycle arrest, diminished

epithelial integrity, inflammatory infiltration, altered gene transcription, and a perturbed luminal environment by variably suppressing or supporting the growth of certain bacterial populations (310, 312-321). The mucosal surface of the small and large intestine has shown increased propensity for radiation-induced mucosal injury because of its high proliferative capacity (312). Thus, we were interested in understanding the effect of high dietary iron and gamma radiation exposure on gene expression in colonic mucosa for pathways associated with microbial signaling, SCFA transport and repair.

SCFA are absorbed from the lumen passively through ionic diffusion, or through transporters such as Slc16a1 and Slc5a8 (322-323). We observed a significant decrease in expression of Slc5a8 in the IRON group relative to the other three groups, whereas Slc16a1 demonstrated minimal changes with either treatment. The highest Slc5a8 and Slc16a1 expression and SCFA concentration observed in the CON group may have resulted from the same effects that induce the reported promotion of Slc16a1 expression in a colonic epithelial cell line, where increased butyrate concentrations upregulated Slc16a1 mRNA and protein levels (322). A decrease in SCFA production and absorption could be detrimental to astronauts' gastrointestinal health, as these metabolites have been reported to have pleiotropic effects on colonocytes, including anti-inflammatory activity, the induction of gene expression, cellular differentiation, apoptosis, cell cycle arrest, and interference with transcription factors critical for proinflammatory cytokine production (62, 324-328).

Expression of four gene targets involved in bacterial recognition and inflammatory responses was reduced by radiation exposure. These targets were TLR9 (a

bacterial recognition receptor), TNFα (a cytokine involved in systemic inflammation) and its receptor, TNFα1b, and IL-6 (an interleukin with both proinflammatory and anti-inflammatory effects). Additionally, TLR4 and TFF3 expression decreased when rats were exposed to high dietary iron. The gene expression patterns indicate that changes occurred in the bacterial recognition signaling pathway (TLR) as a result of dietary iron and radiation, although the treatments had differential effects on mediators of this pathway. Observed effects on TLR expression could also be attributed to changes in the composition of the intestinal microbiota, compromised barrier integrity, or a chronic inflammatory state, all of which have been documented to alter expression of these receptors (329-331). In this study, suppressed luminal SCFA concentrations may indicate that the microbiota was altered by radiation exposure and high dietary iron, which could have contributed to the differential effects on TLR4 and TLR9 expression. Microbial-derived signaling through pattern-recognition receptors affects gene expression, transepithelial electrical resistance, and colonocyte proliferation in normal tissues (332), and plays a pivotal role in maintaining homeostasis between commensal microbiota and the host immune system (333). Alterations in the TLR signaling pathway directly affect the immune response, specifically through downstream activation of the transcription factor NF-κB (334). NF-κB activation alters expression of localized cytokines (IL-1β, IL-10, IL-6, TNFα, IFNγ, and TGFβ) and proinflammatory molecules (COX-2) during an inflammatory response (261). Although we did not observe a significant diet or radiation effect on expression of NF-κB or other proteins mediating the TLR signaling cascade, we did observe a significant radiation effect on TNFα and

IL-6 expression. Additionally, we observed a significant main effect of diet and radiation on TNFα receptor 2 expression (TNFα1b), with significantly upregulated expression in IRON rats. TNFα1b signaling is known to activate the transcription of proinflammatory cytokines through NF-κB (335), which could be one explanation for significant upregulation of IL-6 and upregulation of IL-1b and TNFα expression in IRON animals relative to other groups.

Radiation, in addition to having significant effects on expression of inflammatory cytokines IL-6 and TNFα, induced an increase in MPO concentrations in colon mucosa. MPO, a biomarker of inflammation, is an enzyme found in neutrophils that conjugates bactericidal compounds in the phagosome (336). Increased infiltration of neutrophils into the epithelium occurs in response to an immune challenge, which could explain the observed increase in mucosal MPO concentration in IRON, RAD and IRON+RAD animals in this study. The inflammation may result from the increased presence of ROS in the lumen and in the epithelial cells after radiation or from elevated exposure to oxidants. Additionally, if the epithelial barrier is compromised by these environmental stresses, bacteria and antigens could translocate through the epithelial membrane and be responsible for an increased infiltration of neutrophils and activation of inflammatory mechanisms (317, 320). In this study we observed a significant diet effect on expression of Trefoil factor 3 (TFF3), which is a protein expressed on the apical side of the intestinal epithelial barrier and reported to be involved in epithelial repair and cellular migration (337). An effect of dietary iron on expression of TFF3 could suggest that the luminal environment, specifically a high oxidant-load diet, may have an effect on

epithelial repair or barrier restitution after injury. Persistent inflammation by aberrant TLR signaling, upregulated expression of cytokines such as IL-6, or infiltration of neutrophils into the mucosa can have numerous deleterious effects and increase oxidative stress, which can cause oxidative DNA adducts (338) and nitrative DNA lesions (339). Also, as mentioned previously, chronic inflammation and dysbiosis of the intestinal microbiota is known to persist in intestinal diseases such as inflammatory bowel disease and could increase an astronaut's risk of colorectal cancers (267-269). Moreover, the local colonic inflammatory responses to diet and radiation may further stimulate the systemic alterations in immune function and cytokines discussed earlier.

Conclusion

Increased iron status and radiation exposure combined lead to oxidative stress, immune system dysregulation, alterations of colon microbial metabolism, and changes in intestinal gene expression. Radiation exposure consistently induced dysregulation of both leukocyte distribution and functional capacity of the immune system. To a lesser degree, the elevated iron diet also negatively influenced immunocyte functional responses, at times in an interactive fashion with radiation exposure. Significant radiation effects on localized mucosal cytokine expression (TNFα and IL-6) and reduced levels of the same cytokines in circulation could indicate that the intestinal tract, which harbors the largest and most complex immune cell population in the body, could have an effect on systemic inflammatory responses after radiation exposure. Astronauts are exposed to both increased iron stores and radiation during flight, and this exposure raises

concerns about crew health. These concerns will be greater on exploration missions beyond low Earth orbit, with longer durations and greater exposure to radiation.

CHAPTER V

IMPLICATIONS OF THE SPACE ENVIRONMENT ON INTESTINAL HOMEOSTASIS: CHARACTERIZING ALTERATIONS TO THE INTESTINAL MICROBIOTA AND MUCOSAL ENVIRONMENT

Introduction

Spaceflight exposes astronauts to environmental inputs that are different from that on earth including a typically elevated iron diet, microgravity, and radiation exposure. NASA is concerned with the health risks associated with these environmental insults, particularly radiation exposure, as they have been shown to have deleterious effects on numerous organ systems, and increase the risk of heart disease, cataracts, and can cause bone loss (340-342).

Linear energy transfer (LET), or the amount of energy that is transferred to a substance as the radiation passes through, impacts the extent of radiation exposure on biological systems (118). Low LET radiation, such as gamma and x-rays, is more likely to have indirect effects on cells through the formation of free radicals (e.g., H•, •OH, H_2O_2, and e^-_{aq}), while high LET radiation will directly damage cellular components (118, 125). Both high and low LET radiation exposure can compromise plasma and organelle membrane integrity and cause DNA damage (i.e., base loss, base modification, single or double strand break, and the formation of dimers) (21, 118, 125). Once a cell becomes irradiated (directly or indirectly) the outcome can be mutations, division delay, cellular arrest, and transformation to a possibly carcinogenic cell (21, 119).

Reactive oxygen species are generated within cells immediately after exposure to radiation and could be exacerbated by other environmental factors, including nutrient status. For example, oxidative stress can a be propagated in the intestine by consumption of a diet containing pro-oxidants, such as excess iron, which increases the risk of forming cytotoxic compounds and free radicals (343). Deleterious effects to the intestinal tract have been documented with increased dietary iron such as barrier damage, hyperproliferation, downregulating repair mechanisms, as well as altering the microbiota and luminal concentration of short chain fatty acids (SCFA) (111-113).

Very little research has been done to understand the effect of lose dose radiation exposure (<1 Gy) and microgravity on the luminal environment and intestinal epithelium function. Previous studies looking at large doses of radiation (>8 Gy) have demonstrated exposure can cause detrimental effects such as direct mucosal toxicity, delayed gastric emptying and secretion, and villous shortening (21-22, 120, 129, 344). Additionally, preliminary studies have indicated that radiation exposure can affect the intestinal microbiota, and the presence and composition of these commensal bacterial groups has an effect on radiation induced-lethality (114, 130, 133, 137, 345). Furthermore, our lab group has reported that consumption of a diet with elevated dietary Fe, by itself and in combination with low LET radiation exposure can alter the concentration of fecal SCFA, suggesting alterations to the composition of the intestinal microbiota or a functional change in microbial metabolism. An understanding of how the aforementioned environmental insults affect the microbiota is of utmost importance, as alterations to

commensal bacterial groups have been implicated in the onset and recurrence of chronic intestinal inflammation and gastrointestinal diseases (172-173).

Mitigating the effects of oxidative stress caused by radiation exposure and elevated dietary iron are important areas of research, as no current countermeasures have been thoroughly studied. Moreover, results from this research would also benefit not only astronauts, but others exposed to radiation sources such as medical diagnostic tests, occupational radiation exposure, and doses encountered by airline crews. To our knowledge, no study has characterized the effect of fractionated, low doses (<1-3 Gy) of both low and high LET radiation exposure in combination with microgravity on the luminal environment and intestinal epithelium. We hypothesized that the space environment will alter the microbiota and intestinal epithelium, and that a differential response will be observed in these bacterial populations and the mucosal environment following each insult (i.e., high Fe diet, received radiation dose (high vs. low LET) and weightlessness (HLU and spaceflight)). Therefore the aim of this study was to describe the effect of 1) low LET radiation exposure and high Fe diet, 2) simulated lunar microgravity and high LET radiation exposure, and 3) short term spaceflight, on the intestinal microbiota, mucosal expression of gene targets associated with microbial signaling and epithelial repair, and measurements of colonic injury and inflammation.

Materials and Methods

Animals and diets

Experiment 1 fractionated low LET gamma radiation and high dietary iron in rats

Astronauts total body iron stores are increased following space flight. Excess iron stores, in combination with radiation exposure during space flight, can cause oxidative stress and increase the risk of health problems including cancer.

Thirty two, 12 week old, male Sprague-Dawley rats were acclimated to an adequate iron diet (45 mg iron (ferric citrate)/kg diet) for 3 wk and then assigned to one of four groups: adequate Fe diet/no radiation (CON), adequate Fe diet/radiation (RAD), high Fe diet (650 mg iron (ferric citrate)/kg diet)/no radiation (IRON), and high Fe diet/radiation (IRON+RAD). Animals received the assigned diet for 4 wk. On d 14 of the experiment, animals were exposed to a 0.375 Gy fractionated radiation dose of Cs-137 every other day for 16 d (3 Gy total dose). Animals in both the sham and radiation groups were placed in a restraint tube (Battelle, Geneva, Switzerland) for about 10 min per session to be either irradiated or sham treated. On day 29 (24 h after last radiation exposure), animals were euthanized using isoflourane vapor. The colon was resected, feces removed, and colonic mucosa scraped. The aim of Experiment 1 was to characterize fecal bacterial populations using amplification and 454 pyrosequencing of bacterial 16S rDNA.

Experiment 2 high LET silicon particle exposure and hind limb unloading (HLU) (1/6 G) in mice

During space flight astronauts are exposed to galactic cosmic radiation (GCR) and low gravity environments. Partial gravity (1/6 G) will be experienced while on the lunar surface, and little is known regarding the effect of partial gravity and high LET radiation exposure on the GI tract.

Twenty-eight, 3 mo old, female BalbC/ByJ mice were acclimated to single housing conditions and a standard chow diet for 14 d. After acclimation, half of the animals were suspended in cages by the tail and shoulders. The suspension spring was adjusted to only allow for 1/6 weight bearing (LUN) on all four limbs as described previously (346). The remaining animals served as full weight bearing (WB) controls. Half of the LUN and WB were exposed to one dose of high LET 300 MeV ionizing silicon (50 cGy), simulating GCR, at Brookhaven National Laboratory, NY. All animals were euthanized 21 d following radiation (RAD) exposure by decapitation. The colon was resected, feces removed, and the colonic mucosa scraped. The aim of Experiment 2 was to 1) Characterize fecal bacterial populations using amplification and 454 pyrosequencing of bacteria 16S rDNA and 2) analyze alterations in the expression of genes involved in microbial signaling and tissue repair.

Experiment 3 combined high LET and low LET radiation exposures and microgravity conditions during short term space flight in mice

Fourteen, 49 day old, female C57BL/6 mice were acclimated to standard mouse diet and water for 2 wk. All animals were then loaded into animal enclosure module's

(AEM) and given *ad libitum* access to food and water for the remainder of the study. Half of the animals were flown on Atlantis shuttle mission STS-135 for a period of 13 d. Following landing (3-7 hr), all animals were anesthetized by isoflurane gas and euthanized by decapitation. The colon was resected, feces removed, and a 1 cm section was removed for histological preparations and the remainder was scraped. The aim of Experiment 3 was to 1) Characterize fecal bacterial populations using amplification and 454 pyrosequencing of bacteria 16S rDNA, 2) characterize alterations to gene expression in genes involved in microbial signaling and tissue repair, and 3) assess colonic epithelial injury and inflammation.

Sample collection and processing

Scraped mucosa

After fecal material was removed, the colon was washed twice in RNase free Phosphate-Buffered Saline (PBS) and scraped on a chilled RNase free surface.

Experiment 1 & 2. Mucosa was transferred to an RNase free homogenization tube along with 500 µl of Denaturation Solution (Ambion, Austin, TX), homogenized by pipetting 6-7 times, snap frozen, and then stored at -80°C.

Experiment 3. Mucosa was transferred to an RNase free homogenization tube along with 500 µl of RNA*later* (Ambion, Austin, TX), snap frozen, and then stored at -80°C.

Feces collection and microbial DNA isolation

Upon resection of the colon at termination, fresh fecal samples were collected immediately, transferred to sterile cryotubes, snap frozen, and then stored at -80°C.

DNA was isolated from homogenized fecal samples using a FastDNA SPIN kit according to the manufacturer's instructions (MP Biomedicals, Solon, OH) (Appendix B). Purified DNA was stored at -80°C. A negative control containing H_2O instead of sample was purified in parallel to each set of extractions to screen for contamination of extraction reagents.

Experiment 1 & 3. Bacterial DNA isolated from each sample was used for pyrosequencing and further phylogenetic analysis (described below).

Experiment 2. An aliquot of extracted bacterial DNA was taken from each animal and combined into a composite sample for each experimental group for pyrosequencing and further phylogenetic analysis (i.e., WB/sham irradiated (SHAM); WB/RAD; LUN/SHAM, and LUN/RAD).

Inflammation and injury histological scores

A 1 cm segment was removed from the distal end of the colon and fixed in 70% EtOH solution prior to embedding in paraffin. The degree of inflammation and morphological injury was assessed by H&E staining. Histologic examination was performed in a blinded manner by a board-certified pathologist, and the degrees of inflammation (score of 0–3) and epithelial injury (score of 0–3) in microscopic cross sections of the colon were graded as described previously (150) (Appendix B).

Measurement of gene expression using real-time PCR

Total RNA was isolated from scraped mucosal samples using Phase Lock Gel™ tubes (5 Prime, Gaithersburg, MD) and the ToTALLY RNA™ Kit or RNAqueous® kit (Ambion, Austin, TX) followed by DNase treatment (DNA-*free*™ Kit, Ambion, Austin,

TX). RNA quality was assessed using an Agilent Bioanalyzer prior to storage at -80°C. First strand cDNA was synthesized using random hexamers, oligo dT primer (Promega, Madison, WI), and Superscript™ III Reverse Transcriptase following manufacturer's instructions (Invitrogen, Carlsbad, CA).

Real-time PCR was performed on select genes (TFF3, Slc16a1, IL-6, IL-1β, TNFα, SLC5A8, TGFβ, TLR9, TLR4, TLR2, MyD88, NF-κB, COX-2) using Taqman® Array Plates (Applied Biosystems, Foster City, CA) and a ABI 7900 HT thermocycler (Applied Biosystems, Foster City, CA) (Assay IDs for all primers compiled in Appendix B). To screen for potential contamination of PCR reagents, a negative PCR control of H_2O instead of cDNA template was used. Expression levels were normalized to GAPDH gene expression for Experiment 1, and 18S gene expression in Experiment 2 and 3.

16S rRNA bacterial tag-encoded FLX amplicon pyrosequencing (bTEFAP)

Initial amplification of the V1-V2 region of the bacterial 16S rDNA was performed on total DNA isolated from fecal samples. Master mixes for these reactions used the Qiagen Hotstar Hi-Fidelity Polymerase Kit (Qiagen, Valencia CA) with a forward primer composed of the Roche Titanium Fusion Primer A (5'-CCATCTCATCCCTGCGTGTCTCCGACTCAG -3'), a 10 bp Multiplex Identifier (MID) sequence (Roche, Indianapolis, IN) unique to each of the samples, and the universal bacteria primer 8F (5'-AGAGTTTGATCCTGGCTCAG-3') (199). Incorporation of MID sequences to the PCR amplicons essentially "barcodes" samples and allow for multiplexed assays. Samples are pooled prior to the pyrosequencing reaction. The reverse primer was composed of the Roche Titanium Primer B

(5'-CCTATCCCCTGTGTGCCTTGGCAGTCTCAG -3'), the identical 10 bp MID sequence as the forward primer and the reverse bacteria primer 338R (5'-GCTGCCTCCCGTAGGAGT-3') (200) which span the V1-V2 hypervariable region of the bacterial 16S rDNA. The thermal profile for the amplification of each sample had an initial denaturing step at 94°C for 5 minutes, followed by a cycling of denaturing of 94°C for 45 seconds, annealing at 50°C for 30 seconds and a 90 second extension at 72°C (35 cycles), a 10 minute extension at 72°C and a final hold at 4°C. Each sample was individually gel purified using the E-Gel Electrophoresis System (Life Technologies, Invitrogen). To ensure equal representation of each sample in the sequencing run, each barcoded sample was standardized by calculating equimolar amounts prior to pooling. Pooled samples of the 16S rDNA multiplexed amplicons were sequenced on a Roche 454 Genome Sequencer FLX Titanium instrument (Microbiome Core Facility, Chapel Hill NC) using the GS FLX Titanium XLR70 sequencing reagents and protocols.

bTEFAP data analysis

Analysis of deep sequencing data was carried out using the QIIME pipeline (201). Briefly, the combined raw sequencing data plus metadata describing the samples were de-multiplexed and filtered for quality control. Next, data were denoised using Denoiser software as described previously (202). Chimeric sequences were depleted from the trimmed data set using Chimera Slayer (203). Sequences were grouped into OTUs (Operational Taxonomic Units) at a 97% level to approximate species-level phylotypes using Uclust (204). OTU sequences were aligned and OTU tables containing

the counts of each OTU in each sample were used to calculate mean species diversity of each sample (alpha diversity) and the differentiation among samples (beta diversity). Alpha and beta diversity measures were used to calculate a Chao species richness estimate and a Shannon Weaver diversity index for each OTU. To evaluate the similarities between bacterial communities a combination of Unifrac significance, principal coordinate analysis (PCoA) using Fast Unifrac (205) and network analysis (206-207) were performed to compare samples based on sample time and treatment. ANOVA, the G test of independence, Pearson correlation, or a paired t-test were used within Qiime to identify OTUs that are differentially represented across experimental treatments or measured variables.

Statistical analysis

Data were analyzed using two-way analysis of variance (ANOVA) or one sample ttest (TTEST) in SAS 9.1 (SAS Institute, Inc.) considering a p-value of <0.05 as significant. Data sets from Experiment 3 that were not normally distributed were analyzed using Kruskal-Wallis test considering a p-value of <0.05 as significant.

Results

Experiment 1

Body weight and experimental diet intake

Neither high dietary iron nor the radiation exposure changed body mass or food intake (data not shown).

Microbial taxonomic structure analysis

The number of OTUs classified in the Bacteroidetes phylum were numerically elevated and OTUs in the Firmicutes phylum were significantly lower in the RAD group compared to CON ($p=0.0392$) (Table 18). IRON rats had a numerically increased proportion of OTUs classified as Bacteroidetes (17%) and decreased proportion of Firmicutes (31%) compared to CON. Upon further phylogenetic classification we observe a significant radiation effect on the Lactobacillales and Clostridiales orders ($p=0.03$ and $p=0.02$, respectively) (Table 18 & Figure 16). The proportion of OTUs classified in the Lactobacillales order was numerically higher in RAD and IRON+RAD compared to sham irradiated rats, with IRON+RAD having a significantly higher proportion compared to CON and IRON ($p<0.05$). Additionally, radiation exposure numerically decreased the proportion of OTUs classified in the Clostridiales order for both experimental diets, with CON having significantly higher proportion compared to RAD and IRON+RAD. In general, radiation exposure had a significant effect on the proportion of Unknown OTUs in the Bacteroidetes phylum ($p=0.0324$) with IRON+RAD having significantly higher Unknown OTUs ($p<0.05$) compared to CON, RAD, and IRON groups (Table 18).

Diversity and species richness comparisons

We observe no significant differences in species diversity (Shannon Weaver index) across all experimental groups (Table 19). Species richness (Chao index) was numerically higher in IRON+RAD rats compared to CON and RAD groups, and significantly higher than IRON rats ($p=0.033$, Table 19).

Mucosal gene expression

Gene expression of gene targets associated with TLR signaling pathways, epithelial repair, and SCFA transporters were assessed in a previous study (Chapter IV).

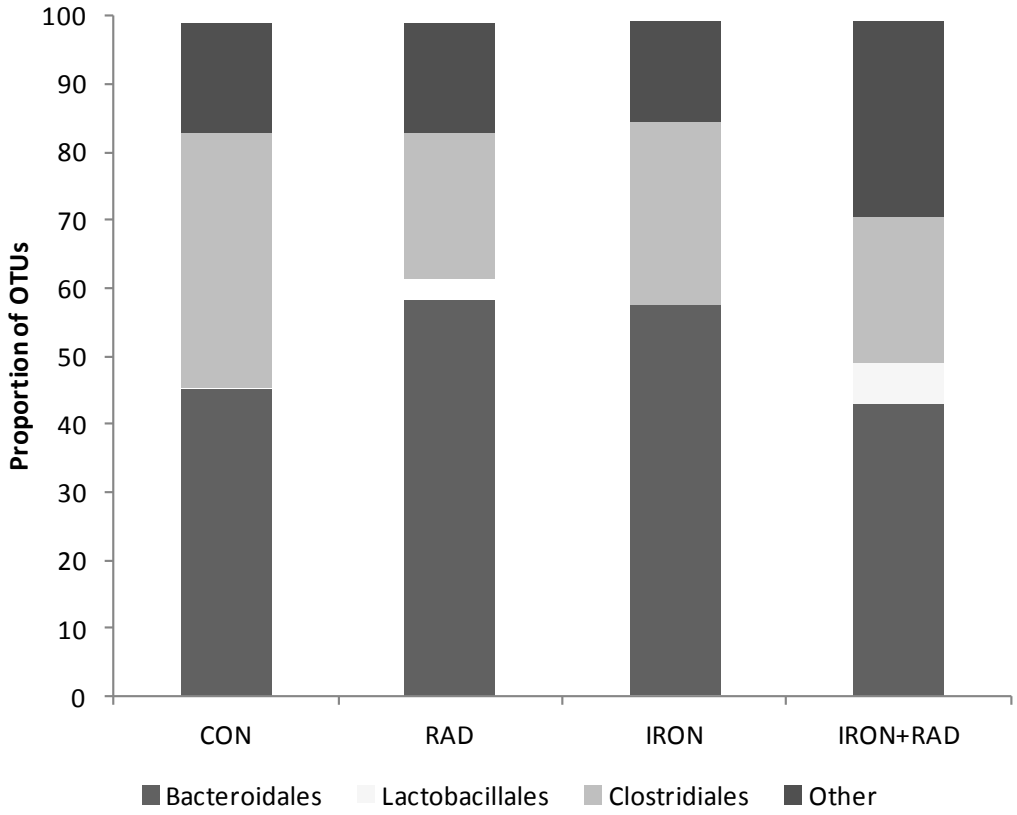

Figure 16. Phylogenetic classification of OTUs (%) at the order level from Experiment 1. The proportion of OTUs classified in the Lactobacillales order was significantly higher in IRON+RAD compared to CON and IRON ($p<0.05$). The proportion of OTUs classified in the Clostridiales order was significantly higher in CON compared to RAD and IRON+RAD ($p<0.05$). Actual values in Table 18.

Table 18. Phylogenetic classification of OTUs (%) from Experiment 1.

Experiment 1									
Phylum	**Family**	**Order**	**CON (N=8)**	**RAD (N=8)**	**IRON (N=8)**	**IRON+RAD (N=8)**	**Diet**	**Radiation**	**Diet* Radiation**
Bacteroidetes			55.18±5.88[a]	68.82±4.22[a]	66.30±4.65[a]	64.26±5.77[a]			
	Bacteroidia	Bacteroidales	45.33±7.04[a]	58.27±5.90[a]	57.68±4.26[a]	43.06±9.53[a]			0.057
	Unknown	Unknown	9.86±1.89[a]	10.55±2.29[a]	8.62±1.36[a]	21.20±4.90[b]		0.032	0.053
Firmicutes			39.55±5.62[b]	25.41±3.67[a]	27.46±3.41[ab]	29.25±4.70[ab]			
	Bacilli	Lactobacillales	0.1±0.03[a]	3.30±0.28[ab]	0.08±0.03[a]	6.05±0.27[b]		0.03	
	Clostridia	Clostridiales	37.56±5.20[b]	21.19±3.06[a]	26.64±3.58[ab]	21.54±4.44[a]		0.02	
	Erysipelotrichi	Erysipelotrichales	1.27±0.67[a]	0.37±0.10[a]	0.31±0.12[a]	1.33±0.85[a]			
Unknown			1.85±0.17[a]	2.31±0.36[a]	2.54±0.47[a]	2.52±0.40[a]			
Unassignable			2.94±0.22[a]	3.09±0.22[a]	3.44±0.86[a]	3.48±0.60[a]			
			Data are LS mean±SEM						
			Means without common superscripts differ (p<0.05)						

Table 19. Chao and Shannon Weaver indices for Experiment 1.

	Experiment 1			
	CON (N=8)	**RAD (N=8)**	**IRON (N=8)**	**IRON+RAD (N=8)**
Shannon Weaver	2.7±0.11[a]	2.62±0.23[a]	2.67±0.23[a]	3.12±0.32[a]
Chao	68.19±2.49[ab]	67.22±5.15[ab]	62.7±4.24[a]	80.44±8.63[b]
	Data are LS means ±SEM.			
	Means without common superscripts differ (p<0.05).			

Experiment 2

Microbial taxonomic structure analysis

As an initial analysis of the effect of weightlessness and high LET radiation on the intestinal microbiota, aliquots of extracted microbial DNA from each animal was combined into a composite sample for each experimental group (i.e., WB SHAM, WB RAD, LUN SHAM, LUN RAD) and bacterial populations were phylogentically classified (Appendix A-6). Compared to WB SHAM, we observe an increase in OTUs classified in the Bacteroidetes phylum and decrease in the Firmicutes phylum in WB RAD (Figure 17A). When comparing SHAM and RAD groups within each environmental treatment (WB vs LUN), we observe differential effects of radiation exposure on the predominant phyla. RAD increased Bacteroidetes and decreased Firmicutes in WB, yet the inverse was observed in LUN RAD mice. Further taxonomical classification at the order level revealed the majority of OTUs classified in the Bacteroidetes phylum were Unknown (Other) at the order level (Figure 17B, Appendix A-6). In WB mice (SHAM and RAD groups) we observe a large proportion of OTUs classified in the Lactobacillales order (38-40%) and lower proportion classified in the Clostridiales order (10-13%) (Figure 17B). In contrast, LUN mice (SHAM and RAD groups) had high proportions in Clostridiales (33-38%) and low proportions in Lactobacillales order (3-7%).

Diversity and species richness comparisons

We observe little differences in bacterial diversity across all experimental groups, with LUN SHAM and LUN RAD mice having numerically higher indices than WB mice

(Table 20). RAD increases bacterial species richness in both WB and LUN groups (27% and 21%, respectively) with the greatest richness observed in LUN RAD mice (90.94).

Table 20. Chao and Shannon Weaver indices for Experiment 2.

	Experiment 2†			
	WB SHAM (N=9)	**WB RAD (N=9)**	**LUN SHAM (N=11)**	**LUN RAD (N=11)**
Shannon Weaver	3.72	3.22	4.55	4.95
Chao	44.43	61.06	72.27	90.94
	† Indices represent analysis of one composite sample containing aliquots from N animals in each group.			
	Data are LS means ±SEM.			
	Means without common superscripts differ (p<0.05).			

Mucosal gene expression

We do not observe a significant effect of diet or treatment on relative expression of any gene targets analyzed, or any significant differences between any experimental groups (Table 21). We observed a numerical elevation in relative expression of IL1b and TGFβ in the LUN SHAM group and TLR4, MyD88, RelA/p65 (regulatory element for NFκB), TFF3, and Slc5a8 in the LUN RAD group compared to WB mice (SHAM & RAD).

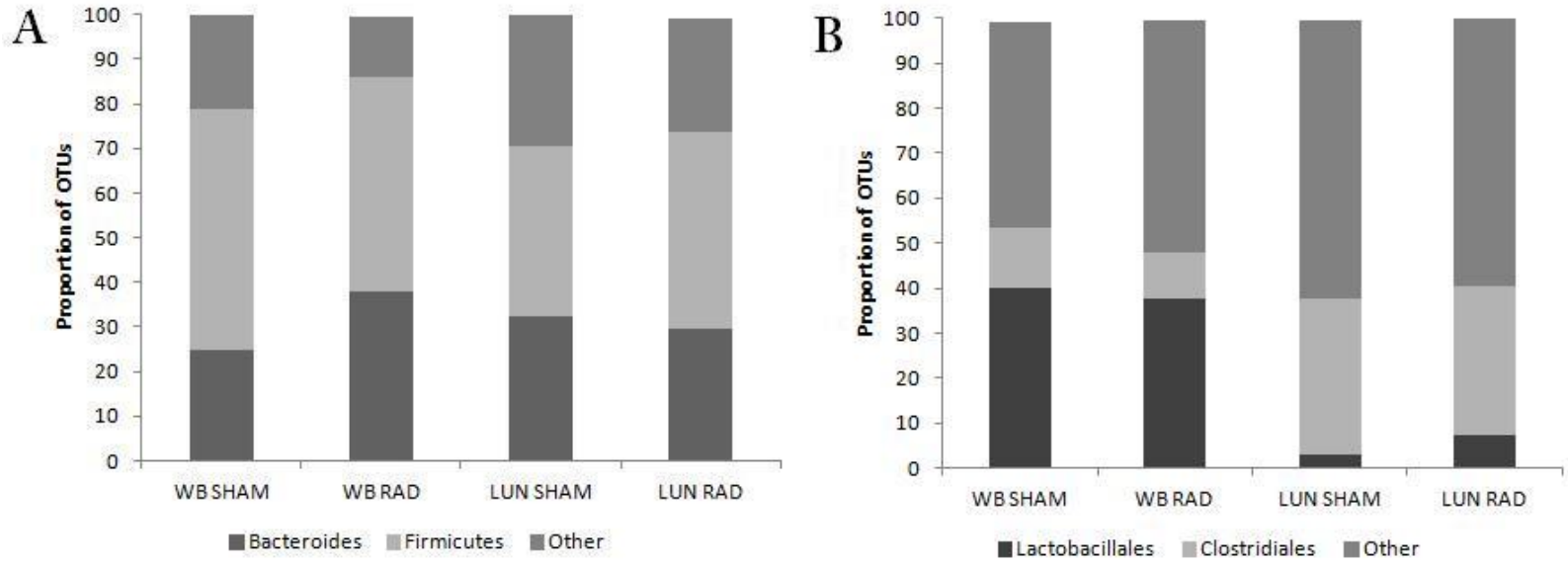

Figure 17. A) Phylogenetic classification of OTUs (%) at the phylum level for Experiment 2. B) Phylogenetic classification of OTUs (%) at the order level for Experiment 2. See Appendix A-6 for actual values.

Experiment 3

Body weight and experimental diet intake

Post flight, we observed significantly lower body weights in flight mice compared to ground controls (Figure 18A). Food intake was not significantly different between groups (not shown), however, water intake during flight was significantly suppressed in flight mice compared to ground mice (Figure 18B).

Microbial taxonomic structure analysis

Unifrac and principal components analysis (PCA) of all sequences for each sample, represented as a discrete data point without overlap, revealed distinct clustering of samples collected from ground and flight mice (Figure 19), yet we observe no significant differences in OTUs at the phylum level (Appendix A-7). Flight mice had a numerically higher proportion of OTUs classified in the Bacteroidetes (8%) and lower proportion of Firmicutes (14%) phylum compared to ground mice (Figure 20). Further phylogenetic classification also showed very few significances at the order level, with ground mice only having significantly higher proportion of OTUs classified as Erysipelotrichales compared to flight mice ($p=0.0467$, Figure 20). In flight mice, we observe a numerically higher proportion of OTUs classified in the Clostridiales order (60%) and numerically lower proportion of Lactobacillales (62%) compared to ground mice (Figure 20).

Diversity and species richness comparisons

We observe no significant differences in species richness or diversity between ground and flight mice, with flight mice having a lower Shannon Weaver and Chao index compared to ground mice (Table 22).

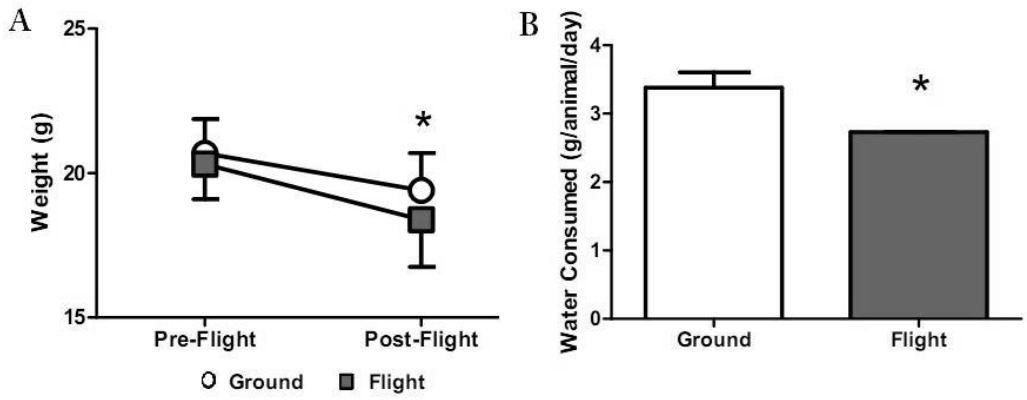

Figure 18. A) Mean body weight was significantly lower in flight mice compared to ground controls post-flight ($p<0.05$). B) Total water consumption was significantly lower in flight mice compared to ground controls. Means with * differ between ground and flight mice ($p<0.05$). Data are LS means ±SEM.

Table 21. Relative expression of selected gene loci for Experiment 2. No significant differences were observed ($p<0.05$).

	BNL†			
	WB SHAM (N=4)	WB RAD (N=5)	LUN SHAM (N=4)	LUN RAD (N=4)
TLR 2	1.56±0.41	1.63±0.12	1.09±0.66	1.17±0.76
TLR 4	0.39±0.10	0.32±0.10	0.30±0.11	0.49±0.09
TLR 9	0.08±0.02	0.06±0.02	0.06±0.02	0.08±0.04
MyD88	0.95±0.15	0.67±0.06	0.59±0.20	1.01±0.25
RelA	0.48±0.06	0.41±0.07	0.46±0.11	0.52±0.10
TNFα	0.04±0.01	0.03±0.01	0.04±0.02	0.04±0.01
IL6	0.01±0.003	0.02±0.057	0.02±0.004	0.02±0.008
IL1b	0.01±0.003	0.01±0.001	0.67±0.003	0.13±0.126
TGFβ	0.52±0.16	0.52±0.08	0.57±0.42	0.27±0.11
TFF3	291±71.5	198±39.8	198±52.5	379±134.9
Slc16a1	16.53±3.56	9.83±2.16	10.71±3.42	13.62±2.71
Slc5a8	3.70±0.44	3.84±1.30	3.05±1.14	6.32±1.68
	† No significant differences observed ($p<0.05$)			
	Data are LS means ±SEM			

Table 22. Chao and Shannon Weaver indices for Experiment 3.

	Experiment 3	
	Ground (N=7)	**Flight (N=7)**
Shannon Weaver	4.46±0.27[a]	4.04±0.27[a]
Chao	84.81±4.74[a]	82.95±14.01[a]
	Data are LS means ±SEM.	
	Means without common	
	superscripts differ ($p<0.05$).	

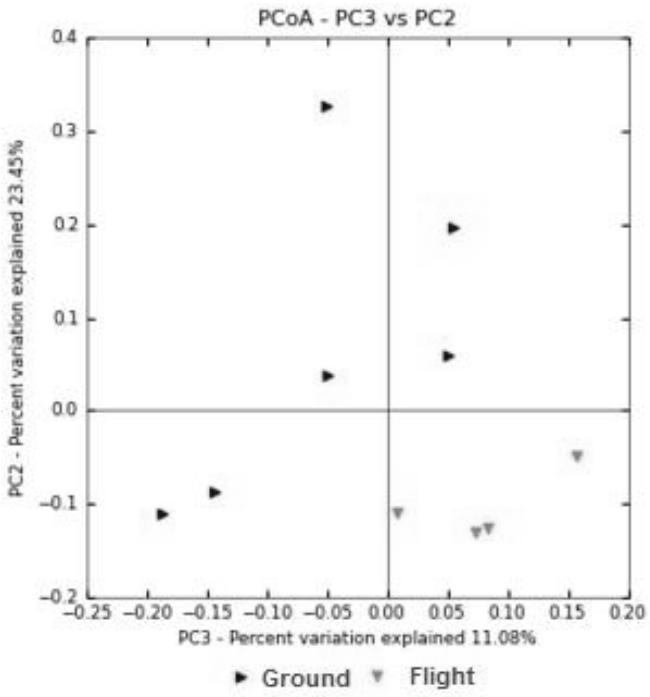

Figure 19. PCA plot of samples from ground and flight mice. Flight mice data points cluster in the bottom right quadrant, illustrating differences in bacterial populations compared to ground controls.

Mucosal gene expression

We observe no significant differences in any gene targets analyzed, except TGFβ, which was significantly higher in flight mice compared to controls (p=0.0453, Table 23). Relative gene expression was numerically higher in TLR2, IL6 and Slc16a1 in flight mice compared to ground control mice.

Table 23. Relative expression of selected gene loci for Experiment 3. Relative expression of TGFβ was significantly higher in flight mice compared to ground control mice. Relative expression of IL1b was not measurable. Means without common superscripts differ ($p<0.05$).

	STS-135	
	Ground (N=6)	Flight (N=5)
TLR 2	0.54±0.21	0.66±0.06
TLR 4	0.20±0.04	0.14±0.03
TLR 9	0.03±0.00	0.02±0.01
MyD88	0.30±0.07	0.26±0.04
RelA	0.18±0.03	0.15±0.03
TNFα	0.01±0.005	0.01±0.002
IL6	0.005±0.002	0.010±0.001
TGFβ	1.7 ± 1.04^{a}	4.1 ± 0.37^{b}
TFF3	107±23.4	102±18.6
Slc16a1	2.82±0.98	3.42±0.39
Slc5a8	0.84±0.19	0.65±0.15
	Data are LS means ±SEM	

Immunohistochemical analysis of distal colon

To understand the effects of spaceflight (i.e., combined weightlessness and mixed radiation exposure) on intestinal injury and inflammation, distal colon was analyzed by a board certified pathologist. We observe no significant differences in intestinal injury and inflammatory infiltration between flight and ground mice (Figure 21).

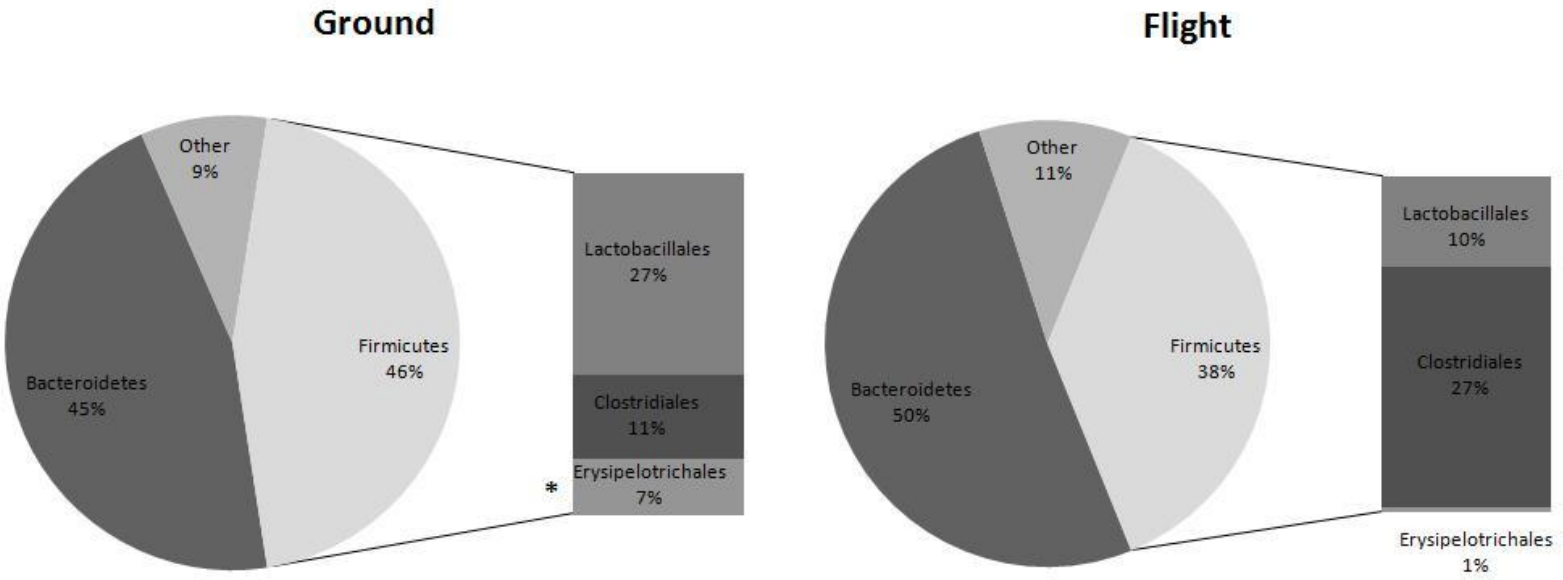

Figure 20. Phylogenetic classification of OTUs from Experiment 3. Ground control mice had a significantly higher proportion of OTUs classified as Erysipelotrichales compared to flight mice ($p<0.05$). Flight mice had a numerically higher proportion of OTUs classified in the Bacteroidetes phylum and Clostridiales order, and a numerically lower proportion of OTUs in the Firmicutes phylum and Lactobacillales order compared to ground control mice. Taxa with * differ between ground and flight mice ($p<0.05$). See Appendix A-7 for actual values.

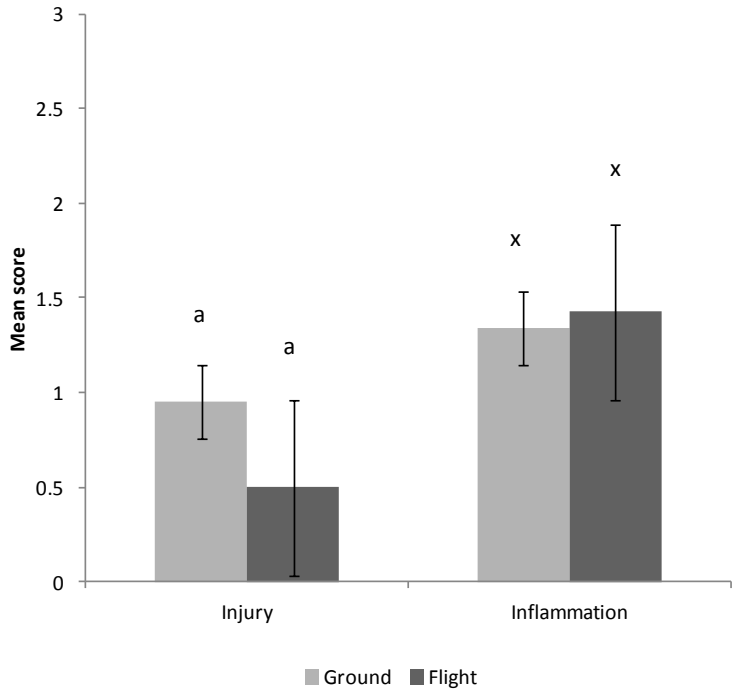

Figure 21. Injury and inflammation scores of distal colon from flight and ground mice in Experiment 3. No significant differences were observed between flight and ground control mice ($p<0.05$). Values are LS mean ± SEM.

Discussion

Astronauts are exposed to different types of radiation from numerous sources including solar particle events, galactic cosmic rays, and charged particles held in the Van Allen belts. These types of radiation have varying LET, and consist of a combination of protons, alpha particles (hydrogen), and a small percentage of heavy ions (e.g., Fe and Si) and electrons, which can penetrate shielding and create secondary particles (21). Radiation exposure and other factors relating to space flight such as diets

high in iron and microgravity can elevate oxidative stress in the body, which has been shown to dysregulate the immune response and is a factor in bone demineralization, muscle atrophy, cardiovascular deconditioning and cataracts (347-351). Recent studies have shown that the intestinal bacterial populations, or microbiota, can be altered by oxidative stress and have been implicated in gastrointestinal diseases such inflammatory bowel disease (IBD) (97, 172, 217-218, 352). Furthermore, recent studies in our lab demonstrated that fecal microbial metabolite concentrations (i.e., short chain fatty acids (SCFA)) are affected by low LET radiation exposure and high dietary iron, suggesting alterations to the microbiota or microbial metabolism in response to space relevant conditions. The initiation and progression of intestinal inflammation is of upmost importance to astronaut health, as it known to increase the risk of colorectal cancers (3-4, 353). Additionally, the effect of radiation on the body has been identified by NASA as one of the most significant risks associated with space flight, and their recent reports estimated that the "probability of causation" for colon cancer is 3rd highest following galactic cosmic radiation exposure (354-355).

We utilized three experimental paradigms to characterize and compare how various insults associated with spaceflight may affect the colonic environment. Understanding how different radiation energies affects the intestinal tract is important, as previous studies have observed differences in cell survival, DNA repair, epithelial cell proliferation, differentiation, and tumor incidence following low and high LET radiation exposure (356-358). Additionally, our experimental design allowed us to compare simulated 1/6 G lunar microgravity (i.e., hind limb unloading (HLU)) to zero gravity of

space flight. Furthermore, it is important to elucidate the combined effects of radiation exposure and microgravity on the colonic environment, as recent studies report a synergistic effect between these exposures and miRNA expression, immune activation, and bone loss (359-361). Very little is known about how the space environment effects intestinal homeostasis, thus, the aim of this study was to characterize the effect of high and low LET radiation exposure, microgravity, and elevated dietary iron on the intestinal microbiota and gene targets associated with microbial derived signaling, metabolite transport, and epithelial repair.

Historically studies have shown that the presence of commensal bacterial populations increased radiation induced lethality in conventionalized (i.e., presence of microbiota) compared to germ free animals (345), but a direct mechanism was not elucidated. More recent studies report alterations to the microbiota after low LET X ray exposure, and observed distinct differences based on received dose, amount of time following exposure, as well as presence of clinical signs such as radiation-induced diarrhea (114, 362). One small pilot study used denaturing gradient gel electrophoresis (DGGE) to identify changes in the bacterial diversity of patients suffering from acute post-radiotherapy diarrhea (total exposure of 4,300-5,400 cGy) (114). They observed that the microbial profiles of the individuals studied (i.e., no radiation, radiation with no diarrhea, and radiation with diarrhea) clustered in unique sets, suggesting that specific bacterial populations could be associated with risk or protection after radiation exposure. Subjects with clinical signs (i.e., diarrhea) had markedly higher proportions of *Bacilli* species and bacteria characterized in the Actinobacteria phylum compared to those

without diarrhea following radiation treatment (114). Another *in vivo* study demonstrated distinct differences in microbial populations based on length of time following 10 Gy X ray exposure. Hierarchical clustering of bacterial populations from samples collected 0, 4, 11, and 21 d post exposure suggested distinct differences in the bacterial populations over time (362). Following phylogenetic classification of bacterial groups, they report an increase in Proteobacteria following both 10 Gy acute and 18 Gy fractionated radiation exposure. Furthermore, the proportion of *Clostridia* in the feces of animals receiving an 18 Gy dose was 1/10 of the value observed in controls. This alteration was not observed in animals that received 10 Gy X ray, suggesting differences based off received dose (362). Those findings suggest that radiation has an effect on the proportion of different bacterial groups present in the intestine. Unfortunately, little phylogenetic classification was performed in the pilot study, which could have provided more insight into which specific bacterial taxa might be involved in the etiology of intestinal dysfunction caused by radiation. Furthermore, these studies used large doses of low LET radiation exposures that are markedly higher than this study (5-22 Gy compared to 3 Gy, respectively), and do not include the effect of high LET radiation exposure on the microbiota.

Phylogenetic classification of fecal intestinal bacterial populations at the phylum level revealed similarities across the various treatments (i.e., low LET radiation, high LET radiation, microgravity, elevated Fe diet). Following low LET radiation exposure (RAD), we observe an increased proportion of bacteria classified in the Bacteroidetes phylum and decreased Firmicutes phylum compared to CON. We also observe similar

alterations to these phyla in IRON animals. High LET radiation exposure and simulated microgravity (i.e., hind limb unloading (HLU)) also increased the proportion of Bacteroidetes and decreased Firmicutes in WB RAD, LUN SHAM and LUN RAD compared to WB SHAM. Unfortunately, since we analyzed a composite sample we were unable to statistically compare these proportions. We observe increased Bacteriodetes and decreased Firmicutes following HLU and high dietary iron exposures individually, however, we do not observe a synergistic effect of low LET radiation exposure and high dietary iron (Experiment 1), or high LET radiation exposure and 1/6 G HLU (Experiment 2). These results suggest that both high and low LET radiation exposure, as well as other environmental insults such as high dietary iron and microgravity, have similar effects on the proportions of bacterial populations at the phylum level. Similar to both experiment 1 and 2, animals exposed to 12 d of space flight had an increased proportion of Bacteroidetes and decrease in Firmicutes compared to ground controls. This suggests that mixed radiation exposure associated with space flight, comprised of both high and low LET radiation, produces similar effects to the predominant phyla as treatment with one energy (i.e., X ray or high charge (Z) energy (E) silicon nuclei (HZE)).

These global observations of the predominant bacterial groups are of interest, as dysbiosis to these phyla have been linked to elevated oxidative stress in the body associated with obesity and IBD (194, 210). Interestingly, increased proportions of Firmicutes and decreased Bacteriodetes have been reported in these studies, which contrast our observations following radiation exposure, microgravity, and an elevated

iron diet. Another contradiction to the results in this study is the report of elevated proportions of pathogenic bacteria in patients with IBD and following low LET X-ray exposure (8, 97, 191, 362). These studies indicated an increase in bacterial taxa (i.e., Enterobacteriaceae, *Escherichia coli*, *Salmonella* spp.) classified in the Proteobacteria phylum, which is a common constituent of the commensal intestinal flora but also contains numerous pathogenic species such as *Vibrio*, *Helicobacter*, *Yersinia pestis*, *Klebsiella* and *Shigella*. We observe ≤0.07% Proteobacteria in all experimental groups analyzed in this study, which is in contrast to previous studies reporting an elevation in this phylum following 10 and 18 Gy X-ray exposure (362). This suggests that the presence of these particular pathogenic bacteria is not a major constituent of the microbiota in our study, and that modulation of this bacterial group by radiation exposure might be dose dependant. This observation is positive, as the virulence of numerous pathogens, including *Escherichia coli* and *Salmonella* and *Bacillus* spp., have been reported to be increased following simulated microgravity and space flight (363-366). Furthermore, it is thought that microgravity has an effect on fighting bacterial infections, as studies have reported that HLU animals have suppressed immune system function and increased lethality when exposed to pathogenic bacteria (e.g., *Klebsiella pneumonia* and *Pseudomonas aeruginosa*) (367-368). Furthermore, it was reported that HLU mice had elevated bacterial organ load following administration of *Klebsiella pneumonia* compared to weight bearing controls, suggesting susceptibility to bacterial translocation from the bowel (367).

To better understand the implications of the observed altered proportions of Firmicutes and Bacteroidetes, we performed further phylogenetic classification and observe distinct differences at the order level across treatments. Within the Firmicutes phylum we observe differences in the Lactobacillales and Clostridiales orders in animals exposed to either low LET radiation or microgravity. Animals exposed to microgravity (both HLU and space flight) had an increased proportion of bacteria classified in the order Clostridiales and decreased proportion of Lactobacillales compared to WB or ground animals. This observation is independent of radiation exposure in experiment 2, as both LUN SHAM and LUN RAD demonstrate these population shifts. Similarly, animals exposed to 12 d space flight also demonstrate an increased proportion of Clostridiales and decreased proportion of Lactobacillales compared to ground controls. These reports are similar to those observed in patients with IBD, as it has been documented in numerous studies a suppression in lactic acid bacteria (LAB) species as well as increased *Clostridium* spp (found in Lactobacillales and Clostridiales order, respectively) (100, 211). Results from experiment 1 contrast these observations, as RAD and IRON+RAD animals have numerically higher proportions of Lactobacillales and significantly lower proportion of Clostridiales compared to sham irradiated animals (i.e., CON & IRON). Observing lower proportions of Clostridiales in these animals may explain our previous observation of suppressed fecal butyrate, since this order harbors bacterial species known to have the capability to produce this metabolite (220-221). An increase in LAB is generally thought to be positive, as these bacterial populations have been shown to provide health benefits to the host (e.g., produce antimicrobial

substances, compete with pathogens for epithelial binding sites) and improves symptoms of chronic intestinal inflammation (123-124, 214-215). However, an increase in luminal H_2O_2 produced by these bacteria could exacerbate the effects of an elevated iron diet by creating highly reactive hydroxyl radicals through iron-mediated Fenton chemistry (343). Although this was not directly measured in this study, increased luminal and epithelial reactive oxygen species (ROS) could potentiate local oxidative stress.

Enhanced oxidative stress has the potential to cause cellular damage and induce an inflammatory response in the colon, and we previously demonstrated that myeloperoxidase activity (i.e., a marker of neutrophil infiltration) is elevated in colonic mucosa following consumption of an elevated iron diet and exposure radiation (Chapter IV). Furthermore, alterations to the microbiota have been shown to initiate an inflammatory state by aberrant signaling through pattern recognition receptors such as toll-like receptors (TLR). We previously reported that low LET radiation exposure and elevated dietary iron altered mucosal gene expression in the TLR signaling cascade. Four gene targets involved in bacterial recognition and inflammatory responses were reduced by low LET radiation exposure; TLR9 (a bacterial recognition receptor), TNF-α (a cytokine involved in systemic inflammation) and its receptor, TNFα1b, and IL-6 (an interleukin with both pro-inflammatory and anti-inflammatory effects). Additionally, TLR4, TFF3 and Slc5a8 expression decreased when exposed to high dietary iron. Alterations in TLR expression could also be attributed to the observed changes in the microbiota, or other factors such as compromised barrier integrity, and colonic inflammation, all of which have been documented to alter expression of these receptors

(7, 187, 369). Microbial-derived signaling through pattern-recognition receptors affects gene expression, transepithelial electrical resistance, colonocyte proliferation in normal tissues (332), and serves as a pivotal role for maintaining homeostasis between commensal microbiota and the host immune system (73). Alterations in the TLR signaling pathway directly affects the immune response, specifically through downstream activation of the transcription factor NF-κB (334). NF-κB activation alters expression of localized cytokines (IL-1β, IL-10, IL-6, TNF-α, IFN-γ and TGF-β) and pro-inflammatory molecules (COX-2) during an inflammatory response (261). Therefore to understand the implications of high LET radiation exposure and microgravity on these processes, we analyzed mucosal gene expression of gene targets associated with the TLR signaling cascade (i.e., TLR2, TLR4, TLR9, MyD88, NFκB, TNFα, IL6, IL1b), short chain fatty acid (SCFA) transport (i.e., Slc16a1, Slc5a8), and epithelial injury repair (i.e., TGFβ, TFF3) in experiment 2 and 3.

Previous studies have shown that high LET radiation exposure and microgravity has a direct effect on gene expression *in vitro* and in muscle tissue (359, 370-373), but to our knowledge no analysis has been published describing these effects in the intestinal tract. We do not observe any significant effect of high LET radiation exposure or HLU for any targets associated with the TLR signaling cascade or SCFA transport. Previous studies have shown that low LET radiation exposure can upregulate the expression of pro-inflammatory cytokines (i.e., INFα, IL-6, IL-1, TNFα) in murine macrophages and increase their concentration in serum (368, 374-375), which contrasts our results from Experiment 1 described above. Zhou et al. reported that HLU acts synergistically with

radiation exposure to markedly elevate circulating INFα, IL-6, and TNFα in mice (374). Although we did not analyze cytokine concentrations in plasma or other organs, we do not observe an increase in the relative expression of IL-6, IL-1b, COX-2 or TNFα in the colonic mucosa of experiment 2 and 3 animals (50 cGy silicon exposure ± HLU and spaceflight, respectively). Additionally, immunohistological assessment of distal colon does not reveal an increase in inflammatory cytokine or neutrophil infiltration following spaceflight. Differences in these observations could be due to the amount of time following radiation exposure and tissue collection in Experiment 2 (21 d), or the effect of low dose gamma irradiation compared to low dose HZE silicon exposure on pro-inflammatory cytokine gene expression.

For both experiment 2 and 3 we observe an upregulation of repair proteins. Relative expression of TFF3 was elevated in LUN RAD animals, which is a protein expressed on the apical side of the epithelial membrane and has been shown to be involved in cellular migration and repair (162). Flight mice had a significantly higher relative expression of repair protein TGFβ compared to ground controls, which acts on the basolateral side of the epithelial membrane (167). Previous studies have demonstrated that HLU can affect the ability to fight bacterial infection, and is thought to be due to impaired barrier integrity of the gastrointestinal tract (367, 374, 376). Immunohistological assessment of distal colon injury in flight animals does not indicate space flight significantly affects epithelial integrity, and these observations were generally described as discrete epithelial lesions with no surface erosion or presence of focal ulcerations. However, our results could suggest repair protein expression is

upregulated to mitigate the observed epithelial lesions following exposure to the space environment. It has been reported that immune system responses following radiation exposure differ across mouse strains and could be a factor when comparing our results to previous studies (377). Future studies with increased sample sizes could allow for more statistical power and further elucidate significant differences between experimental groups for gene targets associated with the TLR signaling cascade. Furthermore, alterations to the microbiota we observe directly following spaceflight may have the ability to initiate an inflammatory state and alter TLR expression if followed for an extended period after return to Earth.

To our knowledge, this is the first study to analyze these experimental paradigms on the intestinal microbiota and colonic mucosal gene expression. Although minimal differences were observed in our selected gene targets, we have illustrated distinct differences in the microbiota following elevated dietary iron consumption, radiation exposure (i.e., high and low LET) and microgravity (HLU and space flight). Previous work in this field has analyzed the effect of radiation exposure on the microbiota after much larger doses of low LET radiation (114, 345, 362), and did not analyze the effect of high LET exposure. Furthermore, this is the first study to perform phylogenetic characterization of the intestinal microbiota in a microgravity environment. Comparing changes to the microbiota following various space flight insults is important, as it is now understood that we cannot directly compare observations across studies utilizing different radiation parameters (i.e., high and low dose; high and low LET). Furthermore, we observe distinct shifts in bacterial populations in animals exposed to microgravity

independent of radiation exposure. Across all experiments in this study we do not observe a marked dysbiosis to the predominant phyla, reduced bacterial diversity, nor an increased proportion of pathogenic genera previously reported during intestinal inflammation. These observations suggest unique alterations to the microbiota when exposed to a space environment compared to other sources of intestinal oxidative stress. A low dose, fractionated radiation exposure was chosen for experiments 1 and 2 to directly compare to the radiation exposure that astronauts experience during short space flight missions. Results from this study can also benefit airline crews and radiation workers who experience low dose exposures. Furthermore, characterizing the effect of high LET radiation exposure on the luminal environment is applicable to patients receiving heavy-ion cancer therapy. Understanding the implications on the intestinal microbiota and microbial signaling in these patients will be useful for estimating the incidence of secondary malignancies. Future studies analyzing alterations to the intestinal bacterial population's genetic code, or metagenome, in patients receiving radiation therapy and astronauts would further elucidate how radiation exposure could affect intestinal homeostasis.

CHAPTER VI

SUMMARY AND CONCLUSIONS

Intestinal homeostasis can be altered in a variety of ways including UC and environmental factors such as radiation exposure and elevated dietary iron. It is well documented that there are alterations to the intestinal microbiota during bouts of inflammation and it is hypothesized that this dysbiosis is a direct contributor to progression of colonic inflammation (172, 211, 213). Mitigating an aberrant immune response and reoccurring bouts of inflammation is important to reduce GI disease progression and the increased risk of colitis associated cancers. Existing therapies for UC such as pharmaceuticals and biological agents may produce an initial response, yet, it is estimated less than 1/3 of patients gain full remission following these treatments (378). Altering dietary constituents has been shown to attenuate the effects of inflammation and treat UC, and those rich in bioactive compounds or plant polyphenols have received interest in recent years. This is thought, in part, due to their antioxidant and anti-inflammatory properties as well as altering bacterial populations (108, 121, 146). Our lab previously reported that sorghum bran diets can increase endogenous antioxidant enzymes such as catalase and superoxide dismutase, and have the ability to reduce aberrant crypt foci in AOM induced colorectal cancer (24), yet, their effect on UC has not been studied.

To our knowledge, this is the first study to demonstrate that sorghum based diets may have the ability to attenuate the symptoms of DSS induced colitis. Our results

indicate that by feeding bran based diets, it is possible to reduce the severity of epithelial injury and alleviate clinical symptoms such as diarrhea commonly associated with DSS induced colitis models and reported in patients suffering from UC. Furthermore, we demonstrate these diets may be able to mitigate colonic injury by upregulating epithelial repair protein (i.e., TFF3 and TGFβ) expression. Sorghum based diets significantly affected excreted fecal SCFA including propionate and butyrate, with Sumac bran having the lowest proportion of excreted butyrate compared total SCFA. Furthermore, we do not observe a decrease in fecal SCFA concentrations commonly reported in patients with UC. One explanation could be an increase in the relative expression of SCFA transporters (i.e., Slc16a1 and Slc5a8), which we observe in sorghum bran fed rats but not cellulose fed rats.

In this body of work, we observe distinct differences in the intestinal microbiota following two experimental paradigms; one using a chemical inducer of inflammation/injury (DSS) and the other using various forms of radiation, weightlessness and diets commonly consumed in the space environment. Pyrosequencing of fecal microbial DNA allowed for deep analysis of the microbiota and we document numerous differential changes to the bacterial populations following each experiment. During DSS induced colitis, we observe that repeated exposures of DSS does alter the intestinal microbiota and produce alterations commonly observed in UC including reduced diversity and species richness. However, when fed a sorghum bran based diet we observe a restoration of both species richness and diversity following recovery from the third DSS exposure, with condensed tannin containing brans having

numerically higher indices at this time point compared to their diet matched controls. Furthermore, it has been shown that the Firmicutes to Bacteroidetes ratio is altered in patients with IBD with an increase in Firmicutes observed in these patients compared to controls. In this study we do not observe an increase in this ratio during DSS induced colitis when feeding a sorghum bran diet, suggesting we may be able to mitigate alterations to these bacterial phyla commonly observed in UC.

To our knowledge, this is the first study to document the effect of the space environment on the intestinal microbiota. Although we do not observe a significant effect of a high iron diet on the fecal microbial populations identified in this study, we do observe significant alterations due to radiation exposure and microgravity. In experiment 1, we observe a significant effect of radiation on the bacterial orders Lactobacillales and Clostridiales. Lactobacillales was significantly higher in IRON+RAD animals compared to rats that were not irradiated (both low Fe and high Fe). Clostridiales was significantly reduced in rats exposed to radiation (both low Fe and high Fe) compared to CON rats, and this observation may be a reason for reduced concentrations of luminal SCFA with IRON+RAD rats having the lowest concentrations compared to all other experimental groups.

Interestingly, we observe a distinct effect of microgravity on the proportion of these bacterial populations with lower Lactobacillales and higher Clostridiales observed in animals exposed to both HLU and spaceflight. These observations may be independent of radiation exposure, as we observe these changes in SHAM and RAD animals in experiment 2. These observations suggest that there are alterations to the

microbiota specifically associated with the space environment and could be detrimental to astronaut health. Moreover, the effect of radiation on the intestinal microbiota that we observe in this study could have implications for patients receiving heavy-ion cancer therapy, airline crews, and radiation workers who experience low dose exposures similar to those utilized in these experiments.

Future Studies

Each experimental paradigm differentially altered the microbiota and mucosal environment and further studies are warranted to elucidate specific mechanisms by which these experimental paradigms alter GI homeostasis. To better understand the progression of disease and inflammation in DSS induced colitis, staggering terminations could further elucidate a phenotype during a more active disease state. Additionally, assessing microbes before feeding the experimental diets and over time would better describe changes by supplementing with sorghum bran. We observe distinct differences when fed sorghum bran diets compared to a cellulose control diet, suggesting that the bioactive compounds in the bran may have the ability to exert the clinical effects in this study. Metabolomics could identify if these bioactive compounds have a systemic effect, as well help elucidate the mechanism that allows these compounds to mitigate the effect of DSS induced colitis.

We observe distinct differences in the microbiota following low dose, low LET radiation exposure and microgravity. Experiments in this study were designed to mimic radiation doses similar to what would be experienced during a short term space flight, however, the microgravity duration in these studies were significantly shorter (12-21 d)

than an International Space Station mission (90-180 days) or future missions extending into deep space. Furthermore, astronauts embarking on deep space missions would experience a much larger dose of radiation, particularly high LET HZE exposures. Therefore, studies analyzing larger doses of radiation and extended microgravity exposure on the microbiota and mucosal environment are warranted.

Across all studies, performing nearest neighbor analysis would be useful to describe bacterial populations that are unclassified or unknown in the RDP database. Additionally, in order to better characterize which microbial populations have a direct affect on TLR signaling, analyzing mucosa microbiota instead of feces could help better understand these interactions. Previous studies have identified specific bacterial population associated with goblet cell mucin that differ from the fecal stream, therefore, characterization of these bacterial populations are warranted. Specific analysis of microbial butyrate producing gene targets would help link our SCFA observations to the microbial populations characterized in this study. Furthermore, analysis of the bacterial population's genome, or metagenome, would give insight on the function of characterized populations and unidentified phylotypes, and further elucidate implications on intestinal inflammation.

REFERENCES

1. Eaden JA, Abrams KR, Mayberry JF. The risk of colorectal cancer in ulcerative colitis: A meta-analysis. Gut. 2001;48:526-35.

2. Jess T, Loftus Jr EV, Velayos FS, Harmsen WS, Zinsmeister AR, Smyrk TC, Schleck CD, Tremaine WJ, Melton LJ, et al. Risk of intestinal cancer in inflammatory bowel disease: A population-based study from Olmsted County, Minnesota. Gastroenterology. 2006;130:1039-46.

3. Rutter MD, Saunders BP, Wilkinson KH, Rumbles S, Schofield G, Kamm MA, Williams CB, Price AB, Talbot IC, et al. Thirty-year analysis of a colonoscopic surveillance program for neoplasia in ulcerative colitis. Gastroenterology. 2006;130:1030-38.

4. Itzkowitz SH, Yio X. Inflammation and cancer IV. Colorectal cancer in inflammatory bowel disease: The role of inflammation. Am J Physiol Gastrointest Liver Physiol. 2004;287:G7-G17.

5. Xavier RJ, Podolsky DK. Unravelling the pathogenesis of inflammatory bowel disease. Nature. 2007;448:427-34.

6. Eckburg PB, Bik EM, Bernstein CN, Purdom E, Dethlefsen L, Sargent M, Gill SR, Nelson KE, Relman DA. Diversity of the human intestinal microbial flora. Science. 2005;308:1635-38.

7. Brint EK, MacSharry J, Fanning A, Shanahan F, Quigley EMM. Differential expression of toll-like receptors in patients with irritable bowel syndrome. Am J Gastroenterol. 2011;106:329-36.

8. Lakatos PL, Fischer S, Lakatos L, Gal I, Papp J. Current concept on the pathogenesis of inflammatory bowel disease-crosstalk between genetic and microbial factors: Pathogenic bacteria and altered bacterial sensing or changes in mucosal integrity take "Toll" ? World J Gastroenterol. 2006;12:1829-41.

9. Chung KT, Lu Z, Chou MW. Mechanism of inhibition of tannic acid and related compounds on the growth of intestinal bacteria. Food Chem Toxicol. 1998;36:1053-60.

10. Okubo T, Ishihara N, Oura A, Serit M, Kim M, Yamamoto T, Mitsuoka T. In vivo effects of tea polyphenol intake on human intestinal microflora and metabolism. Biosci Biotechnol Biochem. 1992;56:588-91.

11. De Filippo C, Cavalieri D, Di Paola M, Ramazzotti M, Poullet JB, Massart S, Collini S, Pieraccini G, Lionetti P. Impact of diet in shaping gut microbiota revealed by a

comparative study in children from Europe and rural Africa. Proc Natl Acad Sci U S A. 2010;107:14691-96.

12. Walker AW, Ince J, Duncan SH, Webster LM, Holtrop G, Ze X, Brown D, Stares MD, Scott P, et al. Dominant and diet-responsive groups of bacteria within the human colonic microbiota. ISME J. 2010;5:220-30.

13. Anderson JW, Baird P, Davis Jr RH, Ferreri S, Knudtson M, Koraym A, Waters V, Williams CL. Health benefits of dietary fiber. Nutr Rev. 2009;67:188-205.

14. Ahn YJ, Lee CO, Kweon JH, Ahn JW, Park JH. Growth-inhibitory effects of *Galla rhois*-derived tannins on intestinal bacteria. J Appl Microbiol. 1998;84:439-43.

15. Okubo T. In vivo effects of tea polyphenol intake on human intestinal microflora and metabolism. Biosci Biotechnol Biochem. 1992;56:588-91.

16. Smith AH, Mackie RI. Effect of condensed tannins on bacterial diversity and metabolic activity in the rat gastrointestinal tract. Appl Environ Microbiol. 2004;70:1104-15.

17. Gibson GR, Probert HM, Loo JV, Rastall RA, Roberfroid MB. Dietary modulation of the human colonic microbiota: Updating the concept of prebiotics. Nutr Res Rev. 2004;17:259-75.

18. Rastall RA, Gibson GR, Gill HS, Guarner F, Klaenhammer TR, Pot B, Reid G, Rowland IR, Sanders ME. Modulation of the microbial ecology of the human colon by probiotics, prebiotics and synbiotics to enhance human health: An overview of enabling science and potential applications. FEMS Microbiol Ecol. 2005;52:145-52.

19. Louis P, Scott KP, Duncan SH, Flint HJ. Understanding the effects of diet on bacterial metabolism in the large intestine. J Appl Microbiol. 2007;102:1197-208.

20. Semann M, Bhmig G, Zlabinger G. Short-chain fatty acids: Bacterial mediators of a balanced host-microbial relationship in the human gut. Wien Klin Wochenschr. 2002;114:289-300.

21. Horneck G, Baumstark-Khan C, Facius R. Radiation biology: Fundamentals of space biology. In: Clément G, Slenzka K, editors.: Springer New York; 2006. p. 291-336.

22. DuBois A, King GL, Livengood DR. Radiation and the gastrointestinal tract: CRC PressI Llc; 1995.

23. Jemal A, Bray F, Center MM, Ferlay J, Ward E, Forman D. Global cancer statistics. CA Cancer J Clin. 2011;61:69-90.

24. Lewis J. Effects of bran from sorghum grains containing different classes and levels of bioactive compounds in colon carcinogenesis. College Station: Texas A&M University; 2008.

25. Dykes L, Rooney LW. Sorghum and millet phenols and antioxidants. J Cereal Sci. 2006;44:236-51.

26. Awika JM, Rooney LW, Waniska RD. Properties of 3-deoxyanthocyanins from sorghum. J Agric Food Chem. 2004;52:4388-94.

27. Burdette A. Anti-inflammatory activity of select sorghum (*Sorghum bicolor*) brans. J Med Food. 2010;13:879.

28. Zoran DL, Turner ND, Taddeo SS, Chapkin RS, Lupton JR. Wheat bran diet reduces tumor incidence in a rat model of colon cancer independent of effects on distal luminal butyrate concentrations. J Nutr. 1997;127:2217-25.

29. Issa J-PJ, Ahuja N, Toyota M, Bronner MP, Brentnall TA. Accelerated age-related CpG island methylation in ulcerative colitis. Cancer Res. 2001;61:3573-77.

30. Santini V, Kantarjian HM, Issa J-P. Changes in DNA methylation in neoplasia: Pathophysiology and therapeutic implications. Ann Intern Med. 2001;134:573-86.

31. D'Acquisto F, May MJ, Ghosh S. Inhibition of nuclear factor kappa b (NF-kb). Mol Interv. 2002;2:22-35.

32. Rogler G, Brand K, Vogl D, Page S, Hofmeister R, Andus T, Knuechel R, Baeuerle PA, Schölmerich J, et al. Nuclear factor [kappa]b is activated in macrophages and epithelial cells of inflamed intestinal mucosa. Gastroenterology. 1998;115:357-69.

33. Yamamoto Y, Gaynor RB. Therapeutic potential of inhibition of the NF-κB pathway in the treatment of inflammation and cancer. J Clin Invest. 2001;107:135-42.

34. Wullaert A. Role of NF-[kappa]b activation in intestinal immune homeostasis. Int J Med Microbiol. 2010;300:49-56.

35. Hooper LV, Gordon JI. Commensal host-bacterial relationships in the gut. Science. 2001;292:1115-18.

36. Kanauchi O, Matsumoto Y, Matsumura M, Fukuoka M, Bamba T. The beneficial effects of microflora, especially obligate anaerobes, and their products on the colonic environment in inflammatory bowel disease. Curr Pharm Des. 2005;11:1047-53.

37. Cario E, Gerken G, Podolsky DK. Toll-like receptor 2 enhances ZO-1-associated intestinal epithelial barrier integrity via protein kinase c. Gastroenterology. 2004;127:224-38.

38. Topping DL, Clifton PM. Short-chain fatty acids and human colonic function: Roles of resistant starch and nonstarch polysaccharides. Physiol Rev. 2001;81:1031-64.

39. Gibson GR, PB Ottaway, RA Rastall. In probiotics: New developments in functional foods. In: Group CH, editor. The gut microflora and its modulation through diet. London, United Kingdom: Chandos Publishing Ltd.; 2000.

40. Hijova E, Chmelarova A. Short chain fatty acids and colonic health. Bratisl Lek Listy. 2007;108:354.

41. Cherbut C. Motor effects of short-chain fatty acids and lactate in the gastrointestinal tract. Proc Nutr Soc. 2003;1:95-99.

42. Tedelind S, Westberg F, Kjerrulf M, Vidal A. Anti-inflammatory properties of the short-chain fatty acids acetate and propionate: A study with relevance to inflammatory bowel disease. World J Gastroenterol. 2007;13:2826.

43. Cummings J, Macfarlane G, Macfarlane S. Intestinal bacteria and ulcerative colitis. Curr Issues Intest Microbiol. 2003;4:9.

44. Deplancke B, Gaskins HR. Microbial modulation of innate defense: Goblet cells and the intestinal mucus layer. Am J Clin Nutr. 2001;73:1131S-41S.

45. Macfarlane G, Blackett K, Nakayama T, Steed H, Macfarlane S. The gut microbiota in inflammatory bowel disease. Curr Pharm Des. 2009;15:1528.

46. Sartor RB, Rath HC, Sellon RK. Microbial factors in chronic intestinal inflammation. Curr Opin Gastroenterol. 1996;12:327-33.

47. Hinnebusch BF, Meng S, Wu JT, Archer SY, Hodin RA. The effects of short-chain fatty acids on human colon cancer cell phenotype are associated with histone hyperacetylation. J Nutr. 2002;132:1012-17.

48. Whitehead RH, Young GP, Bhathal PS. Effects of short chain fatty acids on a new human colon carcinoma cell line (LIM1215). Gut. 1986;27:1457-63.

49. Blottiere HM, Buecher B, Galmiche J-P, Cherbut C. Molecular analysis of the effect of short-chain fatty acids on intestinal cell proliferation. Proc Nutr Soc. 2003;1:101-06.

50. Tonelli F, Dolara P, Batignani G, Monaci I, Caderni G, Spagnesi MT, Luceri C, Amorosi A. Effects of short chain fatty acids on mucosal proliferation and inflammation of ileal pouches in patients with ulcerative colitis and familial polyposis. Dis Colon Rectum. 1995;38:974-78.

51. Waldecker M, Kautenburger T, Daumann H, Busch C, Schrenk D. Inhibition of histone-deacetylase activity by short-chain fatty acids and some polyphenol metabolites formed in the colon. J Nutr Biochem. 2008;19:587-93.

52. De Preter V, Arijs I, Windey K, Vanhove W, Vermeire S, Schuit F, Rutgeerts P, Verbeke K. Impaired butyrate oxidation in ulcerative colitis is due to decreased butyrate uptake and a defect in the oxidation pathway. Inflamm Bowel Dis. 2012;18:1127-36.

53. Thibault R, Blachier F, Darcy-Vrillon B, de Coppet P, Bourreille A, Segain J-P. Butyrate utilization by the colonic mucosa in inflammatory bowel diseases: A transport deficiency. Inflamm Bowel Dis. 2010;16:684-95.

54. Kanauchi O, Iwanaga T, Andoh A, Araki Y, Nakamura T, Mitsuyama K, Suzuki A, Hibi T, Bamba T. Dietary fiber fraction of germinated barley foodstuff attenuated mucosal damage and diarrhea, and accelerated the repair of the colonic mucosa in an experimental colitis. J Gastroenterol Hepatol. 2001;16:160-68.

55. Kanauchi O, Serizawa I, Araki Y, Suzuki A, Andoh A, Fujiyama Y, Mitsuyama K, Takaki K, Toyonaga A, et al. Germinated barley foodstuff, a prebiotic product, ameliorates inflammation of colitis through modulation of the enteric environment. J Gastroenterol. 2003;38:134-41.

56. Inan MS, Rasoulpour RJ, Yin L, Hubbard AK, Rosenberg DW, Giardina C. The luminal short-chain fatty acid butyrate modulates NF-[kappa]b activity in a human colonic epithelial cell line. Gastroenterology. 2000;118:724-34.

57. Wilson AJ, Byron K, Gibson PR. Interleukin-8 stimulates the migration of human colonic epithelial cells in vitro. Clin Sci. 1999;97:385-90.

58. Gibson P, Rosella O. Interleukin 8 secretion by colonic crypt cells in vitro: Response to injury suppressed by butyrate and enhanced in inflammatory bowel disease. Gut. 1995;37:536-43.

59. Huang N, Katz JP, Martin DR, Wu GD. Inhibition of IL-8 gene expression in CACO-2 cells by compounds which induce histone hyperacetylation. Cytokine. 1997;9:27-36.

60. Guillemot F, Colombel J, Neut C, Verplanck N, Lecomte M, Romond C, Paris J, Cortot A. Treatment of diversion colitis by short-chain fatty acids. Dis Colon Rectum. 1991;34:861-64.

61. Wu G, Huang N, Wen X, Keilbaugh S, Yang H. High-level expression of I kappa B-beta in the surface epithelium of the colon: In vitro evidence for an immunomodulatory role. J Leukoc Biol. 1999;66:1049-56.

62. Segain JP, Raingeard de la Bletiere D, Bourreille A, Leray V, Gervois N, Rosales C, Ferrier L, Bonnet C, Blottiere HM, et al. Butyrate inhibits inflammatory responses through NFkappab inhibition: Implications for Crohn's disease. Gut. 2000;47:397-403.

63. Augenlicht LH, Mariadason JM, Wilson A, Arango D, Yang W, Heerdt BG, Velcich A. Short chain fatty acids and colon cancer. J Nutr. 2002;132:3804S-08S.

64. McIntyre A, Gibson P, Young G. Butyrate production from dietary fibre and protection against large bowel cancer in a rat model. Gut. 1993;34:386.

65. Orchel A, Dzierżewicz Z, Parfiniewicz B, Weglarz La, Wilczok T. Butyrate-induced differentiation of colon cancer cells is PKC and JNK dependent. Dig Dis Sci. 2005;50:490-98.

66. Turner ND, Zhang J, Davidson LA, Lupton JR, Chapkin RS. Oncogenic ras alters sensitivity of mouse colonocytes to butyrate and fatty acid mediated growth arrest and apoptosis. Cancer Lett. 2002;186:29-35.

67. Boffa LC, Lupton JR, Mariani MR, Ceppi M, Newmark HL, Scalmati A, Lipkin M. Modulation of colonic epithelial cell proliferation, histone acetylation, and luminal short chain fatty acids by variation of dietary fiber (wheat bran) in rats. Cancer Res. 1992;52:5906-12.

68. Sanderson IR. Short chain fatty acid regulation of signaling genes expressed by the intestinal epithelium. J Nutr. 2004;134:2450S-54S.

69. Donohoe DR, Collins LB, Wali A, Bigler R, Sun W, Bultman SJ. The warburg effect dictates the mechanism of butyrate-mediated histone acetylation and cell proliferation. Mol Cell. 2012.

70. Mackie RI, Sghir A, Gaskins HR. Developmental microbial ecology of the neonatal gastrointestinal tract. Am J Clin Nutr. 1999;69:1035S-45S.

71. Wells JM, Rossi O, Meijerink M, van Baarlen P. Epithelial crosstalk at the microbiota–mucosal interface. Proc Natl Acad Sci U S A. 2010.

72. Cario E. Bacterial interactions with cells of the intestinal mucosa: Toll-like receptors and NOD2. Gut. 2005;54:1182-93.

73. Takeda K, Akira S. Toll-like receptors in innate immunity. Int Immunol. 2005;17:1-14.

74. Abreu MT. Toll-like receptor signalling in the intestinal epithelium: How bacterial recognition shapes intestinal function. Nat Rev Immunol. 2010;10:131-44.

75. Rakoff-Nahoum S, Paglino J, Eslami-Varzaneh F, Edberg S, Medzhitov R. Recognition of commensal microflora by toll-like receptors is required for intestinal homeostasis. Cell. 2004;118:229-41.

76. Li J, Moran T, Swanson E, Julian C, Harris J, Bonen DK, Hedl M, Nicolae DL, Abraham C, et al. Regulation of IL-8 and IL-1β expression in Crohn's disease associated NOD2/ CARD15 mutations. Hum Mol Genet. 2004;13:1715-25.

77. Zaph C, Troy AE, Taylor BC, Berman-Booty LD, Guild KJ, Du Y, Yost EA, Gruber AD, May MJ, et al. Epithelial-cell-intrinsic IKK-[bgr] expression regulates intestinal immune homeostasis. Nature. 2007;446:552-56.

78. Elson CO, Cong Y, McCracken VJ, Dimmitt RA, Lorenz RG, Weaver CT. Experimental models of inflammatory bowel disease reveal innate, adaptive, and regulatory mechanisms of host dialogue with the microbiota. Immunol Rev. 2005;206:260-76.

79. Lee I-A, Bae E-A, Hyun Y-J, Kim D-H. Dextran sulfate sodium and 2,4,6-trinitrobenzene sulfonic acid induce lipid peroxidation by the proliferation of intestinal gram-negative bacteria in mice. J Inflamm. 2010;7:7.

80. Pull SL, Doherty JM, Mills JC, Gordon JI, Stappenbeck TS. Activated macrophages are an adaptive element of the colonic epithelial progenitor niche necessary for regenerative responses to injury. Proc Natl Acad Sci U S A. 2005;102:99-104.

81. Waldner MJ, Neurath MF. Chemically induced mouse models of colitis. Curr Protoc Pharmacol. 2009;1:5.55.1-5.55.15.

82. Kitajima S, Morimoto M, Sagara E. A model for dextran sodium sulfate (DSS)-induced mouse colitis: Bacterial degradation of DSS does not occur after incubation with mouse cecal contents. Exp Anim. 2002;51:203-06.

83. Kobayashi M. Toll-like receptor-dependent production of IL-12p40 causes chronic enterocolitis in myeloid cell-specific Stat3-deficient mice. J Clin Invest. 2003;111:1297.

84. Katakura K. Toll-like receptor 9-induced type I IFN protects mice from experimental colitis. J Clin Invest. 2005;115:695.

85. Rachmilewitz D. Toll-like receptor 9 signaling mediates the anti-inflammatory effects of probiotics in murine experimental colitis. Gastroenterology. 2004;126:520.

86. Takeda K, Clausen BE, Kaisho T, Tsujimura T, Terada N, Förster I, Akira S. Enhanced Th1 activity and development of chronic enterocolitis in mice devoid of Stat3 in macrophages and neutrophils. Immunity. 1999;10:39-49.

87. Kelly D, Conway S, Aminov R. Commensal gut bacteria: Mechanisms of immune modulation. Trends Immunol. 2005;26:326.

88. Smith HW. Observations on the flora of the alimentary tract of animals and factors affecting its composition. J Plant Pathol Microbiol. 1965;89:95-122.

89. Greetham HL, Giffard C, Hutson RA, Collins MD, Gibson GR. Bacteriology of the Labrador dog gut: A cultural and genotypic approach. J Appl Microbiol. 2002;93:640-46.

90. Langendijk P, Schut F, Jansen G, Raangs G, Kamphuis G, Wilkinson M, Welling G. Quantitative fluorescence in situ hybridization of *Bifidobacterium* spp with genus-specific 16S rRNA-targeted probes and its application in fecal samples. Appl Environ Microbiol. 1995;61:3069-75.

91. Ritchie LE, Steiner JM, Suchodolski JS. Assessment of microbial diversity along the feline intestinal tract using 16S rRNA gene analysis. FEMS Microbiol Ecol. 2008;66:590-98.

92. Delgado S, Suárez A, Mayo B. Identification of dominant bacteria in feces and colonic mucosa from healthy Spanish adults by culturing and by 16S rDNA sequence analysis. Dig Dis Sci. 2006;51:744-51.

93. Andersson AF, Lindberg M, Jakobsson H, Bäckhed F, Nyrén P, Engstrand L. Comparative analysis of human gut microbiota by barcoded pyrosequencing. PLoS ONE. 2008;3:e2836.

94. Van de Peer Y, Chapelle S, De Wachter R. A quantitative map of nucleotide substitution rates in bacterial rRNA. Nucleic Acids Res. 1996;24:3381-91.

95. Hamady M, Lozupone C, Knight R. Fast unifrac: Facilitating high-throughput phylogenetic analyses of microbial communities including analysis of pyrosequencing and phylochip data. ISME J. 2009;4:17-27.

96. Frank DN, St. Amand AL, Feldman RA, Boedeker EC, Harpaz N, Pace NR. Molecular-phylogenetic characterization of microbial community imbalances in human inflammatory bowel diseases. Proc Natl Acad Sci U S A. 2007;104:13780-85.

97. Sepehri S, Kotlowski R, Bernstein CN, Krause DO. Microbial diversity of inflamed and noninflamed gut biopsy tissues in inflammatory bowel disease. Inflamm Bowel Dis. 2007;13:675-83.

98. Bibiloni R, Mangold M, Madsen KL, Fedorak RN, Tannock GW. The bacteriology of biopsies differs between newly diagnosed, untreated, Crohn's disease and ulcerative colitis patients. J Med Microbiol. 2006;55:1141-49.

99. Ott SJ, Musfeldt M, Wenderoth DF, Hampe J, Brant O, Fölsch UR, Timmis KN, Schreiber S. Reduction in diversity of the colonic mucosa associated bacterial microflora in patients with active inflammatory bowel disease. Gut. 2004;53:685-93.

100. Heimesaat MM, Fischer A, Siegmund B, Kupz A, Niebergall J, Fuchs D, Jahn H-K, Freudenberg M, Loddenkemper C, et al. Shift towards pro-inflammatory intestinal bacteria aggravates acute murine colitis via toll-like receptors 2 and 4. PLoS ONE. 2007;2:e662.

101. Rath HC, Ikeda JS, Linde HJ, Schölmerich J, Wilson KH, Sartor RB. Varying cecal bacterial loads influences colitis and gastritis in HLA-B27 transgenic rats. Gastroenterology. 1999;116:310-19.

102. Qin J. A human gut microbial gene catalogue established by metagenomic sequencing. Nature. 2010;464:59.

103. Peran L, Camuesco D, Comalada M, Bailon E, Henriksson A, Xaus J, Zarzuelo A, Galvez J. A comparative study of the preventative effects exerted by three probiotics, *Bifidobacterium lactis*, *Lactobacillus casei* and *Lactobacillus acidophilus*, in the TNBS model of rat colitis. J Appl Microbiol. 2007;103:836-44.

104. Hanske L. Xanthohumol does not affect the composition of rat intestinal microbiota. Mol Nutr Food Res. 2005;49:868.

105. Osawa R, Kuroiso K, Goto S, Shimizu A. Isolation of tannin-degrading lactobacilli from humans and fermented foods. Appl Environ Microbiol. 2000;66:3093-97.

106. Bhat TK. Microbial degradation of tannins–a current perspective. Biodegradation. 1998;9:343.

107. Scalbert A. Antimicrobial properties of tannins. Phytochemistry. 1991;30:3875.

108. Minaiyan M, Ghannadi A, Etemad M, Mahzouni P. A study of the effects of Cydonia oblonga Miller (Quince) on TNBS-induced ulcerative colitis in rats. Research in Pharmaceutical Sciences. 2012;7:103.

109. Ahmed AS, Elgorashi EE, Moodley N, McGaw LJ, Naidoo V, Eloff JN. The antimicrobial, antioxidative, anti-inflammatory activity and cytotoxicity of different fractions of four south African *Bauhinia* species used traditionally to treat diarrhoea. J Ethnopharmacol. 2012;143:826-39.

110. Louis P, Flint HJ. Diversity, metabolism and microbial ecology of butyrate-producing bacteria from the human large intestine. FEMS Microbiol Lett. 2009;294:1-8.

111. Sesink ALA, Termont DSML, Kleibeuker JH, Van der Meer R. Red meat and colon cancer: The cytotoxic and hyperproliferative effects of dietary heme. Cancer Res. 1999;59:5704-09.

112. Schepens MAA, Vink C, Schonewille AJ, Dijkstra G, van der Meer R, Bovee-Oudenhoven IMJ. Dietary heme adversely affects experimental colitis in rats, despite heat-shock protein induction. Nutrition. 2011;27:590-97.

113. Ijssennagger N, Derrien M, van Doorn GM, Rijnierse A, van den Bogert B, Müller M, Dekker J, Kleerebezem M, van der Meer R. Dietary heme alters microbiota and mucosa of mouse colon without functional changes in host-microbe cross-talk. PLoS One. 2012;7:e49868.

114. Manichanh C, Varela E, Martinez C, Antolin M, Llopis M, Doré J, Giralt J, Guarner F, Malagelada J-R. The gut microbiota predispose to the pathophysiology of acute postradiotherapy diarrhea. Am J Gastroenterol. 2008;103:1754.

115. Dostal A, Chassard C, Hilty FM, Zimmermann MB, Jaeggi T, Rossi S, Lacroix C. Iron depletion and repletion with ferrous sulfate or electrolytic iron modifies the composition and metabolic activity of the gut microbiota in rats. J Nutr. 2012;142:271-77.

116. Gråsten SM, Pajari A-M, Liukkonen K-H, Karppinen S, Mykkänen HM. Fibers with different solubility characteristics alter similarly the metabolic activity of intestinal microbiota in rats fed cereal brans and inulin. Nutr Res. 2002;22:1435.

117. Awika JM, McDonough CM, Rooney LW. Decorticating sorghum to concentrate healthy phytochemicals. J Agric Food Chem. 2005;53:6230.

118. Kiang J, Garrison BR & Gorbunov NV. Radiation combined injury: DNA damage, apoptosis, and autophagy. Adaptive Medicine. 2010;2:1-10.

119. Pouget J-P, Mather SJ. General aspects of the cellular response to low-and high-LET radiation. Eur J Nucl Med Mol Imaging. 2001;28:541.

120. MacNaughton WK. Review article: New insights into the pathogenesis of radiation-induced intestinal dysfunction. Aliment Pharmacol Ther. 2000;14:523.

121. Paturi G, Paturi T, Mandimika C, Butts S, Zhu N, Roy W, McNabb J. Influence of dietary blueberry and broccoli on cecal microbiota activity and colon morphology in mdr1 -/- mice, a model of inflammatory bowel diseases. Nutrition. 2012;28:324-30.

122. Larrosa M, Yañéz-Gascón MaJ, Selma MaV, González-Sarrías A, Toti S, Cerón JJn, Tomás-Barberán F, Dolara P, Espín JC. Effect of a low dose of dietary resveratrol on colon microbiota, inflammation and tissue damage in a DSS-induced colitis rat model. J Agric Food Chem. 2009;57:2211-20.

123. Garcia Vilela E, De Lourdes De Abreu Ferrari M, Oswaldo Da Gama Torres H, Guerra Pinto A, Carolina Carneiro Aguirre A, Paiva Martins F, Marcos Andrade Goulart E, Sales Da Cunha A. Influence of *Saccharomyces boulardii* on the intestinal permeability of patients with Crohn's disease in remission. Scand J Gastroenterol. 2008;43:842-48.

124. Soo I, Madsen KL, Tejpar Q, Sydora BC, Sherbaniuk R, Cinque B, Di Marzio L, Cifone MG, Desimone C, et al. VSL# 3 probiotic upregulates intestinal mucosal alkaline sphingomyelinase and reduces inflammation. Can J Gastroenterol. 2008;22:237.

125. Pogozelski WK, Xapsos MA, Blakely WF. Quantitative assessment of the contribution of clustered damage to DNA double-strand breaks induced by 60 Co gamma rays and fission neutrons. Radiat Res. 1999;151:442.

126. Gunter Smith PJ. Gamma radiation affects active electrolyte transport by rabbit ileum: Basal Na and Cl transport. Am J Physiol Gastrointest Liver Physiol. 1986;250:G540.

127. Hendry JH, Potten CS, Merritt A. Apoptosis induced by high-and low-LET radiations. Radiat Environ Biophys. 1995;34:59.

128. Merritt AJ, Potten CS, Kemp CJ, Hickman JA, Balmain A, Lane DP, Hall PA. The role of p53 in spontaneous and radiation-induced apoptosis in the gastrointestinal tract of normal and p53-deficient mice. Cancer Res. 1994;54:614.

129. Okunieff P, Mester M, Wang J, Maddox T, Gong X, Tang D, Coffee M, Ding I. In vivo radioprotective effects of angiogenic growth factors on the small bowel of C3H mice. Radiat Res. 1998;150:204.

130. Packey CD, Ciorba MA. Microbial influences on the small intestinal response to radiation injury. Curr Opin Gastroenterol. 2010;26:88.

131. MacNaughton WK, Leach KE, Prud'homme-Lalonde L, Ho W, Sharkey KA. Ionizing radiation reduces neurally evoked electrolyte transport in rat ileum through a mast cell-dependent mechanism. Gastroenterology. 1994;106:324-35.

132. Freeman SL, MacNaughton WK. Ionizing radiation induces iNOS-mediated epithelial dysfunction in the absence of an inflammatory response. Am J Physiol Gastrointest Liver Physiol. 2000;278:G243.

133. Crawford PA, Gordon JI. Microbial regulation of intestinal radiosensitivity. Proc Natl Acad Sci U S A. 2005;102:13254.

134. Egan LJ, Eckmann L, Greten FR, Chae S, Li Z-W, Myhre GM, Robine S, Karin M, Kagnoff MF. Ikb-kinaseβ-dependent NF-κB activation provides radioprotection to the intestinal epithelium. Proc Natl Acad Sci U S A. 2004;101:2452.

135. Wang Y, Meng A, Lang H, Brown SA, Konopa JL, Kindy MS, Schmiedt RA, Thompson JS, Zhou D. Activation of nuclear factor κB in vivo selectively protects the murine small intestine against ionizing radiation-induced damage. Cancer Res. 2004;64:6240.

136. Riehl T, Cohn S, Tessner T, Schloemann S, Stenson WF. Lipopolysaccharide is radioprotective in the mouse intestine through a prostaglandin-mediated mechanism. Gastroenterology. 2000;118:1106.

137. Husebye E, Skar V, Høverstad T, Iversen T, Melby K. Abnormal intestinal motor patterns explain enteric colonization with gram-negative bacilli in late radiation enteropathy. Gastroenterology. 1995;109:1078.

138. Molodecky NA, Soon IS, Rabi DM, Ghali WA, Ferris M, Chernoff G, Benchimol EI, Panaccione R, Ghosh S, et al. Increasing incidence and prevalence of the inflammatory bowel diseases with time, based on systematic review. Gastroenterology. 2012;142:46-54.e42.

139. Latella G, Caprilli R. Metabolism of large bowel mucosa in health and disease. Int J Colorectal Dis. 1991;6:127-32.

140. Wilson AJ, Gibson PR. Short-chain fatty acids promote the migration of colonic epithelial cells in vitro. Gastroenterology. 1997;113:487-96.

141. Turnbaugh PJ, Ridaura VK, Faith JJ, Rey FE, Knight R, Gordon JI. The effect of diet on the human gut microbiome: A metagenomic analysis in humanized gnotobiotic mice. Sci Transl Med. 2009;1:6ra14.

142. Rastmanesh R. High polyphenol, low probiotic diet for weight loss because of intestinal microbiota interaction. Chem Biol Interact. 2011;189:1-8.

143. Larrosa M, Luceri C, Vivoli E, Pagliuca C, Lodovici M, Moneti G, Dolara P. Polyphenol metabolites from colonic microbiota exert anti-inflammatory activity on different inflammation models. Mol Nutr Food Res. 2009;53:1044-54.

144. van Duynhoven J, Vaughan EE, Jacobs DM, A. Kemperman R, van Velzen EJJ, Gross G, Roger LC, Possemiers S, Smilde AK, et al. Metabolic fate of polyphenols in the human superorganism. Proc Natl Acad Sci U S A. 2011;108:4531-38.

145. Lee HC, Jenner AM, Low CS, Lee YK. Effect of tea phenolics and their aromatic fecal bacterial metabolites on intestinal microbiota. Res Microbiol. 2006;157:876-84.

146. Piberger H, Oehme A, Hofmann C, Dreiseitel A, Sand PG, Obermeier F, Schoelmerich J, Schreier P, Krammer G, et al. Bilberries and their anthocyanins ameliorate experimental colitis. Mol Nutr Food Res. 2011;55:1724-29.

147. Seril DN, Liao J, Yang G-Y, Yang CS. Oxidative stress and ulcerative colitis-associated carcinogenesis: Studies in humans and animal models. Carcinogenesis. 2003;24:353-62.

148. Leonardi T, Vanamala J, Taddeo SS, Davidson LA, Murphy ME, Patil BS, Wang N, Carroll RJ, Chapkin RS, et al. Apigenin and naringenin suppress colon carcinogenesis through the aberrant crypt stage in azoxymethane-treated rats. Exp Biol Med. 2010;235:710-17.

149. Warren CA, Paulhill KJ, Davidson LA, Lupton JR, Taddeo SS, Hong MY, Carroll RJ, Chapkin RS, Turner ND. Quercetin may suppress rat aberrant crypt foci formation by suppressing inflammatory mediators that influence proliferation and apoptosis. J Nutr. 2009;139:101-05.

150. Jia Q, Lupton JR, Smith R, Weeks BR, Callaway E, Davidson LA, Kim W, Fan Y-Y, Yang P, et al. Reduced colitis-associated colon cancer in fat-1 (n-3 fatty acid desaturase) transgenic mice. Cancer Res. 2008;68:3985-91.

151. Vanamala J. Suppression of colon carcinogenesis by bioactive compounds in grapefruit. Carcinogenesis. 2006;27:1257.

152. Perse M, Cerar A. Dextran sodium sulphate colitis mouse model: Traps and tricks. J Biomed Biotechnol. 2012.

153. Rose DJ, DeMeo MT, Keshavarzian A, Hamaker BR. Influence of dietary fiber on inflammatory bowel disease and colon cancer: Importance of fermentation pattern. Nutr Rev. 2007;65:51-62.

154. Rodríguez-Cabezas ME, Gálvez J, Lorente MD, Concha A, Camuesco D, Azzouz S, Osuna A, Redondo L, Zarzuelo A. Dietary fiber down-regulates colonic tumor necrosis factor α and nitric oxide production in trinitrobenzenesulfonic acid-induced colitic rats. J Nutr. 2002;132:3263-71.

155. Piefer LA. Quercetin and chlorogenic acid mitigate DSS-induced changes in expression of select pro-inflammatory cytokines and short chain fatty acid transporter genes. College Station: Texas A&M University; 2012.

156. Austin DL, Turner ND, McDonough CM, Rooney LW. Effects of brans from specialty sorghum varieties on in vitro starch digestibility of soft and hard sorghum endosperm porridges. Cereal Chemistry. 2012;89:190-97.

157. Xiang JY, Wu LG, Huang XL, Zhang M, Pen L, Ouyan Q, Gan HT. Amelioration of murine dextran sulfate sodium-induced colitis by nuclear factor-κb decoy oligonucleotides. Amer J Surg. 2009;197:797-805.

158. Murano M, Maemura K, Hirata I, Toshina K, Nishikawa T, Hamamoto N, Sasaki S, Saitoh O, Katsu K. Therapeutic effect of intracolonically administered nuclear factor κB (p65) antisense oligonucleotide on mouse dextran sulphate sodium (DSS)-induced colitis. Clin Exp Immunol. 2000;120:51-58.

159. Osman N, Adawi D, Ahrné S, Jeppsson B, Molin G. Probiotics and blueberry attenuate the severity of dextran sulfate sodium (DSS)-induced colitis. Dig Dis Sci. 2008;53:2464-73.

160. Ciacci C, Lind S, Podolsky D. Transforming growth factor beta regulation of migration in wounded rat intestinal epithelial monolayers. Gastroenterology. 1993;105:93.

161. Loncar MB, Al-azzeh E-d, Sommer PSM, Marinovic M, Schmehl K, Kruschewski M, Blin N, Stohwasser R, Gött P, et al. Tumour necrosis factor α and nuclear factor κB inhibit transcription of human TFF3 encoding a gastrointestinal healing peptide. Gut. 2003;52:1297-303.

162. Kinoshita K. Distinct pathways of cell migration and antiapoptotic response to epithelial injury: Structure-function analysis of human intestinal trefoil factor. Mol Cell Biol. 2000;20:4680.

163. Taupin DR. Intestinal trefoil factor confers colonic epithelial resistance to apoptosis. Proc Natl Acad Sci U S A. 2000;97:799-804.

164. Efstathiou JA, Noda M, Rowan A, Dixon C, Chinery R, Jawhari A, Hattori T, Wright NA, Bodmer WF, et al. Intestinal trefoil factor controls the expression of the adenomatous polyposis coli–catenin and the e-cadherin–catenin complexes in human colon carcinoma cells. Proc Natl Acad Sci U S A. 1998;95:3122-27.

165. Song M, Xia B, Li J. Effects of topical treatment of sodium butyrate and 5-aminosalicylic acid on expression of trefoil factor 3, interleukin 1β, and nuclear factor κB in trinitrobenzene sulphonic acid induced colitis in rats. Postgrad Med J. 2006;82:130-35.

166. Podolsky DK, Gerken G, Eyking A, Cario E. Colitis-associated variant of TLR2 causes impaired mucosal repair because of TFF3 deficiency. Gastroenterology. 2009;137:209-20.

167. Sheng H, Shao J, Dixon DA, Williams CS, Prescott SM, DuBois RN, Beauchamp RD. Transforming growth factor-β1 enhances ha-ras-induced expression of cyclooxygenase-2 in intestinal epithelial cells via stabilization of mRNA. J Biol Chem. 2000;275:6628-35.

168. Janower ML, Robbins LL, Wenlund DE. A review of the use of tannic acid in patients with ulcerative colitis. Radiology. 1967;89:42-43.

169. Kemperman RA, Bolca S, Roger LC, Vaughan EE. Novel approaches for analysing gut microbes and dietary polyphenols: Challenges and opportunities. Microbiology. 2010;156:3224-31.

170. Miene C, Weise A, Glei M. Impact of polyphenol metabolites produced by colonic microbiota on expression of COX-2 and GSTT2 in human colon cells (lt97). Nutr Cancer. 2011;63:653-62.

171. Manichanh C, Rigottier-Gois L, Bonnaud E, Gloux K, Pelletier E, Frangeul L, Nalin R, Jarrin C, Chardon P, et al. Reduced diversity of faecal microbiota in Crohn's disease revealed by a metagenomic approach. Gut. 2006;55:205-11.

172. Andoh A, Imaeda H, Aomatsu T, Inatomi O, Bamba S, Sasaki M, Saito Y, Tsujikawa T, Fujiyama Y. Comparison of the fecal microbiota profiles between ulcerative colitis and crohn's disease using terminal restriction fragment length polymorphism analysis. J Gastroenterol. 2011;46:479-86.

173. Ghosh S, Dai C, Brown K, Rajendiran E, Makarenko S, Baker J, Ma C, Halder S, Montero M, et al. Colonic microbiota alters host susceptibility to infectious colitis by modulating inflammation, redox status, and ion transporter gene expression. Am J Physiol Gastrointest Liver Physiol. 2011;301:G39-G49.

174. Sofa Tedelind FW, Martin Kjerrulf, Alexander Vidal. Anti-inflammatory properties of the short-chain fatty acids acetate and propionate: A study with relevance to inflammatory bowel disease
World J Gastroenterol. 2007;13:2826-32.

175. Cavaglieri CR, Nishiyama A, Fernandes LC, Curi R, Miles EA, Calder PC. Differential effects of short-chain fatty acids on proliferation and production of pro- and anti-inflammatory cytokines by cultured lymphocytes. Life Sci. 2003;73:1683-90.

176. Hond ED, Hiele M, Evenepoel P, Peeters M, Ghoos Y, Rutgeerts P. In vivo butyrate metabolism and colonic permeability in extensive ulcerative colitis. Gastroenterology. 1998;115:584-90.

177. Ahmad MS. Butyrate and glucose metabolism by colonocytes in experimental colitis in mice. Gut. 2000;46:493-9.

178. Ritzhaupt A, Wood IS, Ellis A, Hosie KB, Shirazi-Beechey SP. Identification and characterization of a monocarboxylate transporter (MCT1) in pig and human colon: Its potential to transport l-lactate as well as butyrate. The Journal of Physiology. 1998;513:719-32.

179. Thibault R, Thibault P, De Coppet K, Daly A, Bourreille M, Cuff C, Bonnet Jo, Mosnier J, Galmiche S, et al. Down-regulation of the monocarboxylate transporter 1 is involved in butyrate deficiency during intestinal inflammation. Gastroenterology. 2007;133:1916-27.

180. Vicky De P, Greet Vandermeulen, Paul JR, Kristin Verbeke. T1795 impaired butyrate oxidation in ulcerative colitis is due to decreased butyrate uptake and a defect in the oxidation pathway. Gastroenterology. 2010;138:S.

181. Neurath MF, Becker C, Barbulescu K. Role of NF-κB in immune and inflammatory responses in the gut. Gut. 1998;43:856-60.

182. Karrasch T, Jobin C. NF-κB and the intestine: Friend or foe? Inflamm Bowel Dis. 2008;14:114-24.

183. Ortega-Cava CF, Ishihara S, Rumi MAK, Kawashima K, Ishimura N, Kazumori H, Udagawa J, Kadowaki Y, Kinoshita Y. Strategic compartmentalization of toll-like receptor 4 in the mouse gut. J Immunol. 2003;170:3977-85.

184. Fukata M, Fukata A, Chen A, Klepper S, Krishnareddy A, Vamadevan L, Thomas R, Xu H, Inoue M, et al. Cox-2 is regulated by toll-like receptor-4 (TLR4) signaling: Role in proliferation and apoptosis in the intestine. Gastroenterology. 2006;131:862-77.

185. Cueva C, Sánchez-Patán F, Monagas M, Walton GE, Gibson GR, Martín-Álvarez PJ, Bartolomé B, Moreno-Arribas M. In vitro fermentation of grape seed flavan-3-ol fractions by human faecal microbiota: Changes in microbial groups and phenolic metabolites. FEMS Microbiol Ecol. 2012;83:792-805.

186. Engelbrecht AM, Mattheyse M, Ellis B, Loos B, Thomas M, Smith R, Peters S, Smith C, Myburgh K. Proanthocyanidin from grape seeds inactivates the PI3-kinase/PKB pathway and induces apoptosis in a colon cancer cell line. Cancer Lett. 2007;258:144-53.

187. Lundin A, Bok CM, Aronsson L, Björkholm B, Gustafsson J-A, Pott S, Arulampalam V, Hibberd M, Rafter J, et al. Gut flora, toll-like receptors and nuclear receptors: A tripartite communication that tunes innate immunity in large intestine. Cell Microbiol. 2008;10:1093-103.

188. Loftus Jr EV. Clinical epidemiology of inflammatory bowel disease: Incidence, prevalence, and environmental influences. Gastroenterology. 2004;126:1504-17.

189. Bernstein CN, Blanchard JF, Kliewer E, Wajda A. Cancer risk in patients with inflammatory bowel disease. Cancer. 2001;91:854-62.

190. Swidsinski A, Weber J, Loening-Baucke V, Hale LP, Lochs H. Spatial organization and composition of the mucosal flora in patients with inflammatory bowel disease. J Clin Microbiol. 2005;43:3380-89.

191. Kallinowski F, Wassmer A, Hofmann MA, Harmsen D, Heesemann J, Karch H, Herfarth C, Buhr HJ. Prevalence of enteropathogenic bacteria in surgically treated chronic inflammatory bowel disease. Hepatogastroenterology. 1998;45:1552-58.

192. Martin HM, Campbell BJ, Hart CA, Mpofu C, Nayar M, Singh R, Englyst H, Williams HF, Rhodes JM. Enhanced *Escherichia coli* adherence and invasion in Crohn's disease and colon cancer. Gastroenterology. 2004;127:80-93.

193. Fabia R, Ar'Rajab A, Johansson ML, Andersson R, Willén R, Jeppsson B, Molin G, Bengmark S. Impairment of bacterial flora in human ulcerative colitis and experimental colitis in the rat. Digestion. 1993;54:248-55.

194. Rajilić–Stojanović M, Biagi E, Heilig HGHJ, Kajander K, Kekkonen RA, Tims S, de Vos WM. Global and deep molecular analysis of microbiota signatures in fecal samples from patients with irritable bowel syndrome. Gastroenterology. 2011;141:1792-801.

195. Sokol H, Seksik P, Rigottier-Gois L, Lay C, Lepage P, Podglajen I, Marteau P, Doré J. Specificities of the fecal microbiota in inflammatory bowel disease. Inflamm Bowel Dis. 2006;12:106-11.

196. Cummings JH. Short chain fatty acids in the human colon. Gut. 1981;22:763.

197. Tzounis X, Vulevic J, Kuhnle GGC, George T, Leonczak J, Gibson GR, Kwik-Uribe C, Spencer JPE. Flavanol monomer-induced changes to the human faecal microflora. Br J Nutr. 2008;99:782-92.

198. Turner N. Polyphenol-rich sorghum brans promote fecal water retention and alter short chain fatty acids in Sprague Dawley rats. AACC; 2009.

199. Edwards U, Rogall T, Blocker H, Emde M, Bottger EC. Isolation and direct complete nucleotide determination of entire genes. Characterization of a gene coding for 16S ribosomal RNA. Nucleic Acids Research. 1989 Oct 11;17:7843-53.

200. Fierer N, Hamady M, Lauber CL, Knight R. The influence of sex, handedness, and washing on the diversity of hand surface bacteria. Proc Natl Acad Sci U S A. 2008 Nov 18;105:17994-9.

201. Caporaso JG, Kuczynski J, Stombaugh J, Bittinger K, Bushman FD, Costello EK, Fierer N, Pena AG, Goodrich JK, et al. QIIME allows analysis of high-throughput community sequencing data. Nat Methods. 2010 May;7:335-6.

202. Reeder J, Knight R. Rapidly denoising pyrosequencing amplicon reads by exploiting rank-abundance distributions. Nature Methods. 2010 Sep;7:668-9.

203. Haas BJ, Gevers D, Earl AM, Feldgarden M, Ward DV, Giannoukos G, Ciulla D, Tabbaa D, Highlander SK, et al. Chimeric 16S rRNA sequence formation and detection in sanger and 454-pyrosequenced PCR amplicons. Genome Research. 2011 Mar;21:494-504.

204. Edgar RC. Search and clustering orders of magnitude faster than blast. Bioinformatics. 2010 Oct 1;26:2460-1.

205. Lozupone C, Hamady M, Knight R. Unifrac--an online tool for comparing microbial community diversity in a phylogenetic context. BMC Bioinformatics. 2006;7:371.

206. Ley RE, Hamady M, Lozupone C, Turnbaugh PJ, Ramey RR, Bircher JS, Schlegel ML, Tucker TA, Schrenzel MD, et al. Evolution of mammals and their gut microbes. Science. 2008 Jun 20;320:1647-51.

207. Ley RE, Lozupone CA, Hamady M, Knight R, Gordon JI. Worlds within worlds: Evolution of the vertebrate gut microbiota. Nat Rev Microbiol. 2008 Oct;6:776-88.

208. Biasi F, Astegiano M, Maina M, Leonarduzzi G, Poli G. Polyphenol supplementation as a complementary medicinal approach to treating inflammatory bowel disease. Curr Med Chem. 2011;18:4851-65.

209. Possemiers S, Bolca S, Verstraete W, Heyerick A. The intestinal microbiome: A separate organ inside the body with the metabolic potential to influence the bioactivity of botanicals. Fitoterapia. 2011;82:53-66.

210. Murphy E, Cotter P, Healy S, Marques T, O'Sullivan O, Fouhy F, Clarke S, O'Toole P, Quigley E, et al. Composition and energy harvesting capacity of the gut microbiota: Relationship to diet, obesity and time in mouse models. Gut. 2010;59:1635-42.

211. Nagalingam NA, Kao JY, Young VB. Microbial ecology of the murine gut associated with the development of dextran sodium sulfate-induced colitis. Inflamm Bowel Dis. 2011;17:917-26.

212. Chassard C, Gaillard-Martinie B, Bernalier-Donadille A. Interaction between h2-producing and non-h2-producing cellulolytic bacteria from the human colon. FEMS Microbiol Lett. 2005;242:339-44.

213. Nagalingam NA, Lynch SV. Role of the microbiota in inflammatory bowel diseases. Inflamm Bowel Dis. 2012;18:968-84.

214. Ljungh A, Wadstrom T. Lactic acid bacteria as probiotics. Curr Issues Intest Microbiol. 2006;7:73-90.

215. Pronio A, Montesani C, Butteroni C, Vecchione S, Mumolo G, Vestri A, Vitolo D, Boirivant M. Probiotic administration in patients with ileal pouch–anal anastomosis for ulcerative colitis is associated with expansion of mucosal regulatory cells. Inflamm Bowel Dis. 2008;14:662-68.

216. Verma R, Verma AK, Ahuja V, Paul J. Real-time analysis of mucosal flora in patients with inflammatory bowel disease in india. J Clin Microbiol. 2010;48:4279-82.

217. Noor S, Ridgway K, Scovell L, Kemsley EK, Lund E, Jamieson C, Johnson I, Narbad A. Ulcerative colitis and irritable bowel patients exhibit distinct abnormalities of the gut microbiota. BMC Gastroenterol. 2010;10:134.

218. Takaishi H, Matsuki T, Nakazawa A, Takada T, Kado S, Asahara T, Kamada N, Sakuraba A, Yajima T, et al. Imbalance in intestinal microflora constitution could be involved in the pathogenesis of inflammatory bowel disease. Int J Med Microbiol. 2008;298:463-72.

219. Gophna U, Sommerfeld K, Gophna S, Doolittle WF, van Zanten SJV. Differences between tissue-associated intestinal microfloras of patients with Crohn's disease and ulcerative colitis. J Clin Microbiol. 2006;44:4136-41.

220. Hartmanis MG, Gatenbeck S. Intermediary metabolism in *Clostridium acetobutylicum*: Levels of enzymes involved in the formation of acetate and butyrate. Appl Environ Microbiol. 1984;47:1277-83.

221. Wiegel J, Kuk S-U, Kohring GW. *Clostridium thermobutyricum* sp. a moderate thermophile isolated from a cellulolytic culture, that produces butyrate as the major product. Int J Syst Bacteriol. 1989;39:199-204.

222. Segain J-P, de la Blétière DR, Bourreille A, Leray V, Gervois N, Rosales C, Ferrier L, Bonnet C, Blottière HM, et al. Butyrate inhibits inflammatory responses through NFκB inhibition: Implications for Crohn's disease. Gut. 2000;47:397-403.

223. Onderdonk AB, Richardson JA, Hammer RE, Taurog JD. Correlation of cecal microflora of HLA-B27 transgenic rats with inflammatory bowel disease. Infect Immun. 1998 December 1, 1998;66:6022-23.

224. Croswell A. Prolonged impact of antibiotics on intestinal microbial ecology and susceptibility to enteric *Salmonella* infection. Infect Immun. 2009;77:2741.

225. Larrosa M, Luceri C, Vivoli E, Pagliuca C, Lodovici M, Moneti G, Dolara P. Polyphenol metabolites from colonic microbiota exert anti-inflammatory activity on different inflammation models. Molecular Nutrition & Food Research. 2009;53:1044-54.

226. Crozier A, Del Rio D, Clifford MN. Bioavailability of dietary flavonoids and phenolic compounds. Mol Aspects Med. 2010;31:446-67.

227. Ree T. Tannins: Classification and definition. Nat Prod Rep. 2001;18:641-49.

228. Jimenez-Ramsey LM, Rogler JC, Housley TL, Butler LG, Elkin RG. Absorption and distribution of 14C-labeled condensed tannins and related sorghum phenolics in chickens. J Agric Food Chem. 1994;42:963-67.

229. Borges G, Roowi S, Rouanet JM, Duthie GG, Lean ME, Crozier A. The bioavailability of raspberry anthocyanins and ellagitannins in rats. Mol Nutr Food Res. 2007;51:714-25.

230. Sakakibara H, Ogawa T, Koyanagi A, Kobayashi S, Goda T, Kumazawa S, Kobayashi H, Shimoi K. Distribution and excretion of bilberry anthocyanins in mice. J Agric Food Chem. 2009;57:7681-86.

231. Beard J. Iron deficiency alters brain development and functioning. J Nutr. 2003 May;133:1468S-72S.

232. Smith SM, Zwart SR, Kloeris V, Heer M. Nutritional biochemistry of space flight. New York: Nova Science Publishers; 2009.

233. Smith SM. Red blood cell and iron metabolism during space flight. Nutrition. 2002;18:864-66.

234. Alfrey CP, Rice L, Udden MM, Driscoll TB. Neocytolysis: Physiological down-regulator of red-cell mass. Lancet. 1997 May 10;349:1389-90.

235. Alfrey CP, Udden MM, Leach-Huntoon C, Driscoll T, Pickett MH. Control of red blood cell mass in spaceflight. J Appl Physiol. 1996;81:98-104.

236. Smith SM, Zwart SR, Block G, Rice BL, Davis-Street JE. The nutritional status of astronauts is altered after long-term space flight aboard the international space station. J Nutr. 2005 Mar;135:437-43.

237. National Aeronautics and Space Administration. Nutrition requirements, standards, and operating bands for exploration missions. JSC document #63555. Houston, TX: Lyndon B. Johnson Space Center; 2005.

238. Institute of Medicine. Dietary reference intakes for Vitamin A, Vitamin K, arsenic, boron, chromium, copper, iodine, iron, manganese, molybdenum, nickel, silicon, vanadium, and zinc. Washington, DC: National Academy Press; 2001.

239. Anand J, Goldman J, Steinfeldt L, Montville J, Heendeniya K, Omolewa-Tomobi G, Williams J, Clemens J, Ahuja J, et al. What we eat in America, Nhanes 2007-2008: Documentation and data files: U.S. Department of Agriculture; 2010.

240. Crichton RR. Iron metabolism from molecular mechanisms to clinical consequences. 3rd ed. West Sussex, United Kingdom: John Wiley & Sons Ltd.; 2009.

241. Sempos CT, Looker AC, Gillum RF, Makuc DM. Body iron stores and the risk of coronary heart disease. N Engl J Med. 1994;330:1119-24.

242. Stevens RG, Jones DY, Micozzi MS, Taylor PR. Body iron stores and the risk of cancer. N Engl J Med. 1988 Oct 20;319:1047-52.

243. Zacharski LR, Chow BK, Howes PS, Shamayeva G, Baron JA, Dalman RL, Malenka DJ, Ozaki CK, Lavori PW. Decreased cancer risk after iron reduction in patients with peripheral arterial disease: Results from a randomized trial. J Natl Cancer Inst. 2008 Jul 16;100:996-1002.

244. Zheng H, Cable R, Spencer B, Votto N, Katz SD. Iron stores and vascular function in voluntary blood donors. Arterioscler Thromb Vasc Biol. 2005 Aug;25:1577-83.

245. Feinendegen LE. Significance of basic and clinical research in radiation medicine: Challenges for the future. Br J Radiol. 2005;Sup 27:185-95.

246. Guan J, Wan S, Zhou Z, Ware J, Donahue JJ, Biaglow JE, Kennedy AR. Effects of dietary supplements on space radiation-induced oxidative stress in Sprague-Dawley rats. Radiat Res. 2004;162:572-79.

247. Sener G, Kabasakal L, Atasoy BM, Erzik C, Velioglu-Ogunc A, Cetinel S, Gedik N, Yegen BC. *Ginkgo biloba* extract protects against ionizing radiation-induced oxidative organ damage in rats. Pharmacol Res. 2006;53:241-52.

248. Kennedy AR, Guan J, Ware JH. Countermeasures against space radiation induced oxidative stress in mice. Radiat Environ Biophys. 2007 Jun;46:201-3.

249. Hellweg CE, Baumstark-Khan C. Getting ready for the manned mission to mars: The astronauts' risk from space radiation. Naturwissenschaften. 2007 Jul;94:517-26.

250. Cucinotta FA, Manuel FK, Jones J, Iszard G, Murrey J, Djojonegro B, Wear M. Space radiation and cataracts in astronauts. Radiat Res. 2001;156:460-6.

251. Yusuf SW, Sami S, Daher IN. Radiation-induced heart disease: A clinical update. Cardiol Res Pract. 2011;2011:317659.

252. Borlon C, Chretien A, Debacq-Chainiaux F, Toussaint O. Transient increased extracellular release of H2O2 during establishment of UVB-induced premature senescence. Ann N Y Acad Sci. 2007 Nov;1119:72-7.

253. Iliakis GE, Pantelias GE, Okayasu R, Blakely WF. Induction by H2O2 of DNA and interphase chromosome damage in plateau-phase chinese hamster ovary cells. Radiat Res. 1992 Aug;131:192-203.

254. Stevens RG, Morris JE, Anderson LE. Hemochromatosis heterozygotes may constitute a radiation-sensitive subpopulation. Radiat Res. 2000;153:844-47.

255. Nelson JM, Stevens RG. Ferritin-iron increases killing of chinese hamster ovary cells by x-irradiation. Cell Prolif. 1992 Nov;25:579-85.

256. Morliere P, Salmon S, Aubailly M, Risler A, Santus R. Sensitization of skin fibroblasts to UVA by excess iron. Biochim Biophys Acta. 1997 Mar 15;1334:283-90.

257. Aubailly M, Santus R, Salmon S. Ferrous ion release from ferritin by ultraviolet-a radiations. Photochem Photobiol. 1991 Nov;54:769-73.

258. Biemond P, van Eijk HG, Swaak AJ, Koster JF. Iron mobilization from ferritin by superoxide derived from stimulated polymorphonuclear leukocytes. Possible mechanism in inflammation diseases. J Clin Invest. 1984 Jun;73:1576-9.

259. Abreu MT, Fukata M, Arditi M. TLR signaling in the gut in health and disease. J Immunol. 2005 Apr 15;174:4453-60.

260. Girardin SE, Boneca IG, Viala J, Chamaillard M, Labigne A, Thomas G, Philpott DJ, Sansonetti PJ. Nod2 is a general sensor of peptidoglycan through muramyl dipeptide (mdp) detection. J Biol Chem. 2003 Mar 14;278:8869-72.

261. Xavier RJ, Podolsky DK. Unravelling the pathogenesis of inflammatory bowel disease. Nature. 2007 Jul 26;448:427-34.

262. Lee JY, Hwang DH. The modulation of inflammatory gene expression by lipids: Mediation through toll-like receptors. Mol Cells. 2006 Apr 30;21:174-85.

263. Rakoff-Nahoum S, Medzhitov R. Innate immune recognition of the indigenous microbial flora. Mucosal Immunol. 2008 Nov;1 Suppl 1:S10-4.

264. Zimmermann MB, Chassard C, Rohner F, N'Goran E K, Nindjin C, Dostal A, Utzinger J, Ghattas H, Lacroix C, et al. The effects of iron fortification on the gut microbiota in African children: A randomized controlled trial in Cote D'ivoire. Am J Clin Nutr. 2010 Dec;92:1406-15.

265. Packey CD, Ciorba MA. Microbial influences on the small intestinal response to radiation injury. Curr Opin Gastroenterol. 2010 Mar;26:88-94.

266. Burdelya LG, Krivokrysenko VI, Tallant TC, Strom E, Gleiberman AS, Gupta D, Kurnasov OV, Fort FL, Osterman AL, et al. An agonist of toll-like receptor 5 has radioprotective activity in mouse and primate models. Science. 2008 Apr 11;320:226-30.

267. Cummings JH, Macfarlane GT, Macfarlane S. Intestinal bacteria and ulcerative colitis. Curr Issues Intest Microbiol. 2003 Mar;4:9-20.

268. Deplancke B, Gaskins HR. Microbial modulation of innate defense: Goblet cells and the intestinal mucus layer. Am J Clin Nutr. 2001 Jun;73:1131S-41S.

269. Macfarlane GT, Blackett KL, Nakayama T, Steed H, Macfarlane S. The gut microbiota in inflammatory bowel disease. Curr Pharm Des. 2009;15:1528-36.

270. Zoran DL, Turner ND, Taddeo SS, Chapkin RS, Lupton JR. Wheat bran diet reduces tumor incidence in a rat model of colon cancer independent of effects on distal luminal butyrate concentrations. J Nutr. 1997 Nov;127:2217-25.

271. Latella G, Caprilli R. Metabolism of large bowel mucosa in health and disease. Int J Colorectal Dis. 1991 May;6:127-32.

272. Wilson AJ, Gibson PR. Short-chain fatty acids promote the migration of colonic epithelial cells in vitro. Gastroenterology. 1997 Aug;113:487-96.

273. Larbi A, Kempf J, Pawelec G. Oxidative stress modulation and t cell activation. Exp Gerontol. 2007;42:852-58.

274. Crucian B, Stowe R, Mehta S, Uchakin P, Quiriarte H, Pierson D, Sams C. Immune system dysregulation occurs during short duration spaceflight on board the space shuttle. J Clin Immunol. 2013 Feb;33:456-65.

275. Mehta SK, Stowe RP, Feiveson AH, Tyring SK, Pierson DL. Reactivation and shedding of Cytomegalovirus in astronauts during spaceflight. J Infect Dis. 2000 Dec;182:1761-4.

276. Pierson DL, Stowe RP, Phillips TM, Lugg DJ, Mehta SK. Epstein-Barr virus shedding by astronauts during space flight. Brain Behav Immun. 2005 May;19:235-42.

277. Valyi-Nagy T, Dermody TS. Role of oxidative damage in the pathogenesis of viral infections of the nervous system. Histol Histopathol. 2005;20:957-67.

278. Gueguinou N, Huin-Schohn C, Bascove M, Bueb JL, Tschirhart E, Legrand-Frossi C, Frippiat JP. Could spaceflight-associated immune system weakening preclude the expansion of human presence beyond earth's orbit? J Leukoc Biol. 2009 Nov;86:1027-38.

279. Crucian B, Stowe R, Quiriarte H, Pierson D, Sams C. Monocyte phenotype and cytokine production profiles are dysregulated by short-duration spaceflight. Aviat Space Environ Med. 2011 Sep;82:857-62.

280. Gmunder FK, Konstantinova IV, Cogoli A, Bogomolov W, Grachov AW. Cellular immunity in cosmonauts during long duration spaceflight on board the orbital mir station. Aviat Space Env Med. 1994;65:419-23.

281. Crucian B, Sams C. Immune system dysregulation during spaceflight: Clinical risk for exploration-class missions. J Leukoc Biol. 2009 Nov;86:1017-8.

282. Fischer JG, Glauert HP, Yin T, Sweeney-Reeves ML, Larmonier N, Black MC. Moderate iron overload enhances lipid peroxidation in livers of rats, but does not affect NF-kappab activation induced by the peroxisome proliferator, wy-14,643. J Nutr. 2002 Sep;132:2525-31.

283. Smith RQ. Measurements UNCfRPa. Information needed to make radiation protection recommendation on space missions beyond low-earth orbit. Aviat Space Env Med; 2006;56:3.

284. Zeitlin C, Hassler DM, Cucinotta FA, Ehresmann B, Wimmer-Schweingruber RF, Brinza DE, Kang S, Weigle G, Bottcher S, et al. Measurements of energetic particle radiation in transit to mars on the mars science laboratory. Science. 2013 May 31;340:1080-4.

285. Davidson LA, Nguyen DV, Hokanson RM, Callaway ES, Isett RB, Turner ND, Dougherty ER, Wang N, Lupton JR, et al. Chemopreventive n-3 polyunsaturated fatty acids reprogram genetic signatures during colon cancer initiation and progression in the rat. Cancer Res. 2004 Sep 15;64:6797-804.

286. Crucian BE, Stowe RP, Pierson DL, Sams CF. Immune system dysregulation following short- vs long-duration spaceflight. Aviat Space Environ Med. 2008 Sep;79:835-43.

287. Crim KC, Sanders LM, Hong MY, Taddeo SS, Turner ND, Chapkin RS, Lupton JR. Upregulation of p21waf1/cip1 expression in vivo by butyrate administration can be chemoprotective or chemopromotive depending on the lipid component of the diet. Carcinogenesis. 2008 Jul;29:1415-20.

288. Benjamini Y, Krieger A, Yekutieli D. Adaptive linear set-up procedures that control the false discovery rate. Biometrica. 2006;93:491-507.

289. Zwart SR, Morgan JL, Smith SM. Iron status and its relations with oxidative damage and bone loss during long-duration space flight on the international space station. Am J Clin Nutr. 2013 May 29;98:217-23.

290. Lloyd SA, Bandstra ER, Willey JS, Riffle SE, Tirado-Lee L, Nelson GA, Pecaut MJ, Bateman TA. Effect of proton irradiation followed by hindlimb unloading on bone in mature mice: A model of long-duration spaceflight. Bone. 2012 Oct;51:756-64.

291. Hamilton SA, Pecaut MJ, Gridley DS, Travis ND, Bandstra ER, Willey JS, Nelson GA, Bateman TA. A murine model for bone loss from therapeutic and space-relevant sources of radiation. J Appl Physiol. 2006 Sep;101:789-93.

292. Lloyd SA, Travis ND, Lu T, Bateman TA. Development of a low-dose anti-resorptive drug regimen reveals synergistic suppression of bone formation when coupled with disuse. J Appl Physiol. 2008 Mar;104:729-38.

293. Arboleya L, Castaneda S. Osteoimmunology: The study of the relationship between the immune system and bone tissue. Reumatol Clin. 2013;9:303-15.

294. Angelucci E, Brittenham GM, McLaren CE, Ripalti M, Baronciani D, Giardini C, Galimberti M, Polchi P, Lucarelli G. Hepatic iron concentration and total body iron stores in thalassemia major. New Eng J Med. 2000;343:327-31.

295. Baxter CF, Belcher EH, Harriss EB, Lamerton LF. Anaemia and erythropoiesis in the irradiated rat: An experimental study with particular reference to techniques involving radioactive iron. Br J Haematol. 1955;1:86-103.

296. Merrick BA, Bruno ME, Madenspacher JH, Wetmore BA, Foley J, Pieper R, Zhao M, Makusky AJ, McGrath AM, et al. Alterations in the rat serum proteome during liver injury from acetaminophen exposure. J Pharmacol Exp Ther. 2006 Aug;318:792-802.

297. Geraci JP, Mariano MS. Radiation hepatology of the rat: Parenchymal and nonparenchymal cell injury. Radiat Res. 1993;136:205-13.

298. Birgegard G, Hallgren R, Killander A, Stromberg A, Venge P, Wide L. Serum ferritin during infection. Eur J Haematol. 1978;21:333-40.

299. Gabay C, Kushner I. Acute-phase proteins and other systemic responses to inflammation. N Engl J Med. 1999 Feb 11;340:448-54.

300. Thames HDJ. Effect-independent measures of tissue responses to fractionated irradiation. Int J Radiat Biol Relat Stud Phys Chem Med. 1984;45:1-10.

301. Fowler JF. Review: Total doses in fractionated radiotherapy--implications of new radiobiological data. Int J Radiat Biol Relat Stud Phys Chem Med. 1984 Aug;46:103-20.

302. Cronkite EP, Brecher G. The protective effect of granulocytes in radiation injury. Ann N Y Acad Sci. 1955;59:815-33.

303. Singh VK, Fatanmi OO, Singh PK, Whitnall MH. Role of radiation-induced granulocyte colony-stimulating factor in recovery from whole body gamma-irradiation. Cytokine. 2012;58:406-14.

304. Kusunoki Y, Kyoizumi S, Yamaoka M, Kasagi F, Kodama K, Seyama T. Decreased proportion of cd4 T cells in blood of atomic bomb survivors with myocardial infarction. Radiat Res. 1999;152:539-43.

305. Kandasamy SB. Effect of ionizing radiation on the release of cholecystokinin in the hypothalamus of the rat. Radiat Res. 1998 Sep;150:298-303.

306. Tsay J, Yang Z, Ross FP, Cunningham-Rundles S, Lin H, Coleman R, Mayer-Kuckuk P, Doty SB, Grady RW, et al. Bone loss caused by iron overload in a murine model: Importance of oxidative stress. Blood. 2010 Oct 7;116:2582-9.

307. Gridley DS, Dutta-Roy R, Andres ML, Nelson GA, Pecaut MJ. Acute effects of iron-particle radiation on immunity. Part II: Leukocyte activation, cytokines and adhesion. Radiat Res. 2006;165:78-87.

308. Bogdandi EN, Balogh A, Felgyinszki N, Szatmari T, Perza E, Hildebrant G, Safrany G, Lumniczky K. Effects of low-dose radiation on the immune system of mice after total-body irradiation. Radiat Res. 2010;174:480-89.

309. Louis P, Flint HJ. Diversity, metabolism and microbial ecology of butyrate-producing bacteria from the human large intestine. FEMS Microbiol Lett. 2009 May;294:1-8.

310. Manichanh C, Varela E, Martinez C, Antolin M, Llopis M, Dore J, Giralt J, Guarner F, Malagelada JR. The gut microbiota predispose to the pathophysiology of acute postradiotherapy diarrhea. Am J Gastroenterol. 2008 Jul;103:1754-61.

311. Dostal A, Chassard C, Hilty FM, Zimmermann MB, Jaeggi T, Rossi S, Lacroix C. Iron depletion and repletion with ferrous sulfate or electrolytic iron modifies the composition and metabolic activity of the gut microbiota in rats. J Nutr. 2012 Feb;142:271-7.

312. Dubois A, King G, Livengood D. Radiation and the gastrointestinal tract. Boca Raton, Fl: CRC Press; 1994.

313. MacNaughton WK. Review article: New insights into the pathogenesis of radiation-induced intestinal dysfunction. Aliment Pharmacol Ther. 2000 May;14:523-8.

314. MacNaughton WK, Leach KE, Prud'homme-Lalonde L, Ho W, Sharkey KA. Ionizing radiation reduces neurally evoked electrolyte transport in rat ileum through a mast cell-dependent mechanism. Gastroenterology. 1994 Feb;106:324-35.

315. Kiang JG, Garrison BR, Gorbunov NV. Radiation combined injury: DNA damage, apoptosis, and autophagy. Adaptive Medicine. 2010;2:1-10.

316. Freeman SL, MacNaughton WK. Ionizing radiation induces iNOS-mediated epithelial dysfunction in the absence of an inflammatory response. Am J Physiol Gastrointest Liver Physiol. 2000 Feb;278:G243-50.

317. Gunter-Smith PJ. Gamma radiation affects active electrolyte transport by rabbit ileum: Basal Na and Cl transport. Am J Physiol. 1986 Apr;250:G540-5.

318. Merritt AJ, Potten CS, Kemp CJ, Hickman JA, Balmain A, Lane DP, Hall PA. The role of p53 in spontaneous and radiation-induced apoptosis in the gastrointestinal tract of normal and p53-deficient mice. Cancer Res. 1994 Feb 1;54:614-7.

319. Brennan PC, Carr KE, Seed T, McCullough JS. Acute and protracted radiation effects on small intestinal morphological parameters. Int J Radiat Biol. 1998 Jun;73:691-8.

320. Hendry JH, Potten CS, Merritt A. Apoptosis induced by high- and low-LET radiations. Radiat Environ Biophys. 1995 Mar;34:59-62.

321. Pouget JP, Mather SJ. General aspects of the cellular response to low- and high-LET radiation. Eur J Nucl Med. 2001 Apr;28:541-61.

322. Cuff MA, Lambert DW, Shirazi-Beechey SP. Substrate-induced regulation of the human colonic monocarboxylate transporter, MCT1. J Physiol. 2002 Mar 1;539:361-71.

323. Charney AN, Micic L, Egnor RW. Nonionic diffusion of short-chain fatty acids across rat colon. Am J Physiol. 1998 Mar;274:G518-24.

324. Donohoe DR, Collins LB, Wali A, Bigler R, Sun W, Bultman SJ. The Warburg effect dictates the mechanism of butyrate-mediated histone acetylation and cell proliferation. Mol Cell. 2012 Nov 30;48:612-26.

325. Wilson AJ, Byron K, Gibson PR. Interleukin-8 stimulates the migration of human colonic epithelial cells in vitro. Clin Sci (Lond). 1999 Sep;97:385-90.

326. Hinnebusch BF, Meng S, Wu JT, Archer SY, Hodin RA. The effects of short-chain fatty acids on human colon cancer cell phenotype are associated with histone hyperacetylation. J Nutr. 2002 May;132:1012-7.

327. Tonelli F, Dolara P, Batignani G, Monaci I, Caderni G, Spagnesi MT, Luceri C, Amorosi A. Effects of short chain fatty acids on mucosal proliferation and inflammation of ileal pouches in patients with ulcerative colitis and familial polyposis. Dis Colon Rectum. 1995 Sep;38:974-8.

328. Tedelind S, Westberg F, Kjerrulf M, Vidal A. Anti-inflammatory properties of the short-chain fatty acids acetate and propionate: A study with relevance to inflammatory bowel disease. World J Gastroenterol. 2007 May 28;13:2826-32.

329. Lundin A, Bok CM, Aronsson L, Bjorkholm B, Gustafsson JA, Pott S, Arulampalam V, Hibberd M, Rafter J, et al. Gut flora, toll-like receptors and nuclear receptors: A tripartite communication that tunes innate immunity in large intestine. Cell Microbiol. 2008 May;10:1093-103.

330. Brint EK, MacSharry J, Fanning A, Shanahan F, Quigley EM. Differential expression of toll-like receptors in patients with irritable bowel syndrome. Am J Gastroenterol. 2011 Feb;106:329-36.

331. Kalliomaki M, Satokari R, Lahteenoja H, Vahamiko S, Gronlund J, Routi T, Salminen S. Expression of microbiota, toll-like receptors, and their regulators in the small intestinal mucosa in Celiac disease. J Pediatr Gastroenterol Nutr. 2012 Jun;54:727-32.

332. Vijay-Kumar M, Wu H, Aitken J, Kolachala VL, Neish AS, Sitaraman SV, Gewirtz AT. Activation of toll-like receptor 3 protects against DSS-induced acute colitis. Inflamm Bowel Dis. 2007 Jul;13:856-64.

333. Takeda K, Akira S. Toll-like receptors in innate immunity. Int Immunol. 2005 Jan;17:1-14.

334. Rakoff-Nahoum S, Medzhitov R. Toll-like receptors and cancer. Nat Rev Cancer. 2009 Jan;9:57-63.

335. Baud V, Karin M. Signal transduction by tumor necrosis factor and its relatives. Trends Cell Biol. 2001 Sep;11:372-7.

336. Hampton MB, Kettle AJ, Winterbourn CC. Inside the neutrophil phagosome: Oxidants, myeloperoxidase and bacterial killing. Blood. 1998;92:3007-17.

337. Kinoshita K, Taupin DR, Itoh H, Podolsky DK. Distinct pathways of cell migration and antiapoptotic response to epithelial injury: Structure-function analysis of human intestinal trefoil factor. Mol Cell Biol. 2000 Jul;20:4680-90.

338. Valko M, Leibfritz D, Moncol J, Cronin MT, Mazur M, Telser J. Free radicals and antioxidants in normal physiological functions and human disease. Int J Biochem Cell Biol. 2007;39:44-84.

339. Kawanishi S, Hiraku Y, Pinlaor S, Ma N. Oxidative and nitrative DNA damage in animals and patients with inflammatory diseases in relation to inflammation-related carcinogenesis. Biol Chem. 2006 Apr;387:365-72.

340. Hamilton SA, Pecaut MJ, Gridley DS, Travis ND, Bandstra ER, Willey JS, Nelson G, Bateman TA. A murine model for bone loss from therapeutic and space-relevant sources of radiation. J Appl Physiol. 2006;101:789-93.

341. Yusuf SW, Sami S, Daher IN. Radiation-induced heart disease: A clinical update. Cardiology Research & Practice. 2011:1-9.

342. Radiation health: Mechanisms of radiation-induced cataracts in astronauts. Aviation, Space, and Environmental Medicine. 2009;80:575-76.

343. Prousek J. Fenton chemistry in biology and medicine. Pure Appl Chem. 2007;79:2325-38.

344. C. Brennan Ke Carr T. Seed Js McCullough P, C. Brennan K. E. Carr T. Seed J S. Acute and protracted radiation effects on small intestinal morphological parameters. International Journal of Radiation Biology. 1998;73:691.

345. McLaughlin MM, Dacquisto MP, Jacobus DP, Horowitz RE. Effects of the germfree state on responses of mice to whole-body irradiation. Radiat Res. 1964;23:333-49.

346. Wagner EB, Granzella NP, Saito H, Newman DJ, Young LR, Bouxsein ML. Partial weight suspension: A novel murine model for investigating adaptation to reduced musculoskeletal loading. J Appl Physiol. 2010;109:350-57.

347. Crucian BE, Stowe RP, Mehta SK, Yetman DL, Leal MJ, Quiriarte HD, Pierson DL, Sams CF. Immune status, latent viral reactivation, and stress during long-duration head-down bed rest. Aviation, Space, and Environmental Medicine. 2009;80:A37-A44.

348. Gopalakrishnan R, Genc KO, Rice AJ, Lee S, Evans HJ, Maender CC, Ilaslan H, Cavanagh PR. Muscle volume, strength, endurance, and exercise loads during 6-month missions in space. Aviation, Space, and Environmental Medicine. 2010;81:91-104.

349. Stenger MB, Brown AK, Lee S, Locke JP, Platts SH. Gradient compression garments as a countermeasure to post-spaceflight orthostatic intolerance. Aviation, Space, and Environmental Medicine. 2010;81:883-87.

350. Keyak J, Koyama A, LeBlanc A, Lu Y, Lang T. Reduction in proximal femoral strength due to long-duration spaceflight. Bone. 2009;44:449-53.

351. Cucinotta F, Manuel F, Jones J, Iszard G, Murrey J, Djojonegro B, Wear M. Space radiation and cataracts in astronauts. Radiat Res. 2001;156:460-66.

352. Candela M, Guidotti M, Fabbri A, Brigidi P, Franceschi C, Fiorentini C. Human intestinal microbiota: Cross-talk with the host and its potential role in colorectal cancer. Crit Rev Microbiol. 2011;37:1-14.

353. Munkholm P. Review article: The incidence and prevalence of colorectal cancer in inflammatory bowel disease. Aliment Pharmacol Ther. 2003;18:1-5.

354. Cucinotta FA, Kim M, Chappell LJ. Space radiation cancer risk projections and uncertainties-2010. NASA Tech Pap, NASA/TP-2011-216155. 2011;1:1-20.

355. Cucinotta FA, Kim M-HY, Chappell LJ, Center LBJS. Probability of causation for space radiation carcinogenesis following international space station, near Earth asteroid, and Mars missions: National Aeronautics and Space Administration, Lyndon B. Johnson Space Center; 2012;1:1-45.

356. Portess DI, Bauer G, Hill MA, O'Neill P. Low-dose irradiation of nontransformed cells stimulates the selective removal of precancerous cells via intercellular induction of apoptosis. Cancer Res. 2007;67:1246-53.

357. Schmid TE, Dollinger G, Beisker W, Hable V, Greubel C, Auer S, Mittag A, Tarnok A, Friedl AA, et al. Differences in the kinetics of gamma-h2ax fluorescence decay after exposure to low and high let radiation. Int J Radiat Biol. 2010;86:682-91.

358. Datta K, Suman S, Kallakury BVS, Fornace AJ. Heavy ion radiation exposure triggered higher intestinal tumor frequency and greater β-catenin activation than γ radiation in apc(min/+) mice. PLoS ONE. 2013;8:1-e59295.

359. Girardi C, De Pittà C, Casara S, Sales G, Lanfranchi G, Celotti L, Mognato M. Analysis of miRNA and mRNA expression profiles highlights alterations in ionizing radiation response of human lymphocytes under modeled microgravity. PLoS ONE. 2012;7:e31293.

360. Lloyd SA, Bandstra ER, Willey JS, Riffle SE, Tirado-Lee L, Nelson GA, Pecaut MJ, Bateman TA. Effect of proton irradiation followed by hindlimb unloading on bone in mature mice: A model of long-duration spaceflight. Bone. 2012;51:756-64.

361. Ni H, Balint K, Zhou Y, Gridley DS, Maks C, Kennedy AR, Weissman D. Effect of solar particle event radiation on gastrointestinal tract bacterial translocation and immune activation. Radiat Res. 2011;175:485-92.

362. Lam V, Moulder JE, Salzman NH, Dubinsky EA, Andersen GL, Baker JE. Intestinal microbiota as novel biomarkers of prior radiation exposure. Radiat Res. 2012;177:573-83.

363. Wilson JW, Ott CM, Quick L, Davis R, Zu Bentrup KH, Crabbé A, Richter E, Sarker S, Barrila J, et al. Media ion composition controls regulatory and virulence response of salmonella in spaceflight. PLoS ONE. 2008;3:e3923.

364. Rosenzweig JA, Abogunde O, Thomas K, Lawal A, Nguyen Y-U, Sodipe A, Jejelowo O. Spaceflight and modeled microgravity effects on microbial growth and virulence. Appl Microbiol Biotechnol. 2010;85:885-91.

365. Chopra V, Fadl A, Sha J, Chopra S, Galindo C, Chopra A. Alterations in the virulence potential of enteric pathogens and bacterial–host cell interactions under simulated microgravity conditions. Journal of Toxicology and Environmental Health, Part A. 2006;69:1345-70.

366. Beuls E, Houdt RV, Leys N, Dijkstra C, Larkin O, Mahillon J. *Bacillus thuringiensis* conjugation in simulated microgravity. Astrobiology. 2009;9:797-805.

367. Belay T, Aviles H, Vance M, Fountain K, Sonnenfeld G. Effects of the hindlimb-unloading model of spaceflight conditions on resistance of mice to infection with *Klebsiella pneumoniae*. J Allergy Clin Immunol. 2002;110:262-68.

368. Aviles H, Belay T, Vance M, Sonnenfeld G. Effects of space flight conditions on the function of the immune system and catecholamine production simulated in a rodent model of hindlimb unloading. Neuroimmunomodulation. 2005;12:173-81.

369. Kalliomki M, KalliomÃ¤ki. Expression of microbiota, toll-like receptors, and their regulators in the small intestinal mucosa in Celiac disease. J Pediatr Gastroenterol Nutr. 2012;54:727-32.

370. Nikawa T, Ishidoh K, Hirasaka K, Ishihara I, Ikemoto M, Kano M, Kominami E, Nonaka I, Ogawa T, et al. Skeletal muscle gene expression in space-flown rats. The FASEB Journal. 2004;18:522-24.

371. Templin T, Amundson SA, Brenner DJ, Smilenov LB. Whole mouse blood microrna as biomarkers for exposure to gamma rays and 56Fe ions. Int J Radiat Biol. 2011;87:653-62.

372. Ding L-H, Shingyoji M, Chen F, Hwang J-J, Burma S, Lee C, Cheng J-F, Chen DJ. Gene expression profiles of normal human fibroblasts after exposure to ionizing radiation: A comparative study of low and high doses. Radiat Res. 2005;164:17-26.

373. Azzam EI, de Toledo SM, Gooding T, Little JB. Intercellular communication is involved in the bystander regulation of gene expression in human cells exposed to very low fluences of alpha particles. Radiat Res. 1998;150:497-504.

374. Zhou Y, Ni H, Li M, Sanzari JK, Diffenderfer ES, Lin L, Kennedy AR, Weissman D. Effect of solar particle event radiation and hindlimb suspension on gastrointestinal tract bacterial translocation and immune activation. PLoS ONE. 2012;7:e44329.

375. Hosoi Y, Miyachi H, Matsumoto Y, Enomoto A, Nakagawa K, Suzuki N, Ono T. Induction of interleukin-1β and interleukin-6 mRNA by low doses of ionizing radiation in macrophages. Int J Cancer. 2001;96:270-76.

376. Aviles H, Belay T, Fountain K, Vance M, Sonnenfeld G. Increased susceptibility to *Pseudomonas aeruginosa* infection under hindlimb-unloading conditions. J Appl Physiol. 2003;95:73-80.

377. Pecaut MJ, Gridley DS. The impact of mouse strain on iron ion radio-immune response of leukocyte populations. Int J Radiat Biol. 2010;86:409-19.

378. Clark M, Colombel J-F, Feagan BC, Fedorak RN, Hanauer SB, Kamm MA, Mayer L, Regueiro C, Rutgeerts P, et al. American Gastroenterological Association consensus development conference on the use of biologics in the treatment of inflammatory bowel disease, June 21–23, 2006. Gastroenterology. 2007;133:312-39.

APPENDIX A

TABLES OF RESULTS

Table A-1. Mean body weight (g) throughout the study. High Tannin control rats had higher body weights than Cellulose control rats on d 37, d 39, d 53, and d 58.

			Cellulose		Black bran		Sumac bran		High Tannin				
			Control	DSS	Control	DSS	Control	DSS	Control	DSS	Diet	DSS	Diet* DSS
Body Weight (g)	Initial	d 1	61.70±1.89[a]	61.03±1.97[a]	62.36±1.89[a]	61.48±1.91[a]	63.54±1.65[a]	63.07±1.65[a]	62.77±1.50[a]	62.40±1.48[a]			
	Diet start	d 19	156.11±1.89[a]	155.35±1.97[a]	157.54±1.89[a]	160.12±1.91[a]	159.25±1.65[a]	160.09±1.65[a]	161.78±1.50[a]	157.31±1.48[a]			
	Intake #1 final	d 37	255.67±5.32[a]	261.50±3.58[ab]	261.48±3.54[ab]	264.75±2.84[ab]	267.54±5.03[ab]	262.62±4.23[ab]	268.66±4.05[b]	260.24±4.46[ab]			
	Pre-DSS #1	d 39	269.49±5.80[a]	274.96±3.34[ab]	273.76±3.71[ab]	279.39±2.65[ab]	279.36±4.40[ab]	277.20±4.94[ab]	283.23±4.45[b]	273.81±4.4[ab]			
	Pre-DSS #2	d 53	318.09±6.66[a]	324.76±5.25[ab]	321.66±5.94[ab]	329.01±4.04[ab]	333.17±7.06[ab]	322.30±6.38[ab]	337.88±5.74[b]	323.99±7.16[ab]			
	Intake #2 final	d 58	329.37±6.59[a]	334.66±5.65[ab]	332.59±6.73[ab]	340.34±4.52[ab]	344.89±7.55[ab]	332.52±6.31[ab]	348.55±5.93[b]	335.32±8.26[ab]			
	Pre-DSS #3	d 67	349.71±7.6[a]	356.31±7.04[a]	353.10±7.53[a]	361.56±4.74[a]	365.21±7.95[a]	353.80±7.01[a]	367.91±6.28[a]	356.45±9.04[a]			
	Intake #3	d 77	369.60±9.05[a]	376.47±7.85[a]	373.73±8.04[a]	382.26±5.63[a]	386.37±8.89[a]	372.30±8.28[a]	390.26±8.11[a]	376.60±9.92[a]			
	Termination	d 82	374.27±8.86[a]	382.19±7.81[a]	379.03±7.95[a]	386.97±5.41[a]	391.24±8.9[a]	374.94±8.43[a]	394.8±8.08[a]	381.52±9.94[a]			
			Values are LS mean ± SEM.										
			Means without common superscripts differ (p<0.05).										

Table A-2. SCFA production post DSS#2 on d 44 (umol/24 hr). Diet significantly affected 24 hr SCFA production for propionic, isobutyric, butyric, isovaleric, and valeric. We observe a diet*DSS effect on isobutyric acid.

		Cellulose		Black bran		Sumac bran		High Tannin				
		Control	**DSS**	**Control**	**DSS**	**Control**	**DSS**	**Control**	**DSS**	**Diet**	**DSS**	**Diet* DSS**
Total SCFA prod (umol)/ 24 hr	**Acetic**	89.24±6.70^{b}	60.11±6.34^{ab}	51.17±2.76^{a}	61.65±2.17^{ab}	67.89±2.98^{ab}	68.91±5.52^{ab}	46.41±2.05^{a}	53.54±2.59^{a}			
	Propionic	18.57±0.92^{a}	23.40±1.11^{ab}	20.51±1.22^{a}	27.98±1.20^{abc}	37.32±1.42^{c}	33.40±1.82^{bc}	22.03±0.86^{a}	32.80±1.00^{bc}	0.004		
	Isobutyric	2.45±0.16^{a}	3.55±0.13^{ab}	2.34±0.13^{a}	2.91±0.15^{a}	6.58±0.30^{c}	4.75±0.28^{b}	4.96±0.18^{bc}	6.46±0.27^{c}	<0.0001		0.03
	Butyric	34.47±2.54^{c}	22.26±2.30^{abc}	28.18±1.17^{bc}	22.74±1.08^{abc}	16.99±0.77^{ab}	13.02±0.63^{a}	22.70±0.85^{abc}	22.78±1.16^{abc}	0.0235		
	Isovaleric	4.67±0.39^{a}	7.58±0.28^{a}	5.86±0.31^{a}	7.62±0.36^{a}	17.21±0.81^{c}	12.69±0.58^{b}	12.81±0.50^{b}	15.91±0.78^{bc}	<.0001		
	Valeric	7.60±0.40^{b}	9.23±0.48^{b}	7.45±0.70^{b}	8.0±1.04^{b}	1.38±0.96^{a}	0.96±0.73^{a}	12.99±0.99^{c}	17.54±7.90^{d}	<0.0001		
	Total	157.00±9.62^{a}	126.13±9.35^{a}	115.52±5.81^{a}	130.92±5.53^{a}	147.36±4.67^{a}	133.73±7.49^{a}	121.89±3.70^{a}	149.03±8.97^{a}			
		Values are LS mean ± SEM.										
		Means without common superscripts differ (p<0.05).										

Table A-3. SCFA production on d 66 (umol/24 hr). Diet significantly affected 24 hr SCFA production for propionic, isobutyric, butyric, isovaleric, and valeric. We observe a diet*DSS effect on acetic acid.

		Cellulose		Black bran		Sumac bran		High Tannin				
		Control	**DSS**	**Control**	**DSS**	**Control**	**DSS**	**Control**	**DSS**	**Diet**	**DSS**	**Diet* DSS**
Total SCFA prod (umol)/ 24 hr	**Acetic**	48.15±6.70^{b}	29.06±6.34^{a}	26.08±2.76^{a}	35.66±2.17^{ab}	33.01±2.98^{a}	39.14±5.52^{ab}	30.68±2.05^{a}	31.63±2.59^{a}			0.026
	Propionic	10.73±0.92^{ab}	6.61±1.11^{a}	9.81±1.22^{ab}	12.98±1.20^{b}	19.39±1.42^{c}	19.36±1.82^{c}	14.09±0.86^{b}	13.57±1.01^{ab}	<0.0001		
	Isobutyric	1.54±0.16^{a}	1.28±0.13^{a}	1.23±0.13^{a}	1.53±0.15^{a}	3.53±0.30^{b}	3.13±0.28^{b}	3.47±0.18^{b}	3.80±0.27^{b}	<0.0002		
	Butyric	17.24±2.54^{bc}	10.29±2.30^{a}	16.61±1.17^{bc}	20.55±1.08^{c}	8.43±0.77^{a}	7.09±0.63^{a}	12.54±0.85^{ab}	10.07±1.16^{a}	<0.0003		
	Isovaleric	2.75±0.39^{a}	2.69±0.28^{a}	2.92±0.31^{a}	3.63±0.36^{a}	8.95±0.81^{b}	7.72±0.58^{b}	8.67±0.50^{b}	9.50±0.78^{b}	<0.0004		
	Valeric	4.16±0.40^{abc}	11.01±0.48^{bc}	4.14±0.70^{abc}	4.90±1.04^{abc}	0.53±0.96^{a}	0.65±0.73^{a}	9.04±0.99^{b}	10.14±7.90^{b}	0.0127		
	Total	84.57±9.62^{a}	60.94±9.35^{a}	60.79±5.81^{a}	79.23±5.53^{a}	73.84±4.67^{a}	77.09±7.50^{a}	78.49±3.67^{a}	78.69±8.97^{a}			
		Values are LS mean ± SEM.										
		Means without common superscripts differ (p<0.05).										

Table A-4. SCFA production post DSS#3 on d 72 (umol/24 hr). Diet significantly affected 24 hr SCFA production for propionic, isobutyric, butyric, isovaleric, and valeric.

		Cellulose		Black bran		Sumac bran		High Tannin				
		Control (N=9)	**DSS (N=9)**	**Control (N=9)**	**DSS (N=9)**	**Control (N=9)**	**DSS (N=9)**	**Control (N=9)**	**DSS (N=9)**	**Diet**	**DSS**	**Diet* DSS**
Total SCFA prod (umol)/ 24 hr	**Acetic**	31.82±6.70^{bc}	24.94±6.34^{c}	21.92±2.76^{ab}	27.07±2.17^{bc}	26.70±2.98^{a}	31.05±5.52^{c}	28.89±2.05^{c}	28.80±2.59^{c}			
	Propionic	7.99±0.92^{a}	9.58±1.11^{ab}	9.77±1.22^{ab}	12.65±1.20^{abc}	17.64±1.42^{c}	18.04±1.82^{c}	13.69±0.86^{abc}	15.29±1.01^{bc}	0.0006		
	Isobutyric	1.22±0.16^{a}	1.38±0.13^{a}	1.16±0.13^{a}	1.38±0.15^{a}	3.06±0.30^{bc}	2.67±0.28^{b}	3.56±0.18^{bc}	3.73±0.27^{c}	<0.0001		
	Butyric	15.96±2.54^{c}	8.53±2.30^{ab}	15.31±1.17^{c}	14.75±1.08^{c}	7.50±0.77^{ab}	5.85±0.63^{a}	12.34±0.85^{bc}	11.56±1.16^{abc}	0.002		
	Isovaleric	2.03±0.39^{a}	2.67±0.28^{a}	2.60±0.31^{a}	3.09±0.37^{a}	7.50±0.81^{bc}	6.13±0.58^{b}	8.73±0.50^{c}	8.84±0.78^{c}	<0.0001		
	Valeric	3.69±0.40^{b}	3.56±0.48^{b}	3.85±0.70^{b}	4.31±1.04^{b}	0.60±0.96^{a}	0.32±0.73^{a}	9.41±0.99^{c}	9.56±7.90^{c}	<0.0001		
	Total	62.71±9.62^{a}	50.67±9.35^{a}	54.61±5.81^{a}	63.25±5.53^{a}	63.00±4.67^{a}	64.07±7.50^{a}	76.61±3.67^{a}	77.78±8.97^{a}			
		Values are LS mean ± SEM.										
		Means without common superscripts differ (p<0.05).										

Table A-5. Phylogenetic classification of OTUs (%) at the phylum level on d 47 and d 62.

		Cellulose		Black Bran		Sumac Bran		High Tannin Bran				
			DSS (n=9)		DSS (n=9)		DSS (n=10)		DSS (n=10)	Diet		
Day 47 (Post DSS#2): Phylum level classification (% OTUs)	Actinobacteria		0.64±0.13^{b}		0.12±0.04^{a}		0.37±0.11^{ab}		0.22±0.16^{a}	0.0276		
	Bacteroidetes		2.37±0.81^{a}		9.76±2.77^{b}		19.44±2.75^{c}		7.52±2.34^{ab}	0.0001		
	Firmicutes		83.82±1.47^{c}		69.10±4.94^{b}		44.44±4.78^{a}		63.90±5.63^{b}	<0.0001		
	Proteobacteria		0.70±0.18^{a}		1.52±0.32^{ab}		3.25±0.99^{b}		2.56±0.57^{b}	0.0364		
	Unknown		7.97±1.43^{a}		10.88±1.69^{ab}		16.49±2.38^{b}		13.31±2.90^{ab}			
	Unassignable		4.50±0.51^{a}		8.51±0.91^{ab}		15.95±1.73^{c}		12.44±2.88^{bc}	0.0007		
		Control (n=5)	DSS (n=10)	Control (n=5)	DSS (n=9)	Control (n=5)	DSS (n=10)	Control (n=5)	DSS (n=9)	Diet	DSS	Diet* DSS
Day 62 (Post DSS#3): Phylum level classification (% OTUs)	Actinobacteria	0.52±0.16^{bc}	0.80±0.19^{c}	0.13±0.11^{ab}	0.11±0.04^{ab}	0.04±0.04^{a}	0.02±0.02^{a}	0.58±0.33^{bc}	0.05±0.04^{a}	<0.0001		
	Bacteroidetes	0.55±0.29^{a}	0.95±0.20^{a}	6.06±0.84^{ab}	6.53±1.72^{b}	24.17±4.47^{d}	13.56±1.15^{c}	16.54±3.50^{c}	7.97±0.72^{b}	<0.0001	0.0006	0.0026
	Firmicutes	61.20±4.22^{e}	49.12±3.25^{d}	26.29±3.96^{bc}	33.41±3.32^{c}	23.59±3.46^{b}	9.41±0.60^{a}	53.05±4.62^{de}	27.06±2.23^{bc}	<0.0001	<0.0001	<0.0001
	Proteobacteria	0.18±0.11^{a}	0.11±0.04^{a}	0.61±0.17^{ab}	0.99±0.36^{abc}	4.29±0.40^{d}	2.36±0.79^{c}	3.49±1.20^{cd}	2.13±0.63^{bc}	<0.0001		
	Unknown	20.61±3.28^{a}	27.51±2.39^{b}	39.43±2.55^{de}	33.28±1.84^{cd}	28.10±4.10^{bc}	45.15±0.63^{e}	15.80±2.35^{a}	36.37±1.41^{d}	<0.0001	<0.0001	<0.0001
	Unassignable	16.92±0.93^{b}	21.44±1.19^{c}	27.48±1.03^{de}	25.68±1.22^{d}	19.80±3.41^{bc}	29.50±1.26^{e}	10.38±1.41^{a}	26.28±0.87^{de}	<0.0001	<0.0001	<0.0001
		†Data represents predominant phylogenetic groups (>1%) and are LS mean±SEM.										
		Means without a common superscript differ (p<0.05)										

Table A-6. Phylogenetic classification of OTUs (%) from Experiment 2.

Experiment 2†						
Phylum	**Family**	**Order**	**WB SHAM (N=9)**	**WB RAD (N=9)**	**LUN SHAM (N=11)**	**LUN RAD (N=11)**
Bacteroidetes			24.66	37.89	32.33	29.58
	Bacteroidia	Bacteroidales	0.00	0.82	0.31	0.18
	Unknown	Unknown	24.66	37.07	32.02	29.40
Firmicutes			54.39	48.29	38.18	44.06
	Bacilli	Lactobacillales	40.08	37.67	3.00	7.15
	Clostridia	Clostridiales	13.36	10.10	34.80	33.24
	Erysipelotrichi	Erysipelotrichales	0.00	0.07	0.00	0.00
Unknown			17.15	10.48	22.09	18.95
Unassignable			3.79	3.34	7.39	6.70
† All proportions represent analysis of one composite sample containing aliquots from N animals in each group.						
Data are LS mean±SEM.						

Table A-7. Phylogenetic classification of OTUs (%) from Experiment 3.

Experiment 3				
Phylum	**Family**	**Order**	**Ground (N=7)**	**Fight (N=7)**
Bacteroidetes			45.99±5.71[a]	49.85±5.88[a]
	Bacteroidia	Bacteroidales	18.97±3.03[a]	29.85±4.80[a]
	Unknown	Unknown	27.02±4.49[a]	20.00±5.47[a]
Firmicutes			44.51±6.24[a]	37.43±7.09[a]
	Bacilli	Lactobacillales	26.25±6.77[a]	9.91±4.96[a]
	Clostridia	Clostridiales	10.85±2.10[a]	26.43±7.98[a]
	Erysipelotrichi	Erysipelotrichales	7.11±2.16[b]	0.44±0.24[a]
Unknown			3.42±0.38[a]	4.12±0.90[a]
Unassignable			5.40±0.73[a]	6.68±0.91[a]
Data are LS mean±SEM.				
Means without a common superscript differ (p<0.05).				

APPENDIX B

EXPERIMENTAL PROTOCOLS

Chapter II & III Animals and Diets

Eighty male Sprague-Dawley rats (21 d old) were stratified by body weight and assigned to one of four experimental diets (n=10/ diet). The four diets contain 6% dietary fiber from 1) cellulose, or bran isolated from sorghum grains that contain: 2) high levels of 3-deoxyanthocyanins, 3) high levels of condensed tannins and low levels of 3-deoxyanthocyanins, or 4) both 3-deoxyanthocyanins and condensed tannins. Diets were mixed using the following protocol:

	Control/Cellulose	Sumac Brown	TX430 Black	8830 High Tannin
INGREDIENT	**g/100g**	**g/100g**	**g/100g**	**g/100g**
Dextrose	51.06	44.49	46.11	42.76
Casein	22.35	20.73	20.97	20.76
DL-methionine	0.34	0.34	0.34	0.34
Mineral mix, AIN-76 A	3.91	3.91	3.91	3.91
Vitamin mix AIN-76A	1.12	1.12	1.12	1.12
Choline bitartrate	0.22	0.22	0.22	0.22
Cellulose	6.00	0.00	0.00	0.00
Sorghum bran		16.35	13.08	17.56
Lipid				
Corn oil	15.00	13.55	14.64	13.77

1. Get cart, 2-3 5L jugs, tub big enough to fit jugs and ice, aluminum foil, bench papers, scissors, sharpies, napkins, weigh scale, plastic beaker.
2. Go to Dr. Chapkin's lab to measure out corn oil, where it is also stored. When done, fill remaining barrel of oil with nitrogen gas, seal, date, and store back in freezer. Record lot number.
3. Cover jugs with foil, label, and put on ice.
4. Bring 2 big stainless steel mixing bowls from lab to basement.
5. Measure out test compounds, add to mineral/vitamin, methionine/choline mix and mix well.
6. Start with Bowl 1 of a diet group. Mix by hand diet components .
7. Fit bowl onto electric mixer, cover, and mix dry components for 5 min at #1 setting.
8. Still at setting #1, start mixer for 10 min. During this time, pour oil into mix in 3 separate quantities and times. To get all oil out from jug, use diet to mop it up.

9. Scrape sides of bowl and blade, mix for 5 min more.
10. Lower bowl, scrape sides of bowl and blade. Put bowl back into position and mix for 10 min at #2 setting.
11. Scrape diet off blade, lower and remove bowl. Take a sample of diet mix from four locations in the bowl (send off to analysis).
12. Scoop diet into labeled bags and double-bag. Store in labeled plastic tubs in freezer.
13. Repeat above diet process for all diet groups.
14. Clean up.
Notes: Before starting on a new diet group, remember to wash bowls and scoops and change gloves to prevent cross-contamination. Bowls and scoops need to be sprayed with 70% EtOH after washing and drying. The dry diet components are in powder form, so dust clouds form when pouring; pour slowly to reduce dust. Mineral mix, vitamin mix, and methionine are stored in the freezer, so put back in freezer after measuring out into tubs. The mineral/vitamin/methionine/choline mix might be lumpy, so it is best to use gloved hands to break up the lumps and mix uniformly. Diet samples are taken after mixing for analysis of composition. The small vials are used to collect samples throughout the feeding period and at the end.

Antioxidant capacity, total polyphenol content, tannin content, and proportions of soluble and insoluble fiber were quantified for each experimental diet. Prior to beginning the experimental diet (at 40 d old), animals were maintained on a standard chow diet for 19 d in order to overcome shipping stress.

After 14 d of experimental diets, half of the rats were exposed to three sequential 48 h dextran sodium sulfate (DSS) (MP Biomedicals, Irvine, CA) treatments (3% DSS) in their drinking water, with 14 d between each DSS exposure. Between DSS exposures, distilled water was supplied to treated animals. The remaining half of the animals received distilled water throughout the course of the study.

Body weight and food intake was routinely monitored. Rats were weighed upon arrival, prior to beginning experimental diets, before and after each DSS exposure, and prior to termination. Additionally, experimental diet consumption was measured prior to

the first DSS treatment, following the second DSS treatment, and prior to termination (following third DSS treatment). On day 82, animals were euthanized by CO_2 asphyxiation. The colon was resected, and two 1 cm sections were removed for histological preparations and the remainder will be scraped (see below).

Chapter II & III tissue collection and processing

Scraped mucosa

After fecal material was removed from the colon, it was washed twice in RNase free Phosphate-Buffered Saline (PBS), scraped on a chilled RNase free surface, and transferred to an RNase free homogenization tube along with 500 µl of Denaturation Solution (Ambion, Austin, TX) or 400 µl of protein buffer (see below). Scraped mucosa for RNA analysis was homogenized in Denaturation Solution for 6-7 strokes and then transferred to a 2 ml epitube for storage at -80°C. Scraped mucosa was placed into a homogenizer along with 400 µl of buffer. Protein buffer (10 ml) was mixed on the day of the kill, just prior to use. The protein buffer contained: 1 ml of 500 mM Tris-HCl (pH 7.2) (Sigma), 2.5 ml of 1.0 M Sucrose (Sigma), 100 µl of 200 mM EDTA (pH 7.6) (Sigma), 100 µl of 100 mM EGTA (pH 7.5) (Aldrich), 1.25 µl of 0.4 M NaF (Sigma), 4.554 ml of water; 1 ml of 10% Triton X-100 (Sigma), 100 µl of 10 mM orthovanadate (Sigma), and 400 µl of Protease Inhibitor (Sigma). Mucosa and protein buffer was homogenized for at least 7 strokes (on ice) and transferred into a 2 ml epitube. The sample was aspirated through a 12 gauge needle twice and then incubated on ice for 30 minutes prior to centrifugation at 15,000 g for 20 minutes. The supernatant was

transferred, and the volume was split among the aliquot tubes and then placed into a –80 freezer for storage.

Tissue fixation for immunohistological processing

The two, 1 cm segments removed from the distal end of the colon were fixed in either a 4% PFA (PFA solution was mixed a day before the killing. 50 ml of 10X PBS was dilute to 400 ml with ddH_2O, and then 100 ml of 20% PFA was added. PFA solution was refrigerated overnight.) or 70% EtOH solution prior to embedding in paraffin. Tissue fixed in 70% EtOH was stored at room temperature until embedded in paraffin. Tissue fixed in PFA was incubated on ice for 4 h in a 4% PFA solution, then rinsed and stored at 4°C in 70% EtOH until embedded in paraffin.

Chapter II fecal collections and processing

Fresh fecal samples were collected for fermentation metabolite analysis prior to DSS exposure, and 48 h after each DSS exposure. After the colon was resected from the rat at termination, it was opened longitudinally and fecal samples from the distal and proximal segments of the colon were collected, placed into a tube, and stored on ice. The samples were then immediately placed into a –80°C freezer until further analysis.

Dry matter analysis

Fecal samples were thawed and placed into a weighed pan prior to drying in a 60°C oven for 72 h. Samples were cooled in a vacuum dessicator for 24 h before being weighed. This procedure was repeated until weight became static.

Short chain fatty acid (SCFA) analysis

Fresh fecal samples were collected immediately following defecation. Samples were transferred to sterile cryotubes, snap-frozen in liquid nitrogen, and stored at -80°C. Fecal samples were prepared for analysis by grinding in a mortar and pestle chilled by immersion in liquid nitrogen. The powdered sample (~0.20 g) was weighed into a 1.5-mL centrifuge tube containing 750 mL of the internal standard, 2-ethylbutyric acid (Sigma-Aldrich, St. Louis, MO), in 70% ethanol. Samples were vigorously vortexed and incubated overnight at 47°C to extract the SCFA. To prepare the extracted samples for gas-liquid chromatography, samples were first shaken vigorously for 20 min and then centrifuged at 11,500 g for 20 min at 47°C. A 100 mL aliquot of the supernatant was removed and combined with 100 mL of the second internal standard, 3 mmol/L heptanoic acid prepared in 70% ethanol. Immediately before injection into the gas chromatograph (GC), 20 mL of 0.1mmol/L phosphoric acid was added to the sample and vortexed. One microliter of sample containing the phosphoric acid was then injected into a Varian 3900 gas chromatograph (Walnut Creek, CA) with a splitless capillary inlet and flame ionization detector equipped with a 30 m, 0.53 mm i.d. deactivated glass capillary precolumn (Supelco,Bellfonte, PA). Data were integrated and plotted with a Hewlett Packard Series II Integrator. The GC conditions used were as follows: injector temperature, 1657C; detector temperature, 2207C; column flow, 2.21 mL/min He; make-up flow, 28 mL/min nitrogen; and oven temperature, 1857C (gradient). Standards and a blank were run before and after the daily sample runs to facilitate calibration and data

calculations. Fecal production measurements were used to calculate 24-h SCFA excretion.

- % dry matter= g dry wt/ g wet wt * 100%

$$\frac{\mu\text{mol SCFA}}{\text{g wet wt}} \times \frac{\text{g wet wt}}{\text{g dry wt}} = \frac{\mu\text{mol SCFA}}{\text{g dry wt}}$$

$$\frac{\text{average g feces (stale)}}{24\text{ h}} \times \text{\% dry matter (stale)} = \text{g fecal production (dry wt)/ 24 h}$$

$$\frac{\mu\text{mol SCFA}}{\text{g dry wt}} \times \frac{\text{g fecal production (dry wt)}}{24\text{ h}} = \frac{\mu\text{mol SCFA}}{24\text{ h}}$$

Chapter II, III, and IV inflammation and injury histological scores

The degree of inflammation and morphological injury was assessed by H&E staining. Histologic examination was performed in a blinded manner by a board-certified pathologist, and the degrees of inflammation (score of 0–3) and epithelial injury (score of 0–3) were scored on microscopic cross sections of the colon. The presence of occasional inflammatory cells in the lamina propria was assigned a value of 0; increased numbers of inflammatory cells in the lamina propria as 1; confluence of inflammatory cells, extending into submucosa, as 2; and transmural extension of the infiltrate as 3. For epithelium injury, no mucosal damage was scored as 0; discrete lymphoepithelial lesions were scored as 1; surface mucosal erosion or focal ulceration was scored as 2; and extensive mucosal damage and extension into deeper structures of the bowel wall was scored as 3.

Chapter II immunohistological measurement of proliferation

Cell proliferation was measured using a monoclonal antibody to proliferating cell nuclear antigen (PCNA; Anti-PC-10, Covance, Emeryville, CA). Bound primary antibodies were detected by applying a peroxidase-conjugated antibody to biotinylated anti-mouse immunoglobulin using a Vectastain ABC Elite Kit (Vector Lab, Burlingame, CA) and sequenza slide rack using the following protocol:

1. Deparaffinize slides: xylene (5' x 3), 100% EtOH (5' x 2), 95% EtOH (3' x 2), 70% EtOH (3'), H_2O (3').
2. Leave slides in 3% H_2O_2 for 30 min to remove endogenous peroxidase activity. 3% H_2O_2: 20 ml of 30% H_2O_2 made up to a final volume of 200 ml with methanol.
3. Wash in PBS 5 min, 3 times. Mount slides onto coverplates using PBS and insert into sequenza.
4. Prepare Vectastain Blocking Serum by adding 3 drops of stock Normal Serum (yellow label) to 10 ml of PBS in yellow mixing bottle.
5. Add 3 drops* to each coverplate in sequenza and replace top to maintain humidity. Let stand for 20 min. * Note: 1 drop = 50 μl
6. Wash with PBS by filling each coverplate in the sequenza with one ml of PBS.
7. Add 150 μl of anti-PC10 (use the optimal dilution obtained by dilution series: 1:200) to each coverplate in sequenza and replace top. For the negative control slide use PBS instead of anti-PC10. Let stand for 1 hour.
8. Wash with PBS by filling each coverplate in the sequenza to the top with PBS. Let stand for 5 min.
9. Prepare Vectastain biotynylated anti-mouse IgG by mixing 3 drops of stock normal serum with 10 ml PBS in Blue mixing bottle, then add 1 drop of stock biotinylated antibody (blue labe), Mix Gently. (or use 5 ml of serum solution form step 4, mix with 25 μl of stock biotinylated antibody).
10. Add 3 drops to each coverplate in sequenza and replace top. Let stand for 45 min.
11. Prepare ABC reagent in advance to be used in step 13. The ABC reagent is prepared by adding 2 drops of reagent A (gray label) to 5 ml PBS in the ABC Reagent large mixing bottle. Then add exactly 2 drops of Reagent B (gray label) to the same mixing bottle, mix immediately, and allow ABC Reagent to stand for about 30 minutes before use. This should be done in a darkened area.
12. Wash with PBS by filling each coverplate in the sequenza to the top with PBS. Let stand for 5 min.

13. Apply Vectastain ABC reagent that had been prepared in step 11. Add 3 drops to each coverplate in sequenza, replace top, and let stand for 30 min.
14. Wash with PBS by filling each coverplate in the sequenza to the top with PBS. Remove slides form sequenza and place in PBS for 5 min.
15. Prepare DAB solution. For 200 ml: 2 ml stock DAB (50 mg/ml) bring volume up to 200 ml with PBS. Immediately before staining, add 100 uL of 30% H_2O_2.
16. Leave slides in DAB solution for 1 min, agitate twice.
17. Wash with H_2O 5 min, 3 times.
18. Deactivate all DAB materials (glassware, pipet tips, used stock vials, stir bars) and used DAB solutions with bleach overnight, and flush with excess water in drain next day.
19. Counterstain with Hematoxyline $\leq$ 1 sec.
20. Wash with H_2O 2 min, 2 times.
21. Dehydrate slides: 1 x 1 min 70% ETOH, 1 x 1 min 95% ETOH, 1 x 1 min 100% ETOH, 1 x 2 min Xylene.
22. Apply permount and cover glass.

Negative control slides were prepared in conjunction by substituting anti-PC 10 with a like volume of PBS. Only cells with intense PCNA staining were measured. The total number of proliferating cells, position of the highest proliferating cell and total cell number/crypt column (crypt column height) was assessed in 25 crypt columns/rat.

Chapter II measurement of apoptosis

Paraffin section of the 4% PFA fixed tissues was used to measure apoptosis using the TUNEL assay (EMD Millipore, Billerica, MA) using the following protocol:

***Put 200 ml PBS for Prot. K in 37° C oven and begin bleach rinse.

1. Deparaffinize and rehydrate tissue: Xylene (3X 5 min), let xylene just dry, circle sections w/ PAP pen, dry 1 min, 100% EtOH (2x5 min), 95% EtOH (1X3 min),70% EtOH (1X3 min), PBS (1X5 min). (Get Equilibration Buffer and Reaction Buffer out of freezer-put on ice).
2. Pretreat tissue – 3 min, in 37° Proteinase K (10 μg/ml PBS) = 0.1 ml Proteinase K (Ambion # 2546) in 200 ml PBS.
3. Wash in dH_2O (2x2 min).

4. Quench Endogenous Peroxidase: 0.3% H_2O_2 in 100% Methanol: 3.0 ml 30% H_2O_2 in 297 ml 100% Methanol or 2.0 ml in 198 ml (add fresh H_2O_2 immediately before quenching). 30 min, RT
5. Wash in dH_2O (2x5 min).
6. Wash all slides in PBS 5 min.
7. Gently tap off PBS and carefully blot around sections. (Do this step and following step one slide at a time to avoid drying out sections)
8. Apply EQUILIBRATION BUFFER to all sections: incubate in humidified chamber for 15 sec to 1 hr @ RT. (# of slides X 150 µl) (9 slides X 150µl = 1.35 ml)
9. Tap off equilibration buffer and immediately apply reaction buffer (-controls) or working strength TdT Enzyme with dilution ratio 1/30 (enzyme /reaction buffer). (Get TdT directly from freezer & keep on ice) Apply only reaction buffer to negative control sections:(# sections) X 40µl. For normal sample sections (# sections X 40µl):1080 µl reaction buffer (for 9 slides),36 µl TdT enzyme (for 9 slides).Incubate in a humidified chamber at 37°C, 1 hr. (Prepare Stop/Wash so it can warm to RT)
12. Put slides in coplin jar with Working Strength Stop/Wash Buffer (1ml + 34 ml dH_2O). Agitate for 15 sec; incubate 10 min, RT.Take aliquot of ANTI-DIGOXIGENIN PEROXIDASE (# slides X 125 µl) and allow to warm to room temperature (9 slides x 125µl = 1.125ml).
13. Wash slides in PBS (3X1min).
14. Blot dry the slides quickly (do one slide at a time) and apply ANTI-DIGOXIGENIN PEROXIDASE to all sections; incubate 30 min. in humidity chamber @ RT.
15. Wash in PBS (4X2min). Prepare DAB peroxidase (1:50, substrate:dilution buffer) (#slides x 150µl) and warm to room temperature. Protect from light.
16. Blot dry the slides quickly (do one slide at a time) and stain sections with DAB until light brown color shows up (≤ 20 sec).
17. Wash in dH_2O (3X1 min). Leave in 4^{th} for 5 min. During wash deactivate remaining DAB solution w/ bleach – leave overnight.
18. Counterstain w/ Methyl Green (reusable): Dip quickly into Methyl green. Rinse in dH_2O 5X; dip 1x in the 1^{st} 2 changes and briefly agitate. Dip 10 x in 3^{rd} & leave ~ 30 sec. Leave in the last 2 for 1 min w/o agitation.
19. Dehydrate: 70% EtOH (1X1 min), 95% EtOH (1X1 min), 100% EtOH (1X1 min), Xylene (3X2 min) (dip 10 times/ea).
20. Wet mount w/ Permount (80:20, Permount:Xylene).

Positive control tissues were run in conjunction with each assay. As a negative control, PBS was substituted for 'TdT' in the working solution. Total number of

apoptotic cells and total number of cells/crypt column will be determined in 50 crypt columns/rat, and an apoptotic index (apoptotic cells/crypt column height) was determined for each crypt.

Chapter II activated NF-κB measurement

Activated NF-κB was assessed from scraped mucosa protein supernatant using the manufacturer's protocol for whole cell lysates with the TransAM™ NF-κB Chemi Lysis buffer (Active Motif, Carlsbad, CA). A 20 microliter aliquot of activated NF-κB extract and 30 ul of Complete Binding Buffer was added to a kit provided, oligonucleotide covered plate. The plate was covered and then placed on a rocking plate at room temperature for 1 h. Each well was washed three times with 200 microliters Wash Buffer. Following the wash step, 100 microliters of diluted NF-κB antibody (1:1,000 dilution in 1X Antibody Binding Buffer) was added to each well. The plate was covered and incubated at room temperature for 1 h. Each well was washed three times with 200 microliters Wash Buffer. Following the second wash, 100 microliters of Developing Solution was added to each well. The plate was incubated in the dark for 5 minutes. Following incubation, 100 microliters of Stop Solution was added to each well. Absorbance was read at 450 nm with a reference wavelength of 655 nm. Only activated NF-κB subunits can bind to the oligonucleotide coated plate and are accessible to primary antibodies for detection. A standard curve of working stock recombinant protein diluted in Chemi Lysis buffer (10, 5, 2.5, 1.25, 0.0625, 0.312, 0.156, and 0 nanograms per well) was used to quantify activated NF-κB in each sample. A nuclear extract of

Jurkat cells (2.5 micrograms) was used as a positive control for the p65 NF-κB subunit. An aliquot of protein and lysis buffer was run as a negative control.

Chapter II & IV measurement of gene expression using real-time PCR

Scraped mucosal samples were obtained at termination, placed into RNA protective solution and stored at -80°C until further analysis. Total RNA was isolated from mucosal samples using Phase Lock Gel™ tubes (5 Prime, Gaithersburg, MD) and the ToTALLY RNA™ Kit (Ambion, Austin, TX) followed by DNase treatment (DNA-*free*™ Kit, Ambion, Austin, TX). Epitubes containing homogenized scraped mucosa and Denaturation Solution were removed from -80°C storage and thawed on ice. Total RNA was isolated using the following protocol:

1. In hood, add 1 vol. (starting volume) phenol/CHCl3 :IAA (lower phase).
2. Shake vigorously for 1 min.; store on ice for 5 min. Prepare Heavy PLG tubes by centrifuging for 30 sec at 14000 X g .
3. Tranfer to prepared Phase Lock Gel Tube (Heavy 2 ml version- Cat # 2302830).
4. Centrifuge 16,000 x g, 5 min., 15°C.
5. Transfer upper phase to new 2.0 ml eppie tube. If there is no supernatant add 250 µl more of phenol/CCH_3 and re-centrifuge.
6. Add 1/10 vol. sodium acetate; (Remember to check approx. vol.) Mix by shaking or inversion for about 10 sec.
7. Add 1 vol ACID:phenol/CHCl3 #2 (Starting volume) Do not add more than one starting volume even if the volume of the lysate is greater than the *starting volume*.
8. Shake vigorously for 1 min.; store on ice for 5 min.
9. Transfer to new Phase Lock Gel tube (Heavy 2 ml version- Cat # 2302830).
10. Centrifuge 16,000 x g, 5 min. 15°C.
11. Transfer upper phase to new tube 2.0 ml eppi tube.
12. Measure and record the volume.
13. Add an equal vol. (from previous step, i.e., volume sucked off) isopropanol. Mix well.
14. Store at -20°C, at least 30 min. to overnight.
15. Centrifuge 14,000 x g, 15 min. 4°C.
16. Discard supernatant.

17. Wash pellet with 300 µl of 70% ethanol; flick or gently vortex for ~0.5-3 min.
18. Centrifuge for 5-10 min at low speed (~3000 X g or 7,500 rpm in a microfuge) @RT or 4°C.
19. Carefully remove supernatant and discard. Respin briefly, remove supernatant. Cover w/ Kimwipe and air dry for ~ 5 min.
20. Re-suspend RNA pellet in 50 µl Nuclease Free Water (Applied Biosystems AM9937) If necessary heat to 55-70° and vortex occasionally for all RNA to go into solution.

DNase treatment:

1. To RNA, add 0.1 vol 10X DNase I buffer (Ambion DNA free kit, Applied Biosystems AM####) and 3 µl DNase. Mix gently and incubate at 37°C for 20-30 min.
2. Add 0.1 vol DNase inactivation reagent (after resuspending it). Incubate at RT for 2 min, flicking a few times during incubation.
3. Centrifuge tube ~1 min. Remove supernatant to new tube, leaving reagent behind.
4. Add 0.1 volume (~5 µl) 0.1 mM EDTA in DEPC treated water (Applied Biosystems AM9912). Store at -80°C.

RNA quality was assessed using an Agilent Bioanalyzer prior to storage at -80°C. First strand cDNA was synthesized using random hexamers, oligo dT primer (Promega, Madison, WI), and Superscript™ III Reverse Transcriptase (Invitrogen, Carlsbad, CA) using the following protocol:

1. Add the following components to a nuclease-free microcentrifuge tube: 1 µl of oligo(dT)20 (50 µM), 50–250 ng of random primers, 10 pg–5 µg total RNA, 1 µl 10 mM dNTP Mix (10 mM each dATP, dGTP, dCTP and dTTP at neutral pH), sterile, distilled water to 13 µl.
2. Heat mixture to 65°C for 5 minutes and incubate on ice for at least 1 minute.
3. Collect the contents of the tube by brief centrifugation and add: 4 µl 5X First-Strand Buffer , 1 µl 0.1 M DTT, 1 µl RNaseOUT™ Recombinant RNase Inhibitor (Cat. no. 10777-019, 40 units/µl), 1 µl of SuperScript™ III RT (200 units/µl).
4. Mix by pipetting gently up and down. If using random primers, incubate tube at 25°C for 5 minutes.
5. Incubate at 50°C for 60 minutes.
6. Inactivate the reaction by heating at 70°C for 15 minutes. cDNA was used directly in a PCR reaction or stored at -20°C.

Real-time PCR was performed on select genes (TOLLIP, TFF3, ZO-1, Slc16a1, IL-6, IL-1β, IL-12b, TNFα, SLC5A8, TGFβ, TLR4, TLR2, MyD88, NF-κB, COX-2) using

Taqman® Array Micro Fluidic Cards (Applied Biosystems, Foster City, CA) and a ABI 7900 HT thermocycler (Applied Biosystems, Foster City, CA) using the following protocol:

1. For each sample, determine the total number of reservoirs to be filled, based on the format of your TaqMan Array card. Prepare the PCR reaction mix (cDNA + master mix). Fill the TaqMan Array card with the reaction mix. Centrifuge the TaqMan Array card. Seal the TaqMan Array card.
2. Calculate the total volume required for each reaction component.
3. If frozen, thaw the cDNA samples on ice. Resuspend the cDNA samples by inverting the tube, then gently vortexing.
4. Mix the master mix thoroughly by swirling the bottle.
5. For each sample, label a 1.5-mL microcentrifuge tube, then add the required components to the labeled tube.
6. Cap the microcentrifuge tubes, then gently vortex the tubes to thoroughly mix the solution.
7. Briefly centrifuge the tubes to spin down the contents and eliminate air bubbles.
8. Fill each fill reservoir with sample-specific PCR mix made from a single cDNA sample (1000 ng) + nuclease-free water, 50.0 microliters TaqMan® Gene Expression Master Mix.
9. Allow the TaqMan Array card to reach room temperature, then carefully remove it from its packaging. A minimum of 15 minutes at room temperature is required to equilibrate the card.
10. Place the TaqMan Array card on a lab bench, with the foil side down.
11. Load 100 µL of the desired sample-specific PCR reaction mix into a 100-µL micropipette.
12. Hold the micropipette in an angled position and place the tip in the fill port (the larger of the two holes) IMPORTANT! Do not allow the tip to contact and possibly damage the coated foil beneath the fill port.
13. Dispense the sample-specific PCR reaction mix so that it sweeps in and around the fill reservoir toward the vent port. IMPORTANT! Pipette the entire 100 µL into the fill reservoir. Be careful when pushing the micropipette plunger to its second stop position (to expel the sample-specific PCR reaction mix from the tip). If a large amount of air is released, it can push the reaction mix out of the fill reservoir via the vent port or introduce bubbles into the fill reservoir.
14. After the fill reservoirs have been filled with the sample-specific PCR reaction mix, centrifuge the TaqMan Array card to distribute the reaction mix to the reaction wells. IMPORTANT! You must use a Sorvall® or Heraeus centrifuge with the Sorvall/Heraeus Custom Buckets and card holders. The Custom Buckets and card holders are custom-made for the TaqMan Array cards. Do not use any other centrifuge or bucket/card holder system for this procedure.
15. Place TaqMan Array cards into the Sorvall/Heraeus buckets:
    a. Obtain an empty Sorvall/Heraeus Custom Bucket and card holder.
    b. Place the bucket on a lab bench, with the label facing you.

c. Insert TaqMan Array cards into the card holder, making sure that the fill reservoirs project upwards out of the card holder and the reaction wells face the same direction as the "This Side Out" label. You use blank balance cards to fill any open positions in the card holder. Use the blank balance cards provided with the installation kits. IMPORTANT! Be sure to use the blank balance cards to fill any open positions. The blank balance cards will balance the centrifuge and prevent damage to the card holder. If the card holder is not completely filled, the TaqMan Array card may become displaced during centrifugation, resulting in uneven filling.

d. Place a filled card holder in the bucket so that the "This Side Out" label faces out.

16. Set the centrifuge:
    a. Power on the centrifuge.
    b. Use the front panel controls to set the bucket type to 15679. IMPORTANT! To ensure that the maximum rotational speed stays within the manufacturer's specified limits, be sure to set the correct bucket type.
    c. Use the front panel controls to set the following operations parameters: Parameter EASYSet (touchpad), Up ramp rate 9, Down ramp rate 9, Rotational speed 1200 rpm (331 × g) 1200 rpm, Centrifugation time 2 × 1 min.
17. Place the buckets into the centrifuge:
    a. Press the Open button on the centrifuge to open the centrifuge cover.
    b. Place each loaded bucket onto an open rotor arm of the centrifuge. Make sure each bucket can swing easily within its slotted position on the rotor arm. IMPORTANT! The manufacturer recommends running the centrifuge with all four buckets. If the buckets are not fully loaded with TaqMan Array cards containing the sample-specific PCR reaction mix, place blank balance cards and card holders into the buckets. Make sure the buckets and their contents are balanced; opposing buckets should have matching weights.
    c. Close the centrifuge cover.

18. Run the centrifuge:
    a. Press the Start button. The centrifuge starts, then automatically stops after 1 min, per the programmed sequence.
    b. Repeat step a so that the TaqMan Array cards are centrifuged for a total of two consecutive, 1minute spins. IMPORTANT! To ensure complete distribution of the PCR reaction mix, you must centrifuge the TaqMan Array cards for a total of two consecutive, 1-minute spins.
19. Remove the TaqMan Array cards:
    a. Press the Open button.
    b. When the cover has fully opened, remove the buckets from the centrifuge, then remove the card holders from the buckets.

c. Remove all TaqMan Array cards from the buckets by gently lifting them by their carrier sides.

20. Examine the TaqMan Array cards to be sure filling is complete. The amount of PCR reaction mix remaining in the fill reservoirs should be consistent from reservoir to reservoir.

21. Seal the TaqMan Array Card. Position the sealer:

a. Place the sealer on a sturdy lab bench, approximately waist high so that it can be easily used.

b. Turn the sealer so that the front end (the "starting position" shown below) is closest to you and the back end is farthest from you. In the correct position, the arrows on the sealer are pointing away from you.

c. Place the sealer's carriage in its starting position. IMPORTANT! Never insert a TaqMan Array card into the sealer if the carriage is not in its starting position. The TaqMan Array card will be irreparably damaged if the carriage is moved across it toward its starting position.

22. Insert a TaqMan Array card into the sealer:

a. Orient the TaqMan Array card in the proper direction over the sealer's insert plate. The card's fill reservoir end should be the end closest to the arrows etched in the base of the sealer.

b. Line up the card's rear pin grooves, foil side up, to the stylus pins on the sealer.

c. Gently place the card on top of the insert plate and ensure that the front end of the card is held securely in place by the spring clips.

d. Gently push the card until it is seated securely in the insert plate. Note: When properly seated, the TaqMan Array card's foil surface should be level with the base of the sealer. The four spring clips ensure that the card is held in the proper position.

e. Push the carriage across the base of the sealer in the direction of the arrows. Use a slow, steady, and deliberate motion to push the carriage across the entire length of the TaqMan Array card until the carriage reaches the mechanical stops. It is important to avoid moving the carriage rapidly across the card. The sealer has mechanical stops at both ends to prevent the carriage from coming off. Therefore, do not use excessive force or speed when pushing the carriage. IMPORTANT! Do not move the carriage back before removing the TaqMan Array card.

23. Remove the sealed TaqMan Array card by grasping its sides and lifting it off the sealer's insert plate. In the middle of the sealer's insert plate, there is a thumb slot to help you easily access one side of the card.

24. Inspect the TaqMan Array card for proper sealing. The indentations from the stylus assembly should match up with the card's main channels. If the indentations do not match up, or if the foil is in any way damaged, do not use the TaqMan Array card.

25. Using scissors, trim the fill strip from the TaqMan Array card. Use the edge of the card's carrier as a guide. After the TaqMan Array cards have been loaded and sealed, they are stable for at least 64 hours.
26. Set Up the SDS Plate Document. Start SDS Software v2.1 or later.
27. Select File, New.
28. Complete the New Document dialog box:
    a. From the Assay dropdown menu, select ΔΔCT (RQ) or Relative Quantification.
    b. From the Container dropdown menu, select 384 Wells TaqMan Low Density Array.
    c. Complete the remaining fields as shown, then click OK.
29. Import the SDS Setup File (*.txt) into the new SDS plate document:
    a. In the CD drive, insert the Array Information CD that shipped with your TaqMan Array card.
    b. In the SDS software, select FileImport. In the SDS software, set up the experiment (SDS plate document), using the SDS Setup File included on the Array Information CD (this page).
    c. In the Import dialog box, navigate to the SDS Setup File for your TaqMan Array card, then click Import. The SDS software imports information from the SDS Setup File into the SDS plate document. Note: The SDS software uses the information from the SDS Setup File to automatically configure the plate grid and setup table with detector, detector task, marker, and sample data. For details on the SDS Setup File, see page 26. IMPORTANT! Modifying the contents of the SDS Setup File can corrupt the file, making the file unusable (that is, you will not be able to access information for the TaqMan Array card).
30. Save the SDS plate document:
    a. Select File, Save As.
    b. Navigate to a save location.
    c. Enter a name for the SDS plate document.
    d. For Files of Type, select SDS 7900HT Document (*.sds) or SDS 7900HT Template Document (*.sdt).Note: You can save the plate document as an SDS plate document (*.sds) or SDS template (*.sdt). Saving the plate document as an SDS template is recommended when you want to create duplicate plate documents for a series of TaqMan Array cards with identical assay configurations. For
    e. Click Save.
31. Open the SDS plate document in the SDS software.
32. Select the Instrument tab.
33. Use the default thermal cycling conditions, as shown in the Thermal Cycler tab. Note: When you selected 384 Well TaqMan Low Density Array, the SDS software automatically set the appropriate thermal cycling conditions for the TaqMan Array cards.

34. Select the Real-Time tab. If the software is not connected to the instrument, click Connect to Instrument.
35. If the instrument tray is inside the instrument, click Open/Close to rotate the instrument tray to the OUT position.
36. Verify that the TaqMan Array Micro Fluidic Card Thermal Cycling Block is installed in the instrument tray.
37. Place the prepared TaqMan Array card in the instrument tray with: Well A1 at the top left corner of the tray and the notched corner at the top right and the barcode toward the front of the instrument.
38. Click Start Run. The instrument tray rotates to the IN position. During the run, the instrument displays real-time status information in the Instrument Real-Time tabs and records the fluorescence emissions. During the run, you can view the data (as the data are generated in real-time).
39. When the Run Complete dialog box appears, click OK to close the dialog box, click Open/Close, then remove the TaqMan Array card from the instrument tray.

Expression levels were normalized to 18S gene expression.

Table B-1. Assay ID for selected gene targets in Chapter II.

Gene symbol	Alias	Assay ID
Tollip		Rn01479669_m1
Tff3	ITF, TREFOIL	Rn00564851_m1
Tjp1	ZO-1	Rn02116071_s1
Slc16a1	MCT 1	Rn00562332_m1
Il6ra		Rn00566707_m1
Il1b		Rn01514151_m1
Il12b		Rn00575112_m1
tnf	TNFα	Rn00562055_m1
Slc5a8		Rn01503812_m1
Tgfbi		Rn01442102_m1
Tlr4		Rn00569848_m1
Tlr2		Rn02133647_s1
Myd88		Rn01640052_g1
Rela	NFκB	Rn01502266_m1
Ptgs2	COX-2	Rn01483828_m1

Chapter III and V microbial DNA isolation

Fresh fecal samples were collected immediately following defecation or at termination. Samples were transferred to sterile cryotubes, placed on ice, then stored at -80°C. DNA was isolated from homogenized fecal samples using a FastDNA SPIN kit

for Feces according to the manufacturer's instructions (MP Biomedicals, Solon, OH). Fecal samples were weighed and then homogenized in the FastPrep 24 instrument with kit provided buffers (825 ul Sodium Phosphate Buffer, 275 ul PLS solution, 122 ul MT Buffer) in Lysing Matrix E tubes.

Following homogenization, tubes were centrifuged at 14,000 x g for 5 min, and the supernatant was transferred to a clean 2.0 ml centrifuge tube. Proteins were precipitated from the supernatant by adding 250 ul PPS solution and incubating at 4°C for 10 min. Solution was centrifuged at 14,000 x g for 2 min, and the supernatant was transferred to 15 ml conical tubes containing 1 ml Binding Matrix Solution and placed on a plate rocker for 3 min. Following a 2 min centrifugation at 14,000 x g, the supernatant was decanted and remaining pellet resuspended with 1 ml Wash Buffer #1. This solution was transferred into a kit provided SPIN filter tube and centrifuged for 1 min at 14,000 x g. A 500 ul aliquot of Wash Buffer #2 was added to the SPIN filter and all flow through was discarded following a 2 min centrifugation at 14,000 x g. The SPIN filter was then transferred to a clean catch tube. To elute purified DNA, 50 ul of TES was added to the SPIN filter and the tubes were centrifuged at 14,000 x g for 2 min. Purified DNA was stored at -80°C. A negative control containing H_2O instead of sample was purified in parallel to each extraction batch to screen for contamination of extraction reagents.

Table B-2. Assay ID for selected gene targets in Chapter V.

Gene symbol	Alias	Assay ID
Il1b		Mm00434228_m1
Il6ra		Mm00439653_m1
Myd88		Mm00440338_m1
Rela	NFkB, p65	Mm00501346_m1
Slc16a1	MCT 1	Mm01306379_m1
Slc5a8		Mm00520629_m1
Tff3	ITF, TREFOIL	Mm00495590_m1
Tgfbi	TGFβ	Mm00493634_m1
Tlr 9		Mm00446193_m1
Tlr2		Mm00442346_m1
Tlr4		Mm00445273_m1
tnf	TNFα	Mm00443260_g1
GAPDH		Mm99999915_g1